

# **“Janus” Liquid Crystals Based on Diphenylacetylene**

Tiantian Ma

*Doctor of Philosophy*

University of York  
Department of Chemistry  
December 2013

## Abstract

Supramolecular architecture has the ability to control the fine property and location of specific functional groups which allows them to be applied in various advanced fields. One of the most intriguing aspects is the self-organisation of complex giant molecular systems, especially for the materials with diversely functionalised faces or sides, which can recognise from one side to another, also known as “Janus” materials.

In this project, dendritic supermolecules with more than one type of LC at the periphery (Janus liquid crystals) were developed. These LC molecules have a rigid diphenylacetylene core to which the dendritic linking scaffolds for the periphery groups can be attached. With different LC phase inducing ability, both the end-on and side-on mesogenic units have been used to build the amphiphilic system. The polyphilic materials containing different types of aliphatic chains as end-groups, which can enhance microphase segregation in this family.

Two types (1:3 and 3:3) of Janus liquid crystals with different ratios of peripheral moieties were synthesized, along with their liquid crystal properties being studied. The mesomorphic behaviour of the Janus LCs is determined by the type of the mesogenic units, the microphase segregation effect controlled by the aliphatic chains, and also the steric effect relevant to the central core and dendritic scaffold. The synergy and competition among these factors generated mesophase behaviours which are unique to this type of supermolecular LC system.

A series of side-on functionalized monomeric mesogens, LC dimers and trimers, and LC multipedes which is the intermediate in the synthesis of Janus LCs, were all developed as contrasts to the Janus LCs, for the systematical study in the mesomorphic behavior. Several of the giant molecular LCs based on hexaphenylbenzenes were also obtained from the Janus LC and oligomers via alkyne trimerization. With the unusual molecular conformation and distribution of peripheral groups, they also have novel self-assembling behaviours. Along with the Janus LCs, the supermolecular LCs provided an elegant entry for understanding the connection between the nanoscale structure and the macroscopic physical properties.

## List of Contents

Abstract	ii
List of Tables	vii
List of Figures	viii
Acknowledgements	xiii
Author's Declaration	xiv
<b>Chapter 1 Introduction</b>	<b>1</b>
1.1 Liquid crystals	2
1.1.1 Introduction of liquid crystals	2
1.1.2 Mesogens and mesogenic units	2
1.1.2.1 Classification of liquid crystals	2
1.1.2.2 Mesogens in low molar mass liquid crystals	3
1.1.2.3 Mesogenic units in high molar mass liquid crystals	4
1.1.2.3.1 Liquid crystal polymers and dendrimers	4
1.1.2.3.2 Terminally and laterally attached mesogenic units	5
1.1.3 Liquid crystal phases and identification	8
1.1.3.1 Nematic (N) phase	8
1.1.3.2 Smectic A and C (SmA & SmC) phase	9
1.1.3.3 Columnar (Col) phases	11
1.2 Liquid crystal oligomers	13
1.2.1 Linear liquid crystal oligomers	13
1.2.2 Liquid crystal multipedes	15
1.2.3 Disc-rod liquid crystal oligomers	17
1.3 Dendrimers	20
1.3.1 General concepts and synthesis of dendrimers	20
1.3.2 Self-assembly of dendrimers	21

1.3.3 Functional dendrimers	22
1.3.4 Supermolecular liquid crystal dendrimers	23
1.3.4.1 Introduction to the supermolecular LC system	23
1.3.4.2 Liquid crystal behaviour of supermolecular LC dendrimers	27
1.4 Janus molecular architectures	30
1.4.1 General concept	30
1.4.2 Microphase segregation (microsegregation)	30
1.4.3 Amphiphilic dendrimers	32
1.4.4 Janus liquid crystals	34
1.4.4.1 Introduction to Janus LCs	34
1.4.4.2 The self-assembling and mesophase behavior of Janus LCs	35
1.4.4.2.1 Enhanced microphase segregation ability	35
1.4.4.2.2 Factors affecting the mesomorphic behavior	37
1.4.4.2.2.1 Type of mesogenic units	37
1.4.4.2.2.2 Ratio of mesogenic units	38
1.4.4.2.2.3 The core and the dendritic scaffold	39
<b>Chapter 2 Aims</b>	42
<b>Chapter 3 Mesogenic Monomers</b>	46
3.1 Summary	47
3.2 Synthesis	48
3.3 Mesomorphic behaviour	54
3.4 Discussion	58
3.5 Concluding remark	60
3.6 Experimental	61
<b>Chapter 4 LC Oligomers</b>	77
4.1 Summary	78
4.2 Synthesis	79

4.3 Mesomorphic behaviour	85
4.4 Discussion	87
4.5 Concluding remark	91
4.6 Experimental	92
<b>Chapter 5 LC Mutipedes</b>	<b>103</b>
5.1 Summary	104
5.2 Synthesis	105
5.3 Mesomorphic behaviour	109
5.4 Discussion	114
5.5 Concluding remark	118
5.6 Experimental	119
<b>Chapter 6 1:3 Type Janus LCs</b>	<b>132</b>
6.1 Summary	133
6.2 Synthesis	134
6.3 Mesomorphic behaviour	138
6.4 Discussion	141
6.5 Concluding remark	145
6.6 Experimental	146
<b>Chapter 7 3:3 Type Janus LCs</b>	<b>157</b>
7.1 Summary	158
7.2 Synthesis	159
7.3 Mesomorphic behaviour	165
7.4 Discussion	171
7.5 Microphase segregation and steric effect in 3:3 Janus LCs	177
7.6 Concluding remark	181
7.7 Experimental	182
<b>Chapter 8 Hexaphenylbenzenes</b>	<b>201</b>

8.1 Summary	202
8.2 Synthesis	203
8.3 Mesomorphic behaviour	209
8.4 Discussion	211
8.5 Concluding remark	215
8.6 Experimental	216
<b>Chapter 9 Overall Conclusions</b>	<b>223</b>
Appendix 1 Experimental Techniques	227
Appendix 2 List of Compounds	230
Abbreviations and Acronyms	237
References	239

## List of Tables

<b>Table 1</b>	Transition temperatures ( $T/^{\circ}\text{C}$ ) and associated enthalpies ( $[\Delta H/\text{KJmol}^{-1}]$ ) of the monomers	54
<b>Table 2</b>	Transition temperatures ( $T/^{\circ}\text{C}$ ) and associated enthalpies ( $[\Delta H/\text{KJmol}^{-1}]$ ) of the oligomers	85
<b>Table 3</b>	Transition temperatures ( $T/^{\circ}\text{C}$ ) and associated enthalpies ( $[\Delta H/\text{KJmol}^{-1}]$ ) of the dendritic multipedes	109
<b>Table 4</b>	Transition temperatures ( $T/^{\circ}\text{C}$ ) and associated enthalpies ( $[\Delta H/\text{KJmol}^{-1}]$ ) of the 1:3 Janus materials	138
<b>Table 5</b>	Transition temperatures ( $T/^{\circ}\text{C}$ ) and associated enthalpies ( $[\Delta H/\text{KJmol}^{-1}]$ ) of the 3:3 Janus dendrimers	165
<b>Table 6</b>	Comparison of the structures and the LC behaviors of <b>50</b> , <b>56</b> and <b>74</b>	177
<b>Table 7</b>	Reduced molar entropy ( $\Delta S/R$ ) of SmA-I transition in 3:3 Janus LCs	179
<b>Table 8</b>	Transition temperatures ( $T/^{\circ}\text{C}$ ) and associated enthalpies ( $[\Delta H/\text{KJmol}^{-1}]$ ) of the hexaphenylbenzene derivatives (HPBs)	209

## List of Figures

<b>Figure 1.1</b>	Liquid crystal mesophase	2
<b>Figure 1.2</b>	Liquid crystal sub-categories	3
<b>Figure 1.3</b>	Examples of rod-like and disc-like mesogens	3
<b>Figure 1.4</b>	Side-chain LC polymer and LC dendrimer	4
<b>Figure 1.5</b>	Different attachment of the mesogenic units and mesophases induced	5
<b>Figure 1.6</b>	Commonly used cores in end-on mesogenic units	6
<b>Figure 1.7</b>	Side-on mesogenic units	6
<b>Figure 1.8</b>	Fluorinated chain in liquid crystal	7
<b>Figure 1.9</b>	Nematic phase and the schlieren texture	8
<b>Figure 1.10</b>	Orientations of the director around disclination points	9
<b>Figure 1.11</b>	Smectic A (left) and Smectic C phase (right) arrangement and textures	9
<b>Figure 1.12</b>	Dupin cyclide and the intersection of the cyclide formed in SmA phase	10
<b>Figure 1.13</b>	Columnar phase and its texture	11
<b>Figure 1.14</b>	The conical fan texture (left) and the spine-like texture (right) in columnar phase	12
<b>Figure 1.15</b>	LC dimer and the molecule topology controlled by the parity of the spacer	13
<b>Figure 1.16</b>	Examples of H-shaped (left) and T-shaped (right) LC dimers	14
<b>Figure 1.17</b>	Typical LC trimer (TCBO <sub>n</sub> )	14
<b>Figure 1.18</b>	LC tetrapedes	15
<b>Figure 1.19</b>	PE tetramers and their structure in the smectic phase	16
<b>Figure 1.20</b>	Effect of the attachment position of the mesogenic units on the LC behavior	17
<b>Figure 1.21</b>	Disc-rod LC oligomers and the mesophase miscibility of the mixture	18

<b>Figure 1.22</b>	Segregated SmA phase performed by the disc-rod LC oligomer	19
<b>Figure 1.23</b>	Tree and dendrimer	20
<b>Figure 1.24</b>	Divergent and convergent synthesis method of dendrimers	21
<b>Figure 1.25</b>	Assemblies of dendrimer via core unit interactions	22
<b>Figure 1.26</b>	Dendrimer used in drug delivery	23
<b>Figure 1.27</b>	Structure of a side-chain LC dendrimer	24
<b>Figure 1.28</b>	Mesogen-functionalized side-chain dendrimer	25
<b>Figure 1.29</b>	Liquid-crystalline silsesquioxane dendrimer	26
<b>Figure 1.30</b>	Density of mesogenic units and the LC dendrimer molecule shape	27
<b>Figure 1.31</b>	SmA and SmA <sub>d</sub> biphasic phase affect by different spacer lengths	28
<b>Figure 1.32</b>	Smectic/nematic phase favored by the end-on/side-on mesogenic units	29
<b>Figure 1.33</b>	God Janus and the Janus bead	30
<b>Figure 1.34</b>	Positional ordered mesophases formed via microsegregation	31
<b>Figure 1.35</b>	Self-assembling Janus dendrimers	33
<b>Figure 1.36</b>	Janus dendrimer designed for drug delivery	33
<b>Figure 1.37</b>	Design of Janus liquid crystal	34
<b>Figure 1.38</b>	Janus LC with end-on/side-on mesogenic units	35
<b>Figure 1.39</b>	Microphase segregation in Janus LC tripedes	36
<b>Figure 1.40</b>	Structure of the modulated layered SmA phase and the bicontinuous cubic phase formed by Janus LC	37
<b>Figure 1.41</b>	LC behavior controlled by the ratio between two types of mesogenic moieties	39
<b>Figure 1.42</b>	Different LC behavior with the same mesogenic units affected by the asymmetric core	40
<b>Figure 1.43</b>	Self-assembly via the core unit in Janus LC dendrimer	41
<b>Figure 2.1</b>	Janus LCs with a diphenylacetylene core	43
<b>Figure 2.2</b>	1:1 (left) and 1:3 (middle) type of LC oligomers and the LC multipedes (right)	44

<b>Figure 2.3</b>	Hexaphenylbenzene (HPB) supermolecular LCs	45
<b>Figure 3.1</b>	Laterally substituted 2,5-di(alkoxybenzoyloxy)benzoate	47
<b>Figure 3.2</b>	Typical $^1\text{H}$ NMR spectrum of the aromatic region, showing the central aromatic ring	53
<b>Figure 3.3</b>	Stepwise crystallization and melting of the PDAB monomeric mesogen <b>17</b> (top) and <b>11</b> (bottom) observed by DSC	55
<b>Figure 3.4</b>	Original 3-ring PDAB mesogen	58
<b>Figure 3.5</b>	Mesogenic dimer forms via hydrogen bond	58
<b>Figure 3.6</b>	Comparison of the effect of the side-on attached groups on the mesophase behaviour	60
<b>Figure 4.1</b>	Diphenylacetylene	78
<b>Figure 4.2</b>	$^{13}\text{C}$ NMR spectrum of <b>24</b> showing the carbon with sp <sup>1</sup> hybridisation in diphenylacetylene core	84
<b>Figure 4.3</b>	Parallel alignment of the mesogenic cores in compound <b>19</b> and the nematic phase formed	87
<b>Figure 4.4</b>	Transition temperatures of <b>19</b> (top) and T-shaped LC dimers (bottom)	88
<b>Figure 4.5</b>	The proposed S-shape of the trimer <b>24</b>	89
<b>Figure 4.6</b>	The transition temperatures of <b>24</b> (top) and the H-shaped LC oligomers comprising PDAB side-on mesogenic units (bottom)	89
<b>Figure 4.7</b>	Linear LC trimers with cyanobiphenyl groups, compound <b>32</b> (top) and TCBO10 (bottom)	90
<b>Figure 5.1</b>	Multipedes scaffold based on pentaerythritol	104
<b>Figure 5.2</b>	LC multipedes	105
<b>Figure 5.3</b>	$^1\text{H}$ NMR spectrum of the aromatic region of compound <b>45</b> , showing the 1:3 ratio of the protons of the iodophenyl (red) and the mesogens (blue)	108
<b>Figure 5.4</b>	MALDI-ToF MS of compound <b>43</b>	108
<b>Figure 5.5</b>	DSC heat flow curves of heating (left)/cooling (right) at different rates for compound <b>37</b> (top) and <b>44</b> (bottom) near the isotropisation point	110
<b>Figure 5.6</b>	The “hourglass” and “cone” shape of the tetrapedes and the SmA phase formed	115

<b>Figure 5.7</b>	Postulated molecular assembly in the phase transition of compound <b>37</b> and <b>44</b>	116
<b>Figure 5.8</b>	Comparison of dendritic multipedes with cyanobiphenyl groups and their transition temperatures	117
<b>Figure 5.9</b>	Dendrimer with three side-on mesogenic units and the nematic phase	118
<b>Figure 6.1</b>	1:3 type Janus LC	133
<b>Figure 6.2</b>	Heat flow curve of compound <b>53</b> around the Col-SmA-Iso transition with different heating/cooling rates	139
<b>Figure 6.3</b>	Possible conformations of the 1:3 Janus dendrimers with substituted diphenylacetylene arm (red) and cyanobiphenyl (black) and their mesophase structures	142
<b>Figure 6.4</b>	The cone shape of compound <b>53</b> and the proposed packing of the mesogens showing the transition from the lamellar to the discotic arrangement of the mesogens	143
<b>Figure 6.5</b>	Janus LC molecules with cyanobiphenyls and a perfluorinated chain	144
<b>Figure 7.1</b>	Two types of 3:3 Janus LCs	158
<b>Figure 7.2</b>	<sup>1</sup> H NMR of <b>37</b> (middle), <b>45</b> (top) and <b>59</b> (bottom); chemical shift changes of the protons on the diphenylacetylene core (green circle) while the protons on PDAB (red circle) and CB (blue circle) units unchanged	162
<b>Figure 7.3</b>	<sup>1</sup> H NMR of the TEG region in <b>63</b> (top) and <b>65</b> (bottom) and the 1:2 split peaks	163
<b>Figure 7.4</b>	MALDI-TOF MS of <b>72</b> (top) and <b>59</b> (bottom)	164
<b>Figure 7.5</b>	The dumbbell topology of the 3:3 Janus dendrimers and the different mesophases controlled by steric/microphase segregation effect	171
<b>Figure 7.6</b>	Janus LCs containing end-on and side-on mesogenic units	173
<b>Figure 7.7</b>	Molecular topology of the asymmetric dendritic scaffold with PE and gallate units	175
<b>Figure 7.8</b>	SmA-I transition temperature (°C) of 3:3 Janus LCs with all combination of periphery moieties, roughly coincide with the incompatibility based on CED ( $\delta^2$ ), ignoring the influence of volume fraction ( $f$ ) and central scaffold for simplification	178

<b>Figure 7.9</b>	Different arrangement of Janus molecules in the layer: (a) packing side by side; (b) orientational disordered packing; (c) packing with vertical slippage. The free space was reduced by the twist arrangement (b, c) than the more regulated way of packing (a)	180
<b>Figure 8.1</b>	Structure and topology of hexaphenylbenzene molecule	202
<b>Figure 8.2</b>	Change of the chemical shift of the protons in the core section (red circle) from dimer <b>32</b> (top) to hexamer <b>75</b> (bottom)	206
<b>Figure 8.3</b>	MALDI-TOF MS of compound <b>75</b> (top) and <b>79</b> (bottom)	208
<b>Figure 8.4</b>	The tentatively proposed molecular arrangement in the smectic layered packing of compound <b>75</b>	212
<b>Figure 8.5</b>	The postulated molecular topology of <b>76</b> , showing the perpendicular position of the core and the mesogenic units in <b>76</b>	213
<b>Figure 8.6</b>	The molecular structure of the isomers of <b>78</b> (top) and the cartoons showing the parallel position of the core and the mesogenic units (bottom) of the two isomers of <b>78</b> (left, 1,3,5-substituted; right, 1,2,4-substituted)	214

## Acknowledgments

I would like to thank Dr Isabel M. Saez gratefully for her guidance of this project. Her thoughtful support both on the knowledge and laboratory work guaranteed the success of this project. Without her effort and patience in supervision, the project could not have been accomplished.

I would also like to thank Prof. John W. Goodby for his helpful discussions and suggestions.

Many thanks go to Dr Stephen Cowling for his guidance on the manipulation of the analytic instruments and associated software.

Thanks for all the helpful discussions and the occasional assistance in laboratory work provided by David Stewart, Edward Davis, Richard Mandle and Charles Bradbury. Their support made this project going more successfully.

I would also like to thank Heather Fish and Pedro Aguiar in the Centre for Magnetic Resonance, Karl Heaton in the Centre of Excellence in Mass Spectrometry and Graeme Mcallister for the elemental analysis. Thank for Stephen Hau and Mike Keogh in the store for the supply of chemicals and equipments.

I would like to thank the Department of Chemistry, University of York for supporting this programme through the T. Wild Scholarship.

At last, I would like to thank my family and all my friends heartily. Their backing and company always made everything seems right, and encouraged me to overcome all the difficulties both in study and daily life.

## Author's Declaration

I declare that all the arguments, data, figures and any other materials taken from published or unpublished work of another person have been listed in the references.

I also declare that all the material presented in this thesis is my own work and not written by another person.

# **Chapter 1**

## **Introduction**

## 1.1 Liquid crystals

### 1.1.1 Introduction to liquid crystals (LCs)

A liquid crystal phase is a state of matter formed by some materials, in which the molecules adopt a preferential alignment which has less order than that typical of crystals but more order than liquids. It also shares properties normally associated with both the two other phases (Fig 1.1).

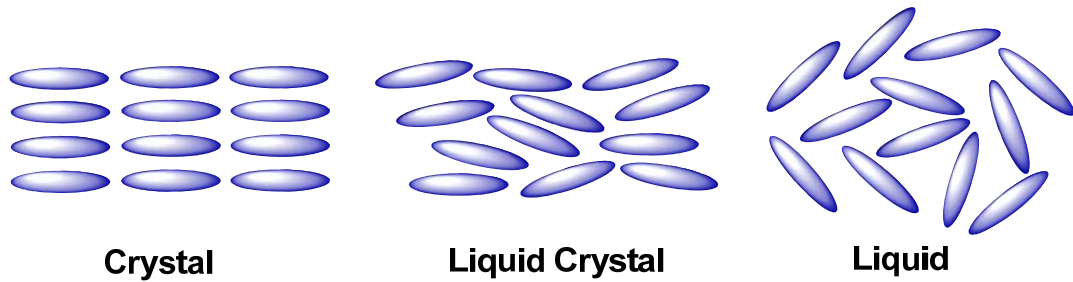


**Figure 1.1** Liquid crystal mesophase

As the fourth state of matter in nature, liquid crystals play an important role in material applications. They are widely used in liquid crystal displays, which rely on the optical properties of certain liquid-crystalline substances in the presence or absence of an applied electric field. Liquid crystals also can be used as temperature sensors, in chromatographic applications, and as anisotropic solvents [1].

### 1.1.2 Mesogens and mesogenic units

#### 1.1.2.1 Classification of liquid crystals

Based on the formation of mesophases, liquid crystals can be divided into two major categories, thermotropic liquid crystals in which phase types vary with temperature, and lyotropic LCs in which the mesomorphic behaviour depends on the concentration in a solvent beside of temperature. In this study the work relate only on thermotropic LCs. According to molecule size and structure, there are low molar mass LCs and high molar mass LCs, under each there are several sub-categories as shown in Fig 1.2.

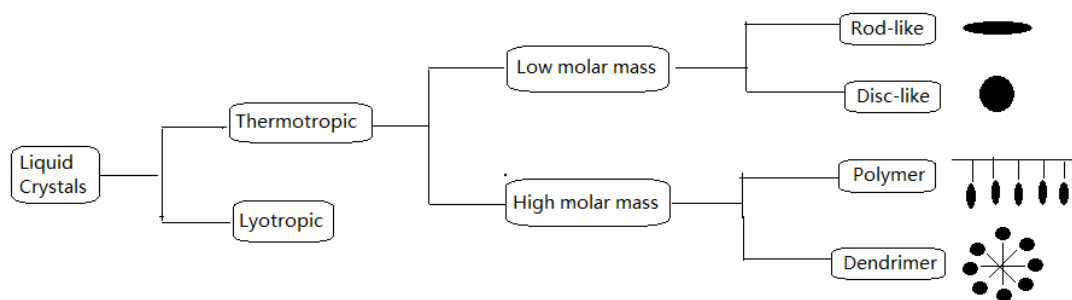


**Figure 1.2** Liquid crystal sub-categories

### 1.1.2.2 Mesogens in low molar mass liquid crystals

The molecules which have molecular structures that are conducive to forming liquid crystal phases are referred as mesogens. The formation of liquid crystal phases in thermotropic liquid crystals is due to the anisotropic structure of the molecular architecture and the electronic and steric interactions between molecules. The interactions between the molecules of anisotropic shape promote orientational and sometimes positional order in an otherwise fluid phase [2]. In low molar mass LCs, the molecules often have rod-like shapes, which are fairly rigid for a least some portion of its length, since it must maintain an elongated shape in order to produce interactions that favor alignment. Another kind of molecular architecture with low molar mass has rigidity in the central part of disc-like shapes, which also enhances the anisotropy (with a much shorter axis than the other two) of the entire molecular structure in order to form the liquid crystal phases by stacking of the disc-shaped molecules one on top of another (Fig 1.3).

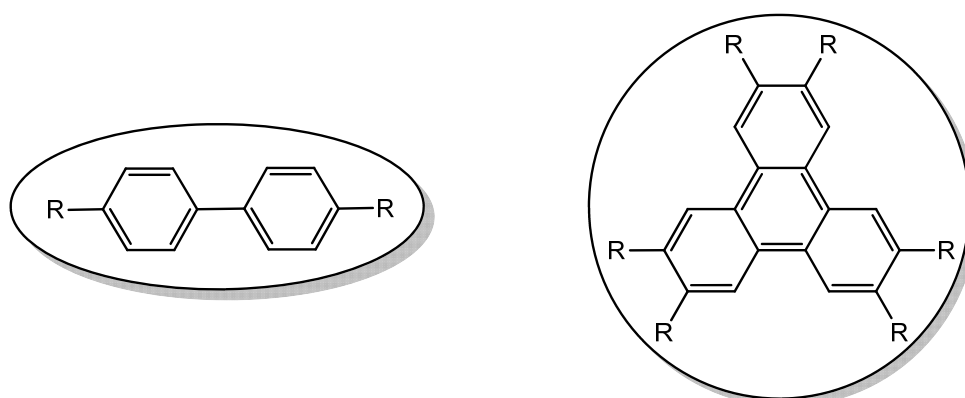


**Figure 1.3** Examples of rod-like and disc-like mesogens

### 1.1.2.3 Mesogenic units in high molar mass liquid crystals

#### 1.1.2.3.1 Liquid crystal polymers and dendrimers

High molar mass liquid crystals are macromolecules, with more complex structures, which can self-assemble to display mesomorphic behaviour. In order to induce liquid crystal mesophase formation, small rigid parts or mesogenic units are commonly required to enhance orientational and positional order for the entire molecular system. To this effect, rigid cores are joined together by flexible aliphatic spacers. For the LC polymers, the mesogenic units can be located in the main chain or in side chains of the polymer, whereas for LC dendrimers they are usually on the periphery of a branched scaffold structure, though there are also a few examples of main-chain LC dendrimers. The mesogenic units in these supermolecules are commonly arranged regularly and symmetrically in identical locations on the scaffold (Fig 1.4). In other words, apart from being supermolecular mesogens, LC polymers and LC dendrimers can be also regarded as elegantly organized assemblies of low molar LC mesogens, with their own unique properties.

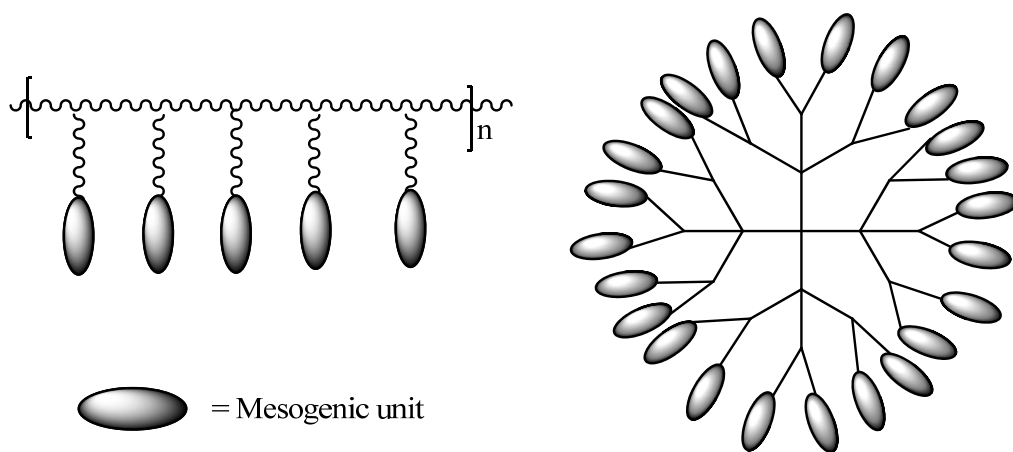


**Figure 1.4** Side-chain LC polymer and LC dendrimer

### 1.1.2.3.2 Terminally and laterally attached mesogenic units

Low molar mass rod-like mesogenic units are required in construction of large LC supermolecular systems. Aliphatic linking spacers are needed to attach the low molar mass mesogens to the backbone of the supermolecular system, and to decouple the motions of the mesogenic units from those of the backbone to guarantee their favorable alignment and interactions. Regarding the way in which the mesogenic units are linked to the backbone, they can be either terminally or laterally attached mesogenic units, also described as end-on or side-on units. The mode of attachment is crucial to the mesomorphic behaviour of the system for the LC dendrimers and side-chain LC polymers; the end-on mesogenic units have a tendency to form layers which induce smectic phases, whereas the side-on units have the ability to enhance the anisotropy and disorder of the system and promote the formation of the nematic phase, by suppressing the tendency to smectic behaviour [3a] (Fig 1.5).

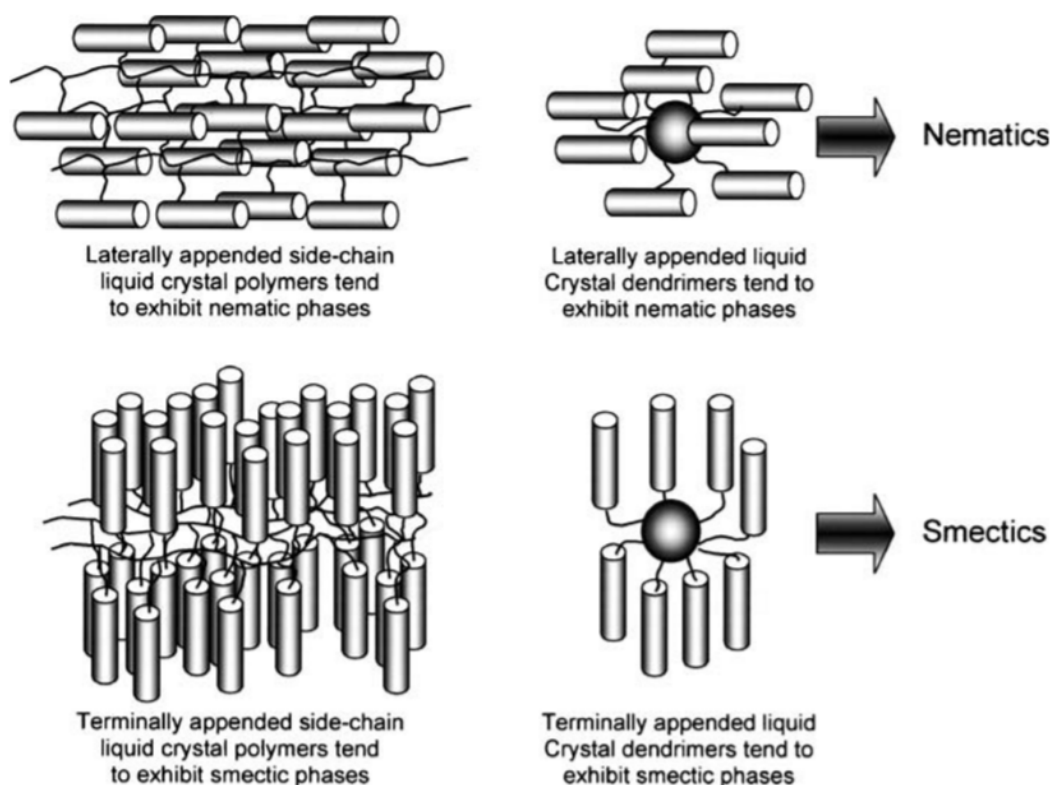


**Figure 1.5** Different attachment of the mesogenic units and mesophases induced (reproduced from Ref [3a])

There are various types of end-on mesogenic groups adopted in the supermolecular LC systems. The most commonly used are the biphenyl series, which has the simplest structure and excellent anisotropy and polarity to promote mesophase. The terminally attached mesogenic units most often used in LC polymers and dendrimers are listed in Fig 1.6.

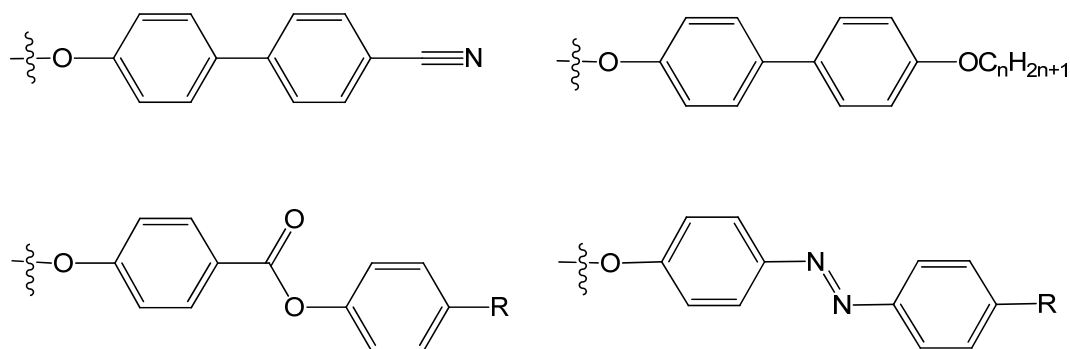


**Figure 1.6** Commonly used cores in end-on mesogenic units

The laterally attached calamitic mesogenic units are often composed of three or more aromatic rings, where one of the rings with a side chain carrying a reactive end-group. These phenyl rings are usually connected with aromatic ester groups, which are relatively stable and also have a certain degree of rigidity. The most commonly used side-on mesogenic groups are the p-phenylene ester of p-alkoxybenzoic acid and their derivatives, as shown below (Fig 1.7).

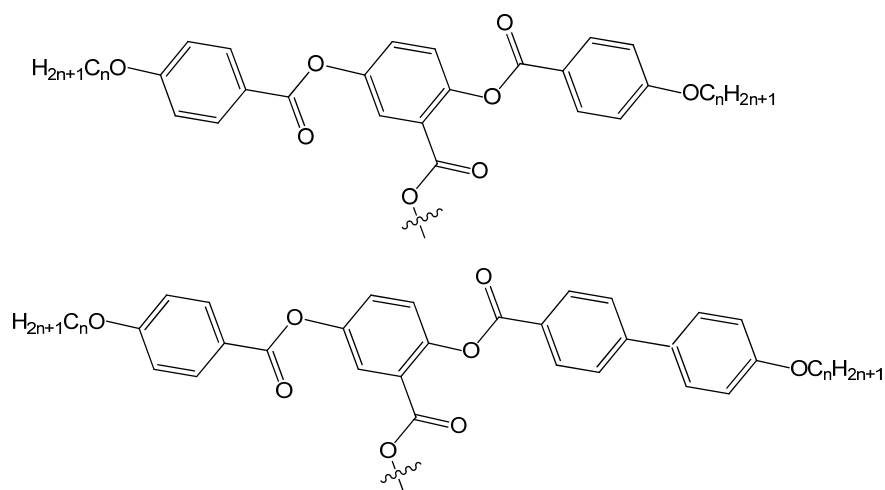


**Figure 1.7** Side-on mesogenic units



### 1.1.3 Liquid crystal phases and identification

#### 1.1.3.1 Nematic (N) phase

Nematic phase is one of the most common liquid crystal phases, in which the molecules have no positional order but they have long-range orientational order, with their long axes roughly parallel (Fig 1.9, left).

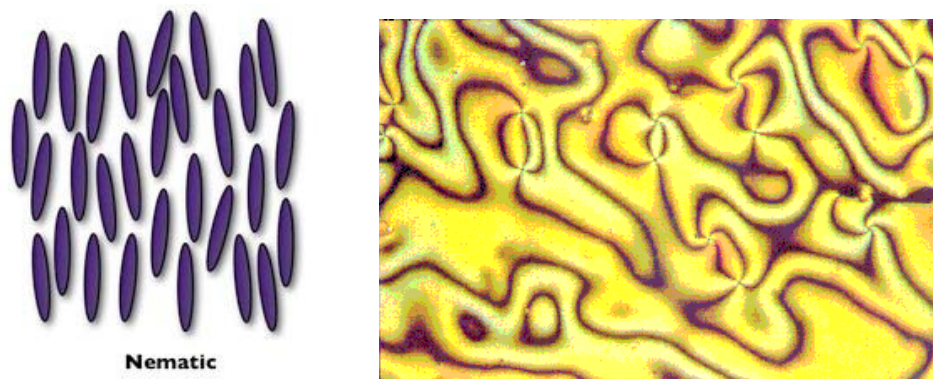


**Figure 1.9** Nematic phase and the schlieren texture (reproduced from [people.ccmr.cornell.edu/~cober/mse124/MSE124LAB3.html](http://people.ccmr.cornell.edu/~cober/mse124/MSE124LAB3.html))

When observing the nematic phase under polarized light with crossed polars, bright and dark areas are observed in the schlieren texture (Fig 1.9, right). In the dark areas, the director of the liquid crystal molecules is oriented either parallel or perpendicular to the axes of the polarized light, while in the bright areas the director adopts any other angle. The dark areas (or brushes) converge into points, also known as defect points. The nematic phase presents four brush and two brush defects. This is generated by disclinations where the director is abruptly changed and the molecules around it, for which the director is in line with one of the polarizer.

Within a plane parallel to the orientation of the nematic phase, the director of molecule around the defect is in a linear relationship with the direction from the disclination relative to the molecules, in the form of  $\theta = m\phi + \theta_0$ . Since the director can point in opposite directions ( $n = -n$ ), the value of  $m$  is confined with  $\pm 1/2$ ,  $\pm 1$ ,  $\pm 3/2$ , etc. The molecular alignment around the defect can be then deduced from the equation and some of the possibilities are showed in Fig 1.10. Since the molecules

align parallel or perpendicular to the axes of polarized light, which appear dark in the texture, there are always two (in the case of **a** and **b** in Fig 1.10) or four (**c** and **d**) dark areas converged into the defect point. Such a texture with both 2- and 4-brushes disclination is a proof of the nematic phase.

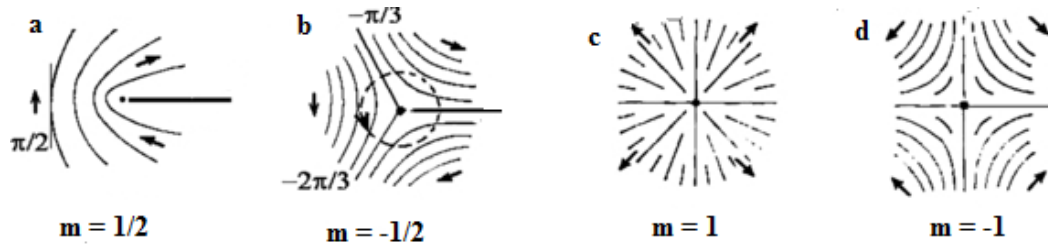


**Figure 1.10** Orientations of the director around disclination points (reproduced from [www.springerimages.com/Images/RSS/1-10.1007\\_978-90-481-8829-1\\_8-13](http://www.springerimages.com/Images/RSS/1-10.1007_978-90-481-8829-1_8-13))

### 1.1.3.2 Smectic A and C (SmA & SmC) phase

Smectic A phases form at lower temperatures than the nematic phase in a phase sequence. In the smectic A phase the molecules are arranged in diffuse layers that can slide over one another, with the molecules oriented along the layer normal. Compared to Smectic A phase, the molecules in Smectic C phase tilt away from the layer normal (Fig 1.11).

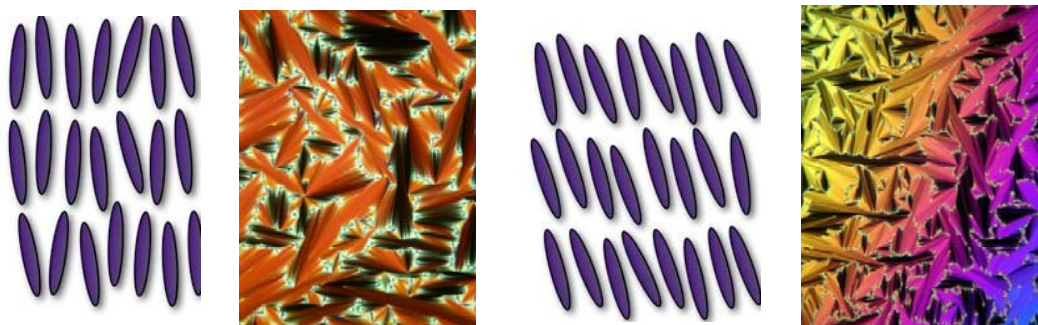


**Figure 1.11** Smectic A (left) and Smectic C phase (right) arrangement and textures (reproduced from [www.eng.cam.ac.uk/photocomp/2008/sf386\\_9.shtml](http://www.eng.cam.ac.uk/photocomp/2008/sf386_9.shtml) and <http://commons.wikimedia.org/wiki/File:F%C3%A4chertextur.jpg>)

The SmA phase commonly shows the focal-conic fan texture under polarized light, and sometimes it comprises colored bright conics formed by the molecules in the lamellar system packing into curved layers, and the black regions arise where the molecules aligned homeotropically. Many black lines can be seen in the texture which correspond to the ellipses and hyperbolae of the focal-conics and indicate sharp changes in the direction of the optic axis. The SmC phase also shows the focal-conic texture when generated from cooling from the SmA phase, while the black region of the homeotropically aligned SmA fills with the schlieren texture from the tilted molecules.

The ellipse and hyperbola, also known as focal-conic pairs, are shown in the form of black crossed, short lines, like a reticle. The layers in the SmA phase adopt usually a curved shape and stack easily into Dupin cyclides (Fig 1.12). Both the hyperbola and ellipse are the places where the molecular director abruptly changes from merging cyclides, so they appear dark under the polarized light in a perpendicular position to each other. The focal-conic pair commonly indicates the presence of the SmA phase, although sometimes they are also observed in some paramorphic textures of lamellar phases.

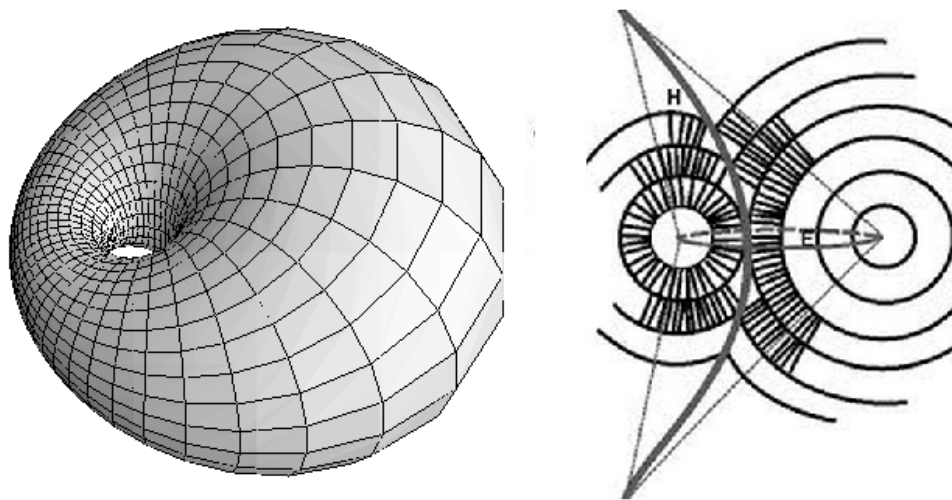


**Figure 1.12** Dupin cyclide and the intersection of the cyclide formed in SmA phase  
(reproduced from [www.geom.uiuc.edu/~banchoff/Lie/Lie.html](http://www.geom.uiuc.edu/~banchoff/Lie/Lie.html))

### 1.1.3.3 Columnar phases

A columnar phase is formed by cylindrical assembly of mesogens. It is usually presented by disc-like molecules which tend to stack into columns, and by some non-discotic mesogens which can also form cylindrical sub-structures. According to the positional order of the columns, there are nematic columnar phase ( $N_{Col}$ ) with no positional order among the columns and other columnar phase with long-range positional order (hexagonal, tetragonal, rectangular and oblique, which refers to the symmetry of the arrangement of the columns). The term “columnar phase (Col)” is usually referred to the phases with long-range order.



**Figure 1.13** Columnar phase and its texture (reproduced from I. Dierking, *Textures of Liquid Crystals*, WILEY-VCH Verlag GmbH & Co. KGaA, Weinheim, 2003)

Though there are several types of columnar phases, their textures are quite similar. The typical texture of columnar phase is the pseudo-focal-conic fan-shaped texture showed in Fig 1.13. The fully formed fan texture in the columnar phase sometimes can be quite similar to that observed in SmA phase, however the fans usually have more circular boundaries compared to the fans in SmA phase, and no focal-conic pairs (hyperbola and ellipse) can be found with the fans.

Similar to the layers in SmA phase, the columnar assemblies formed by disc-like or other mesogens are usually curved. The columns grow in a circular shape and form the circular domain [7]; when the circular domains are parallel to the glass surface (homogeneous alignment), the conical fans can be seen, usually with the accompany

of 2 or 4 orthogonal converged black branches, where the columns aligned parallel to either one of the polarizers (Fig 1.14 left). There is also a spine-like texture in the columnar phase, which forms when the circular domains are perpendicular to the glass surface (homeotropic alignment). No fans but batonnets can be found in this type of texture, which indicate the presence of the line defects (red line in Fig 1.14 right). The middle section of the batonnêt is brighter than the edge, since the directors of molecules are gradually changing, from homogeneous (high birefringence) to homeotropic (low birefringence).

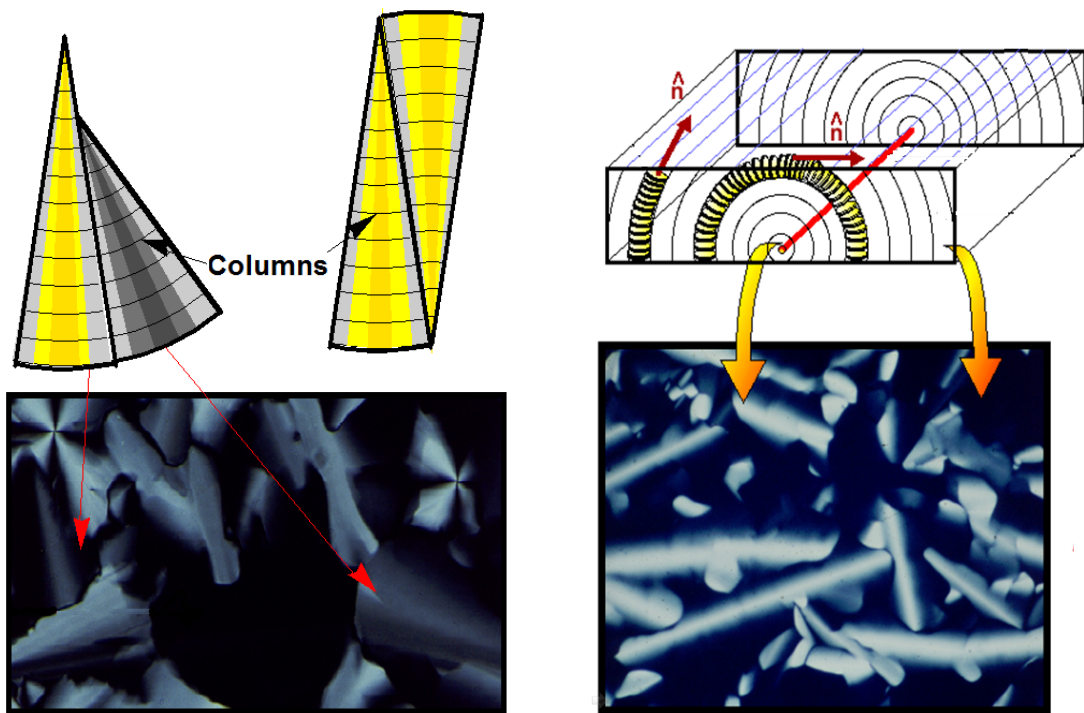


**Figure 1.14** The conical fan texture (left) and the spine-like texture (right) in columnar phase (reproduced from J. W. Goodby lecture notes BLCS winter workshop)

## 1.2 Liquid crystal oligomers

### 1.2.1 Linear liquid crystal oligomers

The molecules of low molar mass LCs contain usually only one rigid mesogenic core. Combination of two mesogenic groups joined with a chain spacer gives LC dimers. Compared to the conventional LC monomers, the dimers have a different degree of flexibility, which allows them to exhibit quite different mesophase behaviour respect to the monomeric constituents. The flexibility is mainly determined by the length of the spacer; the longer the spacer is, the stronger promotion of the nematic phase over smectic phases. The topology of the mesogenic units, as the nature of the monomers and the parity of the spacer chain all affect the mesomorphic behaviour in LC dimers, resulting in a notable odd-even effect, which is caused by the parallel or inclined relative orientations between the two mesogenic units [8] (Fig 1.15).

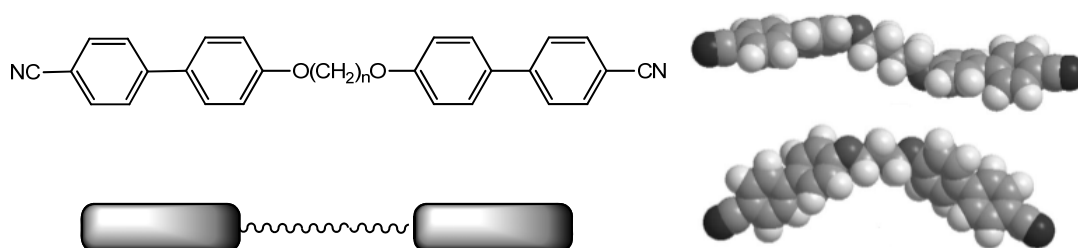


**Figure 1.15** LC dimer and the molecule topology controlled by the parity of the spacer (reproduced from Ref [8c])

Other type of LC dimers can be obtained by the connection of different positions on the mesogenic units. Two mesogenic units can be linked laterally by a spacer, resulting in H-shaped dimers, and one with terminal and another with lateral attachment to the spacer gives T-shaped dimers (Fig 1.16). The H-shaped dimers have similar phase behaviour to the linear dimers, for which the tendency of forming nematic phases increases with the length of the spacer, and also shows a strong odd-even effect [9]. The T-shaped systems usually adopt a nearly co-parallel conformation of the two mesogenic units, which also results in a strong nematic tendency [10].

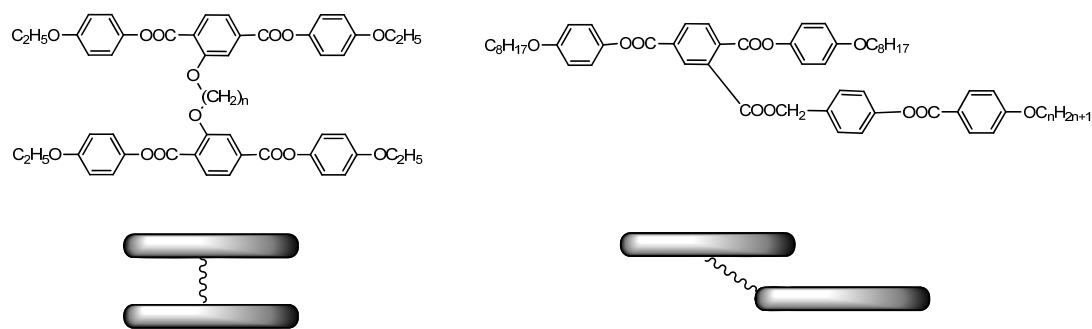


**Figure 1.16** Examples of H-shaped (left) and T-shaped (right) LC dimers

Three mesogenic units joined by two chain spacers gives rise to liquid crystal trimers (Fig 1.17). LC trimers can be seen as a model for main-chain LC polymers, and also have quite different mesomorphic behaviour to the conventional low molar mass LCs. Besides nematic phase tendency and odd-even effects similar to those of dimers, trimers have quite high clearing temperatures and isotropic transition enthalpies, which arise due to the stronger anisotropy of multiple mesogenic units [11].

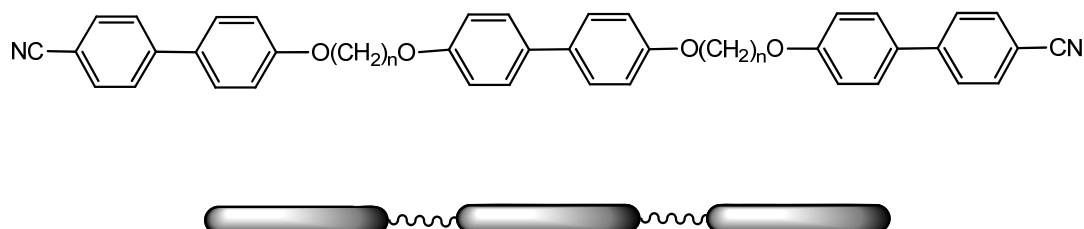


**Figure 1.17** Typical LC trimer (TCBOn)

In these types of LC dimers and trimers, the mesogenic units can be the same (as above) or different, resulting in unsymmetrical dimers or trimers. The mesomorphic behaviour of unsymmetrical oligomers is difficult to predict; but in general terms, the overall phase types observed are influenced by the phase behaviour of the individual components [12].

### 1.2.2 Liquid crystal multipedes

In contrast with the trimers described above, three mesogenic units can also be joined together to a central point (rather than in a succession), resulting in a very different molecular topology. By connecting several mesogenic moieties to the same core unit with a spacer chain, another type of LC oligomer can be obtained in the form of a “multipede” (Fig 1.18). With the simple dendritic structure, the multipedes can be seen as dendrimers of low generation, and are also sometimes referred as “star-shaped” LCs. Compared to LC oligomers with a linear topology, LC multipedes have a better ability to tailor mesophase behaviour since the mesogens, the spacers and the core can be independently modified.

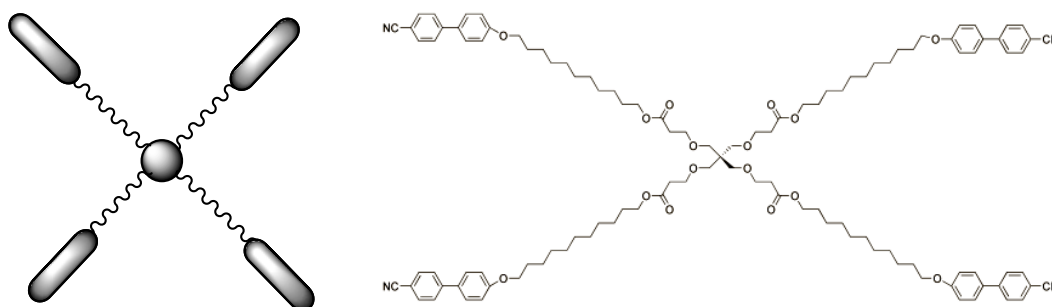


**Figure 1.18** LC tetrapedes (reproduced from Ref [13])

There is a large variety of multifunctional central core scaffold units to build up the LC multipede systems. According to molecular topology controlled mainly by the structure of the central scaffold, the physical properties and mesophase behaviours are largely dependent on the type of mesogenic core unit deployed. The chain spacers which join the core and the mesogenic units also affect the topology of the molecules. These factors also affect the behaviour of LC dendrimers, which will be discussed in detail below.

One of the simplest and most common types of LC multipedes is based on the pentaerythritol (PE) core. The first series of PE-based materials revealed that these multipedes with tetrahedral conformation tend to exhibit monotropic and enantiotropic smectic phases [13]. The four mesogenic units can be segregated into

two pairs which fold into opposite directions, aided by the flexible spacers. Thus, rather than displaying the mesogen extended in a three-dimensional structure, the tetrahedral-shaped molecules are deformed and the mesogenic units are paired and forming layers to achieve the best space filling, which builds up the stable smectic phases (Fig 1.19).

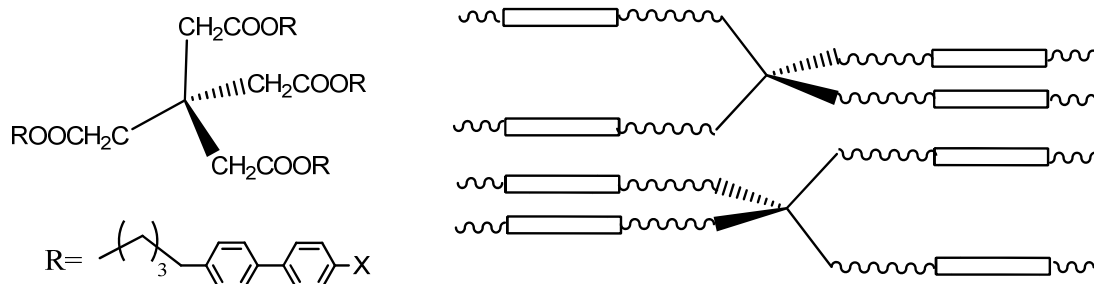


**Figure 1.19** PE tetramers and their structure in the smectic phase

Further study of the tetrahedral LC multipedes was focused on the effect of the attachment position of the linkage of mesogenic units on the mesophase behaviour. By attaching the mesogenic units terminally or laterally to the spacers, the mesophase behaviour can be very different [14] (Fig 1.20). For the uniform tetramers (all end-on or all side-on mesogenic units), the mesomorphic behaviour of the monomers is preserved in the multipedes. However, the attachment to the central scaffold prevents crystallization, so the overall mesomorphic range is greatly enhanced since the tetrapedes do not crystallize but show only glass transitions at low temperatures. As in LC polymers, the nematic phase of the cyanobiphenyl monomers is lost and the tetramers only show the SmA phase. Side-on attachment of the mesogenic units yield tetrapedes that show the same type of mesophase behaviour than the monomers (the chiral nematic phase is preserved and no smectic phase is observed). Moreover, for non-uniform tetrapedes (mixed side-on and end-on attachment of the mesogenic units), the presence of the laterally attached mesogenic unit has a strong effect suppressing the smectic behaviour: one side-on mesogenic unit (25% of all) is enough to eliminate the lamellar mesophases, regardless the type of the other three (rest 75%).

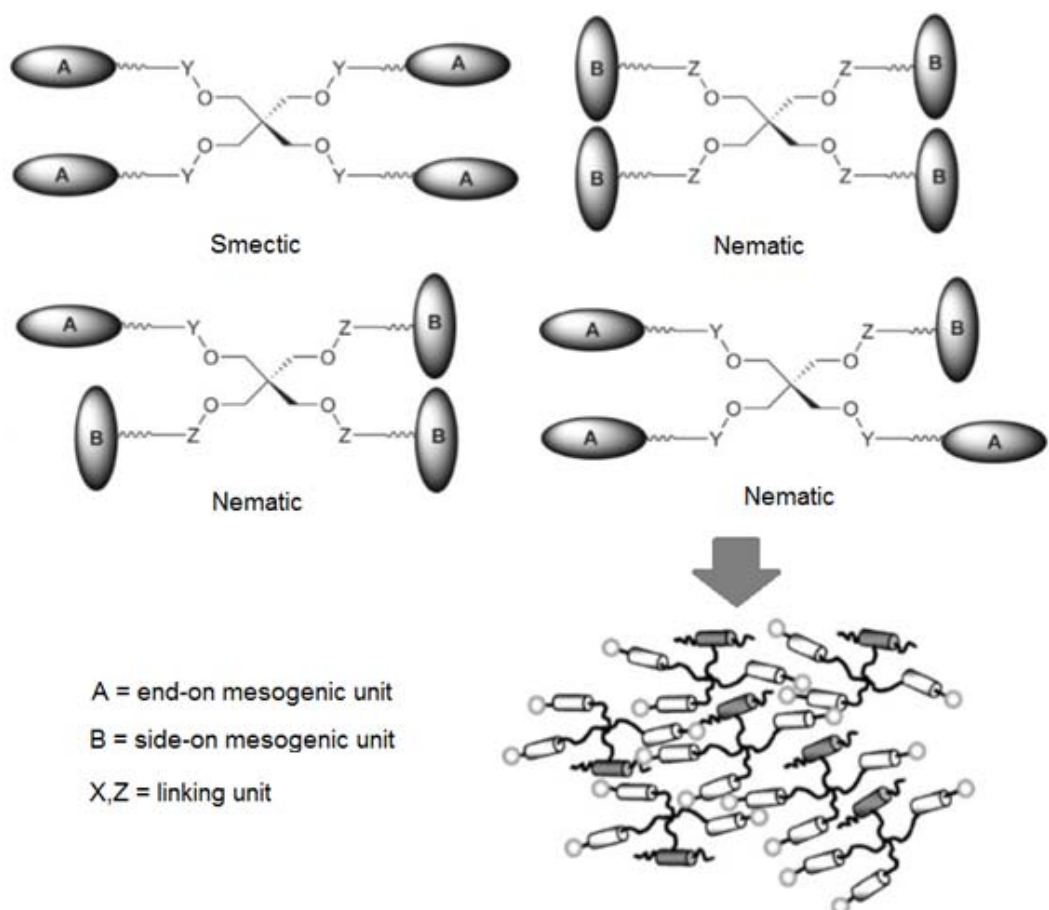


**Figure 1.20** Effect of the attachment position of the mesogenic units on the LC behavior (reproduced from Ref [3a] and [14])

### 1.2.3 Disc-rod liquid crystal oligomers

Mixture of disk-like and rod-like mesogens have been proposed in order to generate the biaxial nematic phase ( $N_B$ ), which has two directional orders. Though this point is only theoretical and in real mixture the phases separate into two uniaxial nematic phases, it is still believed that the problem can be solved by combining the two types of mesogens into one LC molecule to prevent phase separation [15]. Attaching calamitic mesogenic units to a discotic core yields disc-rod LC oligomers, which can behave as shape amphiphiles, being able to mix either with pure rods or with pure discs.

In the experiment of mixing up the disc-rod LC oligomers and disc-like/rod-like mesogens, the oligomers showed complete miscibility over the entire composition

range (Fig 1.21) [15(e)]. Although this system exhibits only a monotropic mesophase, it's still a valid model for the design and development of materials displaying the nematic biaxial phases in the future.

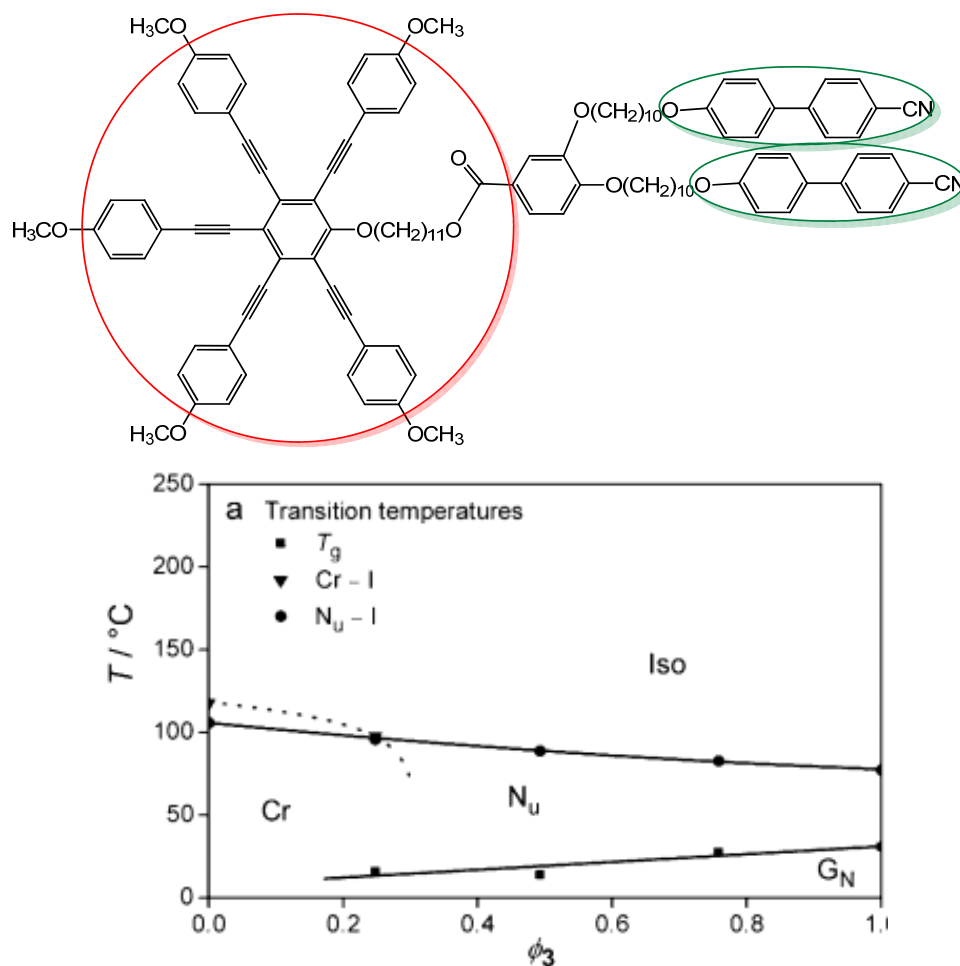


**Figure 1.21** Disc-rod LC oligomers and the mesophase miscibility of the mixture (reproduced from Ref [15e])

Beside the model of  $N_B$  phase, disc-rod LC oligomers are also good candidates for understanding structure–mesophase morphology relationships and are a bridge between calamitic and discotic LCs. A nanophase segregated SmA phase has been observed in the symmetrical disc–rod hybrid system showed in Fig 1.22, that has an electron deficient core and six rod-like mesogenic units [16]. In the mesophase, the calamitic mesogenic units and the discotic core are segregated into different sub-layers, demonstrating the intramolecular recognition among the rods and the

intermolecular interaction among the discotic cores, which results in the tendency of specific packing and aggregation (Fig 1.22).

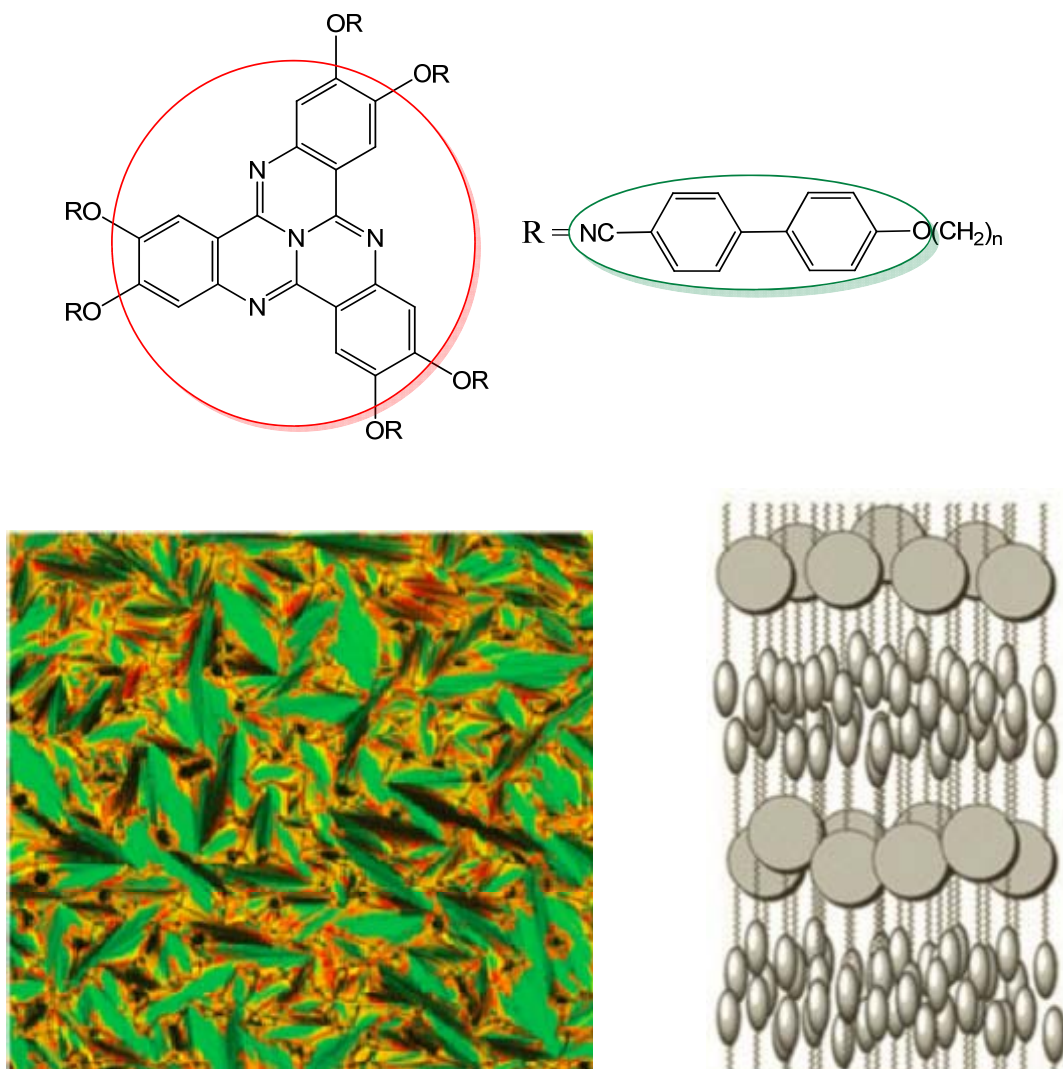


**Figure 1.22** Segregated SmA phase performed by the disc-rod LC oligomer  
(reproduced from Ref [16])

## 1.3 Dendrimers

### 1.3.1 General concepts and synthesis of dendrimers

The name of dendrimer comes from the Greek word "δένδρον" (pronounced dendron), which translates to "tree". Dendrimers are repeatedly branched macromolecules, typically symmetric around the core, that often adopt a spherical three-dimensional molecular conformation (Fig 1.23). The properties of dendrimers are mainly dominated by the functional groups on the molecular surface. Dendritic encapsulation of functional molecules allows for the isolation of the active site, a structure that mimics that of active sites in biomaterials.

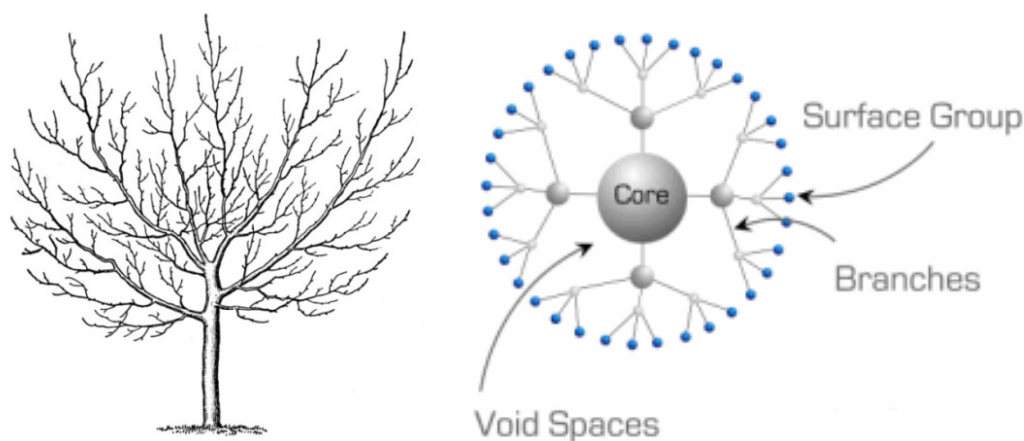


**Figure 1.23** Tree and dendrimer (reproduced from [www.sigmaaldrich.com/materials-science/nanomaterials/dendrimers/dendrons.html](http://www.sigmaaldrich.com/materials-science/nanomaterials/dendrimers/dendrons.html))

Dendrimers can be synthesized either by divergent or convergent methodologies. In the divergent method the dendrimer is assembled from a multifunctional core, which can be extended outward layer by layer by repetition of a series of reactions. A convergent method also can be adopted, which is built from small molecules that end up at the surface of the dendrimer, and reactions proceed by building layer by layer inwards and are eventually attached to a core [17] (Fig 1.24).

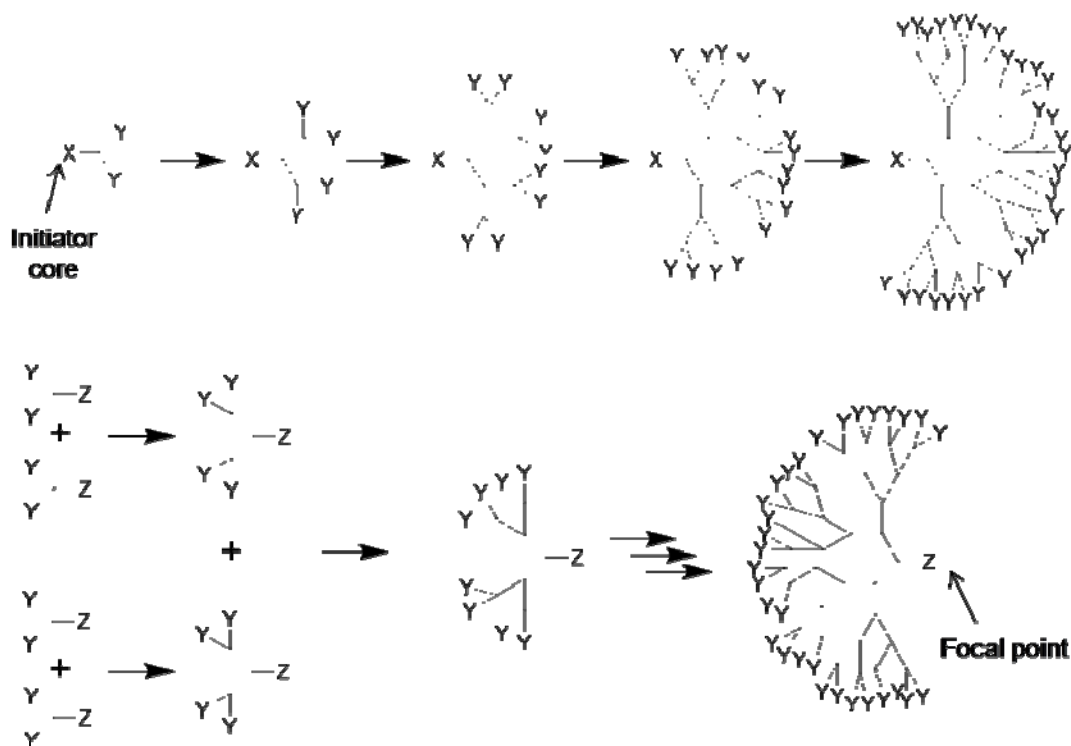


**Figure 1.24** Divergent and convergent synthesis method of dendrimers (reproduced from [en.wikipedia.org/wiki/Dendrimer](http://en.wikipedia.org/wiki/Dendrimer))

Dendrimers are technologically advanced synthetic compounds with monodisperse and precisely branched molecular architectures. Many factors control the properties and application of dendrimers including the number and density of branches and the chemical moieties located inside or at the periphery of the molecule.

### 1.3.2 Self-assembly of dendrimers

Due to the well-defined three-dimensional shapes and multifunctionality, dendrimers are unique nanoscopic building blocks for construction of supramolecular structures. Dendrons generated from certain architectures may self-assemble into functional supramolecular structures, and they have been proposed as mimics of biological macromolecular systems.

The self-assembly process can be triggered by the topology of the macromolecule, the periphery functional group or the core units. Fig 1.25 shows the self-assembly of

a complex trimeric dendrons which forms a columnar structure, induced by metallophilic interactions in the core unit [18]. The process of the self-assembly illustrate the mechanism of hierarchical transfer of structural information, and also provide a simplified model for the design of self-organizable dendronized polymers.

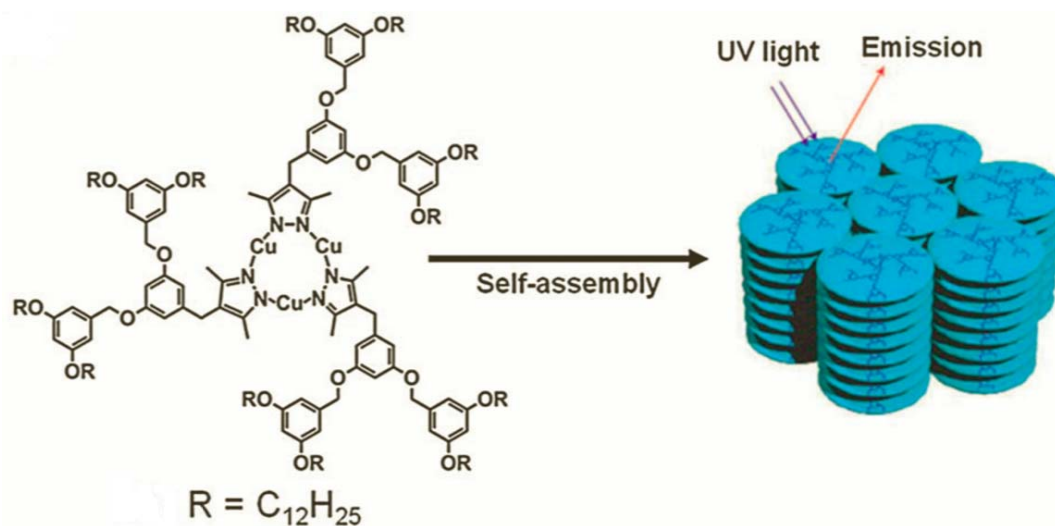


**Figure 1.25** Assemblies of dendrimer via core unit interactions (reproduced from Ref [18])

### 1.3.3 Functional dendrimers

Applications of dendrimers typically involve conjugating other chemical species to the dendrimer surface that can function as sensing agents, affinity ligands, targeting components, radio ligands, imaging agents, pharmaceutically active compounds, catalytic and photoactive moieties among others. Dendrimers have very strong potential for these applications because their structure and monodispersity can lead to perfectly defined multivalent systems.

Fig 1.26 shows an application of a dendrimer in drug delivery [19]: the molecule was decorated with surface glycosides as targeting devices for cellular uptake, and the peptide building block can be biodegraded once they have entered the cell, releasing the active colchicines ready to bind with the tubulin to inhibit their polymerization.

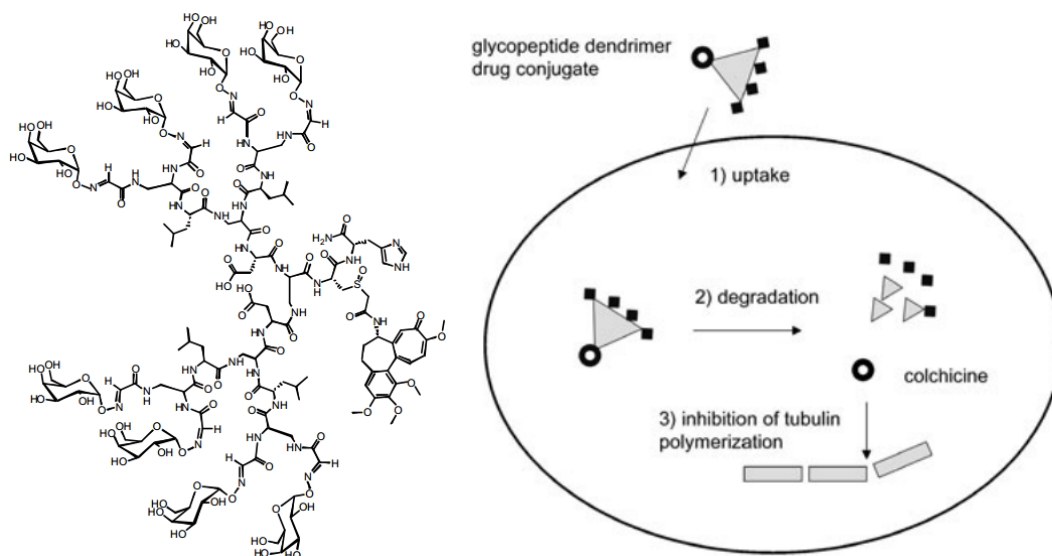


**Figure 1.26** Dendrimer used in drug delivery (reproduced from Ref [19])

### 1.3.4 Supermolecular liquid crystal dendrimers

#### 1.3.4.1 Introduction to the supermolecular LC system

Supermolecular chemistry refers to the area of chemistry “beyond the molecules”, and focuses on the chemical systems made up of a discrete number of assembled molecular subunits or components. Liquid crystal dendrimers have a huge potential in applications in the field of nanoscience, material and biology since their ability to control the location and interactions of specific functional groups within the molecular architecture can be used to tune their self-organising behaviour to very high levels [3].

There are several types of supermolecular systems that exhibit liquid crystal phases. The simplest is a dendrimer or dendron without any mesogenic groups in it; the self-assembly process of the constituent dendrons, aided by microphase segregation,

forms a dendrimer that has mesogenic properties. This type of self-organising LC dendrimers has been pioneered by Percec [20]. The generation number, branching multiplicity, nature of the peripheral chains, the nature of the dendron focal point and the dendrimer core have been used to tune the mesomorphic behaviour. A different type is that composed of hyperbranched polymers or liquid crystal dendrimers that have mesogenic groups forming part of their branching units, called “main-chain” LC polymers or dendrimers. This type has been developed mainly by B. Donnio and D. Guillon, and by V. percec [21]. The most important and common type besides the two above are liquid crystal dendrimers in which the mesogens are located in the periphery to induce LC mesophases, called side-chain LC dendrimers (Fig 1.27). In such supermolecular systems, liquid crystallinity is induced by the constituent mesogens, and it is multiplied by the dendritic construction, although the core also exerts its own effect on the ability to self-assemble.

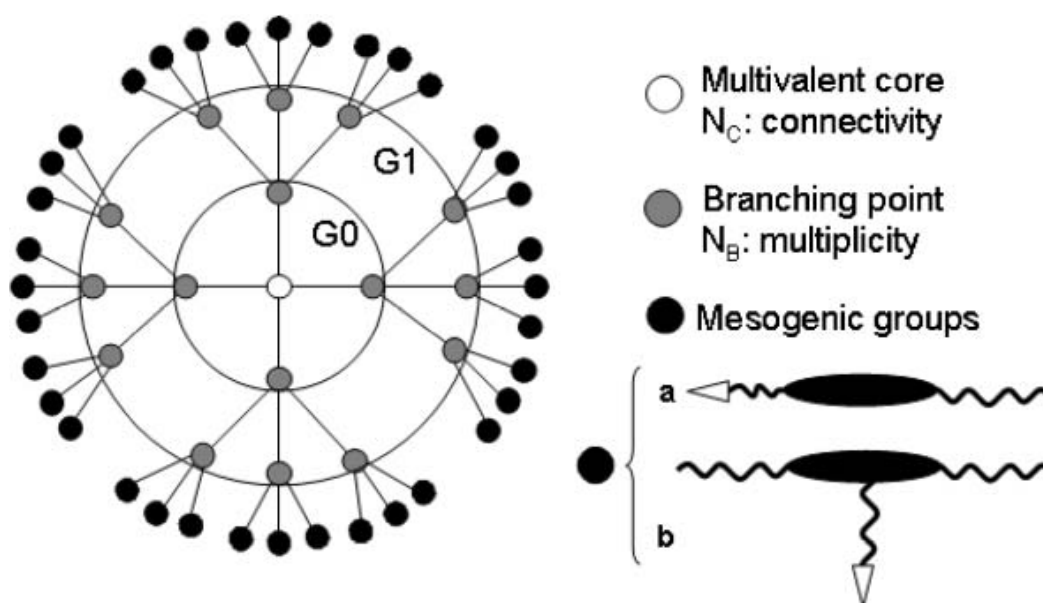


**Figure 1.27** Structure of a side-chain LC dendrimer (reproduced from Ref [3a])

A typical side-chain LC dendrimer combination of a flexible, dendritic carbosilane scaffold with rigid mesogenic units is shown in Fig 1.28 [22]. The liquid crystal dendrimer was obtained by condensation of the dendritic polyol with the acyl chloride of the spacer-functionalized mesogen. Functionalization of the end groups

of a carbosilane dendrimer with mesogenic units, which were attached via a spacer, led to liquid-crystalline dendrimers that form smectic A phases with broad temperature range.

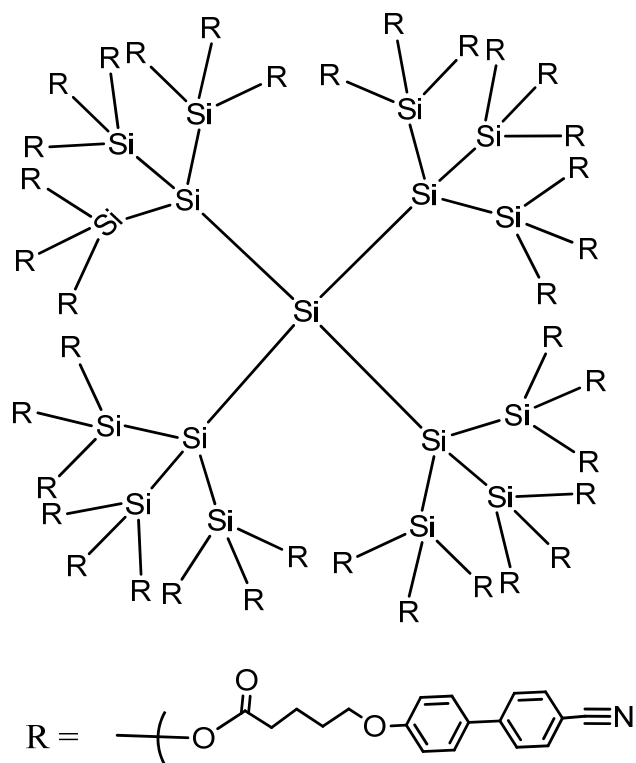


**Figure 1.28** Mesogen-functionalized side-chain dendrimer

Various central scaffolds can be used in the synthesis of the dendritic supermolecular LCs. These being either of a dendrimer type, just a multifunctional core or combinations of both. This field has been reviewed recently by I. M. Saez and J. W. Goodby [3] (Fig 1.29). The scaffold can be either soft and flexible, such as carbosilanes, carbosiloxanes and carbosilazanes, or rigid such as ferrocene or fullerene, where the behaviour of the active core can be tuned by the type of mesophase induced by the peripheral mesogenic units [23a-d]. For example, a first generation liquid crystal dendrimer based on the cubic silsesquioxane core has been reported [23d]. This system was synthesized from the hexadecavinyl (1<sup>st</sup> generation) octasilsesquioxane dendrimer. Platinum-catalyzed hydrosilylation reaction of the parent first-generation vinyl octasilsesquioxane dendrimer with a modified, laterally

substituted mesogen results in the hexadecamer dendrimer which displays enantiotropic chiral nematic, disordered hexagonal columnar and disordered rectangular columnar phases, with a glass transition below room temperature (Fig 1.29).

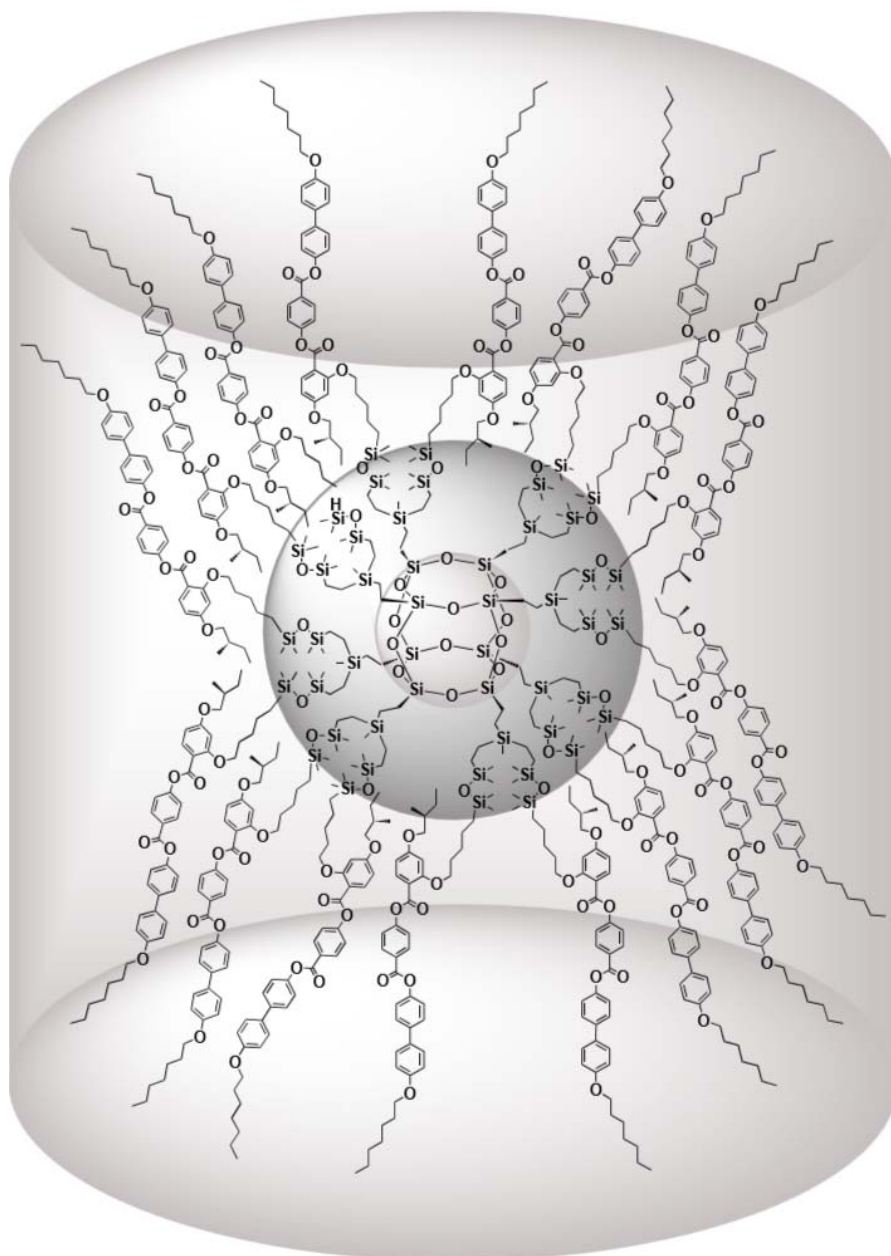


**Figure 1.29** Liquid-crystalline silsesquioxane dendrimer (reproduced from Ref [23d])

### 1.3.4.2 Liquid crystal behaviour of supermolecular LC dendrimers

As a large complex system, the mesophase behaviour of LC dendrimers is controlled by a series of factors. First of all, the mesophase behaviour is affected by the density of mesogens on the surface of the scaffold [3]. The density of mesogenic groups attached to the periphery can effectively change the overall gross shape of the structure of the dendrimer from being rod-like, to disc-like, to spherulitic (Fig 1.30). If there are few mesogenic units on the core, the molecule will take a calamitic shape to minimize the free volume, whereas increasing the number of mesogens reduces the free volume available for their packing and reduces their freedom of movement thus suppressing the ability of generating the rod-like conformational shape, which is replaced by a discotic or spherulitic structure.

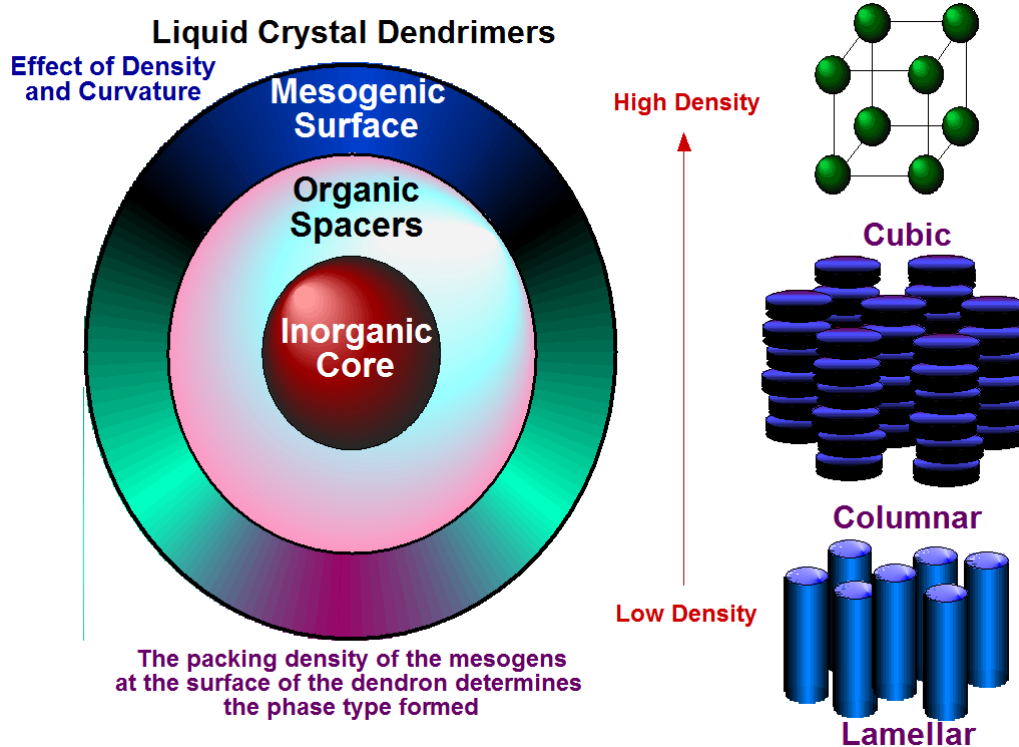


**Figure 1.30** Density of mesogenic units and the LC dendrimer molecule shape (reproduced from Ref [3a])

The flexible spacer between the mesogenic moieties and the core is an important building block, which links the mesogenic units and the central core. The length of the spacer has a significant effect on the self-assembly of the dendrimer. The spacer controls the size, length and flexibility of the dendritic LC molecule, as well as the ability for the free alignment of the mesogenic units. For example, in the tetracyanobiphenyl-siloxane and silane which exhibit SmA phases described by G. H. Mehl and J. W. Goodby [24], it was found that the shorter spacers induced a SmA<sub>d</sub> phase for the mesogenic units and a normal SmA<sub>1</sub> phase for the cores, while the longer spacers yield a more complex SmA<sub>d</sub> biphasic or incommensurate phase at lower temperature (Fig 1.31).

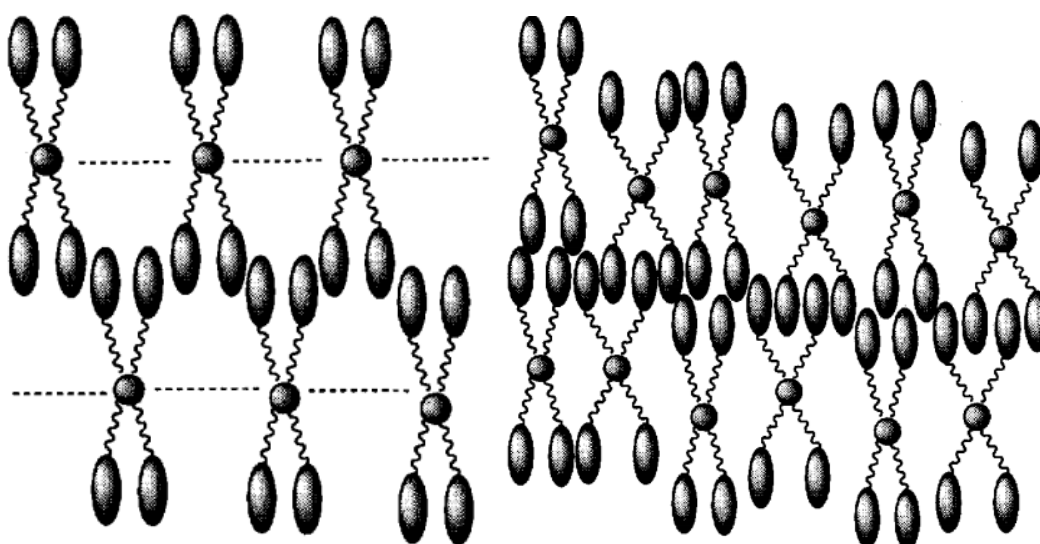


**Figure 1.31** SmA and SmA<sub>d</sub> biphasic phase affect by different spacer lengths  
(reproduced from Ref [24])

The orientation of attachment of rod-like mesogenic units to the central scaffold also affects the mesophases formed in LC dendrimers. With terminally attached mesogenic units, the dendrimer can take a cylindrical conformation easily and assemble into layers, generating lamellar phases. When the groups are attached laterally, the outer shell of the molecule will be much more crowded and disruption to the intermolecular packing occurs, yielding preferentially the nematic phase [3a] (Fig 1.32). It has also been observed that lateral attachment of the mesogenic units to

the core is more difficult for steric reasons, and in certain cases can lead to incomplete derivatisation of the core, which also enhances the nematic behaviour [3c].

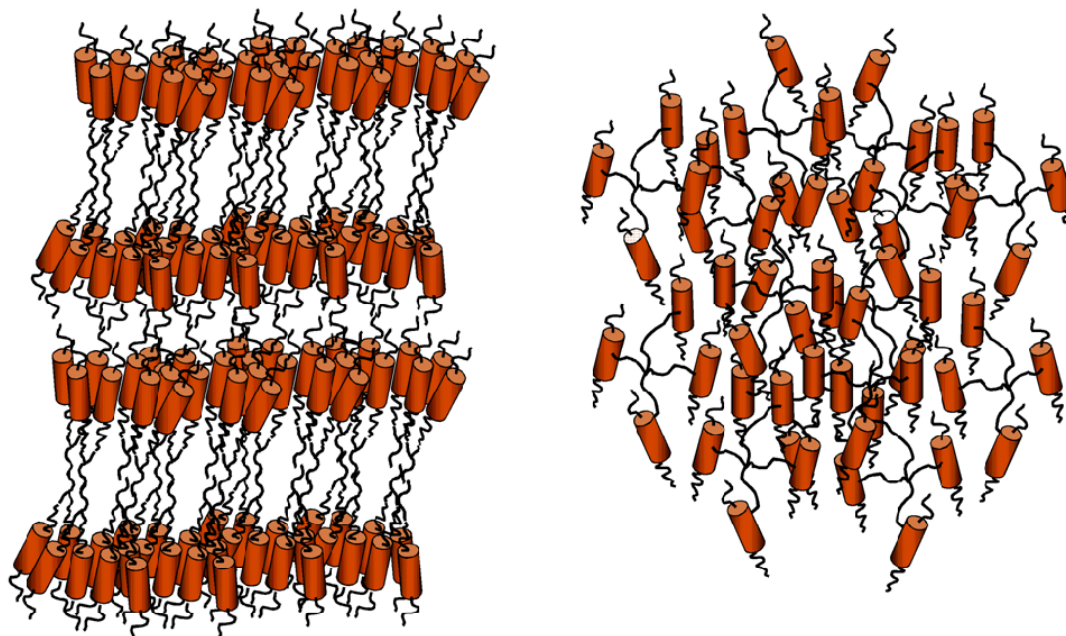


**Figure 1.32** Smectic/nematic phase favored by the end-on/side-on mesogenic units  
(reproduced from Ref [3a])

## 1.4 Janus molecular architectures

### 1.4.1 Introduction

The concept of “Janus grains”, which is a grain has two different sides just like the two-faced god Janus, was given by P.G de Gennes [26]. Janus grains were first made as materials that have common features with surfactants, which has one side polar and another apolar. The interface between the grains allows for chemical exchange between the two sides [25] (Fig 1.33).

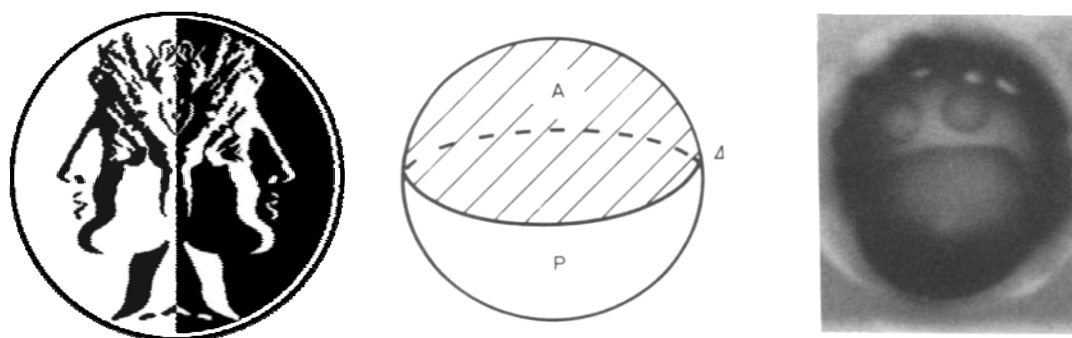


**Figure 1.33** God Janus and the Janus bead (reproduced from Ref [24])

Many Janus materials have been successfully studied now and have found applications in various fields. These are mainly colloidal particles and nanoparticles, with the term “Janus” indicating that the material has two faces or sides diversely functionalized, and include, but are not limited to, the difference in polarity. Understanding of the molecular recognition process in Janus materials is one most intriguing aspects in the self-organization of complex giant molecular systems.

### 1.4.2 Microphase segregation (microsegregation)

In order to present a liquid crystal phase with orientational order, molecules that have anisotropy are required. More ordered mesophases with additional positional order can be derived from molecules that are not only anisotropic but also composed with incompatible segments. The incompatibility can be expressed as different polarity,

rigidity, shape or hydrophilicity, which once a certain limit has been reached, positional segregation will occur between different segments, causing the formation of mesophases with positional order (lamellar, cubic, columnar, etc.) (Fig 1.34).

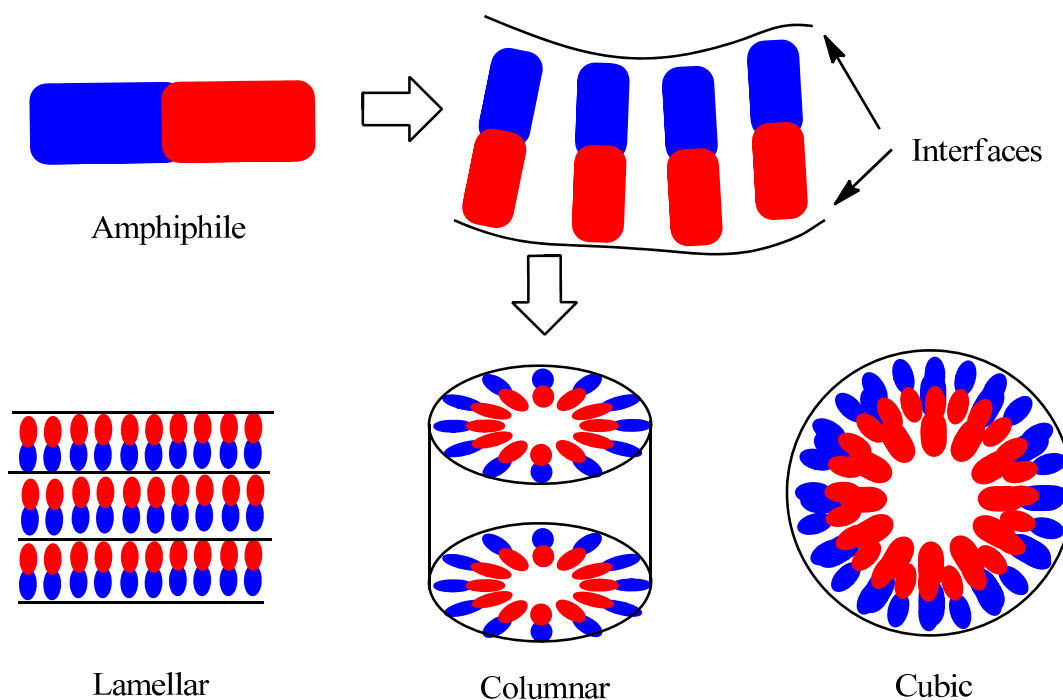


**Figure 1.34** Positional ordered mesophases formed via microsegregation

The concept of “microsegregation” claims that the positionally ordered phases are related to the shape of segregated compartments and the separating interfaces [27]. For example, the typical smectogens based on cyanobiphenyl (CB) derivatives can be regarded as a combination of aromatic core (rigid/polar) and a flexible alkyl chain (flexible/non-polar), the segregation of which allows the formation of SmA phase which has interface with low curvature.

For a flexible diblock mesogen, the expected mesophase behaviour is related to the volume fraction  $f$  and the interaction parameter  $\chi$  of the incompatible segments. The type of mesophase is mainly dependent on  $f$ , which determine the curvature of the interfaces; and the likelihood of the microphase segregation is decided by  $\chi$  which quantified the degree of incompatibility. The value of interaction parameter  $\chi$  is related to the difference of the cohesive energy density (CED) of the segments,

which depend on the type of chemical groups. The perfluorinated chain has one of the lowest CED and usually generates a high  $\chi$  value. With such good microphase segregation ability, perfluorinated chains are commonly employed as mesophase stabilizer in amphiphilic mesogens.

Based on the concept of microphase segregation, the “Janus” materials can be carefully designed as structures with high incompatibility between blocks with the aim of generating materials that can self-assemble into ordered LC phases. This concept is valuable for understanding the connection between the nanoscale structure and the macroscopic phase behaviour.

### 1.4.3 Amphiphilic dendrimers

The term “amphiphile” describes a chemical compound possessing segments with opposite properties. Amphiphilic dendrimers, which are also known as “Janus” dendrimers, bow-tie or block co-dendrimers, describe a dendrimer with different hemispheres, with functional groups either on surface or inner branching structure. The great interest towards these dendritic Janus molecules stems from their bifunctional character, leading to various applications [28]. In a Janus dendrimer, the two different hemispheres could produce a molecule with a perfectly controlled disposition of the peripheral functional groups, which shows enhanced amphiphilicity and self-assembling behaviour. Janus dendrimers can also display mesomorphic behaviour, which has been proven to be a powerful feature to control the supramolecular organization of different chemical structures.

When synthesized with judiciously chosen elements, Janus dendrimers can function as powerful structure-directing amphiphiles of great versatility. V. Percec et al. reported a broad class of synthetic amphiphiles based on pentaerythritol dendrimers prepared by coupling of tailored hydrophilic and hydrophobic branched segments. They demonstrated their facile self-assembly in water to yield a variety of stable bilayer vesicles [28] (Fig 1.35). The bilayer vesicles, which are also referred as dendrimersomes, can offer a molecular periphery suitable for further chemical functionalization. Their modular synthetic strategy also provides access to the systematic tuning of molecular structure and of the self-assembled architecture.

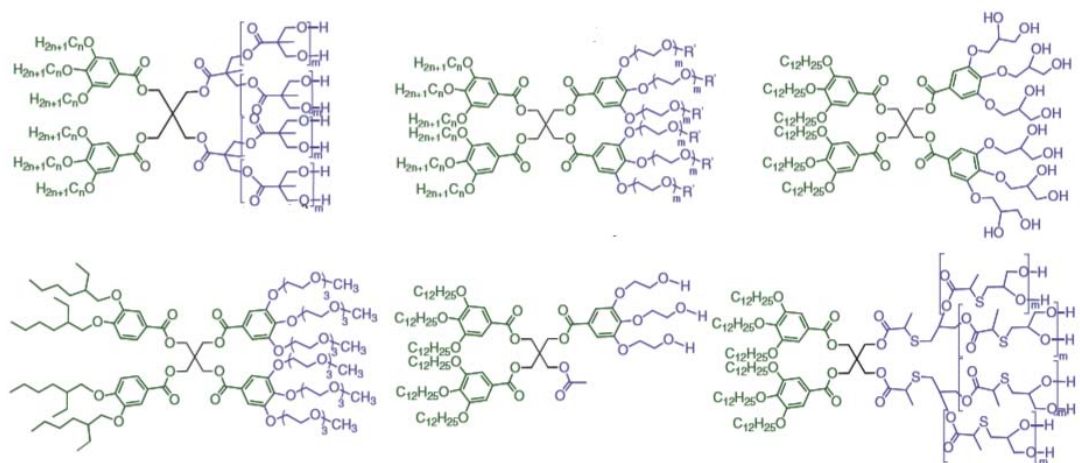


**Figure 1.35** Self-assembling Janus dendrimers (reproduced from Ref [28])

Janus dendrimers can be designed for various applications, especially for drug delivery, due to the capability of self-assembling into nanoscale polymeric structures in aqueous solutions while performing different tasks simultaneously. A series of bisfunctionalized Janus dendrimers (Fig 1.36) was designed for drug delivery to bone, which uses an amino acid group as bone-targeting moiety and naproxen as insoluble model drug [29]. These dendrimers showed enhanced solubility in water, indicating that using an amphiphilic dendrimer was a promising approach to the delivery of multiple copies of drugs poorly soluble in water with increased bone-targeting effect and low cytotoxicity.

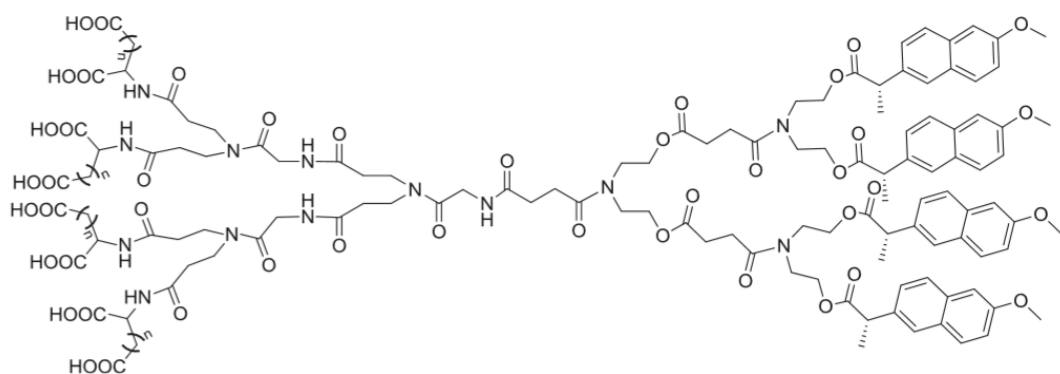


**Figure 1.36** Janus dendrimer designed for drug delivery (reproduced from Ref [29])

## 1.4.4 Janus liquid crystals

### 1.4.4.1 Introduction to Janus LCs

The Janus structure with diversely functionalized faces can be also applied in liquid crystals. Janus LCs are related to asymmetric LC dimers and mutipedes, but with a more advanced structure. Compared to the asymmetric dimers, the dendritic structure of Janus LC can carry more than one mesogenic unit on each side, which provides stronger mesophase inducing ability and the chance to adjust the ratio between the two types of mesogenic units. Compared to the mutipedes, the central core unit of Janus LC enhances the separation of the two types of mesogenic units, which strongly assists the microphase segregation effect, and ensures the “two faces” conformation of the asymmetric system (Fig 1.37). Furthermore, the flexible molecular design in Janus liquid crystals systems is a method potentially capable of incorporating other functional units, ultimately resembling the molecular and functional complexity of living systems [30].

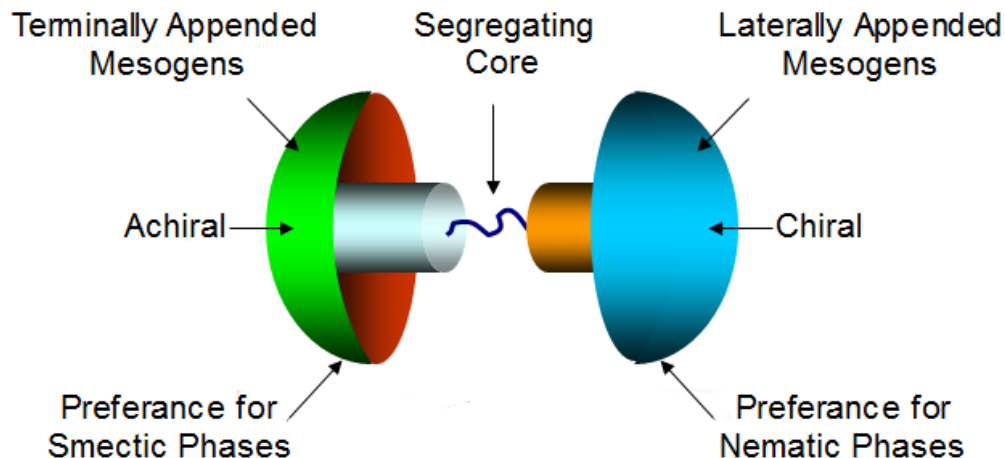


**Figure 1.37** Design of Janus liquid crystal (reproduced from Ref [3a])

The combination of the terminally and laterally attached mesogenic units in a dendrimer has produced a new class macromolecular materials, Janus liquid crystal compounds, introduced by I. M. Saez and J. W. Goodby in 2003 [30] (Fig 1.38). They have high molecular weight; however the mesomorphic temperature range is large, including room temperature. These materials contain two different mesogens

attached to an unsymmetrical core based on pentaerythritol and tris(hydroxymethyl)aminomethane; by placing the mesogenic units either at one side of the core or on the opposite side, different mesomorphic behaviour is observed, demonstrating that the lobes have different recognition abilities.

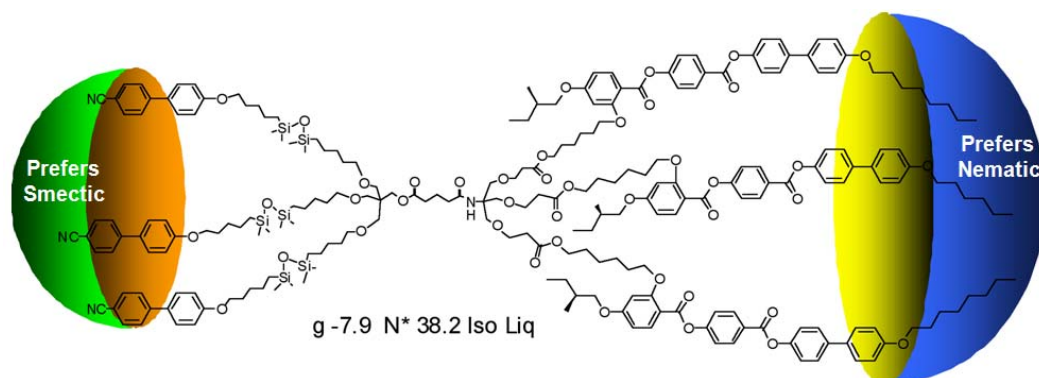


**Figure 1.38** Janus LC with end-on/side-on mesogenic units (reproduced from Ref [30])

#### 1.4.4.2 The self-assembling and mesophase behavior of Janus LCs

##### 1.4.4.2.1 Enhanced microphase segregation ability

Compared to the conventional LC multipedes and dendrimers with identical mesogenic units, the Janus LC architecture can lead to enhanced microphase segregation, caused by the central core units which somehow prevent the intramolecular mixing of mesogenic units on opposite halves.

For example, in model Janus-type tripedes comprising a combination of alkoxy-cyanobipheny (OCB) and alkoxy-azobenzene reported by B. Donnio and D. Guillon [31] (Fig 1.39), the heterolithic system promoted a remarkable mesomorphism, whereas the homolithic tripedes with three cyanobiphenyl groups showed only monotropic behaviour. It can be concluded that the segregation between the two types of mesogenic units in the heterolithic system can result in better differentiated molecular sub-layers than the homolithic system.

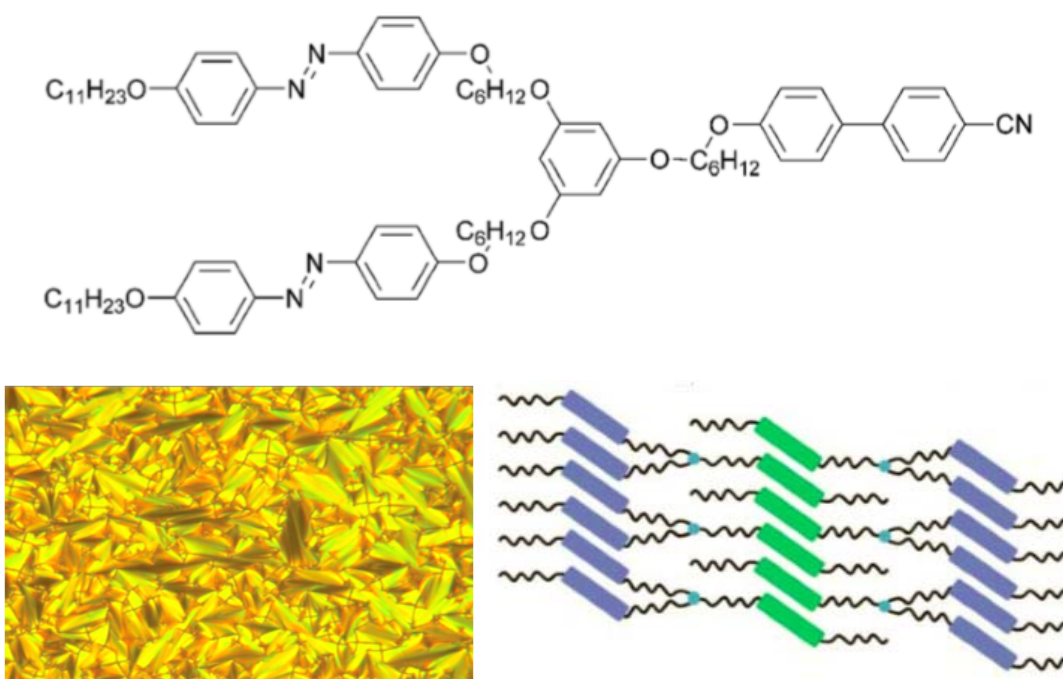


**Figure 1.39** Microphase segregation in Janus LC tripedes (reproduced from Ref [31])

Due to the strong tendency to microphase segregation, Janus LCs can introduce some unique mesophase behaviour which is rarely seen in conventional LCs. A novel lamellar-cubic phase transition was observed in an amphiphilic LC oligomer that has three cyanobiphenyl mesogenic units and one perfluorinated chain linked to the benzene core, reported by A. Yoshizawa [32] (Fig 1.40). This type of Janus LC molecular structure exhibits a modulated layered SmA phase and a bicontinuous cubic phase. This unique mesophase behaviour is caused by the competition between the strong microphase segregation and the steric effect which goes against the regular packing of such mesogens in the lamellar structure. The formation of the

bicontinuous cubic phase is unique among the cyanobiphenyl-based multipedes so far described in the literature.

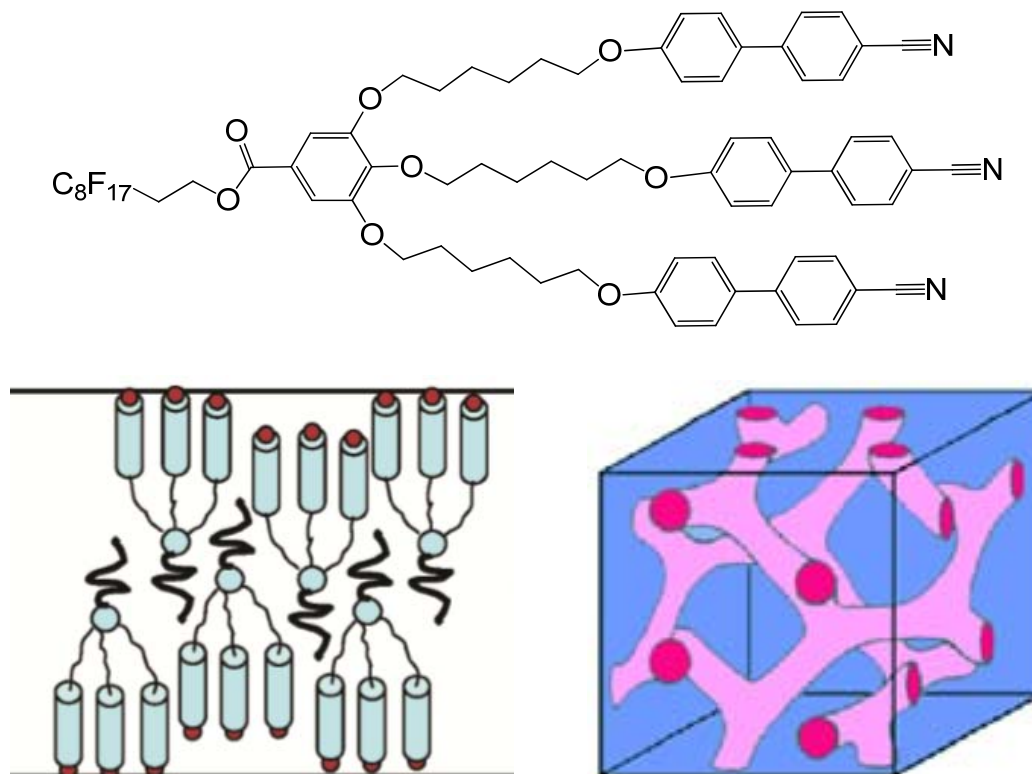


**Figure 1.40** Structure of the modulated layered SmA phase and the bicontinuous cubic phase formed by Janus LC (reproduced from Ref [32])

#### 1.4.4.2.2 Factors affecting the mesomorphic behavior

##### 1.4.4.2.2.1 Type of mesogenic units

Since Janus LCs are incorporated by at least two types of mesogenic units, there are various possibilities of the self-assembling of the molecules and many factors can have an effect on the mesophase behaviour. First of all are the mesogenic units, which usually have different abilities of inducing different mesophases. In general terms, all of the mesogenic units should retain their phase-inducing ability. As described for LC dendrimers, end-on attachment of the mesogenic units results in smectic and nematic behaviour whereas side-on attachment of the mesogenic units to the core suppresses the smectic behaviour and only nematic behaviour is observed

[30]. Similarly, in the Janus LC tetrapedes carrying both side-on and end-on mesogenic moieties, the smectic phase favored by the end-on mesogenic units was totally eliminated by the side-on mesogenic unit, which usually presents the nematic phase.

Since Janus LCs can be also regarded as supermolecular amphiphiles, the mesophase behaviour is also related to the incompatibility between the two types of mesogenic units, resulting in microphase segregation. High incompatibility usually can lead to a more stable LC phase with stronger positional order; whereas low incompatibility may produce only the nematic phase or a mesophase with reduced positional order. The size of the two types of mesogenic units may also affect the overall molecular shape of the Janus LCs, which ultimately defines the interface between molecular assemblies, and can thus result in different mesophase structure. With similar sized moieties on both sides, the Janus LCs tend to exhibit lamellar phases; whereas a huge difference in the size of the two halves usually generates columnar or cubic phases, which have interfaces with a high degree of curvature. These factors can be seen as amplifications of the microphase segregation in low molar mass mesogens, as described in section 1.4.2.

#### 1.4.4.2.2.2 Ratio of mesogenic units

The ratio between the two types of moieties also affects the formation of liquid-crystalline phases. The ratio can greatly influence the incompatibility and fraction between the two mesogenic halves: in the series of amphiphilic LCs possessing perfluorinated chains ( $R_F$ ) and cyanobiphenyl groups (CB) described by Yoshizawa [32], the compound with 1:1 of  $R_F$ /CB units exhibited only SmC phases, whereas 1:2 ratio generated the Col phase and the 1:3 ratio yielded a cubic phase. This is consistent with the effect of segregation induced by the fluorinated chain and the increased curvature induced by the presence of three cyanobiphenyl moieties.

The effect of the ratio of mesogenic units has also been investigated via the synthesis of Janus dendrimers that combine mesogenic bent-core and rod-like molecular segments [33]. A combination of bent-core mesogens and rod-like mesogens in a 1:2 ratio exhibits the nematic phase, whereas the codendrimer with a 1:1 ratio exhibited

well-defined SmCP phases, in which case the bent-core and rod-like mesogens are accommodated separately in different sub-layers (Fig 1.41). This difference in mesophase behaviour can be explained by the cross-sectional area of the rod-like and bent-core mesogenic units used and the balance achieved depending on the relative ratio of both mesogenic units.

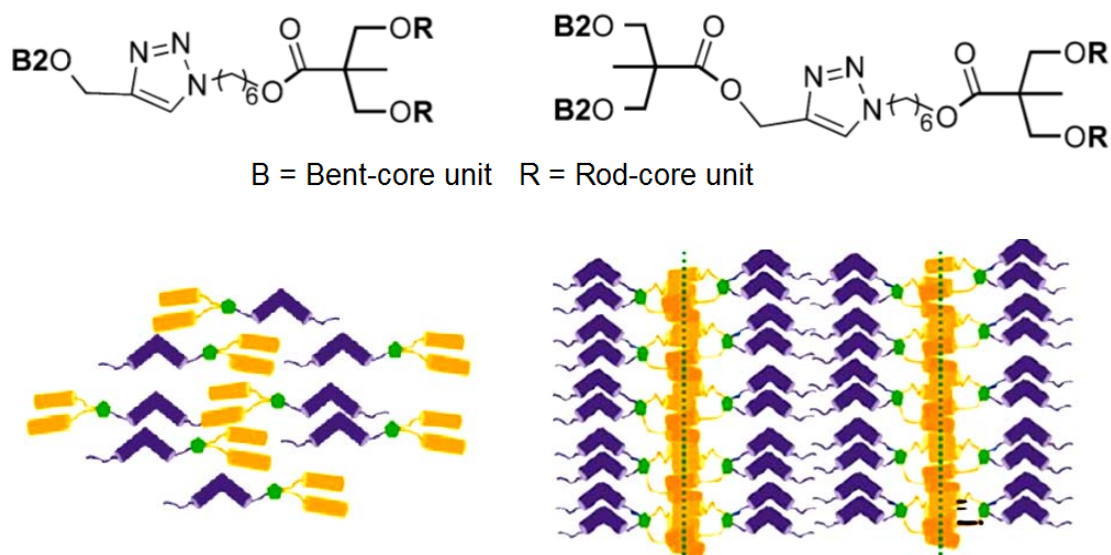


**Figure 1.41** LC behavior controlled by the ratio between two types of mesogenic moieties (reproduced from Ref [33])

#### 1.4.4.2.2.3 The core and the dendritic scaffold

The inner core and dendritic scaffold between the two types of moieties of the co-dendrimer can also affect the phase behaviour by controlling the overall topology of the supermolecule.

In the investigation of the mesomorphic properties of the typical Janus LC with both terminally and laterally attached mesogenic groups [30], the asymmetric dendritic scaffold plays an important role resulting in different phases being exhibited, whereas in both cases the number and type of mesogens are identical (Fig 1.42).

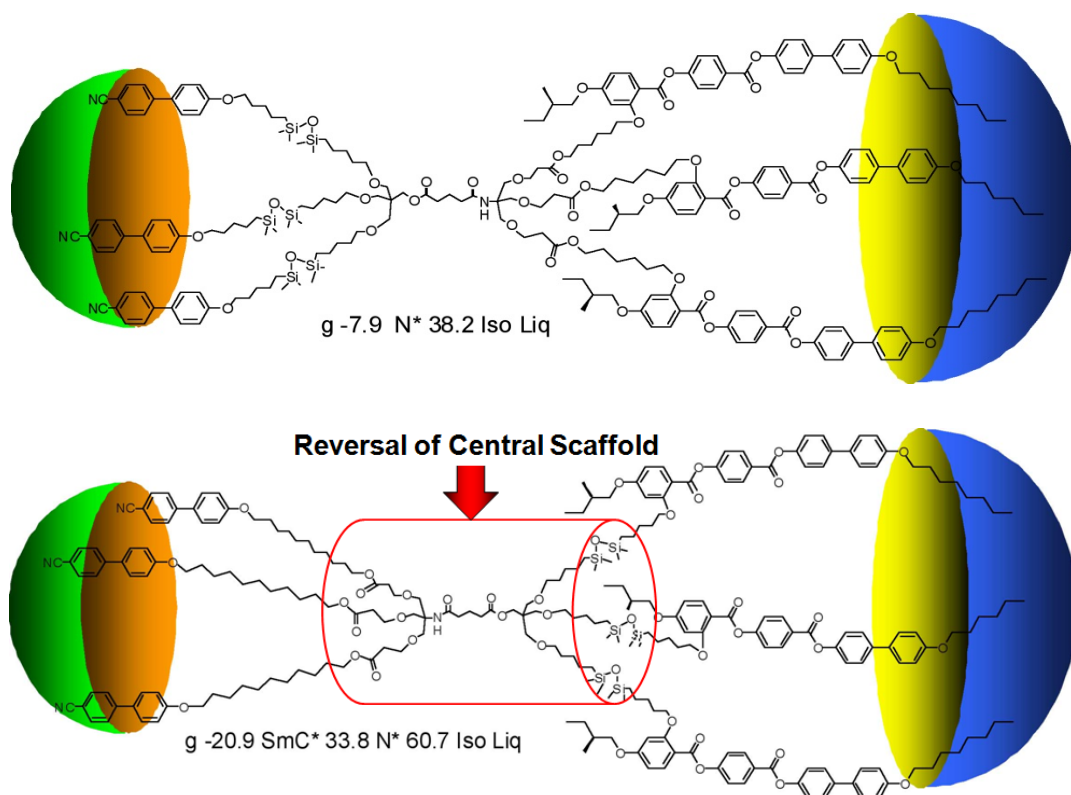


**Figure 1.42** Different LC behavior with the same mesogenic units affected by the asymmetric core (reproduced from Ref [3a])

The core can be crucial in the assembly of molecules if it contains microphase segregation features within their own chemical structures. Similar to the columnar stacking of disc-like dendrimers via core interactions (see section 1.3.2), the affinity between the cores of Janus dendrimers also allows the whole molecule to assemble in various forms. A Janus bisamide dendrimer which combined both the hydrophobic aliphatic chain and the hydrophilic triethyl glycol (TEG) chain exhibits the columnar phase despite not having peripheral mesogenic units or a disc-like shape of molecule [34]. Through the hydrogen bonds between the amide of the core units, four molecules can stack crosswise into a discs and further assemble into columns,

producing a stable columnar phase (Fig 1.43). This mechanism of assembly also applies to Janus LCs with mesogenic units on the periphery of the structure, in which an appropriately designed core unit may assist the self-assembly process along with the mesogenic moieties.

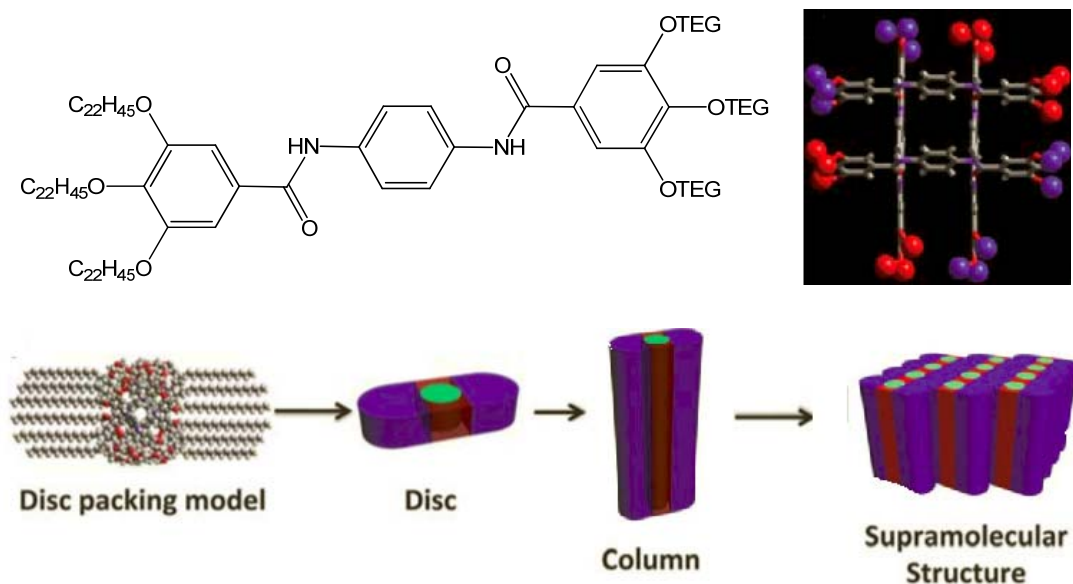
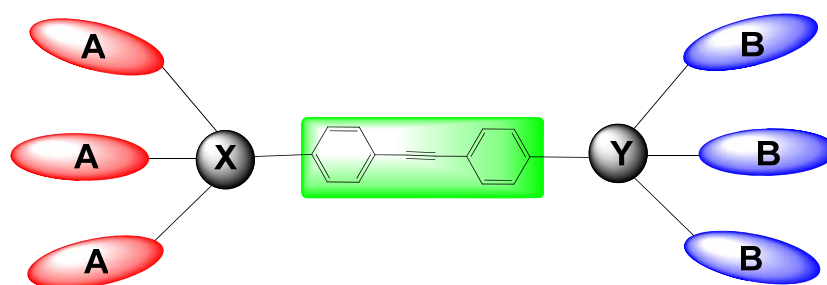


**Figure 1.43** Self-assembly via the core unit in Janus LC dendrimer (reproduced from Ref [34])

# **Chapter 2**

## **Aims**

In this research project, dendritic supermolecules with more than one type of LC at the periphery (“Janus” liquid crystals) are described, which combines the properties of both the supermolecular dendrimer and amphiphilic material. The design is based on diphenylacetylene as an extended rigid core to which dendritic branches carrying mesogenic units are appended (Fig 2.1). Both terminally attached (cyanobiphenyl derivatives, CB) and laterally attached mesogenic units (*p*-phenylene di(*p*-alkoxy)benzoate derivatives, PDAB) have been incorporated as peripheral groups in order to study their effect on LC behaviour of the system. Amphiphilic materials containing hydrocarbon/fluorocarbon chains and hydrocarbon/polyethylenoxy chains (PEG) as end-groups have also been investigated, in order to enhance microphase segregation in this family. Understanding the interactions between these two-faced molecules allows the properties of each face to be tailored in order to create new mesophase structures or phases with specific properties.

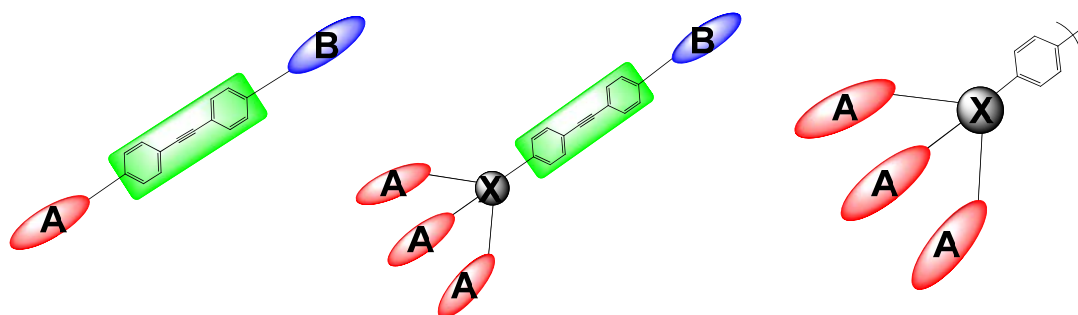


A,B = mesogenic unit or chain group    X,Y = dendritic linking unit

**Figure 2.1** Janus LCs with a diphenylacetylene core

A series of LC oligomers with only one group on each side (Fig 2.2 left), or one group on a side and three on another (Fig 2.2 middle) will be developed as comparisons for the functionalized Janus LCs which have three identical periphery groups on each side of rigid core described above. These LC multipedes with three identical mesogenic units combined by a linking unit (Fig 2.2 right) are also of great value as reference for understanding the behaviour of Janus LCs. These materials are aimed to be investigated, as they are intermediates in the synthesis of the Janus LCs. The relationship between the structure and the mesomorphic behaviour of the

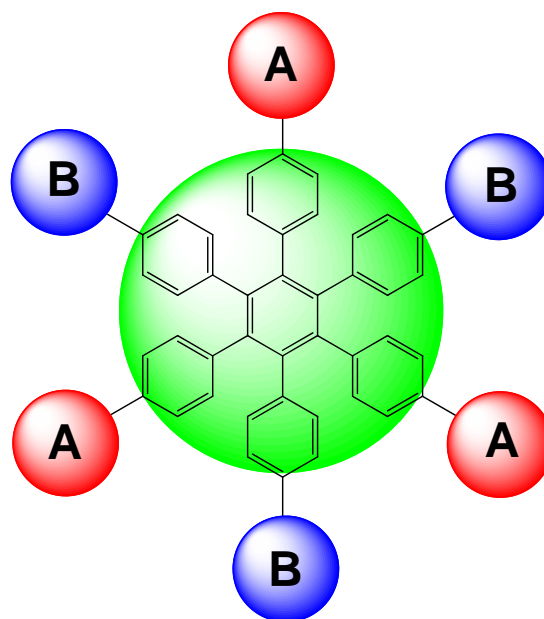
materials will be determined and comparisons with the relevant precursors and derivatives thereof will be established.



A,B = mesogenic unit or chain group    X = dendritic linking unit

**Figure 2.2** 1:1 (left) and 1:3 (middle) type of LC oligomers and the LC multipedes (right)

The diphenylacetylene core can be manipulated synthetically by oligomerisation reactions. The [2+2+2] cycloaddition reaction of the diphenylacetylene core of the oligomers and Janus LCs prepared will be studied, in order to synthesise higher supermolecular LC systems that contain the hexaphenylbenzene core (Fig. 2.3). This type of macromolecule has a nearly planar core section and mesogenic units attached along its periphery. The mesomorphic behaviour of these supermolecular compounds will be studied in terms of the density of mesogenic units around the core and the topology of the attachment of the mesogenic units. The properties of this group of materials will be compared with those of their parent systems and their behaviour examined and compared with the relevant structurally related materials described in the literature. Along with the disc-like core unit which has strong shape incompatibility with the rod-like mesogenic units, the self-recognition process of the HPB LC system may lead to unique mesomorphic properties which are valuable in the study of supermolecular LCs.



A, B = mesogenic unit or mesogenic units with a dendritic linkage, chain group

**Figure 2.3** Hexaphenylbenzene (HPB) supermolecular LCs

# **Chapter 3**

## **Mesogenic Monomers**

### 3.1 Summary

In order to generate the supermolecular liquid crystal systems described in subsequent chapters, both terminally attached and laterally attached mesogenic moieties are required. Cyanobiphenyl derivatives have been chosen as the terminally attached moieties since extensive structure-properties correlations are described and their mesogenic behaviour is well understood. Furthermore, they have been used previously in a number of supermolecular LCs and LC dendrimers, so meaningful comparisons can be established [30].

As for the side-on mesogenic units, side-chain functionalized *p*-phenylene di(*p*-alkoxy)benzoate (PDAB) derivatives (Fig 3.1) were chosen, with the aim of inducing the nematic phase, because this core has been used successfully by Keller [35] in the synthesis of mesogenic LC acrylate and methacrylate polymers that exhibit broad nematic mesophases.

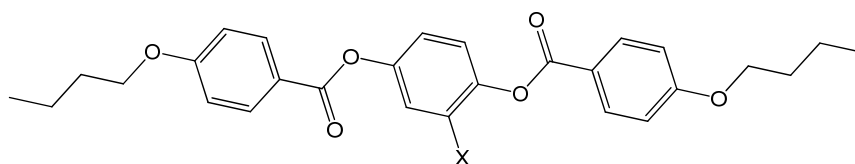


**Figure 3.1** Laterally substituted 2,5-di(alkoxybenzoyloxy)benzoate

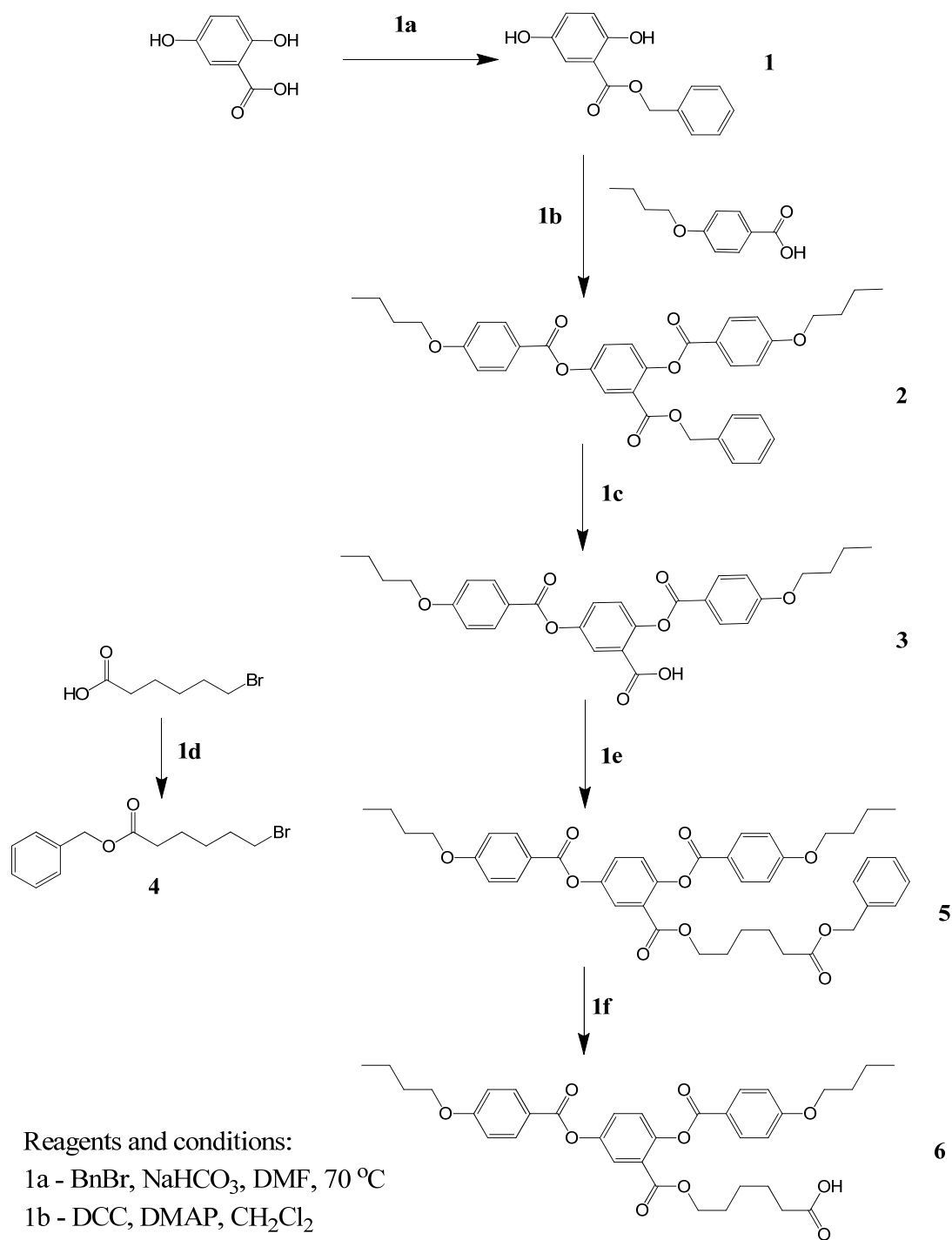
To attach the side-on three-ring monomeric mesogens to the dendritic core, alkyl chain spacers with various lengths were used in order to decouple the motions of the mesogens from those of the dendritic scaffold in order to establish the necessary interactions to produce mesomorphic behaviour. In the synthesis of the 3-rings side-on mesogens, the end of the spacer was decorated with several types of functional groups which allow the mesogenic groups to adapt all kinds of central scaffolds.

This chapter describes a series of functionalized *p*-phenylene di(*p*-alkoxy)benzoate derivatives as the laterally attached mesogens for the later program, and their mesophase properties will be studied separately to learn the effect of the spacer length and end group on the LC behaviour. Different functional groups placed at the

end of the side alkyl spacer were incorporated in order to accomplish their covalent attachment to the dendritic scaffold through a variety of reactions. However, an exhaustive study of structure-properties based on different spacer lengths is outside the scope of this project, therefore only representative examples of each terminal functional group were prepared.

### 3.2 Synthesis

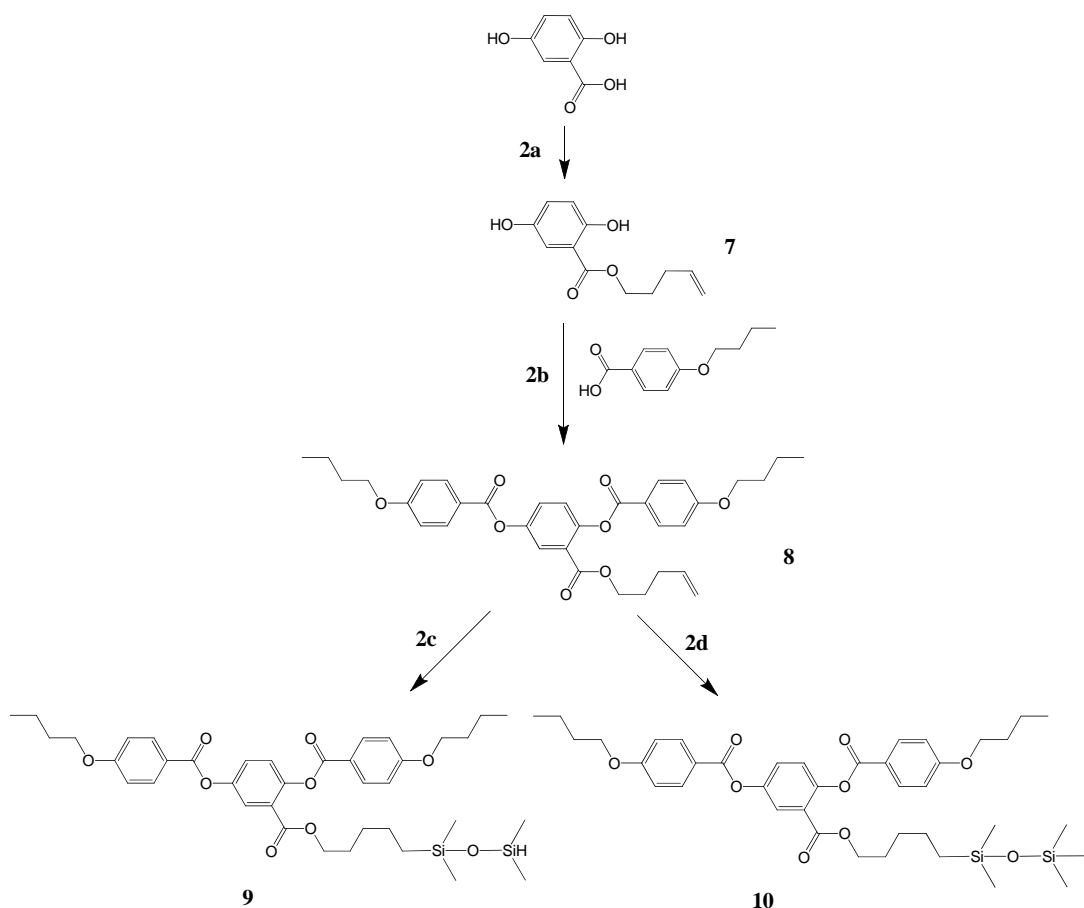
The general strategy for the synthesis of the PDAB mesogens is shown in Scheme 1. It starts with 2,5-dihydroxybenzoic acid. The esterification of the phenolic groups without affecting the carboxylic acid group requires the protection of the acid with a benzyl protecting group [36]. After protection, esterification and deprotection steps, the benzoic acid derivative **3** is obtained, which is a common precursor for a number of derivatives. Several functionalized alkyl chains can be directly attached as spacers via esterification of **3**, either DCC-mediated or by weak base  $\text{NaHCO}_3$  (in order to avoid the hydrolysis of the benzoate esters already present in the molecule). However, this method was not universally adopted because in some cases the esterification reactions do not proceed with high yields. The synthesis of the carboxylic acid derivative **6** is shown in Scheme 1, which required the protection/deprotection sequence to install the terminal carboxylic acid group at the end of the spacer [37].



Reagents and conditions:  
 1a - BnBr, NaHCO<sub>3</sub>, DMF, 70 °C  
 1b - DCC, DMAP, CH<sub>2</sub>Cl<sub>2</sub>  
 1c - Pd/C, H<sub>2</sub>, THF  
 1d - BnOH, DCC, DMAP, CH<sub>2</sub>Cl<sub>2</sub>  
 1e - **4**, NaHCO<sub>3</sub>, DMF, 70 °C  
 1f - Pd/C, H<sub>2</sub>, THF

**Scheme 1**

The synthesis of the alkene derivative **8** is shown in Scheme 2. The sequence shown was used since it is easier to install the olefinic side chain at the beginning of the synthesis rather than on the intermediate **3** [35]. Compound **8** is a very useful mesogen in this study since it can be anchored on the scaffold by Pt-catalysed hydrosilylation reaction. Compound **10** was converted to the hydridosilane **9** by hydrosilylation of **8** with an excess of tetramethyldisiloxane catalysed by Karstedt's catalyst, to allow carrying out the hydrosilylation reaction of an alkene-functionalised scaffold. In order to make meaningful comparisons, the pentamethyldisiloxane derivative **10** was also synthesised by a similar method.



Reagents and conditions:

**2a** - 5-Bromo-1-pentene, NaHCO<sub>3</sub>, DMF, 70 °C

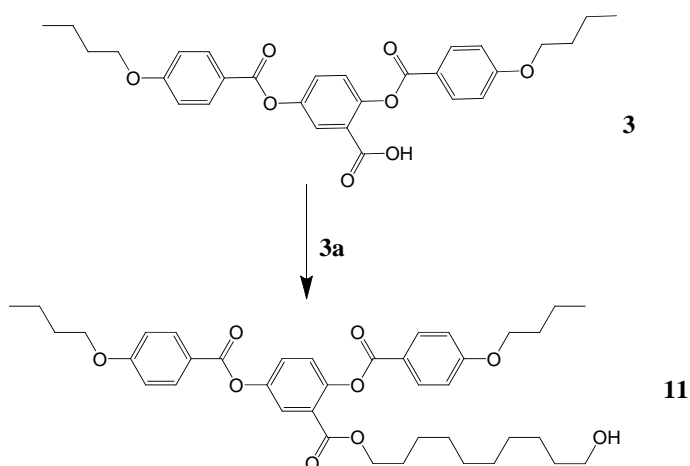
**2b** - DCC, DMAP, CH<sub>2</sub>Cl<sub>2</sub>

**2c** - 1,1,3,3-Tetramethyldisiloxane, Karstedt's catalyst, Toluene

**2d** - Pentamethyldisiloxane, Karstedt's catalyst, Toluene

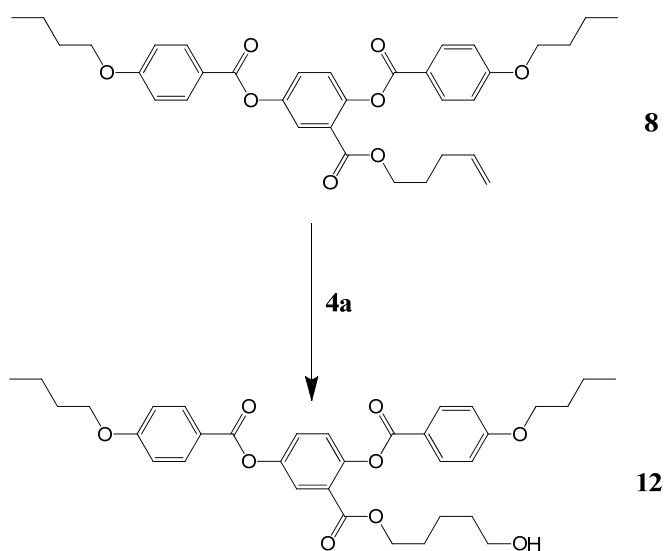
**Scheme 2**

A very useful family of  $\omega$ -hydroxylalkyl mesogens of different alkyl lengths, monomers **11**, **12** and **16**, were also synthesised. Different routes were used depending on the ease of purification and the yield obtained. They involved the monoesterification with a diol (**11**, Scheme 3), BBN hydroboration of the terminal alkene of **8** and following oxidation of the borane (**12**, Scheme 4) and substitution with a THP-protected bromoalcohol followed by deprotection (**16**, Scheme 5).



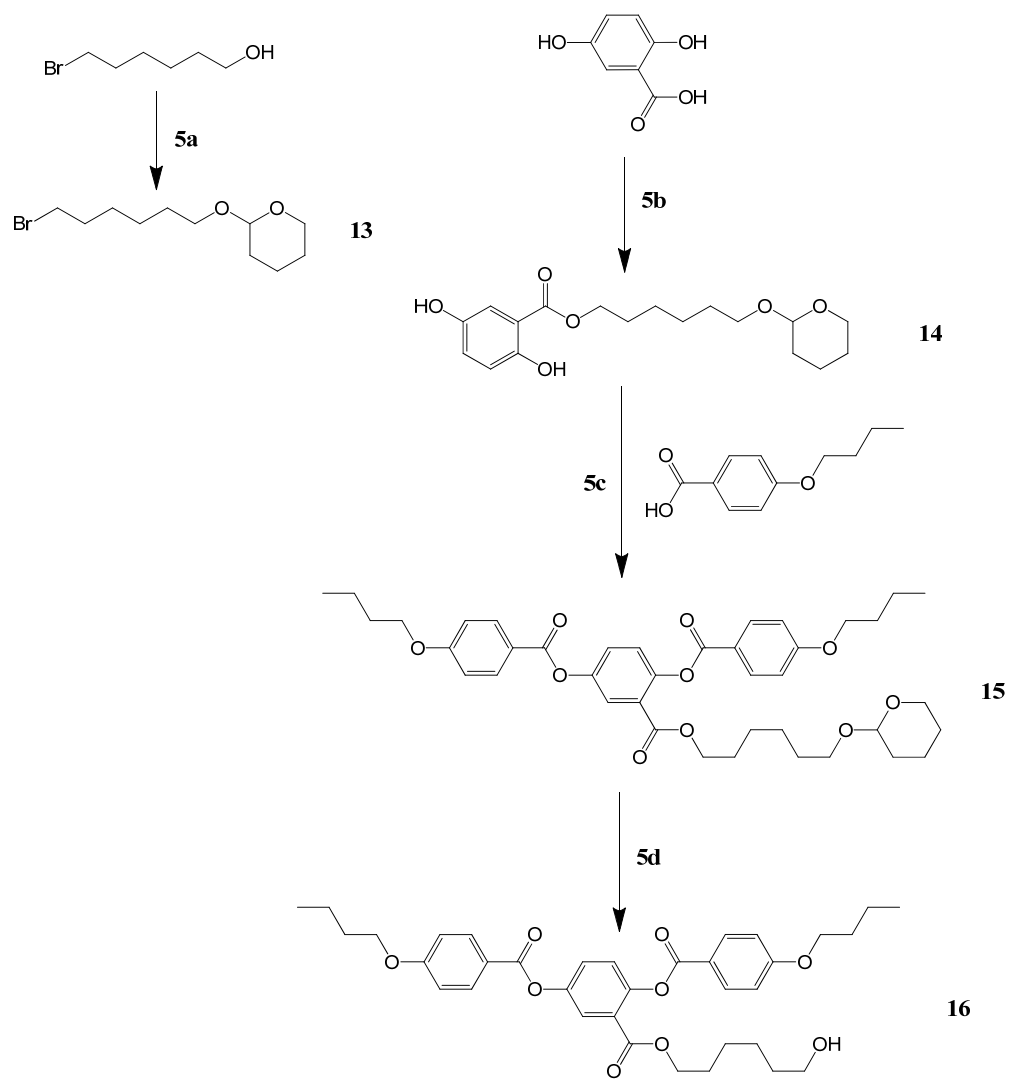
Reagents and conditions:  
3a - 1,10-Decandiol, EDAC, DMAP, CH<sub>2</sub>Cl<sub>2</sub>

**Scheme 3**



Reagents and conditions:  
4a - (i) 9-BBN, THF (ii) MCPBA

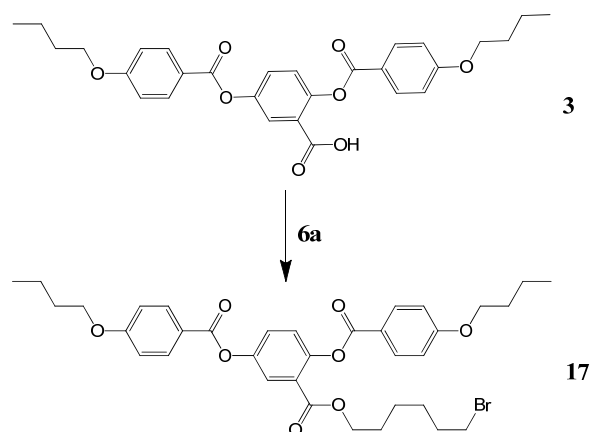
**Scheme 4**



Reagents and conditions:  
 5a - DHP, PTSA,  $\text{CH}_2\text{Cl}_2$   
 5b - **13**,  $\text{NaHCO}_3$ , DMF,  $70^\circ\text{C}$   
 5c - DCC, DMAP,  $\text{CH}_2\text{Cl}_2$   
 5d - PTSA, MeOH

**Scheme 5**

By a direct esterification of **3** with bromo alcohol, the monomer **17** with a terminally brominated chain was obtained (Scheme 6).



Reagents and conditions:  
 6a - 6-Bromo-1-hexanol, DCC, DMAP, CH<sub>2</sub>Cl<sub>2</sub>

**Scheme 6**

The <sup>1</sup>H NMR spectra of this series of materials show five sets of peaks in the aromatic region with integration of 4:1:1:1:4 corresponding to the three ring system, two sets of peaks for the two side phenyl rings and three for the protons labelled a, b, c of the middle ring (Fig 3.2). Since all the monomers have very similar structures, their <sup>1</sup>H NMR showed differences only in the chemical shift of the protons of the side chains due to the different terminal functional groups, as well as the integration of the proton on the methylene spacers between δ1.2~δ1.6 which indicated the length of the alkyl spacer. The monomers were also identified by <sup>13</sup>C NMR and ESI MS to confirm their molar mass, and elemental analysis.

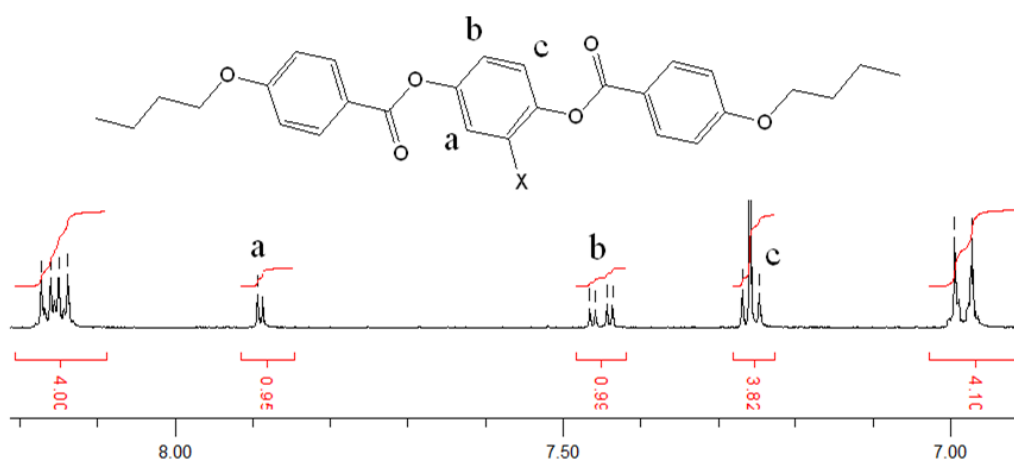


**Figure 3.2** Typical <sup>1</sup>H NMR spectrum of the aromatic region, showing the central aromatic ring



that of the first heating cycle instead of the second or third as the real melting point can be identified only from the former one.

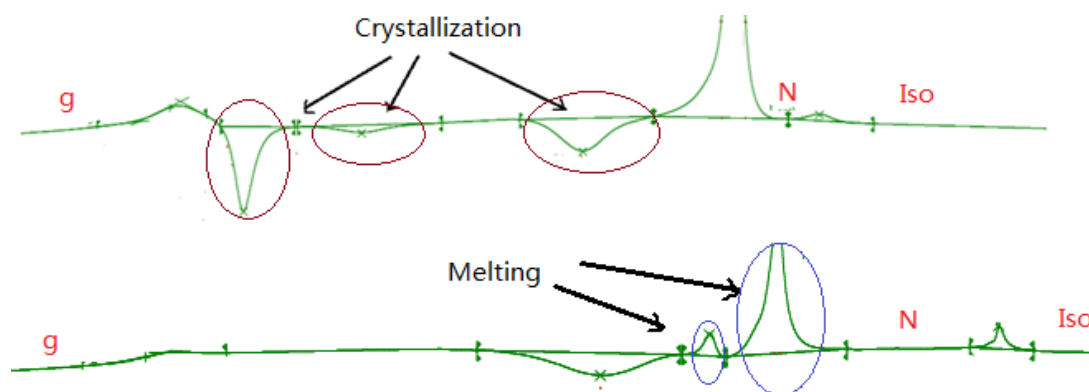
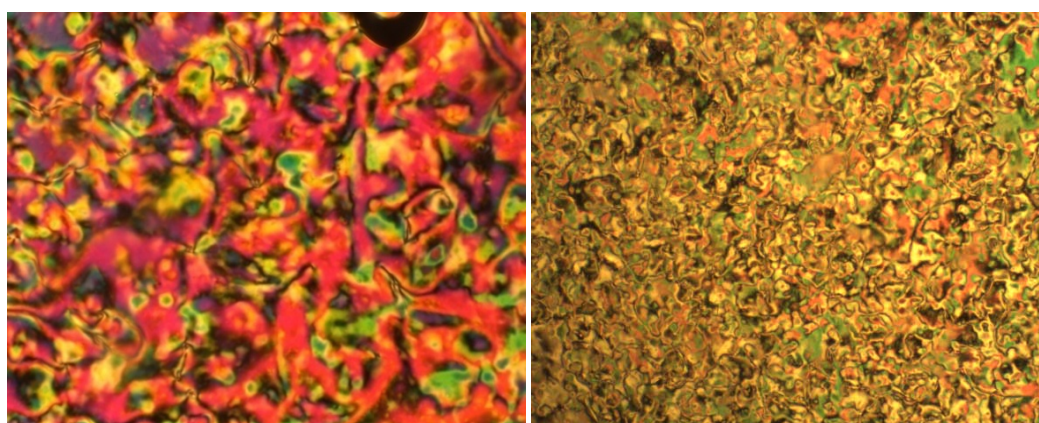


**Figure 3.3** Stepwise crystallization and melting of the PDAB monomeric mesogen **17** (top) and **11** (bottom) observed by DSC

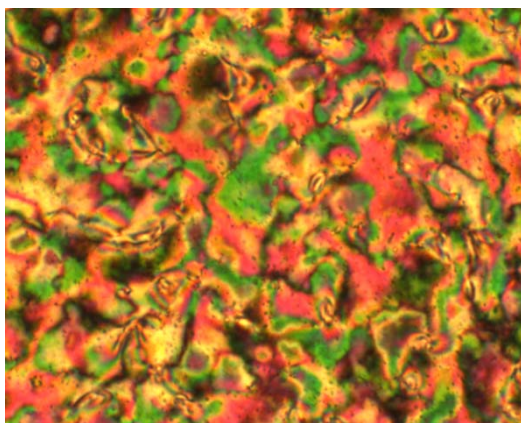
All of the materials exhibit a schlieren texture for the mesophase, which can be easily sheared, with 2- and 4-brush defects, indicating the presence of  $m = \pm 1/2$  and  $m = \pm 1$  disclinations, which confirms the presence of the nematic phase (plate 1a and 1b). Thin preparations display relatively low viscosity (qualitative observation) on shearing the samples.



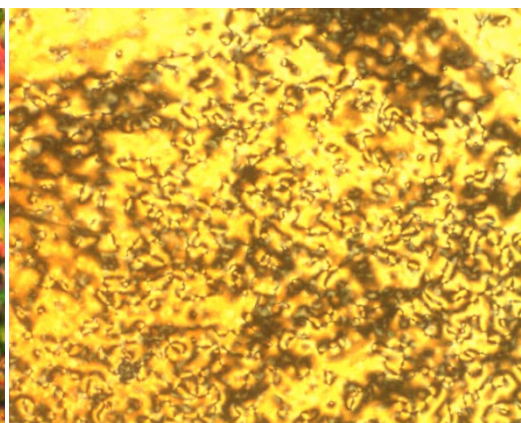
(a)

(b)

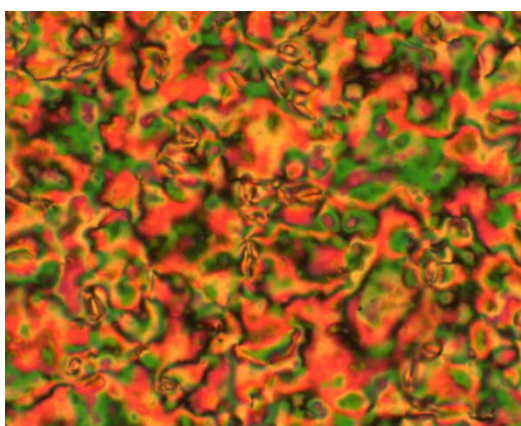
**Plate 1a** The textures of the nematic phase of (a) **6**, 121 °C; (b) **8**, 105 °C (x200)



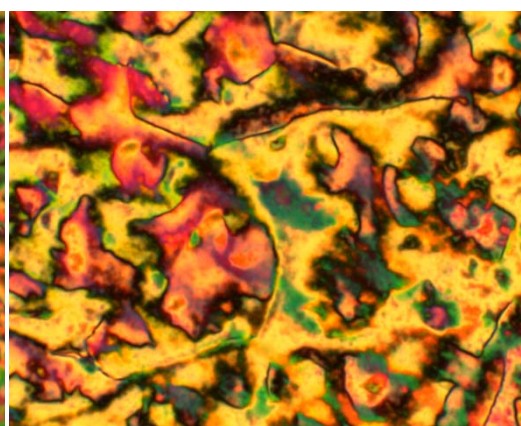
(c)



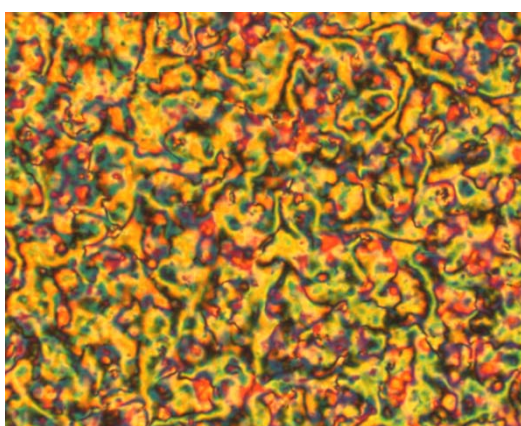
(d)



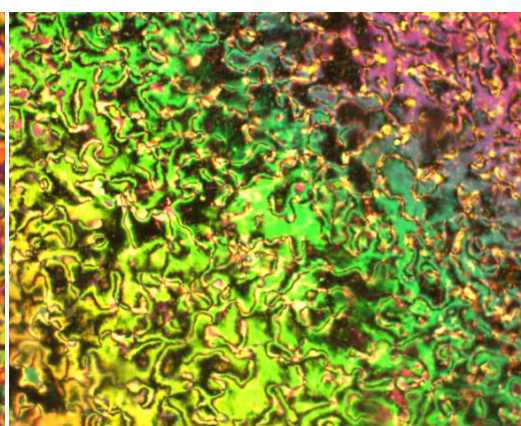
(e)



(f)



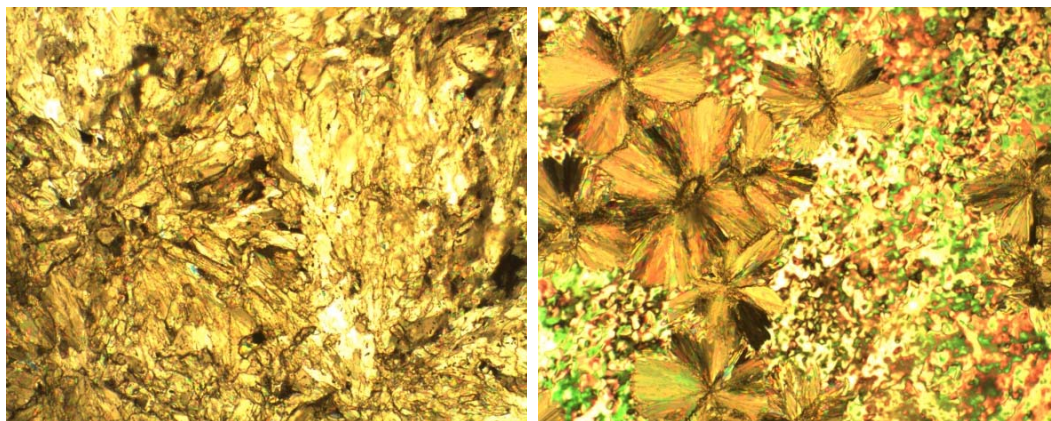
(g)



(h)

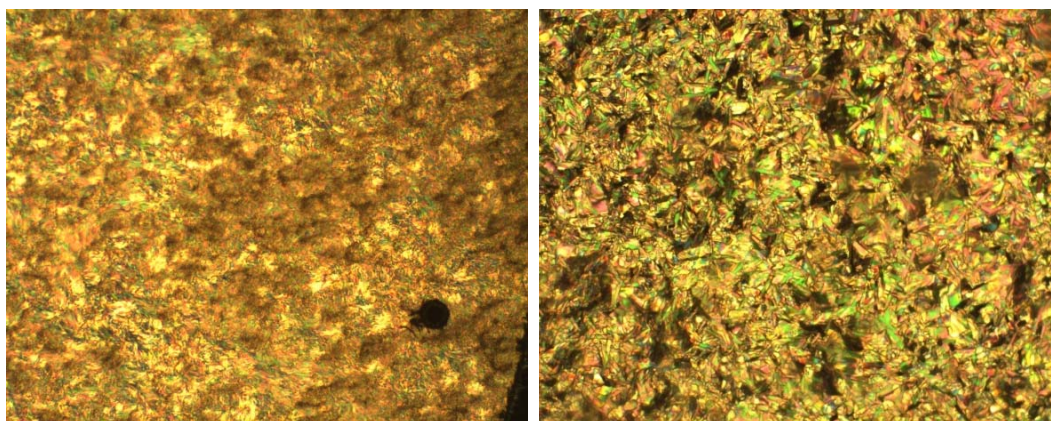
**Plate 1b** The textures of the nematic phase of (c) **9**, 42 °C; (d) **10**, 50°C; (e) **11**, 87.5 °C; (f) **12**, 102 °C; (g) **16**, 99 °C; (h) **17**, 80 °C (x200)

Upon the second and third heating cycles, several of the compounds exhibit partial crystallization from glass state. In these mixed states, the coexistence of crystal state and nematic phase can be observed by POM (Plate 2), as indicated from their DSC traces.



(a)

(b)



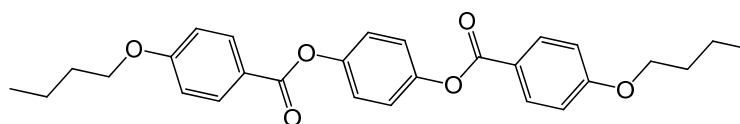
(c)

(d)

**Plate 2** The N-Cr transitions during heating observed in (a) **8**, 80 °C; (b) **11**, 60 °C; (c) **12**, 70 °C; (d) **17**, 68 °C (x200)

### 3.4 Discussion

All of the side-chain functionalised derivatives exhibit the nematic phase, either enantiotropically or monotropically (Table 1). In the preferred molecular conformation, the side chain lies parallel to the aromatic core which maintains the overall rod-like shape of the mesogens; however the broadened molecular breadth in comparison with the unsubstituted analogues reduces the anisotropy of the molecule, which results in a reduction of the liquid crystal phase stability and mesophase range. Comparison of the melting points, clearing points and mesomorphic ranges of the materials described here with those of the unsubstituted nematogen (Fig 3.4) shows that they are greatly reduced by the presence of the side chain, irrespective of the nature of the end group.



Cr 153 N 256 Iso

**Figure 3.4** Original 3-ring PDAB mesogen

Compound **6** exhibits a monotropic nematic phase at high temperature with a narrow mesophase range (plate 1a). The carboxylic acid group in compound **6** induces more polarity to the system than the other functional groups, which results in the relatively higher nematic phase stability and the melting point; however, the carboxylic acid may easily form hydrogen bonding pairing between two molecules to produce mesogenic dimers, which causes the broadening of the average molecular width, resulting in a limited nematic phase range (Fig 3.5).

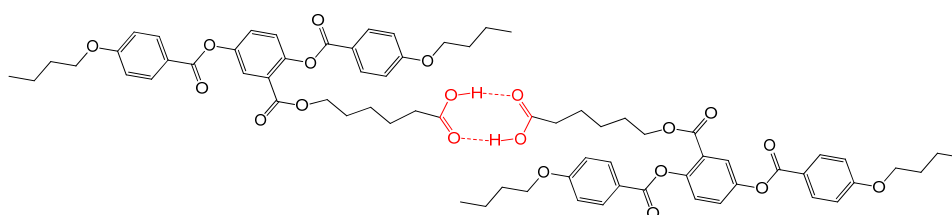


**Figure 3.5** Mesogenic dimer forms via hydrogen bond

Except for the ones decorated with disiloxane groups, this type of mesogen (**8**, **11**, **12**, **16** and **17**) exhibit very similar thermal behaviours. They have melting points and nematic phase stability in interval between 75~110 °C. Compound **11**, **12** and **16** have the hydroxyl terminal group with different spacer lengths. The melting point and the N-I transition temperature decreased with increasing length of the alkyl spacer as expected. Closer comparison of **12** (pentamethylene chain) and **16** (hexamethylene chain) shows a small odd-even effect to be present. The melting point and the nematic phase stability of these three derivatives are higher than most of the other derivatives for the same spacer length, which is expected due to the presence of additional H-bonding between the OH groups.

Compound **8** has an alkene end group which enhances polarisability, producing a nematic phase over a range of 20 degrees, which is the widest of the family. The mesogens **9** and **10** with disiloxane groups behave differently from the others. They exhibit monotropic nematic phases, both have low melting points and nematic phase stabilities, and also strong tendency for crystallization upon cooling. The bulky substituted disiloxane group precludes the effective packing of the side chain, making the molecules much broader which weakens the tendency to form nematic phases.

The overall mesomorphic behaviour of the PDAB monomers is perfectly consistent with that observed for other similarly functionalised mesogens. Saez and Goodby have reported a series of laterally functionalized mesogens (Fig 3.6) [14, 30]. The trends observed in the series described here parallel those observed in the four-ring side substituted mesogens. Especially the trend with respect to the N-I transition temperatures. Similar trends have been observed in the smectic C promoting difluoroterphenyl derivatives described by Goodby and Sia [38]. This may prove that different side-on functional groups have similar effects on the LC behaviour, regardless of the rigid mesogenic core they decorate.

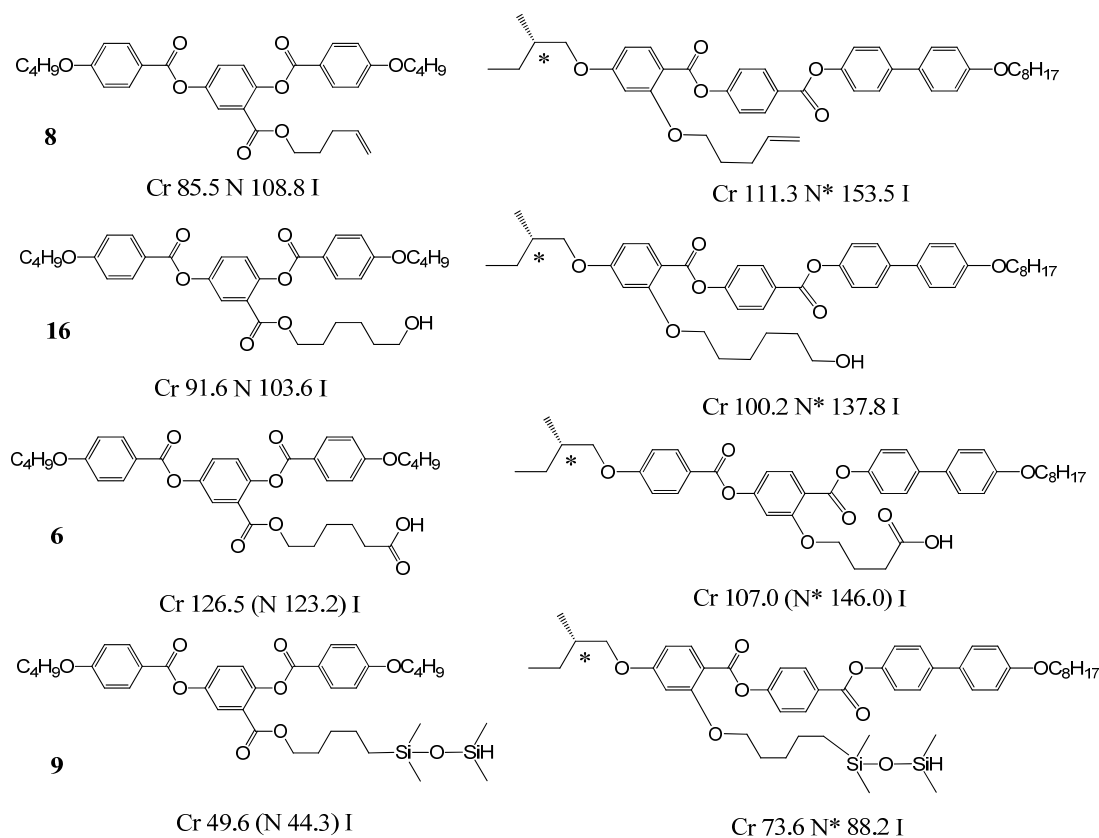


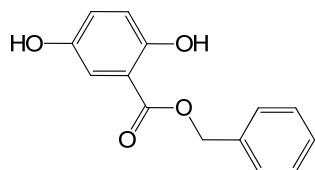
**Figure 3.6** Comparison of the effect of the side-on attached groups on the mesophase behaviour

### 3.5 Concluding remarks

A series of side-chain functionalized *p*-phenylene di(*p*-alkoxy)benzoate mesogens were synthesized and their liquid crystal behaviours were studied. All of the mesogenic monomers exhibit the nematic phase, as the original PDAB derivative without any side chain, though the range, the nematic phase stability and also the melting point is greatly lowered relative to the broadened molecular width and the reduced anisotropy. The specific mesophase behaviour of the PDAB mesogens is influenced by the terminal functional groups of the side chain, according to the polarity, polarisability and size of the functional groups. The length of the aliphatic spacers also plays a role in the LC behavior by providing flexibility to the system. The effect of the side-on PDAB mesogenic unit in the liquid crystal material in higher supermolecular structure will be discussed in later chapters.

### 3.6 Experimental

#### Benzyl 2,5-dihydroxybenzoate (**1**)

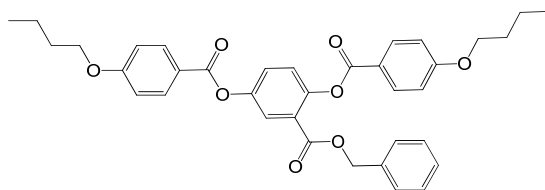


Solid  $\text{NaHCO}_3$  (17.6 g; 210 mmol) was added to a solution of 2,5-dihydroxybenzoic acid (10.8 g; 70 mmol) in dimethylformamide (105 mL). The mixture was heated and stirred at 70 °C for 1 h. Benzyl bromide (8.32 mL; 70 mmol) was added, and the reaction was stirred for 20 h at 70 °C. The mixture was cooled down, diluted with water (300 mL) and extracted with 1:1 ethyl acetate/hexane (150 mL). The organic phase was separated, washed twice with water (150 mL), dried over  $\text{MgSO}_4$  and the solvent removed by evaporation under reduced pressure. The crude product was subjected to column chromatography over silica gel eluting with diethyl ether. The solvent was removed by evaporation under reduced pressure to yield **1** as white crystals.

Yield: 11.0 g (65%)

$^1\text{H}$  NMR (400 MHz,  $\text{CDCl}_3$ )  $\delta\text{H}$  (ppm): 10.32 (s, 2 H, -OH); 7.41 (m, 5 H, ArH); 7.32 (d (J = 3.2 Hz), 1 H, ArHc); 7.01 (d (J = 8.9 Hz) d (J = 3.1 Hz), 1 H, ArHb); 6.89 (d (J = 8.9 Hz), 1 H, ArHa); 5.37 (s, 2 H, -COOCH<sub>2</sub>-)

#### Benzyl 2,5-di(4-butoxybenzoyloxy)benzoate (**2**)



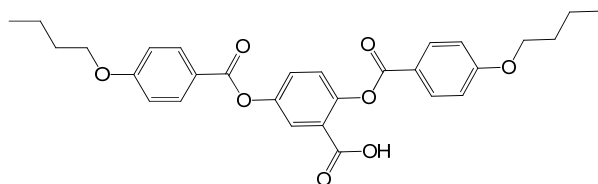
A solution of benzyl 2,5-dihydroxybenzoate (**1**) (11.0 g; 45.2 mmol), 4-butoxybenzoic acid (18.4 g; 94.8 mmol),  $N,N'$ -dicyclohexylcarbodiimide (22.4 g; 108 mmol), 4-(dimethylamino)pyridine (11.4 g; 45.2 mmol) in dichloromethane (500 mL) was stirred at room temperature for 20 h under atmosphere of argon. The

mixture was filtered and the filtrate was washed with water (300 mL), 5% AcOH solution (300 mL), and water (300 mL), and dried over MgSO<sub>4</sub>. After evaporation of the solvent, the crude product was recrystallised from ethanol to yield **2** as a white solid.

Yield: 21.1 g (78%)

<sup>1</sup>H NMR (400 MHz, CDCl<sub>3</sub>) δH (ppm): 8.13 (d (J = 8.9 Hz), 2 H, ArH); 8.07 (d (J = 8.9 Hz), 2 H, ArH); 7.90 (d (J = 2.9 Hz), 1 H, ArHc); 7.46 (d (J = 8.7 Hz) d (J = 2.9 Hz), 1 H, ArHb); 7.26 (d (J = 8.7 Hz), 1 H, ArHa); 7.24 (s, 5 H, ArH); 6.97 (d (J = 8.9 Hz), 2 H, ArH); 6.91 (d (J = 8.9 Hz), 2 H, ArH); 5.19 (s, 2 H, -COOCH<sub>2</sub>-); 4.06 (t (J = 6.5 Hz), 4 H, -C<sub>6</sub>H<sub>4</sub>OCH<sub>2</sub>-); 1.82 (m, 4 H, -C<sub>6</sub>H<sub>4</sub>OCH<sub>2</sub>CH<sub>2</sub>-); 1.50 (m, 4 H, -CH<sub>2</sub>CH<sub>3</sub>); 1.00 (t (J = 7.3 Hz) d (J = 4.6 Hz), 6 H, -CH<sub>3</sub>)

### 2,5-Di(4-butoxybenzoyloxy)benzoic acid (**3**)



Benzyl 2,5-di(4'-butoxybenzoyloxy)benzoate (**2**) (11.6 g; 19.6 mmol) was dissolved in tetrahydrofuran (100 mL) and palladium on carbon (Pd/C, 30 mg) was added. Hydrogen gas was allowed to bubble in the stirred suspension and the reaction stirred for 20 h at room temperature. The reaction was monitored by TLC for completion. The mixture was filtered through a celite pad, the solvent was removed by evaporation under reduced pressure and the crude was recrystallised from ethanol. The white crystalline solid product **3** was collected and dried in air.

Yield: 9.9 g (99.7%)

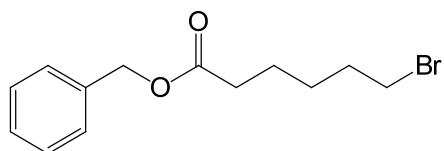
<sup>1</sup>H NMR (400 MHz, CDCl<sub>3</sub>) δH (ppm): 8.14 (d (J = 8.9 Hz), 4 H, ArH); 7.94 (d (J = 2.9 Hz), 1 H, ArHc); 7.51 (d (J = 8.7 Hz) d (J = 2.9 Hz), 1 H, ArHb); 7.30 (d (J = 8.8 Hz), 1 H, ArHa); 6.97 (d (J = 8.9 Hz) d (J = 6.3 Hz), 4 H, ArH); 4.06 (t (J = 6.5 Hz) d (J = 2.8 Hz), 4 H, -C<sub>6</sub>H<sub>4</sub>OCH<sub>2</sub>-), 1.81 (m, 4 H, -C<sub>6</sub>H<sub>4</sub>OCH<sub>2</sub>CH<sub>2</sub>-); 1.52 (m, 4 H, -CH<sub>2</sub>CH<sub>3</sub>); 1.00 (t (J = 7.4 Hz) d (J = 2.5 Hz), 6 H, -CH<sub>3</sub>)

$^{13}\text{C}$  NMR (100.4 MHz,  $\text{CDCl}_3$ )  $\delta\text{C}$  (ppm): 168.1, 165.0, 164.6, 163.9, 163.7, 153.9, 148.8, 148.4, 132.5, 128.1, 125.6, 125.3, 123.6, 121.4, 121.0, 114.4, 68.10, 31.22, 19.27, 13.92

ESI MS:  $m/z = 529.2$  ( $\text{M} + \text{Na}$ ) $^+$

IR ( $\text{cm}^{-1}$ ): 2955, 2932, 2870, 1728, 1690, 1597, 1581, 1512, 1450, 1419, 1250, 1165, 1126, 1065, 1011, 964, 887, 840, 756, 686, 648, 556, 509

#### **Benzyl 6-bromohexanoate (4)**

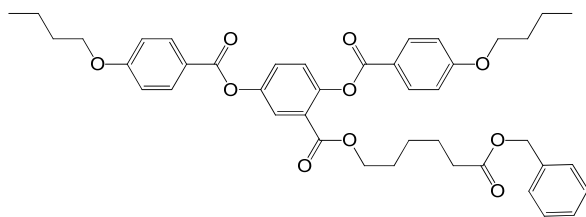


Dicyclohexylcarbodiimide (11.6 g; 56.4 mmol) dissolved in dichloromethane was slowly added to a solution, cooled at 0 °C, of 6-bromohexanoic acid (10 g; 51.3 mmol), benzyl alcohol (5.84 mL; 56.4 mmol) and 4-(dimethylamino)pyridine (0.3 g; 2.46 mmol) in dichloromethane (100 mL). The reaction mixture was stirred at 0 °C for 10 min, and then at room temperature for 20 h. The mixture was filtered, and the filtrate was washed with 1 M  $\text{NaHCO}_3$ , 1 M HCl, water, and dried over  $\text{Na}_2\text{SO}_4$ . The solvent was removed by evaporation under reduced pressure and the oil-like crude was filtered through a short pad of silica gel to yield the pure product **4** as a colorless oil.

Yield: 8.06 g (55%)

$^1\text{H}$  NMR (400 MHz,  $\text{CDCl}_3$ )  $\delta\text{H}$  (ppm): 7.35 (m, 5 H,  $\text{ArH}$ ); 5.11 (s, 2 H,  $\text{C}_6\text{H}_5\text{CH}_2$ -); 3.38 (t ( $J = 6.7$  Hz), 2 H,  $-\text{CH}_2\text{Br}$ ); 2.37 (t ( $J = 7.4$  Hz), 2 H,  $-\text{CH}_2\text{COO}-$ ); 1.85 (m, 2 H,  $-\text{CH}_2\text{CH}_2\text{Br}$ ); 1.46 (m, 2 H,  $-\text{CH}_2\text{CH}_2\text{COO}$ ); 1.67 (m, 2 H,  $-\text{CH}_2\text{CH}_2\text{CH}_2\text{Br}$ )

### Benzyl 6-(2,5-di(4-butoxybenzoyloxy)benzoyloxy)hexanoate (5)

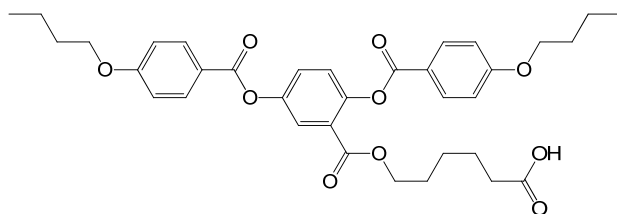


Solid  $\text{NaHCO}_3$  (1.74 g; 20.7 mmol) was added to a stirred solution of **3** (3.5 g; 6.9 mmol) in dimethylformamide (30 mL). The mixture was stirred at 70 °C for 1 h before benzyl 6-bromohexanoate (**4**) (2 g; 6.9 mmol) was added and the mixture was heated at 70 °C for 20 h. The reaction mixture was cooled down, diluted with water (100 mL), and extracted twice with 1:1 ethyl acetate/hexane (60 mL). The organic phase was washed twice with water (100 mL) and dried over  $\text{MgSO}_4$ . After evaporation of the solvents, the crude was recrystallised from dichloromethane/ethanol to yield **7** as a white solid.

Yield: 1.74 g (36%)

$^1\text{H}$  NMR (400 MHz,  $\text{CDCl}_3$ )  $\delta\text{H}$  (ppm): 8.15 (d (J = 8.8 Hz) d (J = 3.1 Hz), 4 H, *ArH*); 7.88 (d (J = 2.9 Hz), 1 H, *ArH*); 7.45 (d (J = 8.8 Hz) d (J = 2.9 Hz), 1 H, *ArH*); 7.34 (m, 5 H, *ArH*); 7.26 (d (J = 8.6 Hz), 1 H, *ArH*); 6.97 (d (J = 8.9 Hz) d (J = 3.3 Hz), 4 H, *ArH*); 5.08 (s, 2 H,  $-\text{COOCH}_2\text{C}_6\text{H}_5$ ); 4.14 (t (J = 6.6 Hz), 2 H,  $-\text{COOCH}_2\text{CH}_2-$ ); 4.05 (m, 4 H,  $-\text{C}_6\text{H}_4\text{OCH}_2-$ ); 2.27 (t (J = 7.5 Hz), 2 H,  $-\text{CH}_2\text{COOCH}_2\text{C}_6\text{H}_5$ ); 1.81 (m, 4 H,  $-\text{C}_6\text{H}_4\text{OCH}_2\text{CH}_2-$ ); 1.50 (m, 6 H,  $-\text{C}_6\text{H}_4\text{OCH}_2\text{CH}_2\text{CH}_2-$ ,  $-\text{C}_6\text{H}_3\text{COOCH}_2\text{CH}_2-$ ); 1.28 (m, 4 H,  $-\text{C}_6\text{H}_3\text{COOCH}_2\text{CH}_2\text{CH}_2\text{CH}_2\text{CH}_2\text{COO}-$ ); 1.00 (t (J = 7.4 Hz) d (J = 3.2 Hz), 3 H,  $-\text{CH}_3$ )

**6-(2,5-Di(4-butoxybenzoyloxy)benzoyloxy)hexanoic acid (6)**



Benzyl 6-(2,5-di(4'-butoxybenzoyloxy)benzoyloxy)hexanoate (**5**) (1.74 g; 2.45 mmol) was dissolved in tetrahydrofuran (20 mL) and Pd/C (30 mg) added. Hydrogen gas was allowed to bubble in the stirred suspension and the reaction stirred for 20 h at room temperature. The mixture was filtered on a celite pad and the solvent was removed by evaporation under reduced pressure. The crude was recrystallised from ethanol to yield **6** as a white crystal.

Yield: 1.28 g (84%)

$^1\text{H}$  NMR (400 MHz,  $\text{CDCl}_3$ )  $\delta\text{H}$  (ppm): 8.16 (d ( $J = 8.9$  Hz) d ( $J = 4.8$  Hz) , 4 H, *ArH*); 7.89 (d ( $J = 2.9$  Hz), 1 H, *ArHc*); 7.45 (d ( $J = 8.8$  Hz) d ( $J = 2.9$  Hz), 1 H, *ArHb*); 7.26 (d ( $J = 8.7$  Hz), 1 H, *ArHa*); 6.98 (d ( $J = 8.9$  Hz), 4 H, *ArH*); 4.17 (t ( $J = 6.5$  Hz), 2 H,  $-\text{COOCH}_2\text{CH}_2-$ ); 4.06 (t ( $J = 6.5$  Hz) d ( $J = 3.2$  Hz), 4 H,  $-\text{C}_6\text{H}_4\text{OCH}_2-$ ), 2.26 (t ( $J = 7.4$  Hz), 2 H,  $-\text{CH}_2\text{COOH}$ ); 1.81 (m, 4 H,  $-\text{C}_6\text{H}_4\text{OCH}_2\text{CH}_2-$ ); 1.52 (m, 8 H,  $-\text{C}_6\text{H}_4\text{OCH}_2\text{CH}_2\text{CH}_2-$ ,  $-\text{COOCH}_2\text{CH}_2\text{CH}_2\text{CH}_2\text{CH}_2\text{COO}-$ ); 1.30 (m, 2 H,  $-\text{CH}_2\text{CH}_2\text{CH}_2\text{CH}_2\text{CH}_2-$ ); 1.00 (t ( $J = 7.4$  Hz) d ( $J = 2.1$  Hz), 6 H,  $-\text{CH}_3$ )

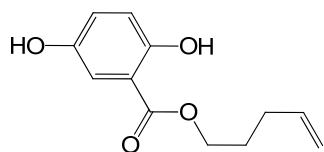
$^{13}\text{C}$  NMR (100.4 MHz,  $\text{CDCl}_3$ )  $\delta\text{C}$  (ppm): 178.4, 163.7, 161.2, 146.5, 137.6, 132.5, 127.2, 125.1, 114.5, 110.2, 109.8, 71.02, 68.11, 65.22, 31.21, 28.11, 25.34, 24.26, 19.28, 13.91

ESI MS:  $m/z = 643.2$  ( $\text{M} + \text{Na}$ ) $^+$

IR ( $\text{cm}^{-1}$ ): 3062, 2947, 2870, 1728, 1705, 1605, 1512, 1466, 1420, 1250, 1157, 1134, 1065, 1003, 926, 841, 756, 687, 640, 570

Elemental analysis: calcd (%) for  $\text{C}_{35}\text{H}_{40}\text{O}_{10}$ : C 67.73, H 6.50; found: C 67.43, H 6.46

### Pent-4-enyl 2,5-dihydroxybenzoate (**7**)

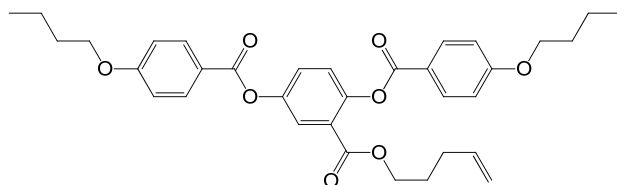


A suspension of 2,5-dihydroxybenzoic acid (5 g; 32.5 mmol) and NaHCO<sub>3</sub> (8.2 g; 97.4 mmol) in dimethylformamide (50 mL) was heated and stirred at 70 °C for 1 h. 5-Bromo-1-pentene (3.85 mL; 32.5 mmol) was added, and the reaction was stirred for 20 h at 70 °C. The mixture was cooled down, diluted with water (150 mL) and extracted with 1:1 ethyl acetate/hexane (70 mL). The organic phase was washed twice with water (70 mL), dried over MgSO<sub>4</sub> and the solvent was removed by evaporation under reduced pressure. The crude product was subject to column chromatography over silica gel with elution with 1:1 hexane/ethyl acetate; removing of the solvents by evaporation yielded **7** as a white powder.

Yield: 5.74 g (80%)

<sup>1</sup>H NMR (400 MHz, CDCl<sub>3</sub>) δH (ppm): 10.5 (s, 2 H, -OH); 7.30 (d (J = 3.1 Hz), 1 H, ArH); 7.01 (d (J = 8.9 Hz) d (J = 3.1 Hz), 1 H, ArH); 6.86 (d (J = 8.9 Hz), 1 H, ArH); 5.81 (d (J<sub>trans</sub> = 17 Hz) d (J<sub>cis</sub> = 10 Hz) t (J = 6.7 Hz), 1 H, -CH<sub>2</sub>CH=CH<sub>2</sub>); 5.07 (d (J<sub>trans</sub> = 17 Hz) m, 1 H, -CH=CH<sub>2</sub>); 5.01 (d (J<sub>cis</sub> = 10 Hz) m, 1 H, -CH=CH<sub>2</sub>); 4.33 (t (J = 6.5 Hz), 2 H, -COOCH<sub>2</sub>-); 2.19 (m, 2 H, -CH<sub>2</sub>CH=CH<sub>2</sub>); 1.85 (m, 2 H, -CH<sub>2</sub>CH<sub>2</sub>CH<sub>2</sub>-)

### Pent-4-enyl 2,5-di(4-butoxybenzoyloxy)benzoate (**8**)



A solution of **7** (5.74 g; 26 mmol), N,N'-dicyclohexylcarbodiimide (12.9 g; 62.4 mmol), 4-(dimethylamino)pyridine (6.54 g; 26 mmol) and 4-butoxybenzoic acid (10.6 g; 54.6 mmol) in dichloromethane (260 mL) was stirred at room temperature for 20 h. The mixture was filtered and the filtrate was washed with water (250 mL),

5% AcOH solution (250 mL), water (250 mL), and dried over MgSO<sub>4</sub>. After evaporation of the solvent, the crude product was recrystallised from ethanol to yield **8** as a white solid.

Yield: 11.3 g (76%)

<sup>1</sup>H NMR (400 MHz, CDCl<sub>3</sub>) δH (ppm): 8.16 (d (J = 8.9 Hz) d (J = 5.2 Hz), 4 H, ArH); 7.89 (d (J = 2.9 Hz), 1 H, ArHc); 7.46 (d (J = 8.7 Hz) d (J = 2.9 Hz), 1 H, ArHb); 7.26 (d (J = 8.7 Hz), 1 H, ArHa); 6.98 (d (J = 9.0 Hz) d (J = 2.6 Hz), 4 H, ArH); 5.67 (d (J<sub>trans</sub> = 17 Hz) d (J<sub>cis</sub> = 10 Hz) t (J = 6.6 Hz), 1 H, -CH<sub>2</sub>CH=CH<sub>2</sub>); 4.93 (d (J<sub>trans</sub> = 17 Hz) m, 1 H, -CH=CH<sub>2</sub>); 4.92 (d (J<sub>cis</sub> = 10 Hz) m, 1 H, -CH=CH<sub>2</sub>); 4.17 (t (J = 6.7 Hz), 2 H, -COOCH<sub>2</sub>-); 4.06 (t (J = 6.5 Hz) d (J = 2.6 Hz), 4 H, -C<sub>6</sub>H<sub>4</sub>OCH<sub>2</sub>-); 2.02 (m, 2 H, -CH<sub>2</sub>CH=CH<sub>2</sub>); 1.82 (m, 4 H, -C<sub>6</sub>H<sub>4</sub>OCH<sub>2</sub>CH<sub>2</sub>-); 1.55 (m, 6 H, -C<sub>6</sub>H<sub>4</sub>OCH<sub>2</sub>CH<sub>2</sub>CH<sub>2</sub>-, -COOCH<sub>2</sub>CH<sub>2</sub>-); 1.00 (t (J = 7.4 Hz), 6 H, -CH<sub>3</sub>)

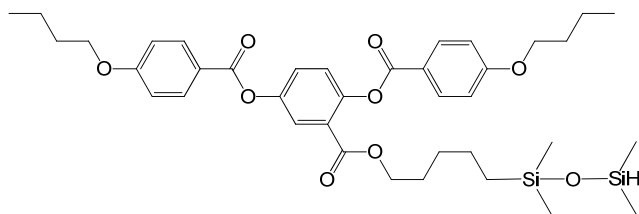
<sup>13</sup>C NMR (100.4MHz, CDCl<sub>3</sub>) δC (ppm): 165.0, 164.7, 164.1, 163.8, 163.6, 148.4, 148.2, 137.4, 132.5, 132.4, 127.2, 125.1, 125.0, 124.9, 121.4, 121.0, 115.2, 114.4, 68.13, 68.08, 65.00, 31.21, 29.98, 27.56, 19.29, 13.92

ESI MS: m/z = 575.3 (M + H)<sup>+</sup>

IR (cm<sup>-1</sup>): 3071, 2955, 2870, 1721, 1605, 1512, 1466, 1389, 1250, 1157, 1165, 1103, 918, 841, 764, 694, 640, 556, 509

Elemental analysis: calcd (%) for C<sub>34</sub>H<sub>38</sub>O<sub>8</sub>: C 71.06, H 6.67; found: C 71.04, H 6.72

### 5-(1,1,3,3-Tetramethyldisiloxy)pentyl 2,5-di(4-butoxybenzoyloxy)benzoate (**9**)



A solution of **8** (0.4 g; 0.7 mmol) in toluene (10 mL) was degassed and placed under argon. Karstedt's catalyst (0.01 mL) was added, followed by 1,1,3,3-tetramethylsiloxane (1.24 mL; 7 mmol) and the mixture was stirred for 20 h at room temperature. The solvent and excess siloxane were removed by evaporation under

vacuum. The product was isolated from the crude by column chromatography, eluting with dichloromethane, to yielded **9** as an air sensitive white sticky solid.

Yield: 0.3 g (60%)

$^1\text{H}$  NMR (400 MHz,  $\text{CDCl}_3$ )  $\delta\text{H}$  (ppm): 8.15 (d ( $J = 8.9\text{Hz}$ ) d ( $J = 5.9\text{ Hz}$ ), 4 H,  $\text{ArH}$ ); 7.87 (d ( $J = 2.9\text{ Hz}$ ), 1 H,  $\text{ArHc}$ ); 7.45 (d ( $J = 8.7\text{ Hz}$ ) d ( $J = 2.8\text{ Hz}$ ), 1 H,  $\text{ArHb}$ ); 7.26 (d ( $J = 8.8\text{ Hz}$ ), 1 H,  $\text{ArHa}$ ); 6.98 (d ( $J = 9.0\text{ Hz}$ ) d ( $J = 3.1\text{ Hz}$ ), 4 H,  $\text{ArH}$ ); 4.65 (sept ( $J = 2.8\text{ Hz}$ ), 1 H,  $-\text{OSi}(\text{CH}_3)_2\text{H}$ ); 4.15 (t ( $J = 6.8\text{ Hz}$ ), 2 H,  $-\text{COOCH}_2-$ ); 4.06 (m, 4 H,  $-\text{C}_6\text{H}_4\text{OCH}_2-$ ), 1.81 (m, 4 H,  $-\text{C}_6\text{H}_4\text{OCH}_2\text{CH}_2-$ ); 1.52 (m, 6 H,  $-\text{C}_6\text{H}_4\text{OCH}_2\text{CH}_2\text{CH}_2-$ ,  $-\text{COOCH}_2\text{CH}_2-$ ); 1.25 (m, 4 H,  $-\text{COOCH}_2\text{CH}_2\text{CH}_2\text{CH}_2-$ ); 1.00 (t ( $J = 7.4\text{ Hz}$ ), 6 H,  $-\text{OCH}_2\text{CH}_2\text{CH}_2\text{CH}_3$ ); 0.45 (m, 2 H,  $-\text{CH}_2\text{Si}-$ ); 0.14 (d ( $J = 2.8\text{ Hz}$ ), 6 H,  $-\text{OSi}(\text{CH}_3)_2\text{H}$ ); 0.03 (s, 6 H,  $-\text{CH}_2\text{Si}(\text{CH}_3)\text{O}-$ )

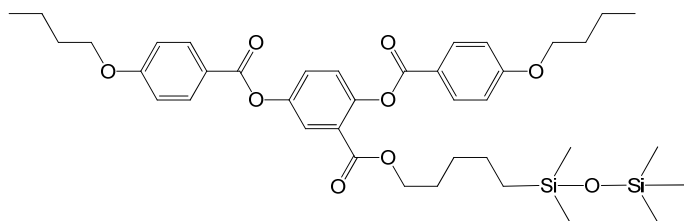
$^{13}\text{C}$  NMR (100.4 MHz,  $\text{CDCl}_3$ )  $\delta\text{C}$  (ppm): 165.1, 164.7, 164.3, 163.8, 163.6, 148.4, 148.2, 132.6, 132.5, 127.2, 125.1, 121.5, 121.1, 114.5, 114.4, 68.13, 65.70, 65.64, 31.21, 29.42, 28.15, 22.84, 19.28, 18.03, 13.91, 0.979, 0.526, 0.241, 0.073

ESI MS:  $m/z = 731.3$  ( $\text{M} + \text{Na}$ ) $^+$

IR ( $\text{cm}^{-1}$ ): 3071, 2955, 2931, 2870, 2122, 1728, 1604, 1512, 1466, 1420, 1250, 1157, 1057, 903, 841, 787, 764, 694, 640, 563.

Elemental analysis: calcd (%) for  $\text{C}_{38}\text{H}_{52}\text{O}_9\text{Si}_2$ : C 64.37, H 7.39; found: C 62.47, H 7.35

### 5-(Pentamethyldisiloxy)pentyl 2,5-di(4-butoxybenzoyloxy)benzoate (**10**)



A solution of the mesogen **8** (0.4 g; 0.7 mmol) in toluene (10 mL) was degassed and placed under argon. Karstedt's catalyst (0.01 mL) was added, followed by pentamethylsiloxane (1.37 mL; 7 mmol) and the mixture was stirred for 20 h at room temperature. The solvent and excess siloxane were removed by evaporation under

vacuum. The crude product was recrystallised from ethanol to yield **10** as white crystals.

Yield: 0.18 g (36%)

$^1\text{H}$  NMR (400 MHz,  $\text{CDCl}_3$ )  $\delta\text{H}$  (ppm): 8.15 (d (J = 8.9 Hz) d (J = 5.9 Hz), 4 H, ArH); 7.88 (d (J = 2.9 Hz), 1 H, ArHc); 7.45 (d (J = 8.8 Hz) d (J = 2.9 Hz), 1 H, ArHb); 7.26 (d (J = 8.7 Hz), 1 H, ArHa); 6.98 (d (J = 8.9 Hz) d (J = 3.2 Hz), 4 H, ArH); 4.15 (t (J = 6.8 Hz), 2 H,  $-\text{COOCH}_2-$ ); 4.06 (m, 4 H,  $-\text{C}_6\text{H}_4\text{OCH}_2-$ ); 1.81 (m, 4 H,  $-\text{C}_6\text{H}_4\text{OCH}_2\text{CH}_2-$ ); 1.52 (m, 6 H,  $-\text{C}_6\text{H}_4\text{OCH}_2\text{CH}_2\text{CH}_2-$ ,  $-\text{COOCH}_2\text{CH}_2-$ ); 1.24 (m, 4 H,  $-\text{COOCH}_2\text{CH}_2\text{CH}_2\text{CH}_2-$ ); 1.04 (t (J = 7.4 Hz), 6 H,  $-\text{OCH}_2\text{CH}_2\text{CH}_2\text{CH}_3$ ); 0.46 (m, 2 H,  $-\text{CH}_2\text{Si}-$ ); 0.04 (s, 6 H,  $-\text{OSi}(\text{CH}_3)_3$ ); 0.00 (s, 6 H,  $-\text{CH}_2\text{Si}(\text{CH}_3)_3$ )

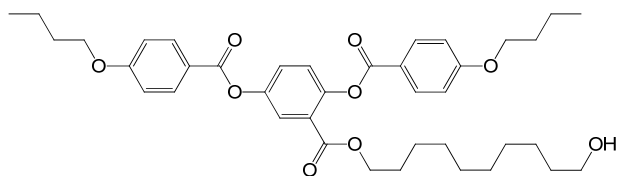
$^{13}\text{C}$  NMR (100.4 MHz,  $\text{CDCl}_3$ )  $\delta\text{C}$  (ppm): 165.0, 164.7, 164.2, 163.8, 163.6, 148.4, 148.2, 132.5, 127.2, 125.1, 121.5, 121.1, 114.5, 114.4, 68.13, 68.08, 65.7, 31.22, 29.54, 28.22, 22.99, 19.28, 18.24, 13.91, 2.056, 1.140, 0.379

ESI MS:  $m/z = 745.3$  (M + Na) $^+$

IR ( $\text{cm}^{-1}$ ): 2955, 2870, 1728, 1605, 1512, 1420, 1250, 1165, 1065, 841, 764, 694, 640, 556

Elemental analysis: calcd (%) for  $\text{C}_{39}\text{H}_{54}\text{O}_9\text{Si}_2$ : C 64.79, H 7.53; found: C 64.66, H 7.46

### 10-Hydroxydecyl 2,5-di(4-butoxybenzoyloxy)benzoate (11)



2,5-Di(4-butoxybenzoyloxy)benzoic acid (**3**) (4.1 g; 8.1 mmol), 1,10-decanediol (4.23 g; 24.3 mmol) were dissolved in dichloromethane (150 mL) with 1-ethyl-3-(3-dimethylaminopropyl)carbodiimide (9.3 g; 48.5 mmol) and 4-(dimethylamino)pyridine (0.6 g; 4.9 mmol). The reaction was stirred under argon for 48 h at room temperature. The solvent was removed by evaporation under reduced

pressure, and the product was isolated from the crude by column chromatography, eluting with 1:10 ethyl acetate/dichloromethane, and recrystallised from dichloromethane/hexane to give **11** as a white solid.

Yield: 3.42 g (64%)

$^1\text{H}$  NMR (400 MHz,  $\text{CDCl}_3$ )  $\delta\text{H}$  (ppm): 8.15 (d (J = 9.0 Hz) d (J = 5.4 Hz), 4 H, *ArH*); 7.89 (d (J = 2.8 Hz), 1 H, *ArH*); 7.45 (d (J = 8.7 Hz) d (J = 2.9 Hz), 1 H, *ArH*); 7.26 (d (J = 8.8 Hz), 1 H, *ArH*); 6.98 (d (J = 9.0 Hz) d (J = 2.7 Hz), 4 H, *ArH*); 4.15 (t (J = 6.8 Hz), 2 H,  $-\text{COOCH}_2-$ ); 4.06 (t (J = 6.5 Hz) d (J = 2.7 Hz), 4 H,  $-\text{C}_6\text{H}_4\text{OCH}_2-$ ); 3.62 (t (J = 6.6 Hz), 2 H,  $-\text{CH}_2\text{OH}$ ); 1.82 (m, 4 H,  $-\text{C}_6\text{H}_4\text{OCH}_2\text{CH}_2-$ ); 1.50 (m, 8 H,  $-\text{C}_6\text{H}_4\text{OCH}_2\text{CH}_2\text{CH}_2-$ ,  $-\text{COOCH}_2\text{CH}_2(\text{CH}_2)_6\text{CH}_2\text{CH}_2\text{OH}$ ); 1.26 (m, 12 H,  $-\text{COOCH}_2\text{CH}_2(\text{CH}_2)_6\text{CH}_2\text{CH}_2\text{OH}$ ); 1.00 (t (J = 7.4 Hz), 6 H,  $-\text{CH}_3$ )

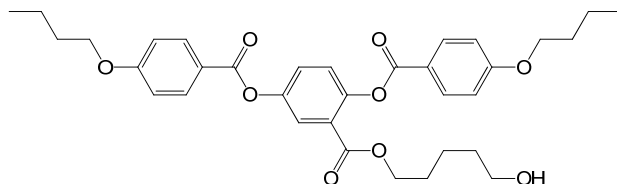
$^{13}\text{C}$  NMR (100.4 MHz,  $\text{CDCl}_3$ )  $\delta\text{C}$  (ppm): 165.0, 164.7, 164.2, 163.8, 163.7, 148.4, 148.2, 132.5, 132.5, 127.2, 125.1, 121.5, 121.1, 114.5, 114.4, 68.14, 68.09, 65.73, 63.13, 32.87, 31.21, 29.55, 29.43, 29.39, 29.21, 28.45, 25.87, 25.79, 19.29, 13.92

ESI MS:  $m/z = 662.5$  ( $\text{M} + \text{H}$ ) $^+$

IR ( $\text{cm}^{-1}$ ): 3449, 3071, 2924, 2862, 1728, 1605, 1512, 1466, 1366, 1312, 1242, 1165, 1126, 1072, 1003, 972, 918, 887, 841, 756, 687, 640, 548

Elemental analysis: calcd (%) for  $\text{C}_{39}\text{H}_{50}\text{O}_9$ : C 70.67, H 7.60; found: C 70.75, H 7.66

### 5-Hydroxypentyl 2,5-di(4-butoxybenzoyloxy)benzoate (**12**)



To a stirred solution of pent-4-enyl 2,5-di(4-butoxybenzoyloxy)benzoate (**8**) (3 g; 5.23 mmol) in tetrahydrofuran (50 mL) kept under nitrogen was added via syringe 9-borabicyclo[3,3,1]nonane (0.5 M in THF; 11.5 mL; 5.75 mmol). The mixture was stirred for 20 h at room temperature under nitrogen. The solution was cooled in an ice/water bath, and solid *m*-chloroperbenzoic acid (70%; 5.2 g; 20.9 mmol) was

added slowly in small portions. After stirring at room temperature for 5 h, the reaction mixture was diluted with water (100 mL) and NaHCO<sub>3</sub> (10%) solution was added to destroy the peroxy acid (monitored by pH test strips). The mixture was extracted with dichloromethane (200 mL), and the organic phase was washed with saturated NaHCO<sub>3</sub> solution (200 mL) and water (200 mL), and dried over Na<sub>2</sub>SO<sub>4</sub>. After evaporation of the solvent, the product was purified by column chromatography, eluting with 1:10 ethyl acetate/dichloromethane, to yield **12** as white crystals.

Yield: 1.09 g (33%).

<sup>1</sup>H NMR (400 MHz, CDCl<sub>3</sub>) δH (ppm): 8.16 (d (J = 8.9 Hz) d (J = 7.1 Hz), 4 H, ArH); 7.90 (d (J = 2.9 Hz), 1 H, ArHc); 7.45 (d (J = 8.7 Hz) d (J = 2.9 Hz), 1 H, ArHb); 7.26 (d (J = 8.7 Hz), 1 H, ArHa); 6.99 (d (J = 8.9 Hz), 4 H, ArH); 4.18 (t (J = 6.6 Hz), 2 H, -COOCH<sub>2</sub>-); 4.06 (t (J = 6.5 Hz), 4 H, -C<sub>6</sub>H<sub>4</sub>OCH<sub>2</sub>-); 3.56 (t (J = 6.5 Hz), 2 H, -CH<sub>2</sub>OH); 1.82 (m, 4 H, -C<sub>6</sub>H<sub>4</sub>OCH<sub>2</sub>CH<sub>2</sub>-); 1.50 (m, 8 H, -C<sub>6</sub>H<sub>4</sub>OCH<sub>2</sub>CH<sub>2</sub>CH<sub>2</sub>-, -COOCH<sub>2</sub>CH<sub>2</sub>CH<sub>2</sub>CH<sub>2</sub>OH); 1.33 (m, 2 H, -CH<sub>2</sub>CH<sub>2</sub>CH<sub>2</sub>OH); 1.00 (t (J = 7.4 Hz), 6 H, -CH<sub>3</sub>)

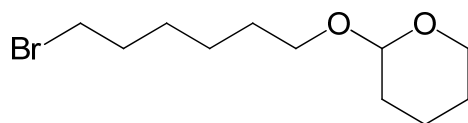
<sup>13</sup>C NMR (100.4 MHz, CDCl<sub>3</sub>) δC (ppm): 165.1, 164.7, 164.2, 163.9, 163.7, 148.4, 148.2, 132.6, 132.5, 127.2, 125.1, 125.0, 121.5, 121.1, 114.5, 114.4, 68.13, 65.48, 62.68, 32.32, 32.21, 28.27, 22.19, 19.29, 13.93

ESI MS: m/z = 593.3 (M + H)<sup>+</sup>

IR (cm<sup>-1</sup>): 3526, 3071, 2932, 2870, 1728, 1605, 1512, 1473, 1389, 1312, 1242, 1165, 1126, 1072, 1033, 972, 918, 889, 841, 756, 687, 640, 548, 517

Elemental analysis: calcd (%) for C<sub>34</sub>H<sub>40</sub>O<sub>9</sub>: C 68.90, H 6.80; found: C 68.68, H 6.80

### 6-Tetrahydropyranyloxy-1-bromohexanol (**13**)

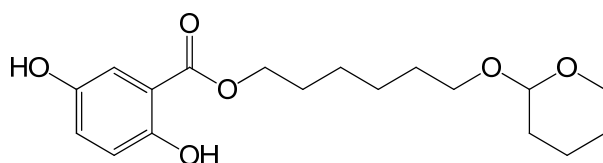


6-Bromohexanol (3 g; 16.6 mmol) was dissolved in dry dichloromethane (50 mL) at room temperature under argon. Dihydropyran (1.8 mL; 20 mmol) and *p*-toluenesulfonic acid (50 mg; 0.29 mmol) were added and the solution stirred for 20 h at room temperature. The resulting solution was poured into saturated NaHCO<sub>3</sub> and extracted with dichloromethane. The organic layer were washed with saturated NaCl, dried over MgSO<sub>4</sub>, filtered and concentrated. The product was obtained from the crude by column chromatography with ethyl 1:4 acetate/petroleum ether to yield **13** as a colourless oil.

Yield: 4.27 g (97%)

<sup>1</sup>H NMR (400 MHz, CDCl<sub>3</sub>) δH (ppm): 4.57 (m, 1 H, C(2)*H* of THP); 3.86 (m, 1 H, C(6)*H* of THP); 3.73 (m, 1 H, C(6)*H* of THP); 3.49 (m, 1 H, -CHHO-THP); 3.39 (m, 3 H, -CHHO-THP, BrCH<sub>2</sub>-); 1.62 (m, 14 H, BrCH<sub>2</sub>CH<sub>2</sub>CH<sub>2</sub>CH<sub>2</sub>CH<sub>2</sub>-, C(3)*H*<sub>2</sub>, C(4)*H*<sub>2</sub>, C(5)*H*<sub>2</sub> of THP)

### 6-(Tetrahydropyranyloxy)hexyl-2,5-dihydroxybenzoate (**14**)

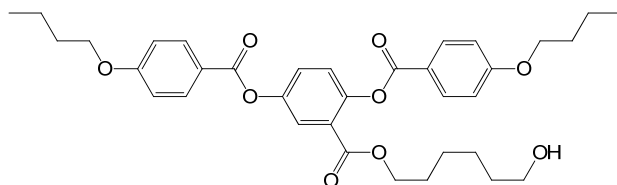


Solid NaHCO<sub>3</sub> (4.06 g; 48.3 mmol) was added to a solution of 2,5-dihydroxybenzoic acid (2.5 g; 16.1 mmol) in dimethylformamide (100 mL). The mixture was heated and stirred at 70 °C for 1 h. 6-Tetrahydropyranyloxy-1-bromohexanol (**13**) (4.27 g; 16.1 mmol) was added, and the reaction was stirred for 20 h at 70 °C. The mixture was cooled down, diluted with water (200 mL) and extracted with 1:1 ethyl acetate/hexane (100 mL). The organic phase was separated, washed twice with water (100 mL), dried over MgSO<sub>4</sub> and the solvent was removed by evaporation under reduced pressure. The crude was purified by column chromatography over silica gel



THP, C(3)H<sub>2</sub>, C(4)H<sub>2</sub>, C(5)H<sub>2</sub> of THP); 1.26 (m, 4 H, -COOCH<sub>2</sub>CH<sub>2</sub>CH<sub>2</sub>CH<sub>2</sub>-); 0.99 (t (J = 7.4 Hz), 6 H, -CH<sub>3</sub>)

### 6-Hydroxyhexyl 2,5-di(4-butoxybenzoyloxy)benzoate (**16**)



**15** (4.22 g; 6.1 mmol) was dissolved in methanol (150 mL) and p-toluenesulfonic acid (100 mg) was added. The solution was stirred for 72 h at room temperature and the reaction was quenched by the addition of saturated NH<sub>4</sub>Cl solution. The organic product phase was extracted with dichloromethane, dried over MgSO<sub>4</sub>, filtered and dried concentrated in vacuo. The product was purified by column chromatography, using 1:1 hexane/ethyl acetate, and recrystallised from ethanol to give **16** as white crystals.

Yield: 3.13 g (85%)

<sup>1</sup>H NMR (400 MHz, CDCl<sub>3</sub>) δ<sub>H</sub> (ppm): 8.15 (d (J = 8.6 Hz) d (J = 6.3 Hz), 4 H, ArH); 7.89 (d (J = 2.9 Hz), 1 H, ArH); 7.45 (d (J = 8.7 Hz) d (J = 2.8 Hz), 1 H, ArH); 7.26 (d (J = 8.7 Hz), 1 H, ArH); 6.98 (d (J = 8.7 Hz); 4 H, ArH); 4.16 (t (J = 6.6 Hz), 2 H, -COOCH<sub>2</sub>-); 4.06 (t (J = 6.4 Hz) d (J = 0.8 Hz), 4 H, -C<sub>6</sub>H<sub>4</sub>OCH<sub>2</sub>-); 3.58 (t (J = 6.5 Hz), 2 H, -CH<sub>2</sub>OH); 1.82 (m, 4 H, -C<sub>6</sub>H<sub>4</sub>OCH<sub>2</sub>CH<sub>2</sub>-); 1.50 (m, 8 H, -C<sub>6</sub>H<sub>4</sub>OCH<sub>2</sub>CH<sub>2</sub>CH<sub>2</sub>-, -COOCH<sub>2</sub>CH<sub>2</sub>CH<sub>2</sub>CH<sub>2</sub>CH<sub>2</sub>CH<sub>2</sub>OH); 1.26 (m, 4 H, -COOCH<sub>2</sub>CH<sub>2</sub>CH<sub>2</sub>CH<sub>2</sub>CH<sub>2</sub>CH<sub>2</sub>OH); 1.00 (t (J = 7.4 Hz), 6 H, -CH<sub>3</sub>)

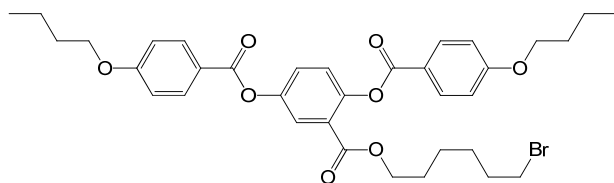
<sup>13</sup>C NMR (100.4 MHz, CDCl<sub>3</sub>) δ<sub>C</sub> (ppm): 165.1, 164.7, 164.2, 163.9, 163.7, 148.4, 148.2, 132.6, 132.5, 127.2, 125.1, 125.0, 121.5, 121.1, 114.5, 114.4, 68.14, 65.57, 62.85, 32.58, 31.21, 28.32, 25.71, 25.36, 19.29, 13.92

ESI MS: m/z = 629.3 (M + Na)<sup>+</sup>

IR (cm<sup>-1</sup>): 3541, 3078, 2924, 2855, 2222, 1921, 1728, 1605, 1512, 1489, 1474, 1389, 1312, 1250, 1165, 1134, 1065, 1003, 918, 887, 841, 756, 687, 640, 556

Elemental analysis: calcd (%) for C<sub>35</sub>H<sub>42</sub>O<sub>9</sub>: C 69.29, H 6.98; found: C 69.39, H 7.02

### 6-Bromohexyl 2,5-di(4-butoxybenzoyloxy)benzoate (**17**)



A solution of 2,5-di(4-butoxybenzoyloxy)benzoic acid (**3**) (0.3 g; 0.6 mmol), N,N'-dicyclohexylcarbodiimide (0.17 g; 0.8 mmol), 4-(dimethylamino)pyridine (0.07 g; 0.6 mmol) in dichloromethane (15 mL) was stirred while the 6-bromohexanol (0.11 mL; 0.8 mmol) was added. The reaction was stirred for 20 h at room temperature. The solid was filtered, and the filtrate was washed with water (30 mL), 5% AcOH (30 mL), and water (30 mL) and dried over MgSO<sub>4</sub>. After evaporation of the solvent, the crude was filtered through a short silica gel pad and recrystallised with ethanol/dichloromethane to yield **17** as white crystals.

Yield: 0.14 g (36%)

<sup>1</sup>H NMR (400 MHz, CDCl<sub>3</sub>) δ<sub>H</sub> (ppm): 8.16 (d (J = 9.0 Hz) d (J = 5.9 Hz), 4 H, ArH); 7.89 (d (J = 2.9 Hz), 1 H, ArH<sub>c</sub>); 7.46 (d (J = 8.7 Hz) d (J = 2.9 Hz), 1 H, ArH<sub>b</sub>); 7.26 (d (J = 8.7 Hz), 1 H, ArH<sub>a</sub>); 6.99 (d (J = 8.9 Hz) d (J = 1.7 Hz), 4 H, ArH); 4.16 (t (J = 6.6 Hz), 2 H, -COOCH<sub>2</sub>CH<sub>2</sub>-); 4.06 (t (J = 6.5 Hz), 4 H, -C<sub>6</sub>H<sub>4</sub>OCH<sub>2</sub>-); 3.35 (t (J = 6.8 Hz), 2 H, -CH<sub>2</sub>Br); 1.79 (m, 6 H, -C<sub>6</sub>H<sub>4</sub>OCH<sub>2</sub>CH<sub>2</sub>-, -CH<sub>2</sub>CH<sub>2</sub>Br); 1.51 (m, 6 H, -C<sub>6</sub>H<sub>4</sub>OCH<sub>2</sub>CH<sub>2</sub>CH<sub>2</sub>-, -COOCH<sub>2</sub>CH<sub>2</sub>-); 1.28 (m, 4 H, -CH<sub>2</sub>CH<sub>2</sub>CH<sub>2</sub>CH<sub>2</sub>Br); 1.00 (t (J = 7.4 Hz), 6 H, -CH<sub>3</sub>)

<sup>13</sup>C NMR (100.4 MHz, CDCl<sub>3</sub>) δ<sub>C</sub> (ppm): 165.0, 164.7, 164.3, 163.9, 163.7, 148.4, 148.1, 132.5, 127.2, 125.1, 125.0, 121.5, 121.1, 114.5, 114.4, 68.20, 65.50, 33.82, 32.67, 31.29, 28.40, 27.90, 25.22, 19.34, 13.96

ESI MS: m/z = 691.2 (M + Na)<sup>+</sup>

IR (cm<sup>-1</sup>): 3070, 2955, 2932, 2870, 1728, 1605, 1512, 1466, 1420, 1381, 1250, 1157, 1134, 1057, 1003, 964, 887, 841, 764, 687, 640, 509

Elemental analysis: calcd (%) for  $C_{35}H_{41}BrO_8$ : C 62.78, H 6.17; found: C 62.82, H 6.18

# **Chapter 4**

## **LC Oligomers**

## 4.1 Summary

In order to achieve Janus supermolecular mesogenic systems, a central scaffold unit that allows for different functionalization on each of the halves is indispensable. Diphenylacetylene is a suitable building block with these characteristics, as it allows the modular assembly of different functionalization on each aromatic ring.



**Figure 4.1** Diphenylacetylene

Diphenylacetylene (tolane) has a linear shape and a rigid structure (Fig 4.1). As a core unit in a Janus system, it can separate the two halves of the molecule, avoiding the para-substituents X and Y from possible internal hindrance of rotation and movement. The core itself, with its linear configuration, can also enhance the mesomorphic behaviour. This simple structure can be synthesized by several routes, either independently or through the combination of appropriate building blocks. The triple bond between the two phenyl rings also provides possibilities for further manipulation to afford more complex structures.

Several families of low molar mass materials incorporating the diphenylacetylene core showing mesomorphic behaviour have been described [39]. Additionally, this building block has been used as a mesogenic segment in a number of main-chain dendrimers, demonstrating its ability to generate and aid mesomorphic behaviour [40].

This chapter describes the synthesis of several symmetrical and unsymmetrical mesogenic oligomers based on the diphenylacetylene core. These materials are models for the higher dendrimers described in later chapters and provide a general platform for understanding their mesomorphic behaviour.

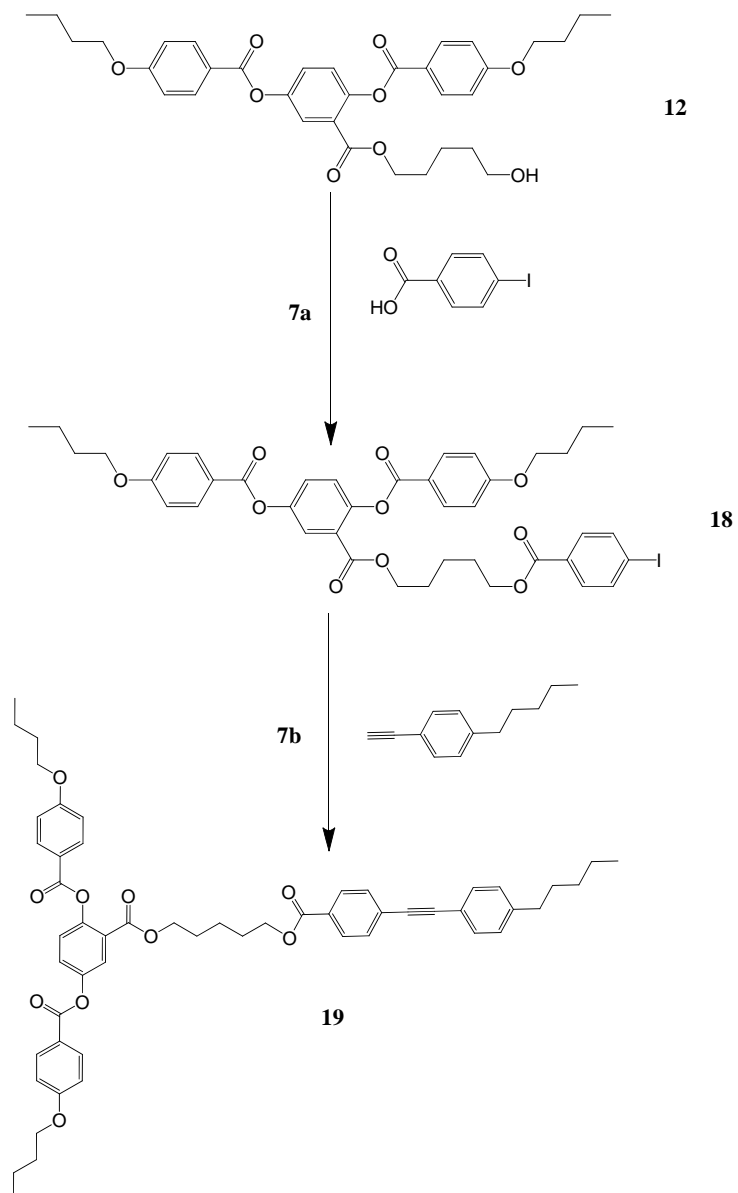
## 4.2 Synthesis

From the synthetic point of view two approaches can be followed:

- (a) Build up the tolane core first and then functionalise each side (divergent approach).
- (b) Prepare the two mesogenic building blocks necessary to construct the tolane and assemble them in the last step (convergent approach). This is done by the Sonogashira coupling of a phenyl acetylene derivative and an iodobenzene derivative.

If the two sides of the molecule are identical, methodology (a) is easier to implement. However, if the sides are to be different (Janus structures), method (b) is the most appropriate.

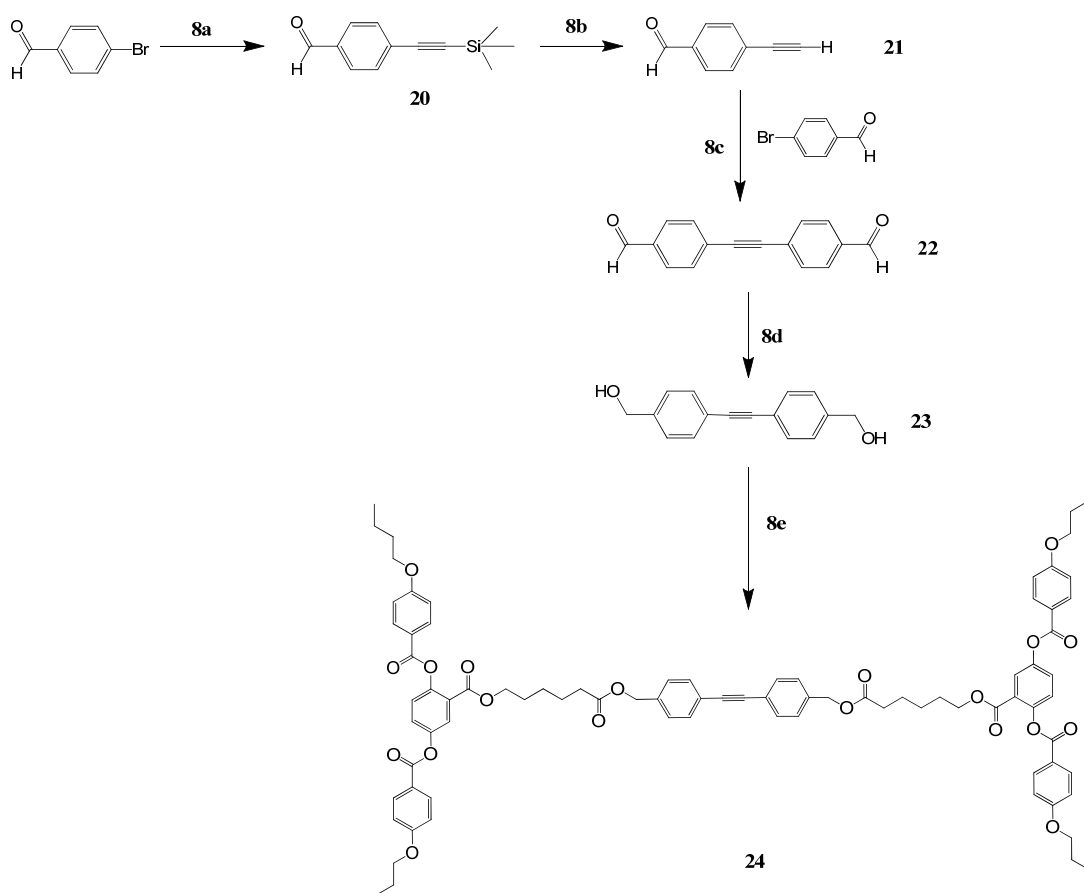
An asymmetric trimer, **19**, with one side-on mesogen and an alkyl chain was made from the 2,5-di(4'-butoxybenzoyloxy)benzoate ester with the hydroxyl terminal group **11** in two steps, first the esterification with 4-iodobenzoic acid followed by the Sonogashira coupling reaction with 1-ethynyl-4-pentyl benzene (Scheme 7).



Reagents and conditions:  
 7a - DCC, DMAP, CH<sub>2</sub>Cl<sub>2</sub>  
 7b - Pd(PPh<sub>3</sub>)<sub>2</sub>Cl<sub>2</sub>, CuI, Et<sub>3</sub>N

**Scheme 7**

A different route, as outlined for method (a), involves the synthesis of the tolane core first, followed by the addition of the mesogenic units (Scheme 8). The diphenylacetylene synthesis begins with 4-bromobenzaldehyde, which reacted with trimethylsilylacetylene (TMSA) and was deprotected later to give the 4-ethynylbenzaldehyde **21**, which was subjected to Sonogashira coupling with p-bromobenzaldehyde again to yield the the tolane dialdehyde **22** [41]. The dialdehyde **22** was then reduced to the diol **23**, which is used as the core in the synthesis of the LC trimer **24** with two laterally attached PDAB mesogenic units by esterification.



Reagents and conditions:

8a - TMSA, Pd(PPh<sub>3</sub>)<sub>2</sub>Cl<sub>2</sub>, PPh<sub>3</sub>, CuI, Et<sub>3</sub>N, 65 °C

8b - K<sub>2</sub>CO<sub>3</sub>, MeOH

8c - Pd(PPh<sub>3</sub>)<sub>2</sub>Cl<sub>2</sub>, PPh<sub>3</sub>, CuI, Et<sub>3</sub>N, 65 °C

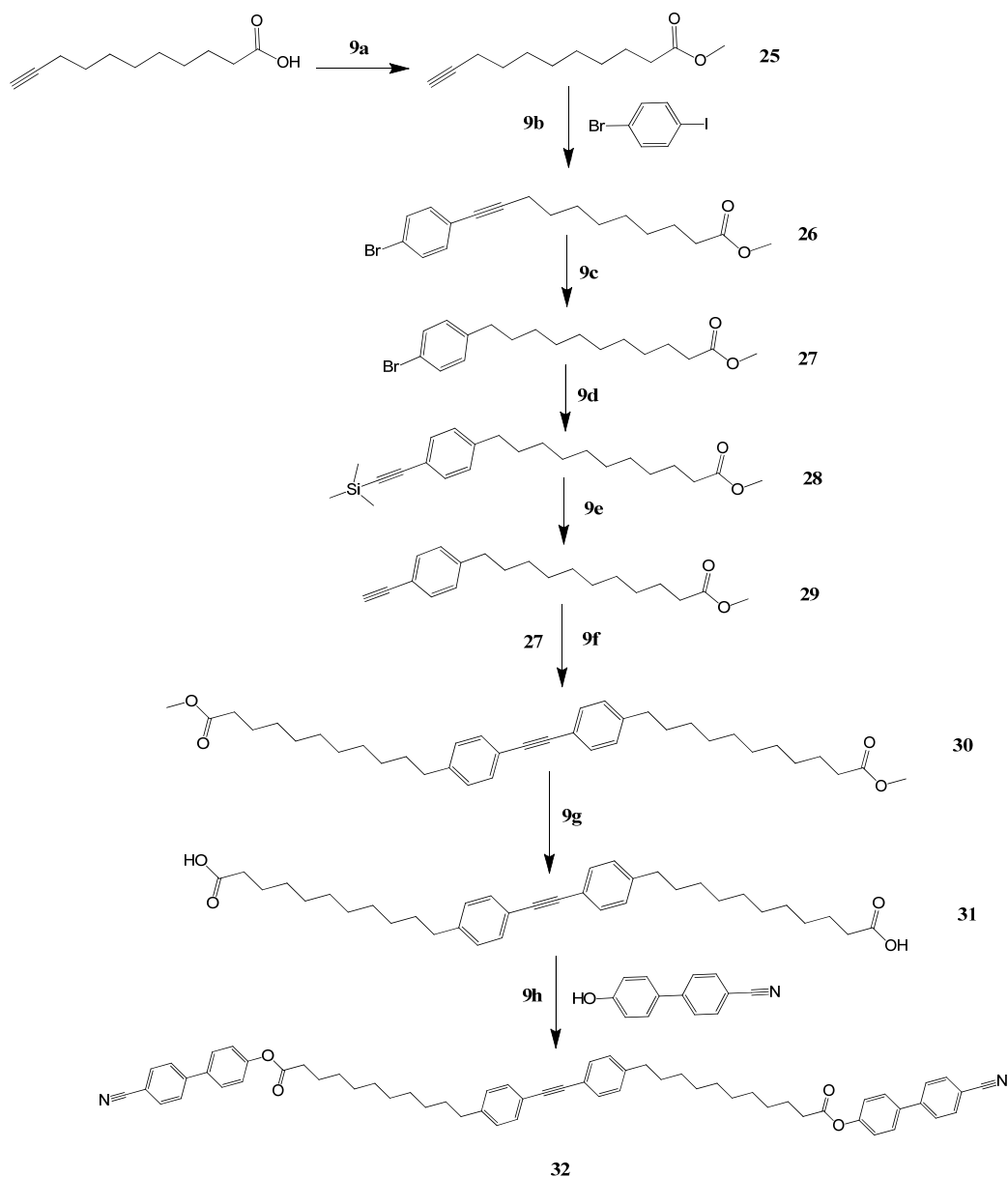
8d - (i) NaBH<sub>4</sub>, THF; (ii) HCl

8e - **6**, DCC, DMAP, CH<sub>2</sub>Cl<sub>2</sub>

**Scheme 8**

The reason for choosing a tolanediol as a core, as opposed to the diphenylacetylene dicarboxylic acid, is that the diacid is very insoluble and difficult to functionalise, whereas the diol is freely soluble and the esterification reactions easier to accomplish.

A unique diphenylacetylene core, **31**, with long alkyl spacer chains directly linked to the core was synthesised in multiple steps (Scheme 9) including the Sonogashira coupling three times and protection/deprotection steps for the alkyne and the methyl ester groups (**25~31**), following the route developed by K. Müllen [42]. The diacid **31** was later used to make the trimer **32** with two end-on mesogens. Although a very long synthetic route, the advantage of this synthesis is that the diacid **31** is much more soluble than tolane dicarboxylic acid, making it a more versatile building block for further substitution with mesogenic units.



Reagents and conditions:

9a - conc.  $\text{H}_2\text{SO}_4$ , MeOH; 9b -  $\text{Pd}(\text{PPh}_3)_4$ , CuI, piperidine; 9c - Pd/C,  $\text{H}_2$ , THF;

9d - TMSA,  $\text{Pd}(\text{PPh}_3)_2\text{Cl}_2$ ,  $\text{PPh}_3$ , CuI,  $\text{Et}_3\text{N}$ , 70 °C; 9e -  $\text{K}_2\text{CO}_3$ , MeOH;

9f -  $\text{Pd}(\text{PPh}_3)_2\text{Cl}_2$ ,  $\text{PPh}_3$ , CuI,  $\text{Et}_3\text{N}$ , 65 °C; 9g - KOH, EtOH/ $\text{H}_2\text{O}$ , 35 °C; 9h - DCC, DMAP, THF

### Scheme 9

The symmetric oligomers were made based on the prepared diphenylacetylene core, while the asymmetric ones always took the core formation as the final step. The diol core **23** was made in four steps whereas the di-acid core **31** takes seven steps, including three Sonogashira couplings. The carboxylic acid group was protected until the final step to give the diacid **31**, while the diol **23** was made from the reduction of

the aldehyde. Both of the cores (the diacid **31** and the diol **23**) were synthesized with medium total yield. The trimers **24** and **32** was made by Steglich esterification with mesogen **6** and hydroxycyanobiphenol respectively in similar conditions; however, the yield of **32** is not as good as **24**, which may be due cause by the intramolecular and intermolecular hydrogen bond forming between the carboxylic groups.

The successful synthesis of the diphenylacetylene core in the oligomers was ascertained by  $^{13}\text{C}$  NMR spectroscopy, in which the resonances between 88~94 ppm indicate the existence of the triple bond between the aromatic rings. In T-shaped trimer **19** there are two resonances with chemical shift of 92.72 ppm and 88.20 ppm respectively, due by the asymmetric structure. In the symetric ones there is only one resonance in that region, at 89.51 ppm for the H-shaped trimer **24** and at 93.03 for the linear trimer **32** (Fig 4.2).

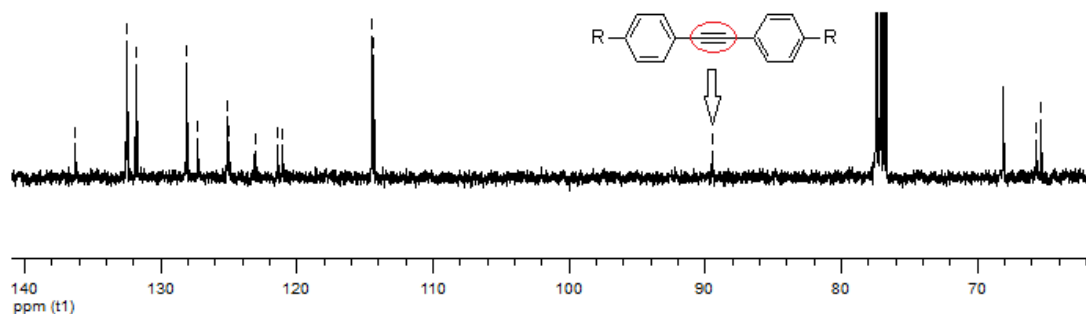


**Figure 4.2**  $^{13}\text{C}$  NMR spectrum of **24** showing the carbon with sp<sup>1</sup> hybridisation in diphenylacetylene core

### 4.3.3 Mesomorphic behaviour

Differential scanning calorimetry was used to determine the phase transition temperatures and associated enthalpies of the liquid crystal oligomers, as shown in Table 2.

No	Cr		N		Iso
19	●*	98.2 [31.2]	●	141.2 [3.8]	●
24	●*	133.7 [91.9]	( ●	115.9 [3.5] )	●
32	●	174.1 [56.5]	●	206.2 [19.3]	●

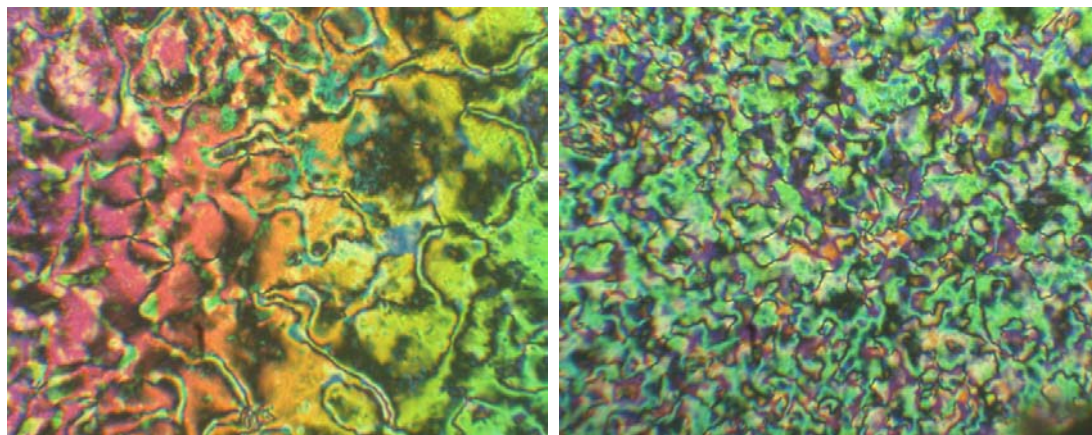
Note (\*): phase transition observed on the first heating cycle, see discussion below

**Table 2** Transition temperatures ( $T/^{\circ}\text{C}$ ) and associated enthalpies ( $[\Delta H/\text{KJmol}^{-1}]$ ) of the oligomers

Similar to the mesogenic monomers in the last chapter, the LC oligomers with PDAB side-on mesogenic units also crystallize slowly. However, the crystallisation is only partially suppressed and frequently happened on heating from the glassy state. For these materials, the melting points and enthalpies given are those of the first heating cycle.

The mesophase identification transition was monitored by polarized light optical microscopy.

Compound **19** and **24** exhibit the typical schlieren texture of nematic phase, with 2- and 4-brush defects clearly identifiable in the textures (Plate 3).



(a)

(b)

**Plate 3** Schlieren textures of (a) **19**, 130 °C; (b) **24**, 110 °C (x200)

Many black threads with 2- and 4-brush singularities as well as homeotropic regions were found in the texture of **32**. The viscosity of the mesophase was quite low, which allowed the material to flow freely. These features allowed the identification of the texture as belonging to a nematic phase.

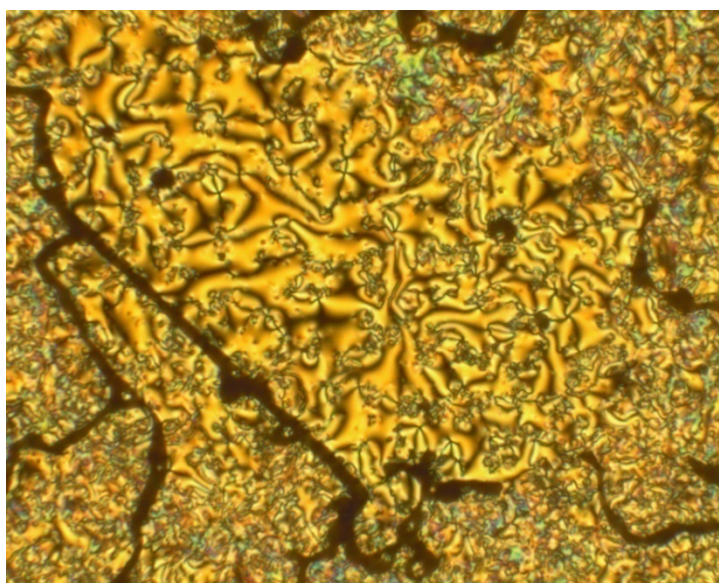


**Plate 4** Schlieren texture of the nematic phase of **32**, 200 °C (x200)

#### 4.4 Discussion

As described in Table 2, the liquid crystal dimer **19** and trimers **24** and **32** exhibit exclusively the nematic phase. Dimer **19** has a structure related to the LC monomers described in Chapter 3, as the functional group at the end of the side chain was replaced by the diphenylacetylene moiety. In the extended conformation of the mesogenic dimer **19**, the flexible spacer allows the two rigid mesogenic cores (side-on PDAB and diphenylacetylene) to adopt a parallel position to each other in order to reduce the free volume (Fig 4.3). In comparison with the mesogenic monomer **6**, dimer **19** has a higher N-I transition temperature since the diphenylacetylene part adds polarisability to the PDAB mesogenic core and stabilizes the nematic phase. On the other hand, the molecular breath is smaller in **19** than in **6**, and at the same time the alkyl chain attached to the biphenyl acetylene effectively induce flexibility to the system and lower the melting-point (similar to the monomers), produced a relatively wide range of the nematic phase.

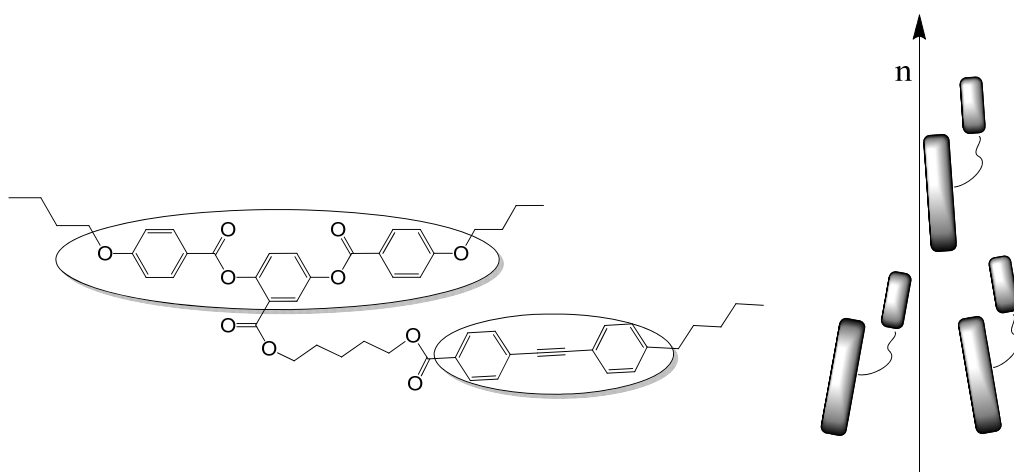
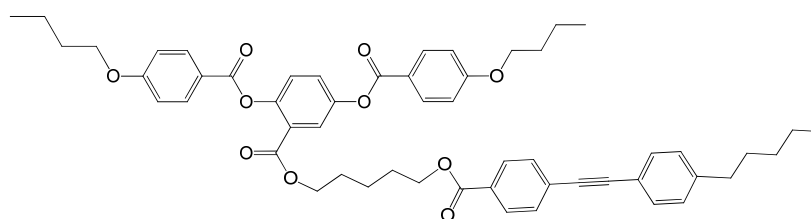


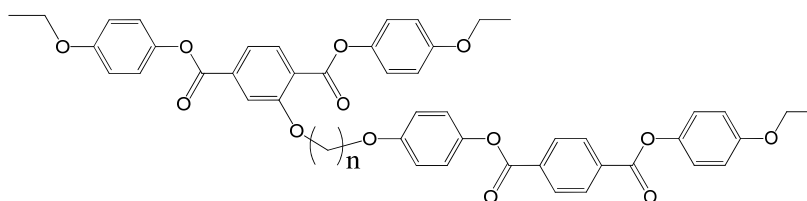
**Figure 4.3** Parallel alignment of the mesogenic cores in compound **19** and the nematic phase formed

There are only a few previous studies of T-shaped LC dimers with a flexible spacer between the two mesogenic cores. A series of T-shaped dimers with two identical three-ring mesogenic units was reported by J. Jin et. al. (Fig 4.4) [9]. Compared to **19**, the dimers with different spacer lengths all exhibit nematic phases with much higher N-I transition temperatures, due to the increased polarisabilities induced by the

larger core, and also the higher rigidity caused by the short end chains. It was also found that the enthalpy and entropy of the N-I transition increased along with the length of the spacer, which indicated that a better alignment of the cores was allowed by the longer and more flexible spacers. This is strong evidence of the co-parallel position of the two mesogenic units, which was mainly affected by the flexibility of the spacer, and this must also apply in the case of the dimer **19**.



Cr 98.2 [31.2] N 141.2 [3.8] I



n = 4 Cr 137.4 [55.5] N 232.1 [1.1] I

n = 8 Cr 147.4 [46.4] N 221.5 [3.4] I

n = 12 Cr 112.1 [36.4] N 196.4 [4.2] I

**Figure 4.4** Transition temperatures of **19** (top) and T-shaped LC dimers (bottom)

With the same side-on mesogenic group, the mesogenic trimer **24** also exhibits the nematic phase, but in this case is monotropic in nature (Plate 3b). In the most stable conformation for this H-shape trimer the lateral alignment of the rigid cores in the mesophase forms an approximate S-shaped conformation (Fig 4.5). In comparison with the LC monomers and the dimer **19**, the trimer **24** with an S-shape should have the highest polarisability and also nematic phase stability. However, the further broadening of the molecular width deforms the overall rod-like molecular structure, thus reducing the anisotropy resulting in the relatively low N-I transition temperature. Without enough terminal chains to induce more flexibility to the system

compared to the increased polarisability, the melting point of trimer **24** is relatively high, which results in a monotropic nematic phase with a short temperature range.

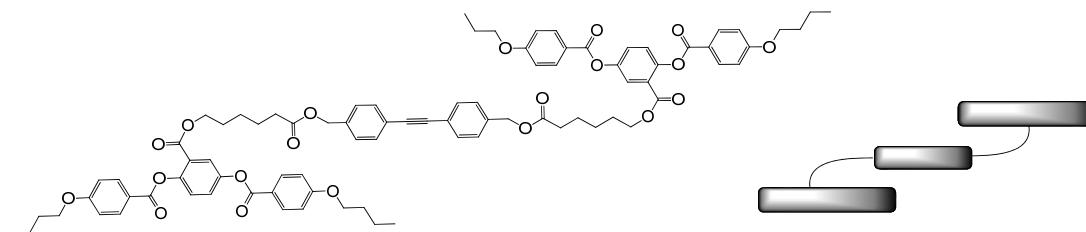


**Figure 4.5** The proposed S-shape of the trimer **24**

By studying the H-shaped dimers reported by J. Jin et. al. and W. Wedler et.al, it can be found that the H-shaped dimers with a long enough spacer usually exhibit only the nematic phase whereas a short spacer may induce smectic phases (Fig 4.6) [9, 10].

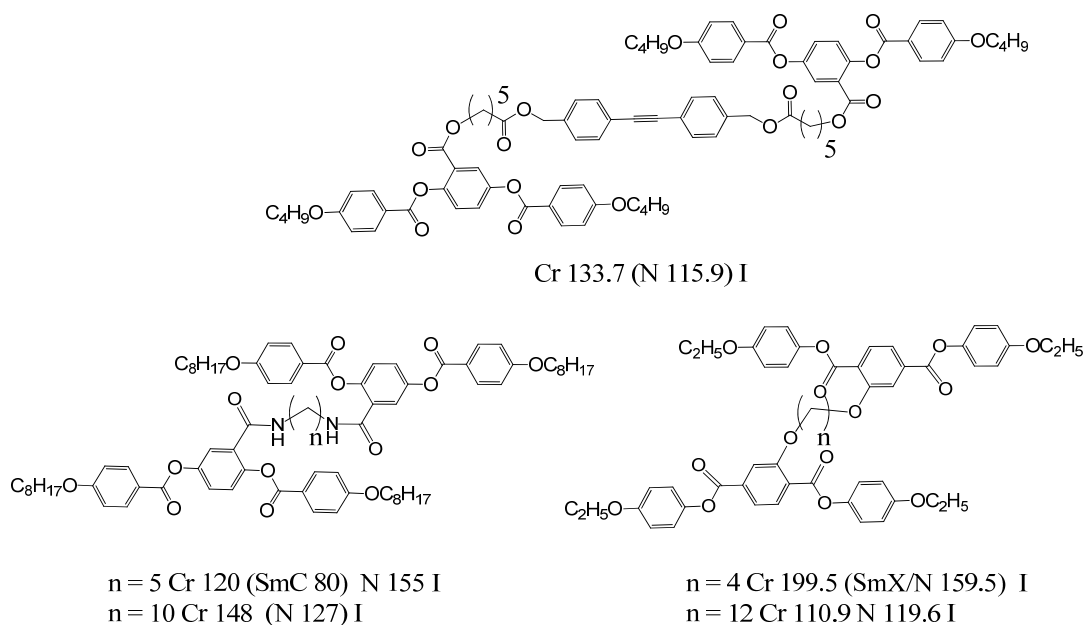
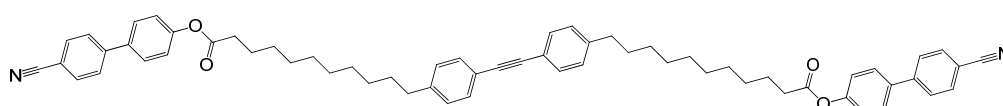


**Figure 4.6** The transition temperatures of **24** (top) and the H-shaped LC oligomers comprising PDAB side-on mesogenic units (bottom)

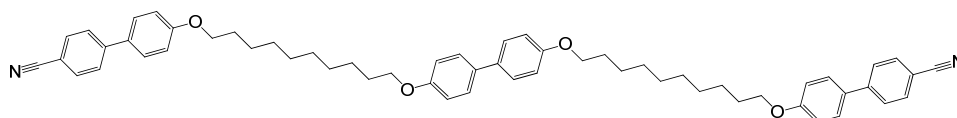
In analogy to the T-shaped dimers, the nematic phase stability of H-shaped dimers decreases with increasing the length of the spacer, however the N-I transition enthalpy was not affected to the same extent. Comparison of **19** with the side-on dimers with long spacers, it can be seen that they all have N-I transition temperatures in the same range; the introduction of the diphenylacetylene in **19** not only added anisotropy to the system but also has broadened the molecular architecture, resulting in almost no contribution to the stability of the nematic phase.

Two cyanobiphenyl groups were linked to the biphenyl acetylene core with two long aliphatic chain spacers to give LC trimer **32**. This linear type of mesogenic trimers usually takes a stretched conformation in order to minimize the intramolecular energy. It has also been reported that such systems usually form stable nematic phases, which have quite high N-I transition temperatures, caused by the considerable polarisability of the three mesogenic cores aided by the anisotropy compared to the monomers or dimers.

C. Imrie and coworkers have studied the LC behaviour of a series of mesogenic trimers known as TCBO<sub>n</sub> [11]. The phase transition temperatures in the trimers show a pronounced odd-even effect depending on the length of the spacers, which determines the overall conformation of the molecule (in an all-trans manner or in a bent form).



Cr 174 N 206 I



Cr (155 SmA) 191 N 213 I

**Figure 4.7** Linear LC trimers with cyanobiphenyl groups, compound **32** (top) and TCBO10 (bottom)

TCBO10 (Fig 4.7 bottom) has similar melting point and N-I transition temperature compared to **32**, due to their closely related molecule structure. However a monotropic smectic A phase was observed in TCBO10, which may be due to the stronger lateral attraction between the alkyloxy biphenyl group compared to the biphenyl acetylene group. No smectic behaviour was observed in **32**.

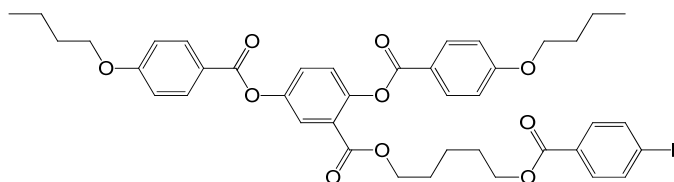
In addition, it is worthwhile to notice that the oligomers described in this chapter have a relatively high enthalpy of N-I transition in comparison with the monomers, especially for the trimer **32**. This might be due to the increased molecular alignment within the nematic phase, caused by the multiple mesogenic units which contributed to the overall transition enthalpy/entropy of the system.

#### 4.5 Concluding remarks

Three LC oligomers based on diphenylacetylene core were developed and in their mesophase behaviour studied. The T-shaped and H-shaped oligomers exhibit stable nematic phases, which is a strong evidence on the favoured parallel position of the rigid mesogenic units within the molecule, allowed by flexible aliphatic spacers. The linear conformation generated in the LC trimer results in high mesophase stability, melting point and meophase range. As LC oligomers with only a few mesogenic units, the rigid core unit plays a crucial role in the mesophase behaviour, which somewhat obscures the effect of the mesogenic groups attached to it; such a problem is not quite evident when the dendritic structure is introduced, on which much more mesogenic groups can be attached on. However, the rigidity of the core can still affect the overall topology of the system; the influence of the diphenylacetylene core on higher mesogenic structures will be studied in later chapters.

## 4.6 Experimental

### 5-(2,5-Di(4'-butoxybenzoyloxy)benzoyloxy)pentyl 4-iodobenzoate (**18**)

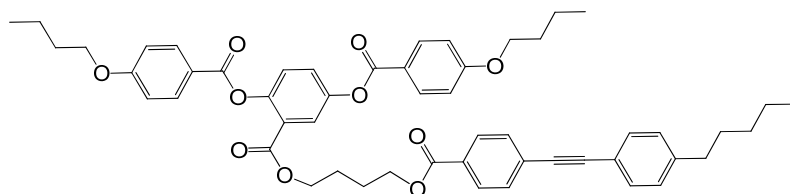


A solution of **12** (1.09 g; 1.84 mmol), 4-iodobenzoic acid (0.5 g; 2 mmol), *N,N'*-dicyclohexylcarbodiimide (0.5 g; 2.4 mmol), 4-(dimethylamino)pyridine (0.46 g; 1.84 mmol) in dichloromethane (30 mL) was stirred at room temperature for 20 h. The suspension was filtered and the filtrate was washed sequentially with water (30 mL), 5% AcOH solution (40 mL), water (40 mL), and dried over  $\text{MgSO}_4$ . After evaporation of the solvent, the crude product was purified by column chromatography eluting with dichloromethane. Evaporation of the solvent afforded **18** as a white solid.

Yield: 1.1 g (73%)

$^1\text{H}$  NMR (400 MHz,  $\text{CDCl}_3$ )  $\delta\text{H}$  (ppm): 8.14 (d ( $J = 8.9$  Hz) d ( $J = 4.2$  Hz), 4 H, *ArH*); 7.88 (d ( $J = 2.9$  Hz), 1 H, *ArH*); 7.77 (d ( $J = 8.5$  Hz), 2 H, *ArH*); 7.70 (d ( $J = 8.5$  Hz), 2 H, *ArH*); 7.46 (d ( $J = 8.7$  Hz) d ( $J = 2.9$  Hz), 1 H, *ArH*); 7.25 (d ( $J = 8.5$  Hz), 1 H, *ArH*); 6.97 (d ( $J = 8.9$  Hz) d ( $J = 4.8$  Hz), 4 H, *ArH*); 4.19 (m, 4 H,  $-\text{COOCH}_2-$ ); 4.04 (m, 4 H,  $-\text{C}_6\text{H}_4\text{OCH}_2-$ ); 1.79 (m, 4 H,  $-\text{C}_6\text{H}_4\text{OCH}_2\text{CH}_2-$ ); 1.52 (m, 8 H,  $-\text{C}_6\text{H}_4\text{OCH}_2\text{CH}_2\text{CH}_2-$ ,  $-\text{COOCH}_2\text{CH}_2-$ ); 1.38 (m, 2 H,  $-\text{COOCH}_2\text{CH}_2\text{CH}_2-$ ); 0.98 (m, 6 H,  $-\text{CH}_3$ )

**5-(2,5-Di(4-butoxybenzoyloxy)benzoyloxy)pentyl 4-(4-pentylphenylethyl-nyl)-benzoate (19)**



A Schlenk flask containing 5-(2,5-Di(4-butoxybenzoyloxy)benzoyloxy)pentyl 4-iodobenzoate (**18**) (1 g; 1.2 mmol), Pd(PPh<sub>3</sub>)<sub>2</sub>Cl<sub>2</sub> (0.022 g; 0.03 mmol) and CuI (0.006 g; 0.03 mmol) was degassed and flushed with argon. Triethylamine (20 mL), flushed with argon for 20 min, was transferred via a cannula. 1-Ethynyl-4-pentyl benzene (0.3 mL; 1.5 mmol) was added by syringe. The reaction mixture was stirred at room temperature for 20 h. The solvent was removed, and the residue dissolved in dichloromethane and passed through a short silica gel column. The column was flushed with hexane and then with dichloromethane. The dichloromethane solution was removed by evaporation under reduced pressure, and the crude product was recrystallised from dichloromethane/ethanol to yield **19** as white crystals.

Yield: 0.41 g (40%).

<sup>1</sup>H NMR (400 MHz, CDCl<sub>3</sub>) δH (ppm): 8.15 (d (J = 8.8 Hz) d (J = 6.3 Hz), 4 H, ArH); 7.98 (d (J = 8.5 Hz), 2 H, ArH); 7.90 (d (J = 2.9 Hz), 1 H, ArHc); 7.55 (d (J = 8.5 Hz), 2 H, ArH); 7.46 (m, 3 H, ArH); 7.26 (d (J = 14.4 Hz) d (J = 5.7 Hz), 1 H, ArHa); 7.17 (d (J = 8.1 Hz), 2 H, ArH); 6.97 (d (J = 8.9 Hz) d (J = 1.7 Hz), 4 H, ArH); 4.22 (m, 4 H, -COOCH<sub>2</sub>-); 4.04 (m, 4 H, -C<sub>6</sub>H<sub>4</sub>OCH<sub>2</sub>-); 2.62 (t (J = 7.7 Hz), 2 H, -C<sub>6</sub>H<sub>4</sub>CH<sub>2</sub>-); 1.80 (m, 4 H, -C<sub>6</sub>H<sub>4</sub>OCH<sub>2</sub>CH<sub>2</sub>-); 1.57 (m, 10 H, -C<sub>6</sub>H<sub>4</sub>OCH<sub>2</sub>CH<sub>2</sub>CH<sub>2</sub>-, -COOCH<sub>2</sub>CH<sub>2</sub>-, -C<sub>6</sub>H<sub>4</sub>CH<sub>2</sub>CH<sub>2</sub>-); 1.28 (m, 6 H, -COOCH<sub>2</sub>CH<sub>2</sub>CH<sub>2</sub>-, -C<sub>6</sub>H<sub>4</sub>CH<sub>2</sub>CH<sub>2</sub>CH<sub>2</sub>CH<sub>2</sub>-); 0.99 (m, 6 H, -COOCH<sub>2</sub>CH<sub>2</sub>CH<sub>2</sub>CH<sub>3</sub>-, -C<sub>6</sub>H<sub>4</sub>CH<sub>2</sub>CH<sub>2</sub>CH<sub>2</sub>CH<sub>2</sub>CH<sub>3</sub>-), 0.88 (t (J = 6.9 Hz), 3 H, -C<sub>6</sub>H<sub>4</sub>CH<sub>2</sub>CH<sub>2</sub>CH<sub>2</sub>CH<sub>2</sub>CH<sub>3</sub>)

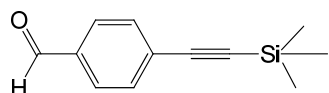
<sup>13</sup>C NMR (100.4 MHz, CDCl<sub>3</sub>) δC (ppm): 166.1, 164.7, 164.2, 163.7, 144.1, 132.5, 131.7, 132.5, 129.5, 128.6, 125.1, 121.5, 121.1, 114.5, 114.4, 100.0, 92.72, 88.20, 68.12, 65.29, 64.90, 36.85, 35.99, 31.51, 31.20, 30.98, 28.37, 28.21, 22.59, 22.56, 19.27, 14.09, 13.90, 10.40

ESI MS: m/z = 867.4 (M + H)<sup>+</sup>

IR (cm<sup>-1</sup>): 3063, 2955, 2932, 2870, 2214, 1713, 1605, 1512, 1474, 1420, 1250, 1157, 1126, 1065, 964, 934, 841, 764, 687, 640, 548, 509

Elemental analysis: calcd (%) for C<sub>54</sub>H<sub>58</sub>O<sub>10</sub>: C 74.80, H 6.74; found (%): C 74.80, H 6.69

#### 4-Trimethylsilylethynyl benzaldehyde (**20**)



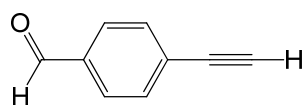
4-Bromobenzaldehyde (10 g; 54 mmol) was dissolved in triethylamine (50 mL) and argon was flushed for 30 min. A catalytic mixture of Pd(PPh<sub>3</sub>)<sub>2</sub>Cl<sub>2</sub> (0.06 g; 0.08 mmol), PPh<sub>3</sub> (0.11 g; 0.41 mmol) and CuI (0.02 g; 0.1 mmol) was added and the temperature raised to 65 °C. Trimethylsilyl acetylene (10 mL; 67.5 mmol) was added via syringe and the mixture was stirred at 65 °C for 5 h. Upon cooling, triethylamine hydrobromide was filtered off. The solvent was distilled at room temperature under reduced pressure until precipitation occurred. The solid residue was washed several times with water and dried at 50 °C in vacuo to afford **20** as a yellow powder.

Yield: 10.5 g (96%)

<sup>1</sup>H NMR (400 MHz, CDCl<sub>3</sub>) δ<sub>H</sub> (ppm): 10.0 (s, 1 H, -CHO); 7.82 (d (J = 8.4 Hz), 2 H, Ar H); 7.60 (d (J = 8.3 Hz), 2 H, ArH); 0.27 (s, 9 H, -Si(CH<sub>3</sub>)<sub>3</sub>)

<sup>13</sup>C NMR (100.4 MHz, CDCl<sub>3</sub>) δ<sub>C</sub> (ppm): 191.6, 135.6, 132.6, 129.5, 129.4, 103.9, 99.13, -0.134

#### 4-Ethynyl benzaldehyde (**21**)



**20** (10 g; 49 mmol) was treated with potassium carbonate (0.7 g; 5 mmol) in methanol (60 mL) at room temperature for 3 h. The solvent was removed by evaporation under vacuum, and the crude was extracted with dichloromethane. The

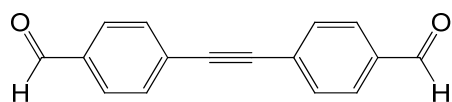
solution was washed with NaHCO<sub>3</sub>, dried over MgSO<sub>4</sub>, and passed through a short silica gel pad to yield **21** as a yellow powder.

Yield: 4.93 g (77%)

<sup>1</sup>H NMR (400 MHz, CDCl<sub>3</sub>) δ<sub>H</sub> (ppm): 10.0 (s, 1 H, -CHO); 7.85 (d (J = 8.4 Hz), 2 H, ArH); 7.64 (d (J = 8.3 Hz), 2 H, ArH); 3.30 (s, 1 H, -C≡CH)

<sup>13</sup>C NMR (100.4 MHz, CDCl<sub>3</sub>) δ<sub>C</sub> (ppm): 191.5, 132.8, 129.6, 82.70, 81.15

#### **Tolane-4,4'-dicarbaldehyde (22)**



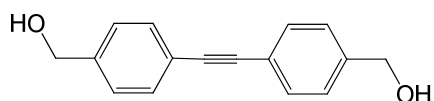
4-Bromobenzaldehyde (2.53 g; 13.7 mmol) was dissolved in triethylamine (20 mL) and the solution was flushed with argon for 15 min. A catalytic mixture of Pd(PPh<sub>3</sub>)<sub>2</sub>Cl<sub>2</sub> (0.06 g; 0.08 mmol), PPh<sub>3</sub> (0.11 g; 0.41 mmol) and CuI (0.02 g; 0.1 mmol) was added and the temperature raised to 65 °C. 4-Ethynyl benzaldehyde (**21**) (1.79 g; 13.7 mmol) dissolved in toluene (10 mL) was added and the mixture was stirred at 65 °C for 20 h. Upon cooling, the mixture was filtered and the precipitate washed with triethylamine (3 × 40 mL), and washed with water (3 × 100 mL). The remaining solid was dried in vacuo to yield **22** as a yellow powder.

Yield: 2.95 g (92%)

<sup>1</sup>H NMR (400 MHz, CDCl<sub>3</sub>) δ<sub>H</sub> (ppm): 10.0 (s, 2 H, -CHO); 7.90 (d (J = 8.5 Hz), 4 H, ArH); 7.10 (d (J = 8.3 Hz), 4 H, ArH)

<sup>13</sup>C NMR (100.4 MHz, CDCl<sub>3</sub>) δ<sub>C</sub> (ppm): 191.5, 136.0, 132.4, 129.7, 128.8, 92.2

### 4,4'-bis(hydroxymethyl)tolane (**23**)

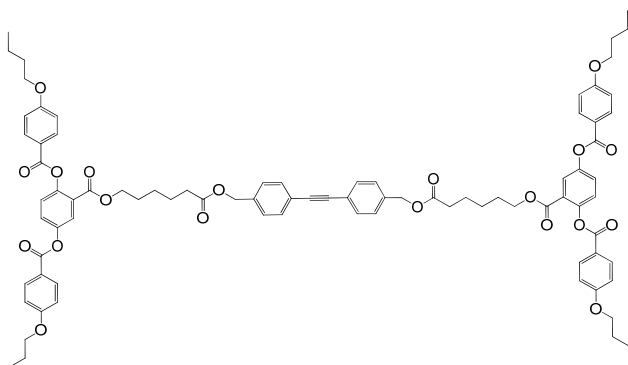


Tolan-4,4'-dicarbaldehyde (**22**) (0.1 g; 0.43 mmol) and sodium borohydride (16 mg; 0.43 mmol) were dissolved in tetrahydrofuran (10 mL), and the mixture was stirred at room temperature for 20 h under argon. The solution was acidified with water/hydrochloric acid, the aqueous layer was saturated with sodium chloride, and the mixture was extract twice with dichloromethane. After evaporation of the solvent, the crude product was recrystallised from ethanol to afford **23** as yellow crystals.

Yield: 0.08 g (79%)

<sup>1</sup>H NMR (400 MHz, (CD<sub>3</sub>)<sub>2</sub>SO) δH (ppm): 7.51 (d (J = 8.2 Hz), 2 H, ArH); 7.36 (d (J = 8.2 Hz), 2 H, ArH); 5.30 (t (J = 5.7 Hz), 2 H, -OH); 4.53 (d (J = 5.7 Hz), 4 H, -CH<sub>2</sub>OH)

### 4,4'-(1,2-ethynediyl)benzylbis(6-(2,5-Di(4-butoxybenzoyloxy)benzoyloxy)hexan)-oate (**24**)



A solution of 6-(2,5-Di(4-butoxybenzoyloxy)benzoyloxy)hexanoic acid (**6**) (0.2 g; 0.32 mmol), N,N'-dicyclohexylcarbodiimide (0.08 g; 0.38 mmol), 4-(dimethylamino)pyridine (0.04 g; 0.32 mmol) and 4,4'-bis(hydroxymethyl)tolane (**23**) (0.038 g; 0.16 mmol) in dichloromethane (10 mL) was stirred at room temperature for 20 h under nitrogen. The mixture was filtered and the filtrate was washed with water, 5% AcOH solution, water, and dried over MgSO<sub>4</sub>. After evaporation of the

solvent, the crude product was washed twice with hot ethanol to yield **24** as a white solid.

Yield: 0.14 g (61%).

$^1\text{H}$  NMR (400 MHz,  $\text{CDCl}_3$ )  $\delta\text{H}$  (ppm): 8.15 (m, 8 H, ArH); 7.89 (d (J = 2.9 Hz), 2 H, ArHc); 7.50 (d (J = 8.3 Hz), 4 H, ArH); 7.45 (d (J = 8.7 Hz) d (J = 2.9 Hz), 2 H, ArHb); 7.30 (d (J = 8.4 Hz), 4 H, ArH); 7.26 (d (J = 8.7 Hz), 2 H, ArHa); 6.97 (d (J = 8.9 Hz) d (J = 1.2 Hz), 8 H, ArH); 5.08 (s, 4 H,  $-\text{COOCH}_2\text{C}_6\text{H}_4-$ ); 4.16 (t (J = 6.6 Hz), 4 H,  $-\text{COOCH}_2\text{CH}_2-$ ); 4.04 (m, 8 H,  $-\text{C}_6\text{H}_4\text{OCH}_2-$ ); 2.29 (t (J = 7.5 Hz), 4 H,  $-\text{CH}_2\text{COO}-$ ); 1.81 (m, 8 H,  $-\text{C}_6\text{H}_4\text{OCH}_2\text{CH}_2-$ ); 1.52 (m, 16 H,  $-\text{C}_6\text{H}_4\text{OCH}_2\text{CH}_2\text{CH}_2-$ ,  $-\text{COOCH}_2\text{CH}_2\text{CH}_2\text{CH}_2\text{CH}_2\text{COO}-$ ); 1.29 (m, 4 H,  $-\text{CH}_2\text{CH}_2\text{CH}_2\text{CH}_2\text{CH}_2-$ ); 0.99 (t (J = 7.4 Hz) d (J = 2.1 Hz), 12 H,  $-\text{CH}_3$ )

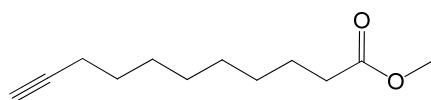
$^{13}\text{C}$  NMR (100.4 MHz,  $\text{CDCl}_3$ )  $\delta\text{C}$  (ppm): 173.3, 165.0, 064.7, 164.2, 163.8, 163.7, 148.4, 148.2, 136.3, 132.5, 131.9, 128.1, 127.3, 125.1, 125.0, 123.1, 121.4, 121.1, 114.5, 114.4, 89.51, 68.13, 68.10, 65.73, 65.32, 34.08, 31.21, 28.20, 25.51, 24.54, 19.29, 13.94

ESI MS:  $m/z = 1465.6$  (M + Na) $^+$

IR ( $\text{cm}^{-1}$ ): 3071, 2955, 2932, 2870, 1720, 1605, 1512, 1466, 1420, 1242, 1157, 1057, 1003, 964, 841, 818, 756, 687, 640

Elemental analysis: calcd (%) for  $\text{C}_{86}\text{H}_{90}\text{O}_{20}$ : C 71.55, H 6.28; found (%): C 71.34, H 6.29

### Methyl 10-undecynoate (**25**)



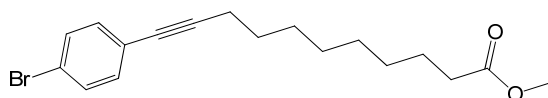
Concentrated sulfuric acid (2.0 mL) was added to a solution of 10-undecynoic acid (12.0 g; 65.8 mmol) in methanol (300 mL). The mixture was heated to reflux for 2 h, poured into a saturated  $\text{NaHCO}_3$  water solution and extracted with dichloromethane. The organic layer was dried over  $\text{MgSO}_4$  and after removal of the solvent by evaporation under reduced pressure, the product was obtained from the residue by

column chromatography over flash-grade silica gel, eluting with dichloromethane/petroleum ether (1:1), to yield **25** as a colourless oil.

Yield: 12.0 g (95%)

$^1\text{H}$  NMR (400 MHz,  $\text{CDCl}_3$ )  $\delta\text{H}$  (ppm): 3.67 (s, 3 H,  $-\text{COOCH}_3$ ); 2.30 (t ( $J = 7.5$  Hz), 2 H,  $-\text{CH}_2\text{COO}-$ ); 2.18 (t ( $J = 7.1$  Hz) d ( $J = 2.7$  Hz), 2 H,  $\text{HC}\equiv\text{C}-\text{CH}_2-$ ); 1.99 (t ( $J = 2.7$  Hz), 1 H,  $\text{HC}\equiv\text{C}-$ ); 1.61 (m, 2 H,  $-\text{CH}_2\text{CH}_2\text{COO}-$ ); 1.52 (m, 2 H,  $\text{HC}\equiv\text{C}-\text{CH}_2\text{CH}_2-$ ); 1.38 (m, 2 H,  $-\text{CH}_2\text{CH}_2\text{CH}_2\text{COO}-$ ); 1.31 (m, 6H,  $\text{HC}\equiv\text{C}-\text{CH}_2\text{CH}_2\text{CH}_2\text{CH}_2\text{CH}_2-$ )

### Methyl 11-(4-bromophenyl)-10-undecynoate (**26**)

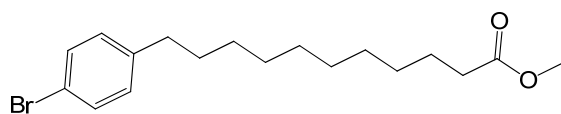


Methyl 10-undecynoate (**25**) (6.0 g; 31.2 mmol) was added to a solution of 4-bromoiodobenzene (17.3 g; 61.2 mmol), CuI (0.24 g; 1.26 mmol),  $\text{Pd}(\text{PPh}_3)_4$  (0.7 g; 0.61 mmol) in piperidine (100 mL) and the resulting mixture was stirred at room temperature for 20 h under argon. The mixture was poured into a saturated solution of  $\text{NH}_4\text{Cl}$  and extracted with dichloromethane. The organic layer was washed with a saturated solution of  $\text{NH}_4\text{Cl}$ , water and dried with  $\text{MgSO}_4$ . After removal of the solvent by evaporation under vacuum, the product was isolated from the residue by column chromatography, eluting with petroleum ether, to yield the **25** as a colourless oil.

Yield: 9.86 g (91%)

$^1\text{H}$  NMR (400 MHz,  $\text{CDCl}_3$ )  $\delta\text{H}$  (ppm): 7.40 (d ( $J = 8.4$  Hz), 2 H,  $\text{ArH}$ ); 7.24 (d ( $J = 8.5$  Hz), 2 H,  $\text{ArH}$ ); 3.66 (s, 3 H,  $-\text{COOCH}_3$ ); 2.37 (t ( $J = 7.1$  Hz), 2 H,  $-\text{C}\equiv\text{C}-\text{CH}_2-$ ); 2.30 (t ( $J = 7.5$  Hz), 2 H,  $-\text{CH}_2\text{COO}-$ ); 1.60 (m, 4 H,  $-\text{CH}_2\text{CH}_2\text{COO}-$ ,  $-\text{C}\equiv\text{C}-\text{CH}_2\text{CH}_2-$ ); 1.44 (m, 2 H,  $-\text{CH}_2\text{CH}_2\text{CH}_2\text{COO}-$ ); 1.32 (m, 6 H,  $-\text{C}\equiv\text{C}-\text{CH}_2\text{CH}_2\text{CH}_2\text{CH}_2\text{CH}_2-$ )

### Methyl 11-(4-bromophenyl)undecanoate (**27**)

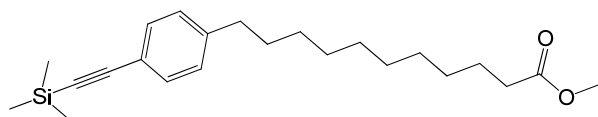


A mixture of methyl 11-(4-bromophenyl)-10-undecynoate (**26**) (9.50 g, 27.4 mmol) and palladium (10%) on activated carbon (2 g) in tetrahydrofuran (200 mL) was stirred at room temperature for 48 h under a hydrogen atmosphere. After removal of the catalyst by filtration, the solvent was removed under reduced pressure. The product was isolated from the residue by column chromatography over flash-grade silica gel, eluting with dichloromethane/petroleum ether (1:1). Evaporation of the solvent afforded **27** as colorless needles.

Yield: 8.66 g (89%)

$^1\text{H}$  NMR (400 MHz,  $\text{CDCl}_3$ )  $\delta\text{H}$  (ppm): 7.38 (d ( $J = 8.3$  Hz), 2 H,  $\text{ArH}$ ); 7.04 (d ( $J = 8.3$  Hz), 2 H,  $\text{ArH}$ ); 3.66 (s, 3 H,  $-\text{COOCH}_3$ ); 2.54 (t ( $J = 7.7$  Hz), 2 H,  $\text{BrC}_6\text{H}_4\text{CH}_2-$ ); 2.30 (t ( $J = 7.6$  Hz), 2 H,  $-\text{CH}_2\text{COO}-$ ); 1.59 (m, 4 H,  $-\text{CH}_2\text{CH}_2\text{COO}-$ ,  $\text{BrC}_6\text{H}_4\text{CH}_2\text{CH}_2-$ ); 1.27 (m, 12 H,  $\text{BrC}_6\text{H}_4\text{CH}_2\text{CH}_2(\text{CH}_2)_6-$ )

### Methyl 11-(4-(trimethylsilylethynyl)phenyl)undecanoate (**28**)



Methyl 11-(4-bromophenyl)undecanoate (**27**) (4 g; 11.3 mmol) was dissolved in triethylamine (50 mL) and the solution was flushed with argon for 15 min. A catalytic mixture of  $\text{Pd}(\text{PPh}_3)_2\text{Cl}_2$  (0.08 g; 0.11 mmol),  $\text{PPh}_3$  (0.15 g; 0.57 mmol) and  $\text{CuI}$  (0.03 g; 0.14 mmol) was added and the temperature raised to 70 °C. Trimethylsilyl acetylene (3.2 mL; 22.5 mmol) was introduced via syringe and the mixture stirred at 70 °C for 20 h. Upon cooling, the precipitate of triethylamine hydrobromide was filtered off. The solvent was distilled at room temperature under reduced pressure until precipitation occurred. The product was purified by column chromatography, eluting with 1:1 dichloromethane/petroleum ether, to yield **28** as a colorless oil.

Yield: 3.1 g (76%)

$^1\text{H}$  NMR (400 MHz,  $\text{CDCl}_3$ )  $\delta\text{H}$  (ppm): 7.37 (d ( $J = 8.3$  Hz), 2 H,  $\text{ArH}$ ); 7.10 (d ( $J = 8.3$  Hz), 2 H,  $\text{ArH}$ ); 3.66 (s, 3 H,  $-\text{COOCH}_3$ ); 2.57 (t ( $J = 7.7$  Hz), 2 H,  $-\text{C}_6\text{H}_4\text{CH}_2-$ ); 2.30 (t ( $J = 7.5$  Hz), 2 H,  $-\text{CH}_2\text{COO}-$ ); 1.59 (m, 4 H,  $-\text{CH}_2\text{CH}_2\text{COO}-$ ,  $-\text{C}_6\text{H}_4\text{CH}_2\text{CH}_2-$ ); 1.27 (m, 12 H,  $-\text{C}_6\text{H}_4\text{CH}_2\text{CH}_2(\text{CH}_2)_6-$ ); 0.24 (s, 9 H,  $-\text{Si}(\text{CH}_3)_3$ )

### Methyl 11-(4-ethynylphenyl)undecanoate (**29**)

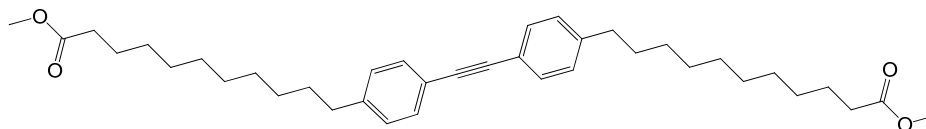


The TMS-protected acetylene **28** (2.5 g; 6.7 mmol) was treated with potassium carbonate (0.1 g; 0.67 mmol) in methanol (20 mL) at room temperature for 20 h. The solvent was removed by evaporation under reduced pressure, and dichloromethane was added. The solution was washed with  $\text{NaHCO}_3$ , dried over  $\text{MgSO}_4$ , and passed a short silica gel pad. Evaporation of the solvent afforded **29** as a yellow powder.

Yield: 1.89 g (94%)

$^1\text{H}$  NMR (400 MHz,  $\text{CDCl}_3$ )  $\delta\text{H}$  (ppm): 7.40 (d ( $J = 8.2$  Hz), 2 H,  $\text{ArH}$ ); 7.13 (d ( $J = 8.2$  Hz), 2 H,  $\text{ArH}$ ); 3.66 (s, 3 H,  $-\text{COOCH}_3$ ); 3.03 (s, 1H,  $-\text{C}\equiv\text{CH}$ ); 2.59 (t ( $J = 7.7$  Hz), 2 H,  $-\text{C}_6\text{H}_4\text{CH}_2-$ ); 2.30 (t ( $J = 7.6$  Hz), 2 H,  $-\text{CH}_2\text{COO}-$ ); 1.59 (m, 4 H,  $-\text{CH}_2\text{CH}_2\text{COO}-$ ,  $-\text{C}_6\text{H}_4\text{CH}_2\text{CH}_2-$ ); 1.27 (m, 12 H,  $-\text{C}_6\text{H}_4\text{CH}_2\text{CH}_2(\text{CH}_2)_6-$ )

### Bis(4-(10-methoxycarbonyldecyl)phenyl)acetylene (**30**)



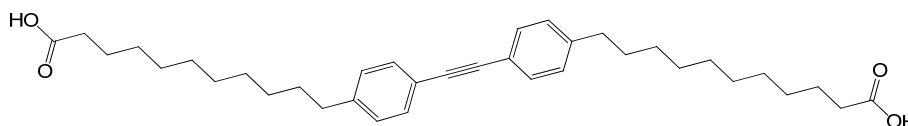
Methyl 11-(4-bromophenyl)undecanoate (**27**) (4.7 g; 13.2 mmol) and methyl 11-(4-ethynylphenyl)undecanoate (**29**) (4.2 g; 14 mmol) were dissolved in triethylamine (50 mL) and the solution flushed with argon for 15 min. A catalytic mixture of  $\text{Pd}(\text{PPh}_3)_2\text{Cl}_2$  (0.3 g; 0.43 mmol),  $\text{PPh}_3$  (0.44 g; 1.67 mmol) and  $\text{CuI}$  (0.08 g; 0.42

mmol) was added and mixture was heated at 65 °C and stirred for 20 h. Upon cooling, the solvent was removed by evaporation under vacuum, and the product was obtained from the crude by column chromatography eluting with 1:1 dichloromethane/petroleum ether. Evaporation of the solvent yielded **30** as a white powder.

Yield: 5.92 g (74%)

<sup>1</sup>H NMR (400 MHz, CDCl<sub>3</sub>) δH (ppm): 7.43 (d (J = 8.2 Hz) d (J = 1.8 Hz), 4 H, ArH); 7.14 (d (J = 8.2 Hz) d (J = 2.5 Hz), 4 H, ArH); 3.66 (s, 6 H, -COOCH<sub>3</sub>); 2.60 (t (J = 7.7 Hz), 4 H, -C<sub>6</sub>H<sub>4</sub>CH<sub>2</sub>-); 2.30 (t (J = 7.6 Hz), 4 H, -CH<sub>2</sub>COO-); 1.60 (m, 8 H, -CH<sub>2</sub>CH<sub>2</sub>COO-, -C<sub>6</sub>H<sub>4</sub>CH<sub>2</sub>CH<sub>2</sub>-); 1.27 (m, 24 H, -C<sub>6</sub>H<sub>4</sub>CH<sub>2</sub>CH<sub>2</sub>(CH<sub>2</sub>)<sub>6</sub>-)

### Bis(4-(10-hydroxycarbonyldecyl)phenyl)acetylene (**31**)

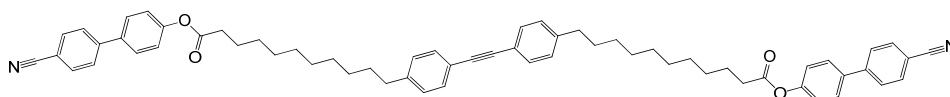


A flask was charged with the appropriate amount of bis(4-(10-methoxycarbonyldecyl)phenyl)acetylene (**30**) (0.2 g; 0.52 mmol), KOH (0.2 g; 8.7 mmol) and ethanol/water (13.05 mL/1.45 mL) to give a 0.2 M solution of the diester. The flask was capped and the mixture was allowed to stir at 35 °C for 20 h. The ethanol was removed under reduced pressure, and distilled water was added to the remaining residue until the entire mixture became homogeneous. The resulting aqueous mixture was acidified with 2M HCl until pH = 1 and the mixture stirred for 20 h. The white precipitate formed was filtered off, washed with dichloromethane, water and dried under vacuum to afford diacid **31** as a white powder.

Yield: 0.14 g (74%)

<sup>1</sup>H NMR (400 MHz, DMSO-d<sub>6</sub>) δH (ppm): 7.43 (d (J = 8.1 Hz), 4 H, ArH); 7.23 (d (J = 8.2 Hz), 4 H, ArH); 2.59 (t (J = 7.6 Hz), 4 H, -C<sub>6</sub>H<sub>4</sub>CH<sub>2</sub>-); 2.18 (t (J = 7.2 Hz), 4 H, -CH<sub>2</sub>COOH); 1.52 (m, 8 H, -C<sub>6</sub>H<sub>4</sub>CH<sub>2</sub>CH<sub>2</sub>-, -CH<sub>2</sub>CH<sub>2</sub>COOH); 1.25 (m, 24 H, -C<sub>6</sub>H<sub>4</sub>CH<sub>2</sub>CH<sub>2</sub>(CH<sub>2</sub>)<sub>6</sub>-)

**Bis(4-(10-(4,4-cyanobiphenyloxy)carbonyldecyl)phenyl)acetylene (32)**



The di-acid **31** (0.2 g; 0.37 mmol) and 4,4'-hydroxycyanobiphenol (0.16 g; 0.82 mmol) were dissolved in tetrahydrofuran (15 mL). N,N'-dicyclohexylcarbodiimide (0.18 g; 0.87 mmol) and 4-(dimethylamino)pyridine (0.09 g; 0.73 mmol) were added to the solution and the reaction mixture stirred under argon for 72 h at room temperature. The solvent was removed by evaporation under vacuum, and the crude product was purified by column chromatography eluting with 1:15 ethyl acetate/dichloromethane. Evaporation of the solvent yielded **32** as a white solid.

Yield: 0.13 g (39%)

$^1\text{H}$  NMR (400 MHz,  $\text{CDCl}_3$ )  $\delta\text{H}$  (ppm): 7.72 (d (J = 8.4 Hz), 4 H, ArH); 7.65 (d (J = 8.4 Hz), 4 H, ArH); 7.58 (d (J = 8.6 Hz), 4 H, ArH); 7.42 (d (J = 8.1 Hz), 4 H, ArH); 7.20 (d (J = 8.6 Hz), 4 H, ArH); 7.15 (d (J = 8.1 Hz), 4 H, ArH); 2.60 (m, 8 H, - $\text{C}_6\text{H}_4\text{CH}_2$ -,  $-\text{CH}_2\text{COO}$ -); 1.77 (m, 4 H,  $-\text{CH}_2\text{CH}_2\text{COO}$ -); 1.61 (m, 4 H, - $\text{C}_6\text{H}_4\text{CH}_2\text{CH}_2$ -); 1.30 (m, 24 H,  $-\text{C}_6\text{H}_4\text{CH}_2\text{CH}_2(\text{CH}_2)_6$ -)

$^{13}\text{C}$  NMR (100.4 MHz,  $\text{CDCl}_3$ )  $\delta\text{C}$  (ppm): 162.6, 158.6, 154.3, 151.3, 149.2, 132.7, 131.5, 128.5, 128.4, 127.8, 122.4, 93.03, 35.98, 34.49, 29.55, 29.49, 29.30, 29.17, 24.99

ESI MS:  $m/z = 923.5$  (M + Na) $^+$

IR ( $\text{cm}^{-1}$ ): 2916, 2847, 2222, 2114, 1921, 1751, 1605, 1489, 1381, 1204, 1165, 1111, 1003, 926, 826, 725, 648, 563, 532

Elemental analysis: calcd (%) for  $\text{C}_{62}\text{H}_{64}\text{N}_2\text{O}_4$ : C 82.63, H 7.16, N 3.11 found: C 82.27, H 7.16, N 2.82

# **Chapter 5**

## **LC Multipedes**

## 5.1 Summary

Once the protocol for building up the dendritic core had been established, the linear oligomers described in the previous chapter were studied as simple models for understanding the mesomorphic behaviour of the dendritic materials presented in the following chapters. The dendritic branching was sought to be incorporated onto the core to build up the complexity in order to study tri-, tetra- and hexa-substituted supermolecular liquid crystals.

The LC mutipedes using pentaerythritol (PE) as the branching unit described in this chapter contain three mesogens attached to PE by flexible spacers, leaving the fourth arm available for building up the diphenylacetylene segment that eventually will form the core of Janus liquid crystal dendrimers. Despite its tetrahedral geometry, PE has already been used as scaffold in LC mutipedes including tetramers and segregated mutipedes which carry two different mesogenic units [14]. The nature of the mesogenic group, the topology of the attachment to the core (end-on or side-on) and the spacer length were used to tailor the mesomorphic properties (Fig 5.1).

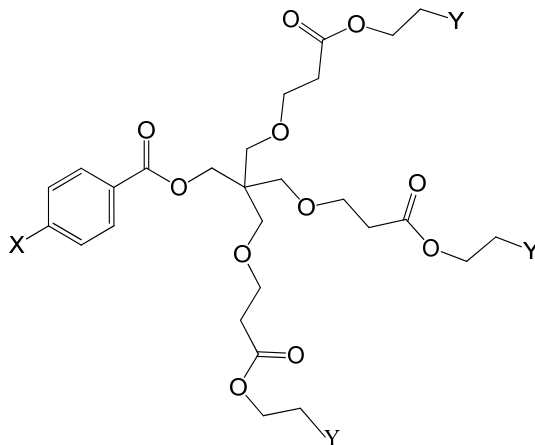


**Figure 5.1** Mutipede scaffold based on pentaerythritol

The role of the flexible spacer is to decouple the motions of the mesogens from those of the scaffold and allow the establishment of the necessary alignment of the rigid cores.

In this chapter, two series of mesogenic multipedes based on PE are described, one with iodophenyl at the focal point of the dendron and the second one with a phenylethynyl moiety; each series with cyanobiphenyl (end-on) mesogenic units and with PDAB (side-on) mesogenic units (Fig 5.2). Additionally, the mesomorphic properties of the dendrons without any mesogenic unit, just only partially fluorinated chains instead, are discussed. The dependence of the mesomorphic behaviour on mesogenic groups and on the PE scaffold is presented.

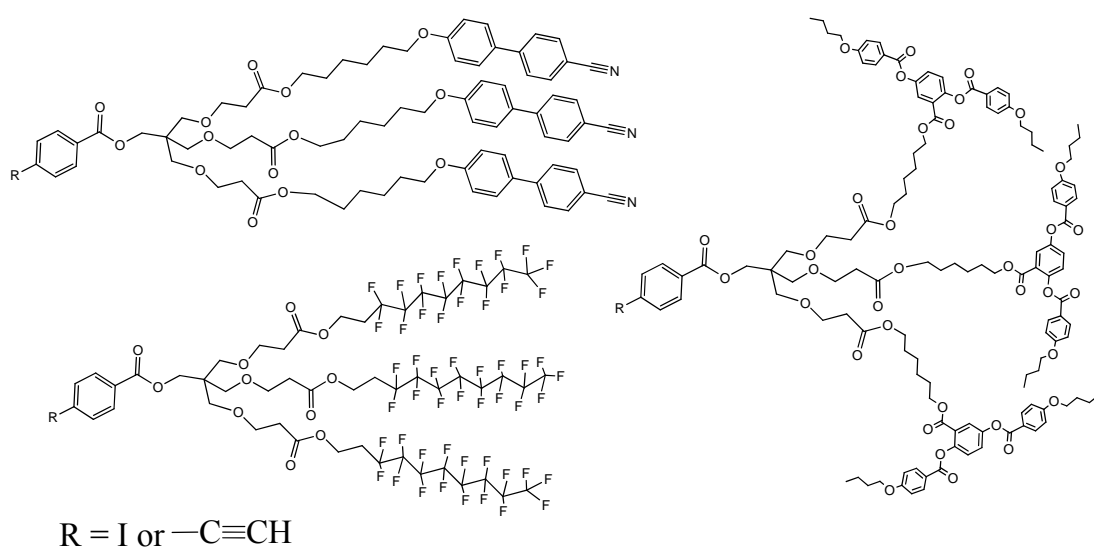
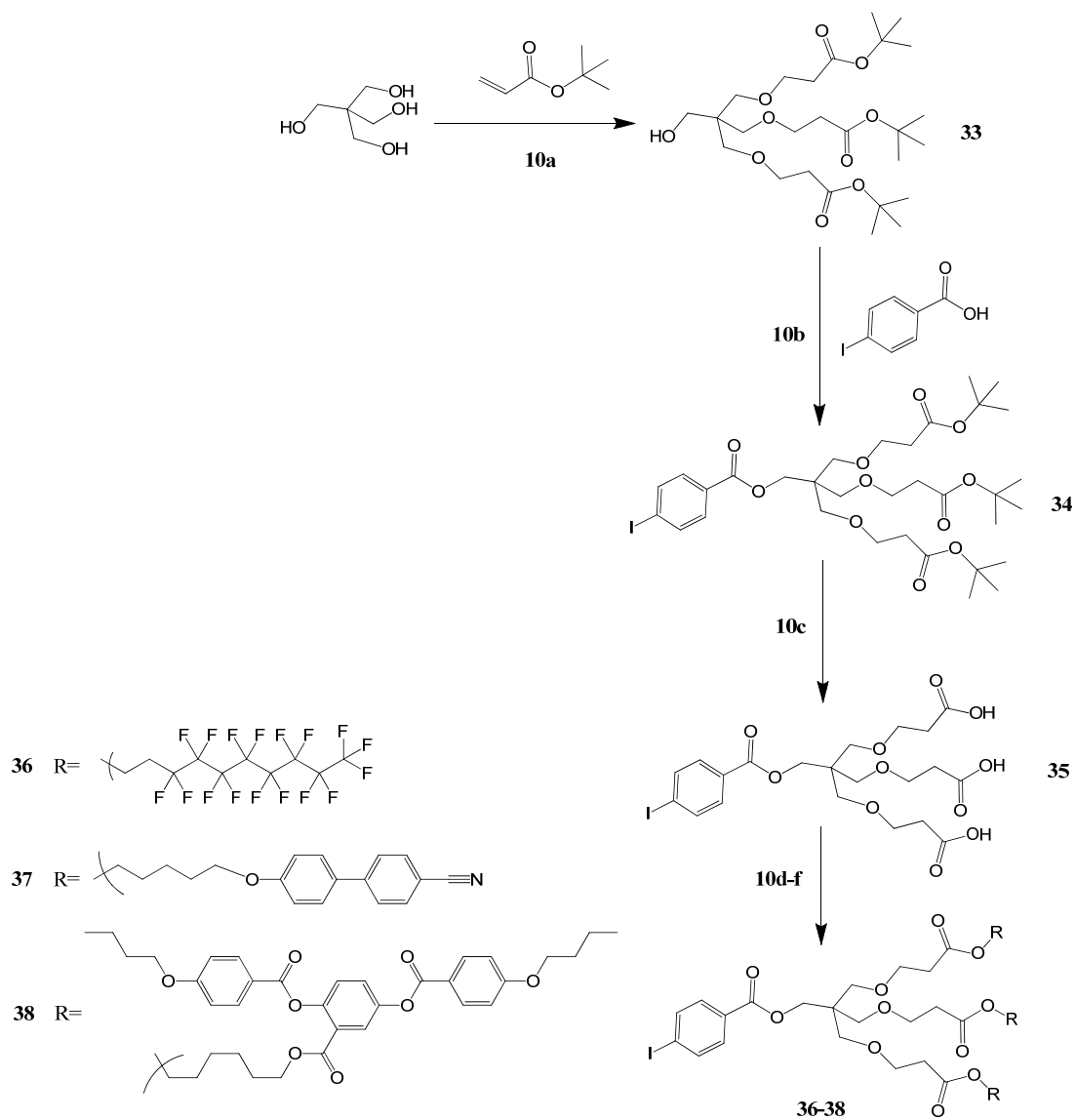


**Figure 5.2** LC multipedes

## 5.2 Synthesis

Synthesis of PE scaffold is based on nucleophilic conjugate addition of PE to t-butyl acrylate in presence of strong base (in order to provide a carboxylic acid group at the end of the arm to which a mesogens could be attached) following the method described by Dupuy [43]. The focal point of the trisubstituted PE **33** was esterified with either iodobenzoic acid or 4-ethynylbenzoic acid to afford **34** and **41** respectively. Deprotection of the carboxylic acid t-butyl ester yielded the dendritic tri-acids **35** and **42**, which were subjected to esterification with the mesogenic alcohols to yield the LC multipedes **36-38** and **43-46** (Schemes 10 and 11). The

fluorinated dendrons **36** and **43** were synthesised by esterification with 1H,1H,2H,2H-perfluorodecanol.



Reagents and conditions:

10a -  $[\text{nBu}_4\text{N}]^+[\text{OH}]^-$ ,  $\text{H}_2\text{O}$

10b - DCC, DMAP,  $\text{CH}_2\text{Cl}_2$

10c - TFA,  $\text{CH}_2\text{Cl}_2$

10d - 1H,1H,2H,2H-perfluorodecanol, DCC, DMAP, THF

10e -  $\text{HO}(\text{CH}_2)_6(\text{C}_6\text{H}_4)_2\text{CN}$ , DCC, DMAP, THF

10f - **16**, DCC, DMAP, THF

**Scheme 10**



Despite the increasing complexity of the molecules, their  $^1\text{H}$  NMR spectra consists of the combination of the sets of signals of the mesogens and those of the scaffold, which could be followed easily since they appear in a ratio of 3:1 respectively, proving the stoichiometry of the asymmetric dendritic structure (Fig 5.3). The protons of the starting mesogens usually preserve their chemical shift value for the dendrons.

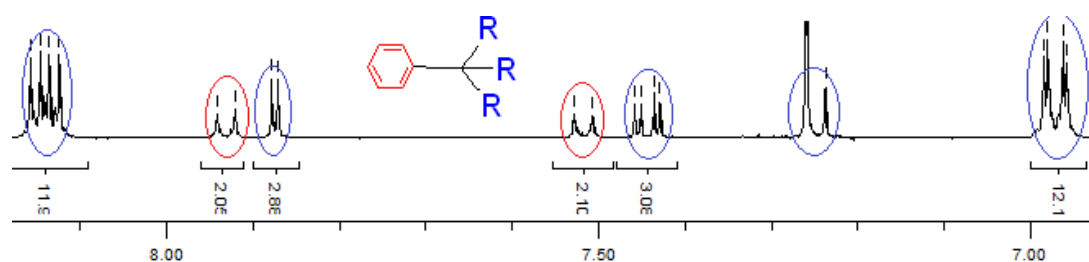


**Figure 5.3**  $^1\text{H}$  NMR spectrum of the aromatic region of compound **45**, showing the 1:3 ratio of the protons of the iodophenyl (red circle) and the mesogens (blue circle)

The structural integrity of the materials was also analyzed by MALDI-TOF MS to ensure the formation of the macromolecular species, and to discard the possibility of the presence of molecular species with missing arms arising from incomplete esterification in the final reaction step. For example, Fig 5.4 shows the MALDI-TOF MS of **43**, with the molecular ion and the calculated molecular mass.

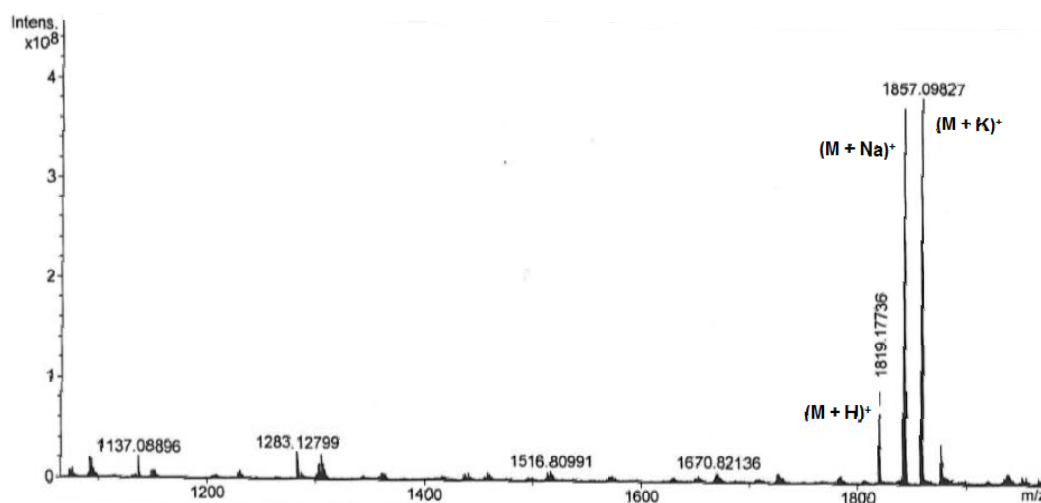


**Figure 5.4** MALDI-TOF MS of compound **43**

### 5.3 Mesomorphic behaviour

The dendritic LC multipedes were examined by differential scanning calorimetry and polarized light optical microscopy. The phase transitions and associated enthalpies are listed in Table 3.

No	g	Cr	SmA	N	Iso
<b>36</b>	-	• 37.4 [12.5]	• 49.1 [4.7]	-	•
<b>37</b>	• 1.7	-	•* 33.7 [0.7]	•* 37.1 [0.4]	•
<b>38</b>	• 0.5	-	-	• 58.2 [2.3]	•
<b>43</b>	-	• 31.5 [11.0]	• 49.2 [5.1]	-	•
<b>44</b>	• 2.0	-	•†	•† 43.9 [6.7]	•
<b>45</b>	• 3.2	-	-	• 56.1 [2.0]	•
<b>46</b>	• -2.1	-	-	• 59.8 [3.9]	•

Note (\*): Overlapped transition peak, phase transition analyzed at 1 °C/min; (†): Overlapping transitions, see discussion below

**Table 3** Transition temperatures (T/°C) and associated enthalpies ([ΔH/KJmol<sup>-1</sup>]) of the dendritic multipedes

Multiple LC phases were observed for the cyanobiphenyl derivatives **37** and **44** just below the clearing point. The phase transitions can be seen clearly by POM, however the associated endotherms in the DSC heat flow curves are partially overlapped at a rate of 10 °C/min. At slower heating/cooling rate, the SmA-N and N-Iso transitions of compound **37** were resolved and can be analyzed (Fig 5.4 top). Similarly the broad isotropisation transition observed for **44** shows signs of containing several

transitions, noticeable on the cooling thermogram recorded at 5 °C/min (possibly three transitions) and the position of the maxima could be determined at 1 °C/min (Fig 5.4, bottom). By analyzing the cooling curve at 1 °C/min, the peaks of phase transition of compound **44** can be roughly determined as 48.4 °C, 47.2 °C and 46.4 °C.

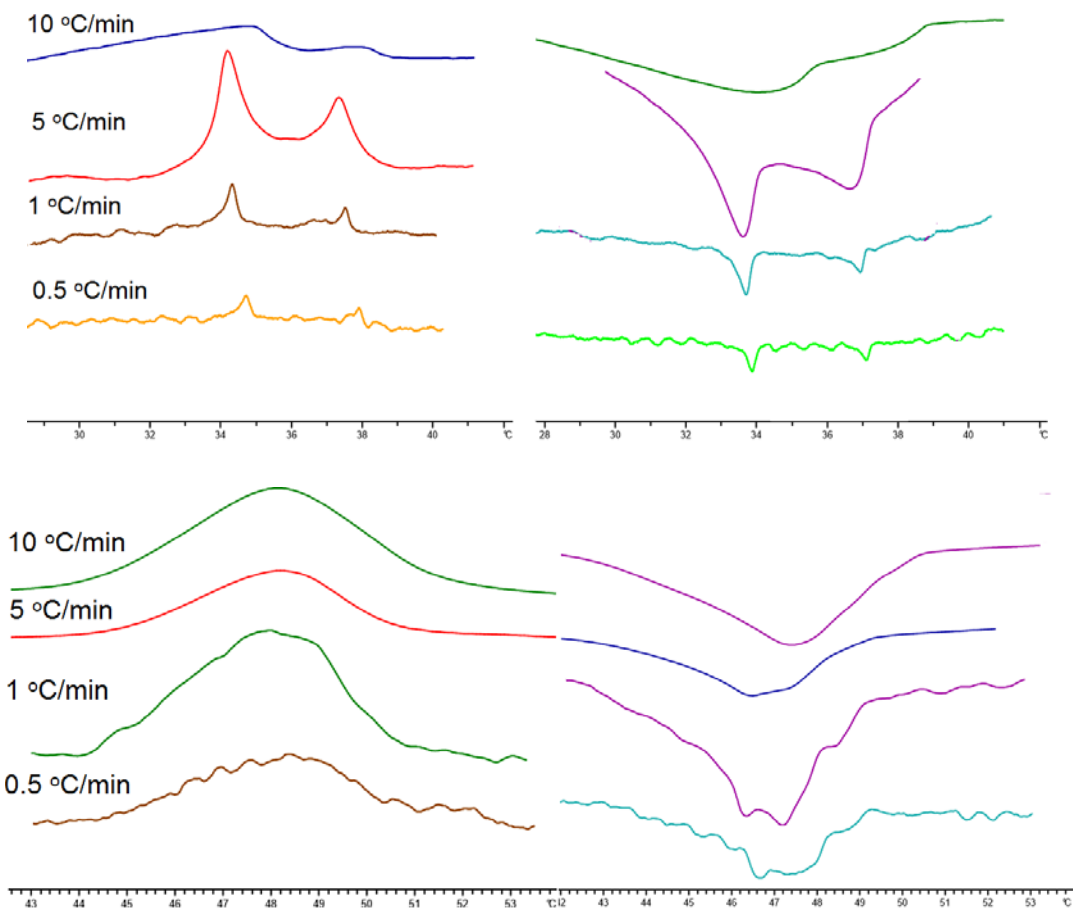
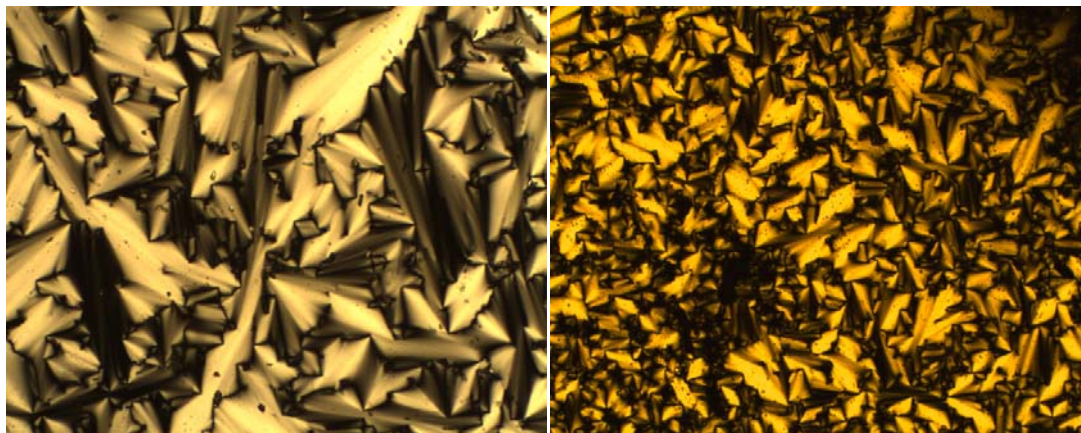


**Figure 5.5** DSC heat flow curves of heating (left)/cooling (right) at different rates for compound **37** (top) and **44** (bottom) near the isotropisation point

In general the materials described required some period of annealing in order to observe clearly the typical defects associated with the textures.

Compound **36** and **43** formed typical focal-conic fan textures of smectic A phase which is the natural texture of the mesophase observed on cooling from the isotropic. In the texture of compound **36** the hyperbola and ellipse pairs can be found as crossed black lines, which form from the molecular packing into curved layer of

Dupin cyclides (Plate 5). Such areas of the sharp changes in optic axis can be also found in the texture of compound **43**, which has a better formed fan shapes.

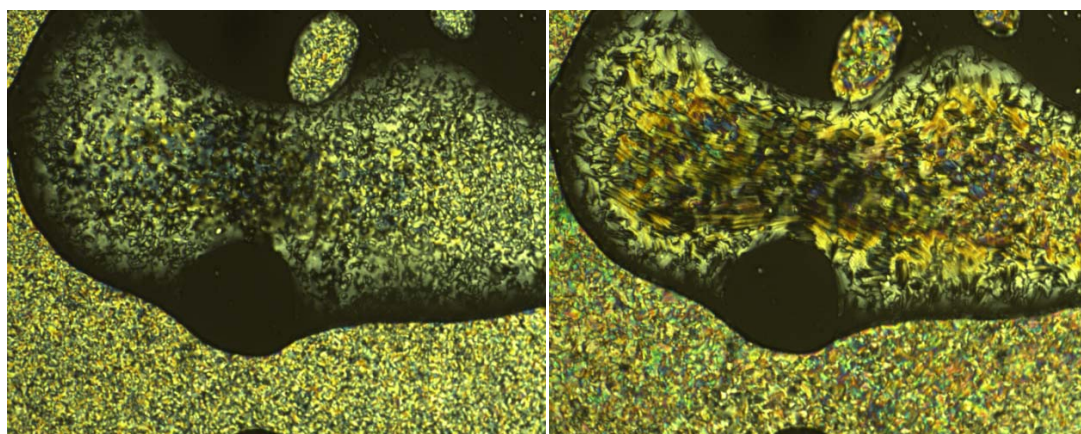


(a)

(b)

**Plate 5** The focal-conic fan textures of (a) **36**, 45 °C (b) **43**, 52 °C (x200)

Textures of compound **37** can be better observed on the thin free-standing regions of the sample. A schlieren texture with 2- and 4-brush defect points appeared directly from isotropic liquid; with further cooling, fan shapes are forming gradually on the base of the schlieren texture. There are lots of visible parallel straight dark lines running on the fans formed, which indicated the discontinuities in the focal-conic domains of smectic A phase (Plate 6).

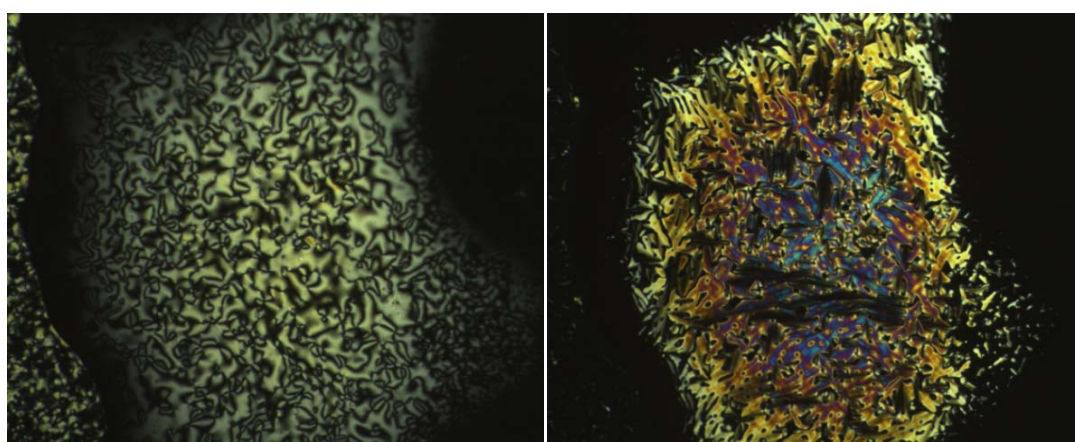


(a)

(b)

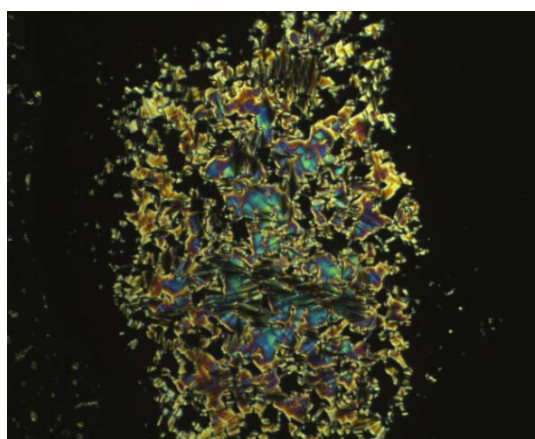
**Plate 6** Textures of **37**: (a) Schlieren texture, 36 °C; (b) Focal-conic fan texture, 32 °C (x200)

Compound **44** also presents distinct textures in thin areas of the sample (Plate 7). The schlieren texture of the nematic phase (a) and the focal-conic fan texture of SmA phase (c) is quite similar to **37**, besides the focal-conic pairs in the SmA phase texture can be seen more clearly for **44**; however a pseudo focal-conic fan like texture with smooth faced fans was also observed with the accompany of spine-like defects (b), which corresponds to the middle transition observed by DSC. However, from the combination of DSC and POM observations it is still unclear whether if the middle phase is a columnar phase or it is just a modification of the smectic phase.



(a)

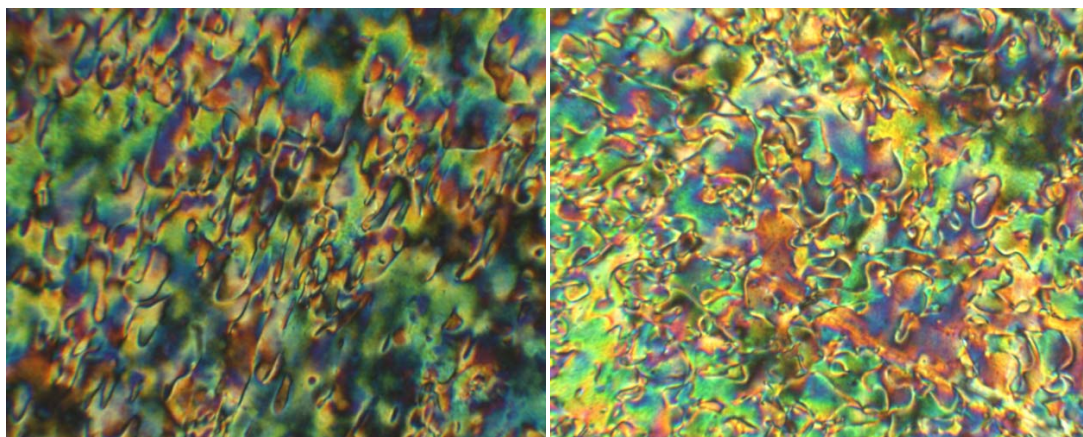
(b)



(c)

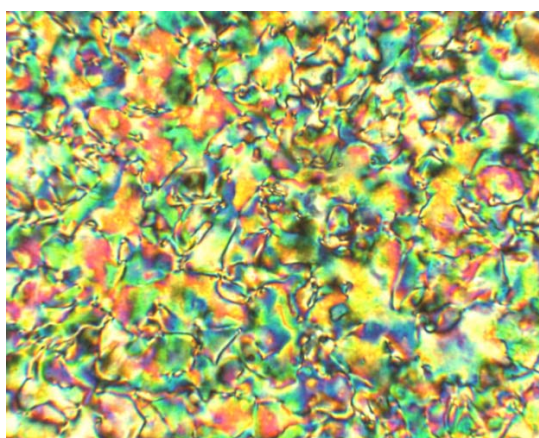
**Plate 7** Textures of **44**: (a) Schlieren texture, 50 °C; (b) Pseudo focal-conic fan texture, 48 °C; (c) Focal-conic fan texture, 40 °C (x200)

In contrast, compounds **38**, **45** and **46** with side-on PDAB mesogenic units all displayed nematic phases, as shown in plate 8. These textures have a close resemblance with the phase formed by the PDAB mesogenic monomers themselves.



(a)

(b)



(c)

**Plate 8** The Schlieren textures of (a) **38**, 58 °C; (b) **45**, 50 °C; (c) **46**, 55 °C (x200)

## 5.4 Discussion

The mesophase behaviour of the multipedes is mainly controlled by the mesogenic units. Though there are two series of compound (36~38, 43~46) based on the iodophenyl and ethynylphenyl groups respectively on the short branch, the differences on liquid crystal behaviour between them are insignificant for the dendrons with the same mesogenic units. It can be also found that for all the with mesogenic units the crystallisation is suppressed, showing instead the glass transition, and the isotropisation temperatures are relatively low, below 60 °C, consistent with the branched structure of the scaffold.

By taking the pentaerythritol as the central dendritic scaffold, the mesogenic dendritic molecule still maintained enough anisotropy to induce LC phases. This means that for the multipedes the mesogenic units have certain directional order due to the flexible structure of the scaffold and the presence of the spacers which ensures an optimized mesogenic conformation. Considering the opposing effects of intermolecular forces between the mesogens and the steric hindrance, there are two structural models for of the LC dendritic molecules based on pentaerythritol (Fig 5.6). First is the “hourglass” model, in which two of the four branches point in one direction and the other two in the opposite direction. This model was confirmed for some rigid symmetric tetrapedes compound based on pentaerythritol [13]. By adopting the hourglass shape, the supermolecule can be stretched to reduce the free volume and maximise the intermolecular interactions thus leading to an effective packing into layers. In other model, the “cone” shape, three branches are in one direction and the fourth is opposite. For an asymmetric tetrapede the molecule with three identical long and flexible branches, this cone shape conformation allows for a microphase segregation effect, which also promotes the formation of lamellar phases. In both of the models, the mesogenic units can take a relatively parallel position to make a contribution to the anisotropy of the entire system. The two possible models of the asymmetric dendritic mutipedes are related to the fourth branch. If the branch is short and small, the other three can be extended which results in the hourglass shape; a longer or bulky group on the fourth branch will prevent the packing of the mesogens in pairs and may force the molecule take the cone shape. The more stable conformation also depends on the microsegregation ability of the fourth arm relative to the other arms. Both of the hourglass and cone on formations of the asymmetric

molecules can form smectic layers or bilayers by packing with an anti-parallel position as showed in Fig 5.6.

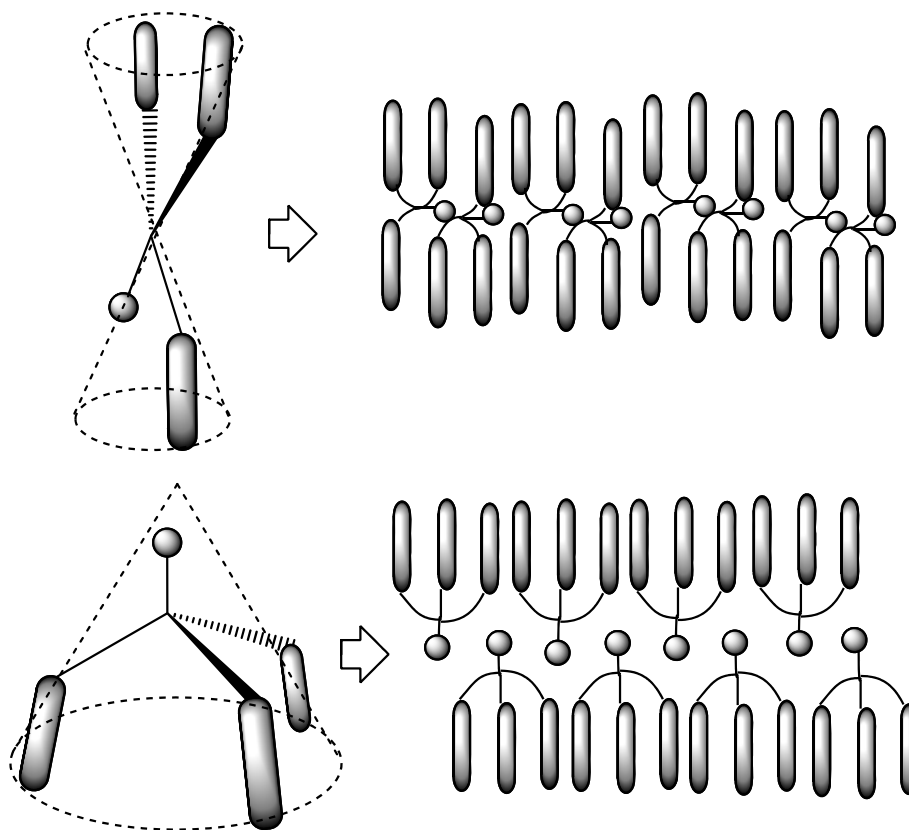


**Figure 5.6** The “hourglass” and “cone” shape of the tetrapedes and the SmA phase formed

Compounds **36** and **43**, comprising of three perfluorinated chains, strong microsegregation must occur between the incompatible hydrocarbon core and the fluorinated branches, making likely the cone shape conformation, which leads to the formation of the SmA phase where the stiff fluorinated chains are segregated into layers. They are also the only compounds in this group that crystallized rapidly at room temperature.

Unlike the perfluorinated chains, the cyanobiphenyl groups do not have such strong incompatibilities with the phenyl group on the short arm. These two mesogenic tetrapedes, **37** and **44**, exhibit the smectic A phase at room temperature as well as a

short range nematic phase just before the clearing point. The presence of the nematic phase indicates that the short arm must introduce a certain amount of disorder (Fig 5.7) in the system since the uniform tetramer (four cyanobiphenyl groups) displays only the SmA phase. This is not observed in **36** and **43** because the strong microphase segregation effect of the perfluorinated chains must be able to overcome the disorder introduced by a different fourth arm.

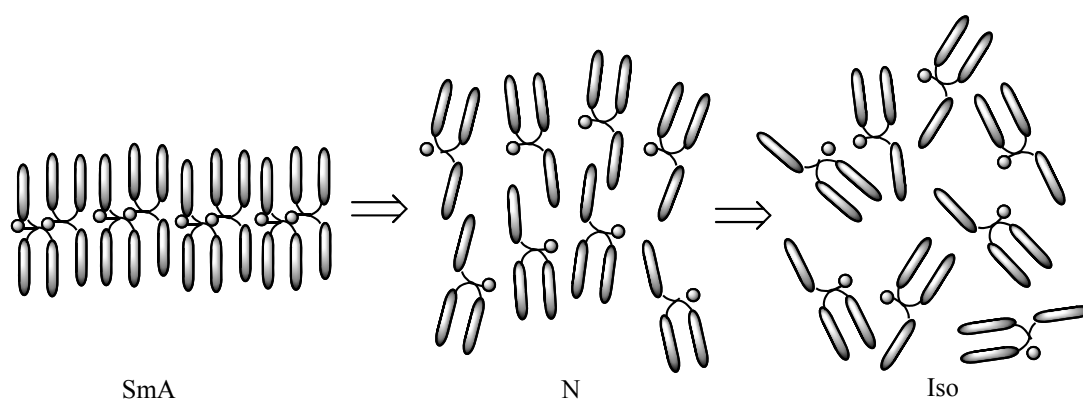
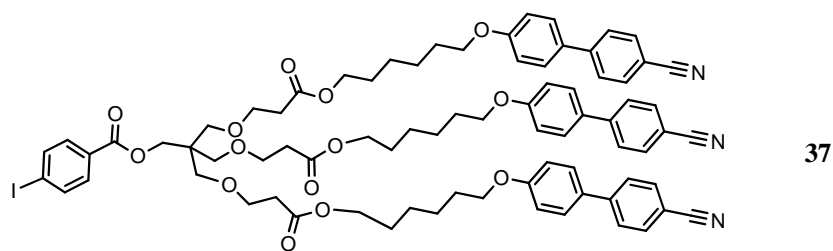


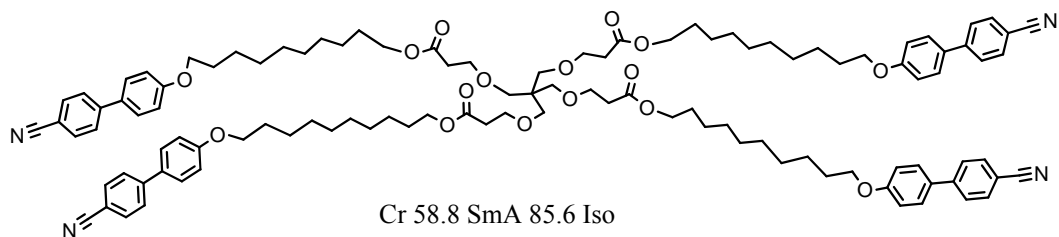
**Figure 5.7** Postulated molecular assemblies in the phase transition of **37** and **44**

A previous study on segregated LC supermolecules based on PE with three and four cyanobiphenyl moieties was carried out by I. M. Saez et al. [3a, 14]. These mutipedes exhibit the smectic A phase (Fig 5.8). Compared to compound (a) and (b), **37** and **44** have much lower clearing points due to the unsymmetrical structure and the higher disordering of the fourth arm; however they do not crystallise, showing a low temperature glass transition which results in a comparable mesophase range despite having only three mesogens.



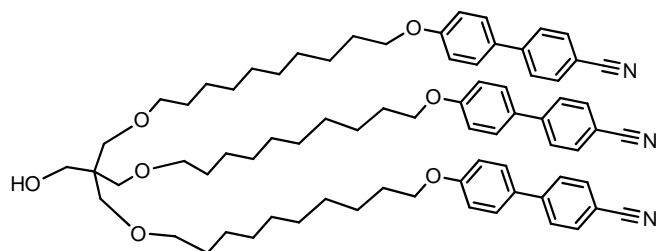
g 1.7 SmA 33.7 N 37.1 I

(a)



Cr 58.8 SmA 85.6 Iso

(b)



Cr 26.2 SmC 43.5 SmA 96.2 I

**Figure 5.8** Comparison of dendritic multipedes with cyanobiphenyl groups and their transition temperatures

Compounds **38**, **45** and **46** exhibit only the nematic phase, as the laterally attached PDAB mesogenic groups have a strong tendency to induce the formation of this phase, and do not crystallize, showing glass transitions only. Compound **46** has a longer spacer chain between the central scaffold and the mesogenic groups than **45**, but their N-Iso transition temperatures are very close which means that the length of the spacer doesn't have a significant effect on the thermal stability of the mesophase. For all the dendritic mesogens with laterally attached mesogenic units, the supermolecules take on a distorted conformation, in which the mesogenic cores are distributed around the central scaffold of the dendrimer with a rough directional order (Fig 5.9). In such a distorted form, the dendritic mesogens have even more

difficulty in packing into layers therefore the nematic phase is preferred by the dendron since the directional order of the mesogenic units is maintained.

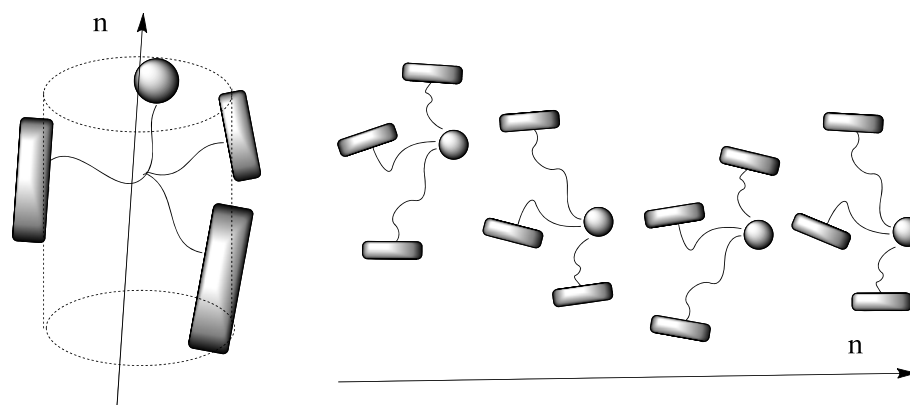


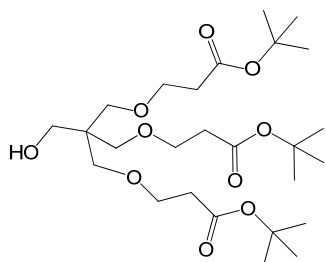
**Figure 5.9** Dendrimer with three side-on mesogenic units and the nematic phase

### 5.5 Concluding remarks

Pentaerythritol (PE) based dendritic LC multipedes were developed as the branching units for constructing the dendrimers described later on. Both the nematic phase and SmA phase were observed in the multipedes with cyanobiphenyl; it is a rare mesophase behaviour among all the dendritic oligomer contains cyanobiphenyl, which may be caused by their unique unsymmetrical structure. The microphase segregation induced by the perfluorinated chains induces the formation of the smectic phase even when there are no mesogenic units *per se* in the multipede. The multipedes with the side-on PDAB mesogens show exclusively the nematic phase. The mesophase behavior of the LC multipedes is valuable as a reference for studying more complicated Janus type LCs in later chapters.

## 5.6 Experimental

### 6,6-Bis(4-oxa-tertbutylpentanoyl)-7-hydroxy-4-oxa-tertbutylheptanoate (**33**)

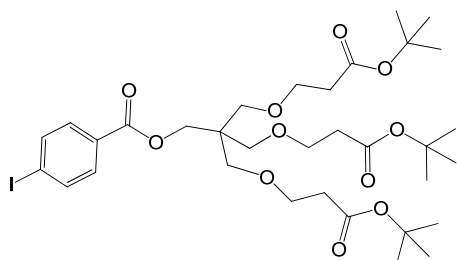


Pentaerythritol (6 g; 44 mmol) and  $[\text{nBu}_4\text{N}]^+[\text{OH}]^-$  in  $\text{H}_2\text{O}$  (40%, 20 mL) were dissolved under an atmosphere of argon. Tert-butyl acrylate (20.1 g; 157 mmol) was added and the reaction was stirred for 72 h at room temperature. The mixture was poured into water and extracted with ethyl acetate, dried over  $\text{MgSO}_4$ , and the solvent was removed by evaporation *in vacuo*. The crude product was subjected to column chromatography, eluting with 1:3 then 1:2 ethyl acetate/petroleum ether, to yield **33** as a colorless oil.

Yield: 8.14 g (36%)

$^1\text{H}$  NMR (400 MHz,  $\text{CDCl}_3$ )  $\delta_{\text{H}}$  (ppm): 3.61 (m, 8 H,  $-\text{CH}_2\text{OH}$ ,  $-\text{C}(\text{CH}_2\text{OCH}_2-)_3$ ); 3.42 (s, 6 H,  $-\text{C}(\text{CH}_2\text{O}-)_3$ ); 2.86 (t (J = 6.5 Hz), 1 H,  $-\text{OH}$ ); 2.44 (t (J = 6.3 Hz), 6 H,  $-\text{CH}_2\text{COO}-$ ); 1.44 (s, 27 H,  $-\text{C}(\text{CH}_3)_3$ )

### 2,2,2-Pentaerythritol tris(t-butylpropanoate)-4-iodobenzoate (**34**)



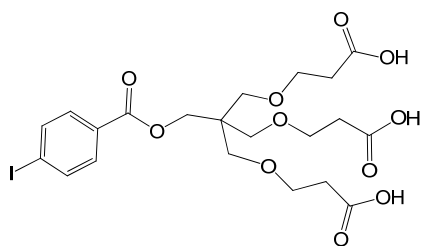
Compound **33** (0.5 g; 0.9 mmol) and 4-iodobenzoic acid (0.25 g; 1 mmol) were dissolved in dichloromethane (30 mL) with  $\text{N,N}'$ -dicyclohexylcarbodiimide (0.25 g; 1.2 mmol) and 4-(dimethylamino)pyridine (0.12 g; 1 mmol). The reaction was stirred under argon for 20 h at room temperature. The precipitate was filtered off and the

solvent was removed by evaporation *in vacuo*. The product was isolated by column chromatography, eluting with 1:1 hexane/diethyl ether, to yield **34** as a colorless oil.

Yield: 0.55 g (81%)

$^1\text{H}$  NMR (400 MHz,  $\text{CDCl}_3$ )  $\delta_{\text{H}}$  (ppm): 7.81 (d (J = 8.5 Hz), 2 H, ArH); 7.72 (d (J = 8.5 Hz), 2 H, ArH); 4.30 (s, 2 H,  $-\text{COOCH}_2-$ ); 3.61 (t (J = 6.4 Hz), 6 H,  $-\text{C}(\text{CH}_2\text{OCH}_2-)_3$ ); 3.46 (s, 6 H,  $-\text{C}(\text{CH}_2\text{O}-)_3$ ); 2.42 (t (J = 6.4 Hz), 6 H,  $-\text{CH}_2\text{COO}-$ ); 1.43 (s, 27 H,  $-\text{C}(\text{CH}_3)_3$ )

### 2,2,2-Pentaerythritol (4-iodobenzoate)trispropanoic acid (**35**)

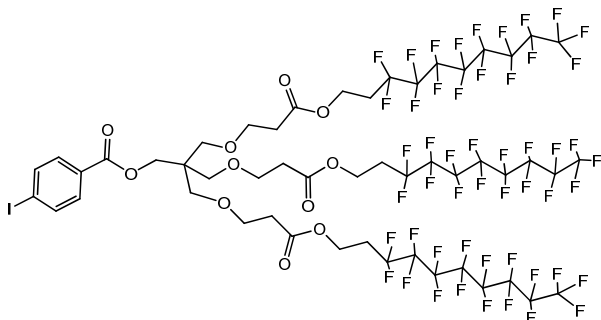


The tri-ester **34** (0.55 g; 0.73 mmol) was dissolved in dichloromethane (10 mL) and trifluoroacetic acid (1.7 mL; 22 mmol) was added. The mixture was stirred for 20 h at room temperature. The solvent was removed by evaporation, and the residue was left to stand in desiccator over  $\text{P}_2\text{O}_5$  for three days to yield the tri-acid **35** as a yellow solid.

Yield: 0.42 g (99%)

$^1\text{H}$  NMR (400 MHz,  $\text{CDCl}_3$ )  $\delta_{\text{H}}$  (ppm): 7.81 (d (J = 8.6 Hz), 2 H, ArH); 7.70 (d (J = 8.5 Hz), 2 H, ArH); 4.29 (s, 2 H,  $-\text{COOCH}_2-$ ); 3.67 (t (J = 5.7 Hz), 6 H,  $-\text{C}(\text{CH}_2\text{OCH}_2-)_3$ ); 3.49 (s, 6 H,  $-\text{C}(\text{CH}_2\text{O}-)_3$ ); 2.57 (t (J = 5.6 Hz), 6 H,  $-\text{CH}_2\text{COOH}$ )

**Pentaerythritol tris(3,3,4,4,5,5,6,6,7,7,8,8,9,9,10,10,10-heptafluorodecyl propanoate)-4-iodobenzoate (36)**



The tri-acid **35** (0.19 g; 0.33 mmol) and 1H,1H,2H,2H-perfluorodecanol (0.5 g; 1.08 mmol) were dissolved in tetrahydrofuran (20 mL) with N,N'-dicyclohexylcarbodiimide (0.24 g; 1.18 mmol) and 4-(dimethylamino)pyridine (0.12 g; 0.98 mmol). The reaction was stirred under argon for 72 h at room temperature. The solvent was removed by evaporation, and the product was separated from the crude by column chromatography, eluting with 1:5 ethyl acetate/dichloromethane, to yield **36** as a white solid.

Yield: 0.55 g (87%)

$^1\text{H}$  NMR (400 MHz,  $\text{CDCl}_3$ )  $\delta_{\text{H}}$  (ppm): 7.80 (d ( $J = 8.5$  Hz), 2 H, ArH); 7.70 (d ( $J = 8.6$  Hz), 2 H, ArH); 4.37 (t ( $J = 6.5$  Hz), 6 H,  $-\text{CH}_2\text{COOCH}_2-$ ); 4.26 (s, 2 H,  $\text{IC}_6\text{H}_4\text{COOCH}_2-$ ); 3.64 (t ( $J = 6.2$  Hz); 6 H,  $-\text{C}(\text{CH}_2\text{OCH}_2-)_3$ ); 3.44 (s, 6 H,  $-\text{C}(\text{CH}_2\text{O}-)_3$ ); 2.47 (m, 12 H,  $-\text{CH}_2\text{COO}-$ ,  $-\text{CH}_2\text{COOCH}_2\text{CH}_2-$ )

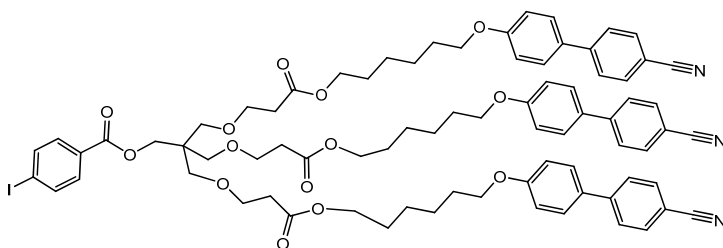
$^{13}\text{C}$  NMR (100.4 MHz,  $\text{CDCl}_3$ )  $\delta_{\text{C}}$  (ppm): 171.2, 137.8, 131.0, 129.9, 120.9, 104.3, 100.7, 69.73, 66.69, 64.45, 56.41, 56.35, 55.85, 44.72, 35.01, 34.86, 30.50

MALDI-ToF MS:  $m/z = 1943.0$  ( $\text{M} + \text{Na}$ ) $^+$

IR ( $\text{cm}^{-1}$ ): 2932, 2878, 2122, 1744, 1713, 1589, 1481, 1458, 1366, 1196, 1142, 1111, 1011, 964, 849, 756, 702, 656, 602, 509

Elemental analysis: calcd (%) for  $\text{C}_{51}\text{H}_{36}\text{O}_{11}\text{F}_{51}\text{I}$ : C 31.89, H 1.89; found: C 32.28, H 1.76

**Pentaerythritol tris(6-(4'-cyanobiphenyl-4-yloxy)hexyloxy)propanoate) 4-iodobenzoate (37)**



The tri-acid **35** (0.4 g; 0.69 mmol) and 4,4'-(6-hydroxylhexyloxy)cyanobiphenyl (0.67 g; 2.27 mmol) were dissolved in tetrahydrofuran (20 mL) with *N,N'*-dicyclohexylcarbodiimide (0.52 g; 2.5 mmol) and 4-(dimethylamino)pyridine (0.25 g; 2.1 mmol). The reaction was stirred under argon for 72 h at room temperature. The solvent was removed by evaporation under reduced pressure, and the product was isolated by column chromatography, eluting with 1:10 ethyl acetate/dichloromethane, to yield the **37** as a white sticky solid.

Yield: 0.9 g (92%)

$^1\text{H}$  NMR (400 MHz,  $\text{CDCl}_3$ )  $\delta_{\text{H}}$  (ppm): 7.78 (d ( $J = 8.6$  Hz), 2 H, ArH); 7.69 (m, 8 H, ArH); 7.63 (d ( $J = 8.6$  Hz), 6 H, ArH); 7.52 (d ( $J = 8.8$  Hz), 6 H, ArH); 6.97 (d ( $J = 8.8$  Hz), 6 H, ArH); 4.28 (s, 2 H,  $\text{IC}_6\text{H}_4\text{COOCH}_2$ -); 4.06 (t ( $J = 6.7$  Hz), 6 H,  $-\text{CH}_2\text{COOCH}_2$ -); 3.98 (t ( $J = 6.4$  Hz), 6 H,  $-\text{CH}_2\text{O}(\text{C}_6\text{H}_4)_2\text{CN}$ ); 3.65 (t ( $J = 6.4$  Hz), 6 H,  $-\text{C}(\text{CH}_2\text{OCH}_2)_3$ ); 3.46 (s, 6 H,  $-\text{C}(\text{CH}_2\text{O}-)_3$ ); 2.51 (t ( $J = 6.4$  Hz), 6 H,  $-\text{CH}_2\text{COO}$ -); 1.80 (m, 6 H,  $-\text{CH}_2\text{COOCH}_2\text{CH}_2$ -); 1.64 (m, 6 H,  $-\text{CH}_2\text{CH}_2\text{O}(\text{C}_6\text{H}_4)_2\text{CN}$ ); 1.46 (m, 12 H,  $-\text{CH}_2\text{COOCH}_2\text{CH}_2(\text{CH}_2)_2$ -)

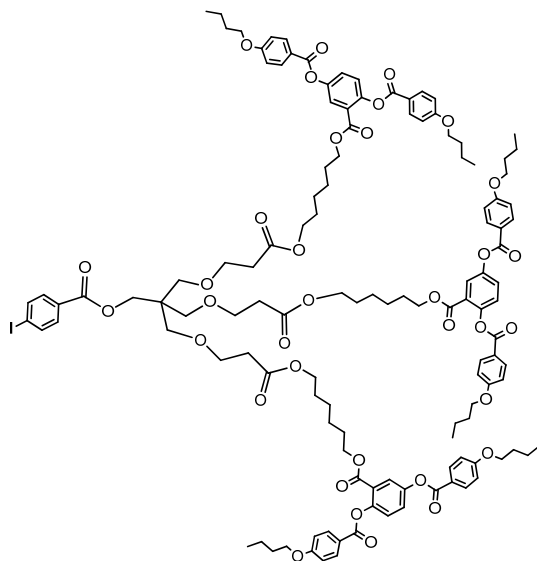
$^{13}\text{C}$  NMR (100.4 MHz,  $\text{CDCl}_3$ )  $\delta_{\text{C}}$  (ppm): 171.7, 159.8, 145.3, 137.8, 132.7, 131.4, 131.1, 128.4, 127.2, 119.2, 115.1, 110.2, 69.88, 68.01, 67.04, 64.55, 44.74, 35.12, 29.21, 28.63, 25.81

MALDI-ToF MS:  $m/z = 1436.5$  ( $\text{M} + \text{Na}$ ) $^+$

IR ( $\text{cm}^{-1}$ ): 3040, 2940, 2862, 2222, 1728, 1605, 1489, 1474, 1389, 1250, 1173, 1103, 1092, 1003, 818, 756, 656, 532

Elemental analysis: calcd (%) for  $\text{C}_{78}\text{H}_{84}\text{N}_3\text{O}_{14}\text{I}$ : C 66.23, H 5.99, N 2.97; found: C 66.02, H 5.94, N 2.76

**Pentaerythritol tris(6-(2,5-di(4-butoxybenzoyloxy)benzoyloxy)hexyloxy)propanoate 4-iodobenzoate (38)**



The tri-acid **35** (0.14 g; 0.25 mmol) and 6-hydroxylhexyl 2,5-di(4-butoxybenzoyloxy)benzoate (**16**) (0.5 g; 0.83 mmol) were dissolved in tetrahydrofuran (20 mL) with *N,N'*-dicyclohexylcarbodiimide (0.19 g; 0.9 mmol) and 4-(dimethylamino)pyridine (0.1 g; 0.75 mmol). The reaction was stirred under argon for 72 h at room temperature. The solvent was removed by evaporation, and the product was isolated from the crude by column chromatography, eluting with 1:5 ethyl acetate/dichloromethane, to yield **38** as a white sticky solid.

Yield: 0.5 g (85%)

$^1\text{H}$  NMR (400 MHz,  $\text{CDCl}_3$ )  $\delta_{\text{H}}$  (ppm): 8.14 (m, 12 H, *ArH*); 7.88 (d ( $J = 2.9$  Hz), 3 H, *ArH*); 7.77 (d ( $J = 8.5$  Hz), 2 H, *ArH*); 7.68 (d ( $J = 8.5$  Hz), 2 H, *ArH*); 7.44 (d ( $J = 8.7$  Hz) d ( $J = 2.9$  Hz), 3 H, *ArH*); 7.25 (d ( $J = 8.5$  Hz), 3 H, *ArH*); 6.97 (m, 12 H, *ArH*); 4.25 (s, 2 H,  $\text{IC}_6\text{H}_4\text{COOCH}_2$ -); 4.14 (t ( $J = 6.7$  Hz), 6 H,  $-\text{CH}_2\text{COO}(\text{CH}_2)_5\text{CH}_2\text{OCO}-$ ); 4.05 (m, 12 H,  $-\text{C}_6\text{H}_4\text{OCH}_2$ -); 3.97 (t ( $J = 6.8$  Hz), 6 H,  $-\text{CH}_2\text{COOCH}_2$ -); 3.62 (t ( $J = 6.4$  Hz), 6 H,  $-\text{C}(\text{CH}_2\text{OCH}_2)_3$ ); 3.43 (s, 6 H,  $-\text{C}(\text{CH}_2\text{O})_3$ ); 2.48 (t ( $J = 6.4$  Hz), 6 H,  $-\text{CH}_2\text{COO}-$ ); 1.80 (m, 12 H,  $-\text{C}_6\text{H}_4\text{OCH}_2\text{CH}_2$ -); 1.50 (m, 24 H,  $-\text{C}_6\text{H}_4\text{OCH}_2\text{CH}_2\text{CH}_2$ -,  $-\text{CH}_2\text{COOCH}_2\text{CH}_2\text{CH}_2\text{CH}_2\text{CH}_2\text{CH}_2\text{OCO}-$ ); 1.22 (m, 12 H,  $-\text{CH}_2\text{COOCH}_2\text{CH}_2(\text{CH}_2)_2$ -); 1.03 (t ( $J = 7.4$  Hz) d ( $J = 3.3$  Hz), 18 H,  $-\text{CH}_3$ )

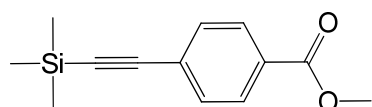
$^{13}\text{C}$  NMR (100.4 MHz,  $\text{CDCl}_3$ )  $\delta_{\text{C}}$  (ppm): 171.6, 163.7, 137.8, 132.5, 132.5, 127.2, 125.1, 125.0, 125.0, 121.5, 121.1, 114.5, 114.4, 68.10, 66.98, 65.47, 64.48, 44.69, 35.02, 31.21, 28.50, 28.39, 25.59, 19.28, 13.93

MALDI-ToF MS:  $m/z = 2348.9$  ( $\text{M} + \text{H}$ ) $^+$

IR ( $\text{cm}^{-1}$ ): 2955, 2870, 1728, 1605, 1512, 1466, 1420, 1242, 1157, 1119, 1057, 1003, 972, 849, 756, 687, 648, 594, 509

Elemental analysis: calcd (%) for  $\text{C}_{126}\text{H}_{147}\text{O}_{35}\text{I}$ : C 64.44, H 6.31; found: C 63.84, H 6.19

### Methyl 4-(trimethylsilylethynyl)benzoate (**39**)

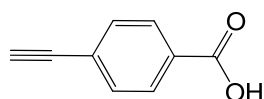


Methyl 4-iodobenzoate (5 g; 19.1 mmol) was dissolved in triethylamine (60 mL), and the solution purged with argon for 15 min. A catalytic mixture of  $\text{Pd}(\text{PPh}_3)_2\text{Cl}_2$  (56 mg; 0.08 mmol),  $\text{PPh}_3$  (84 mg; 0.32 mmol) and  $\text{CuI}$  (0.1 g; 0.54 mmol) was added. Trimethylsilyl acetylene (4 mL; 28.7 mmol) was added by syringe. The mixture was stirred for 20 h at room temperature. The triethylamine hydroiodide was filtered off, and the solvent was distilled at room temperature under reduced pressure. The product was isolated by column chromatography, eluting with 1:1 dichloromethane/petroleum ether, to yield **39** as a white solid.

Yield: 4.4 g (99%)

$^1\text{H}$  NMR (400 MHz,  $\text{CDCl}_3$ )  $\delta_{\text{H}}$  (ppm): 7.97 (d ( $J = 8.5$  Hz), 2 H,  $\text{ArH}$ ); 7.51 (d ( $J = 8.6$  Hz), 2 H,  $\text{ArH}$ ); 3.91 (s, 3 H,  $-\text{COOCH}_3$ ); 0.26 (s, 9 H,  $-\text{Si}(\text{CH}_3)_3$ )

#### 4-Ethynylbenzoic acid (**40**)

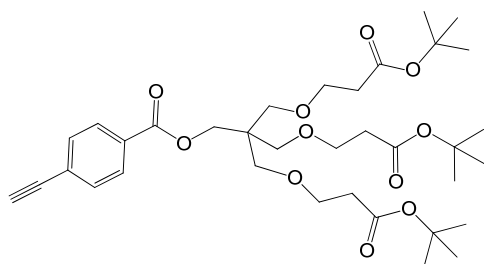


Methyl 4-(trimethylsilylethynyl)benzoate (**39**) (1 g; 4.3 mmol) was dissolved in ethanol (20 mL) and 1 M NaOH (4.4 mL; 4.3 mmol) was added to the solution at 0 °C. The solution was stirred at 0 °C for 2 h, then at room temperature for 20 h. The ethanol was removed by evaporation under vacuum; more water was added into the mixture and washed with diethyl ether. The aqueous phase was acidified with 1 M HCl and the mixture was extracted with diethyl ether. The organic layer was washed twice with water, dried on MgSO<sub>4</sub> and the solvent removed by evaporation to give **40** as a pale yellow solid.

Yield: 0.57 g (90%)

<sup>1</sup>H NMR (400 MHz, CDCl<sub>3</sub>) δ<sub>H</sub> (ppm): 8.06 (d (J = 8.5 Hz), 2 H, ArH); 7.59 (d (J = 8.5 Hz), 2 H, ArH); 3.26 (s, 1 H, -C≡CH)

#### 2,2,2-Tris(3-tert-butoxy-3-oxopropyl)ethyl 4-ethynylbenzoate (**41**)

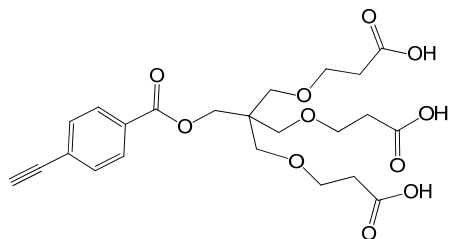


4-Ethynylbenzoic acid (**40**) (0.44 g; 3 mmol) and 2,2,2-tris(3-tert-butyl-3-oxopropyl)ethan-1-ol (**33**) (1.53 g; 3 mmol) were dissolved in tetrahydrofuran (30 mL) with 1-ethyl-3-(3-dimethylaminopropyl)carbodiimide (0.69 g; 3.6 mmol) and 4-(dimethylamino)pyridine (0.37 g; 3 mmol). The reaction was stirred under argon for for 20 h at room temperature. The solvent was removed by evaporation, and the product was isolated from the crude by column chromatography, eluting with 1:10 ethyl acetate/dichloromethane, to yield **41** as a colorless oil.

Yield: 1.64 g (86%)

$^1\text{H}$  NMR (400 MHz,  $\text{CDCl}_3$ )  $\delta_{\text{H}}$  (ppm): 7.97 (d ( $J = 8.5$  Hz), 2 H, ArH); 7.55 (d ( $J = 8.4$  Hz), 2 H, ArH); 4.31 (s, 2 H,  $-\text{COOCH}_2-$ ); 3.61 (t ( $J = 6.4$  Hz), 6 H,  $-\text{C}(\text{CH}_2\text{OCH}_2-)_3$ ); 3.47 (s, 6 H,  $-\text{C}(\text{CH}_2\text{O}-)_3$ ); 3.23 (s, 1 H,  $-\text{C}\equiv\text{CH}$ ); 2.42 (t ( $J = 6.4$  Hz), 6 H,  $-\text{CH}_2\text{COO}-$ ); 1.42 (s, 27 H,  $-\text{C}(\text{CH}_3)_3$ )

**2,2,2-Tris(3-hydroxyl-3-oxopropoxymethyl)ethyl 4-ethynylbenzoate (42)**

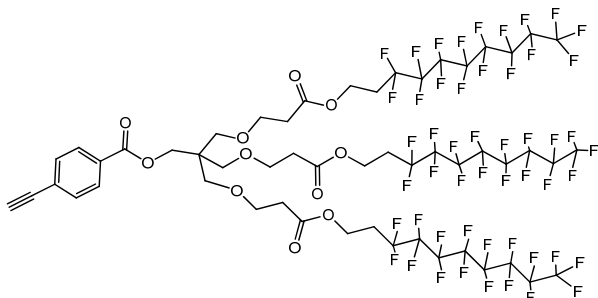


The tri-ester **41** (1.64 g; 2.53 mmol) was dissolved in dichloromethane (20 mL) and trifluoroacetic acid was added (5.8 mL; 76 mmol). The mixture was stirred for 20 h at room temperature. The solvent was removed by evaporation under reduced pressure, and the residue was left in a desiccator over  $\text{P}_2\text{O}_5$  for 24 h to give **42** as a brown solid.

Yield: 1.0 g (74%)

$^1\text{H}$  NMR (400 MHz,  $\text{CDCl}_3$ )  $\delta_{\text{H}}$  (ppm): 7.96 (d ( $J = 8.4$  Hz), 2 H, ArH); 7.55 (d ( $J = 8.4$  Hz), 2 H, ArH); 4.30 (s, 2 H,  $-\text{COOCH}_2-$ ); 3.67 (t ( $J = 6.1$  Hz), 6 H,  $-\text{C}(\text{CH}_2\text{OCH}_2-)_3$ ); 3.50 (s, 6 H,  $-\text{C}(\text{CH}_2\text{O}-)_3$ ); 3.24 (s, 1 H,  $-\text{C}\equiv\text{CH}$ ); 2.58 (t ( $J = 5.6$  Hz), 6 H,  $-\text{CH}_2\text{COOH}$ )

**Pentaerythritol tris(3,3,4,4,5,5,6,6,7,7,8,8,9,9,10,10,10-heptafluorodecyl propanoate)-4-ethynylbenzoate (43)**



The tri-acid **42** (94 mg; 0.2 mmol) and 1H,1H,2H,2H-perfluorodecanol (0.3 g; 0.65 mmol) were dissolved in tetrahydrofuran (15 mL) with 1-ethyl-3-(3-dimethylaminopropyl)carbodiimide (0.14 g; 0.7 mmol) and 4-(dimethylamino)pyridine (24 mg; 0.2 mmol). The reaction was stirred under argon for 48 h at room temperature. The solvent was removed by evaporation under vacuum, and the product was separated from the crude by column chromatography, eluting with 1:10 ethyl acetate/dichloromethane, to yield **43** as a white solid.

Yield: 0.25 g (70%)

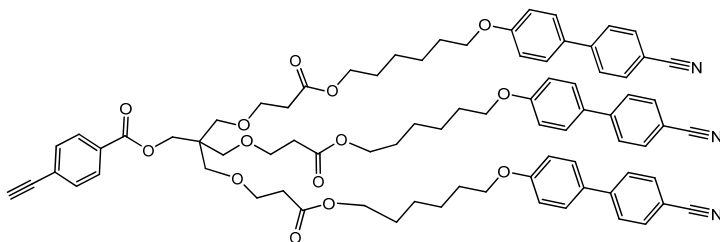
$^1\text{H}$  NMR (400 MHz,  $\text{CDCl}_3$ )  $\delta_{\text{H}}$  (ppm): 7.95 (d (J = 8.5 Hz), 2 H, ArH); 7.55 (d (J = 8.5 Hz), 2 H, ArH); 4.36 (t (J = 6.5 Hz), 6 H,  $-\text{CH}_2\text{COOCH}_2-$ ); 4.27 (s, 2 H,  $\text{IC}_6\text{H}_4\text{COOCH}_2-$ ); 3.65 (t (J = 6.2 Hz); 6 H,  $-\text{C}(\text{CH}_2\text{OCH}_2-)_3$ ); 3.46 (s, 6 H,  $-\text{C}(\text{CH}_2\text{O}-)_3$ ); 3.22 (s, 1 H,  $-\text{C}\equiv\text{CH}$ ); 2.54 (t (J = 6.2 Hz), 6 H,  $-\text{CH}_2\text{COO}-$ ); 2.46 (m, 6 H,  $-\text{CH}_2\text{COOCH}_2\text{CH}_2-$ )

$^{13}\text{C}$  NMR (100.4 MHz,  $\text{CDCl}_3$ )  $\delta_{\text{C}}$  (ppm): 171.2, 165.6, 132.2, 130.4, 129.4, 126.9, 82.77, 80.07, 69.75, 66.70, 64.44, 56.40, 44.74, 34.87, 30.50, 30.28

MALDI-ToF MS:  $m/z = 1841.1$  (M + Na) $^+$

IR ( $\text{cm}^{-1}$ ): 3310, 2924, 2870, 1744, 1605, 1466, 1404, 1335, 1227, 1211, 1142, 1111, 972, 864, 756, 702, 656, 556, 532

**Pentaerythritol tris(6-(4'-cyanobiphenyl-4-yloxy)hexyloxy)propanoate) 4-ethynylbenzoate (**44**)**



The tri-acid **43** (0.13 g; 0.28 mmol) and 4,4'-(6-hydroxylhexyloxy)cyanobiphenyl (0.33 g; 1.11 mmol) were dissolved in tetrahydrofuran (10 mL) with 1-ethyl-3-(3-dimethylaminopropyl)carbodiimide (0.19 g; 1 mmol) and 4-(dimethylamino)pyridine (0.1 g; 0.83 mmol). The reaction was stirred under argon for 48 h at room temperature. The solvent was removed by evaporation, and the product was isolated by column chromatography, eluting with 1:10 ethyl acetate/dichloromethane, to yield **44** as a white sticky solid.

Yield: 0.3 g (82%)

$^1\text{H}$  NMR (400 MHz,  $\text{CDCl}_3$ )  $\delta_{\text{H}}$  (ppm): 7.95 (d (J = 8.6 Hz), 2 H, ArH); 7.68 (d (J = 8.6 Hz), 6 H, ArH); 7.63 (d (J = 8.6 Hz), 6 H, ArH); 7.52 (m, 8 H, ArH); 6.97 (d (J = 8.8 Hz), 6 H, ArH); 4.29 (s, 2 H,  $-\text{C}_6\text{H}_4\text{COOCH}_2-$ ); 4.06 (t (J = 6.7 Hz), 6 H,  $-\text{CH}_2\text{O}(\text{C}_6\text{H}_4)_2\text{CN}$ ); 3.98 (t (J = 6.4 Hz), 6 H,  $-\text{CH}_2\text{COOCH}_2-$ ); 3.65 (t (J = 6.4 Hz), 6 H,  $-\text{C}(\text{CH}_2\text{OCH}_2)_3$ ); 3.47 (s, 6 H,  $-\text{C}(\text{CH}_2\text{O}-)_3$ ); 3.22 (s, 1 H,  $-\text{C}\equiv\text{CH}$ ); 2.52 (t (J = 6.4 Hz), 6 H,  $-\text{CH}_2\text{COO}-$ ); 1.80 (m, 6 H,  $-\text{CH}_2\text{CH}_2\text{O}(\text{C}_6\text{H}_4)_2\text{CN}$ ); 1.64 (m, 6 H,  $-\text{CH}_2\text{COOCH}_2\text{CH}_2-$ ); 1.45 (m, 12 H,  $-\text{CH}_2\text{COOCH}_2\text{CH}_2(\text{CH}_2)_2-$ )

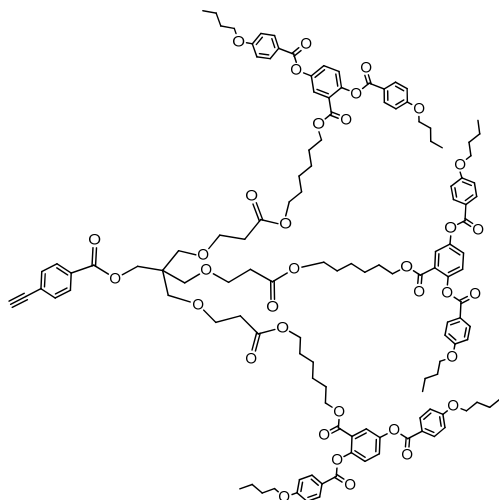
$^{13}\text{C}$  NMR (100.4 MHz,  $\text{CDCl}_3$ )  $\delta_{\text{C}}$  (ppm): 171.7, 165.6, 159.8, 145.3, 132.7, 132.2, 131.4, 130.5, 129.5, 128.4, 127.2, 126.8, 119.2, 115.1, 110.1, 82.87, 80.21, 69.87, 68.00, 67.04, 64.67, 64.54, 44.76, 35.12, 29.20, 28.63, 25.80

MALDI-ToF MS:  $m/z = 1334.6$  ( $\text{M} + \text{Na}$ ) $^+$

IR ( $\text{cm}^{-1}$ ): 3248, 2924, 2862, 2222, 2106, 1728, 1605, 1489, 1466, 1366, 1242, 1173, 1103, 1065, 1011, 856, 818, 772, 733, 633, 556, 532

Elemental analysis: calcd (%) for  $\text{C}_{80}\text{H}_{85}\text{N}_3\text{O}_{14}$ : C 73.21, H 6.53, N 3.20; found: C 72.58, H 6.59, N 3.17

**Pentaerythritol tris(6-(2,5-di(4-butoxybenzoyloxy)benzoyloxy)hexyloxy)propanoate 4-ethynylbenzoate (45)**



The tri-acid **43** (72 mg; 0.15 mmol) and 6-hydroxylhexyl 2,5-di(4-butoxybenzoyloxy)benzoate (**16**) (0.3 g; 0.5 mmol) were dissolved in tetrahydrofuran (15 mL) with 1-ethyl-3-(3-dimethylaminopropyl)carbodiimide (0.1 g; 0.55 mmol) and 4-(dimethylamino)pyridine (55 mg; 0.45 mmol). The reaction was stirred under argon for 48 h at room temperature. The solvent was removed by evaporation under reduced pressure, and the product was isolated from the crude by column chromatography, eluting with 1:10 ethyl acetate/dichloromethane, to yield **45** as a white sticky solid.

Yield: 0.25 g (74%)

$^1\text{H}$  NMR (400 MHz,  $\text{CDCl}_3$ )  $\delta_{\text{H}}$  (ppm): 8.14 (m, 12 H, ArH); 7.93 (d (J = 8.5 Hz), 2 H, ArH); 7.87 (d (J = 2.9 Hz), 3 H, ArH); 7.52 (d (J = 8.5 Hz), 2 H, ArH); 7.44 (d (J = 8.7 Hz) d (J = 2.9 Hz), 3 H, ArH); 7.25 (d (J = 9.0 Hz), 3 H, ArH); 6.97 (d (J = 8.9 Hz) d (J = 1.9 Hz), 12 H, ArH); 4.26 (s, 2 H,  $-\text{C}_6\text{H}_4\text{COOCH}_2-$ ); 4.14 (t (J = 6.7 Hz), 6 H,  $-\text{CH}_2\text{COO}(\text{CH}_2)_5\text{CH}_2\text{OCO}-$ ); 4.05 (m, 12 H,  $-\text{C}_6\text{H}_4\text{OCH}_2-$ ); 3.97 (t (J = 6.8 Hz), 6 H,  $-\text{CH}_2\text{COOCH}_2-$ ); 3.62 (t (J = 6.5 Hz), 6 H,  $-\text{C}(\text{CH}_2\text{OCH}_2)_3$ ); 3.44 (s, 6 H,  $-\text{C}(\text{CH}_2\text{O})_3$ ); 3.21 (s, 1 H,  $-\text{C}\equiv\text{CH}$ ); 2.48 (t (J = 6.5 Hz), 6 H,  $-\text{CH}_2\text{COO}-$ ); 1.80 (m, 12 H,  $-\text{C}_6\text{H}_4\text{OCH}_2\text{CH}_2-$ ); 1.50 (m, 24 H,  $-\text{C}_6\text{H}_4\text{OCH}_2\text{CH}_2\text{CH}_2-$ ,  $-\text{CH}_2\text{COOCH}_2\text{CH}_2\text{CH}_2\text{CH}_2\text{CH}_2\text{CH}_2\text{OCO}-$ ); 1.22 (m, 12 H,  $-\text{CH}_2\text{COOCH}_2\text{CH}_2(\text{CH}_2)_2-$ ); 0.99 (t (J = 7.4 Hz) d (J = 3.6 Hz), 18 H,  $-\text{CH}_3$ )

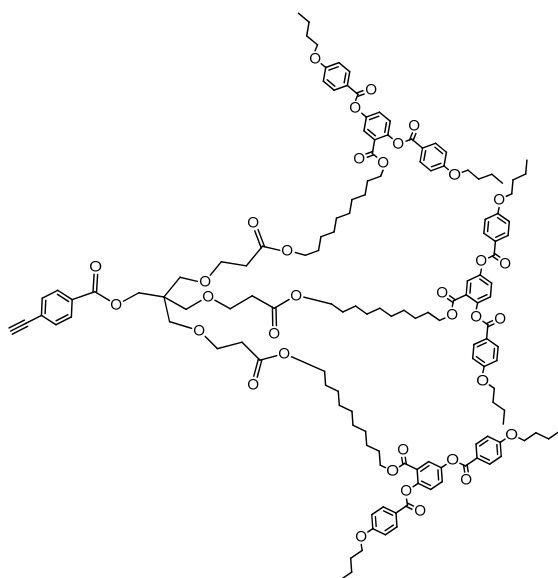
$^{13}\text{C}$  NMR (100.4 MHz,  $\text{CDCl}_3$ )  $\delta_{\text{C}}$  (ppm): 171.6, 165.0, 164.7, 164.2, 163.8, 163.7, 148.4, 148.2, 132.5, 132.5, 132.2, 129.5, 127.2, 125.1, 125.0, 125.0, 121.5, 121.1, 114.5, 114.4, 102.7, 79.97, 69.83, 68.12, 68.09, 66.98, 65.47, 64.47, 44.72, 35.02, 31.20, 28.49, 28.39, 25.58, 19.28, 13.92

MALDI-ToF MS:  $m/z = 2267.9$  ( $\text{M} + \text{Na}$ ) $^+$

IR ( $\text{cm}^{-1}$ ): 3256, 3078, 2932, 2870, 1721, 1605, 1512, 1466, 1373, 1242, 1157, 1119, 1057, 1003, 972, 910, 849, 764, 733, 694, 640, 525

Elemental analysis: calcd (%) for  $\text{C}_{128}\text{H}_{148}\text{O}_{35}$ : C 68.43, H 6.64; found: C 68.40, H 6.81

**Pentaerythritol tris(6-(2,5-di(4-butoxybenzoyloxy)benzoyloxy)decyloxy)propanoate 4-ethynylbenzoate (46)**



The tri-acid **43** (66 mg; 0.14 mol) and 10-hydroxydecyl 2,5-di(4-butoxybenzoyloxy)benzoate (**11**) (0.3 g; 0.45 mmol) were dissolved in tetrahydrofuran (15 mL) with 1-ethyl-3-(3-dimethylaminopropyl)carbodiimide (95 mg; 0.49 mmol) and 4-(dimethylamino)pyridine (50 mg; 0.41 mmol). The reaction was stirred under argon for 72 h at room temperature. The solvent was removed by evaporation under vacuum, and the product was isolated by column chromatography with 1:10 ethyl acetate/dichloromethane to yield **46** as a white sticky solid.

Yield: 0.1 g (30%)

$^1\text{H}$  NMR (400 MHz,  $\text{CDCl}_3$ )  $\delta_{\text{H}}$  (ppm): 8.15 (d (J = 8.9 Hz) d (J = 5.3 Hz), 12 H, ArH); 7.95 (d (J = 8.5 Hz), 2 H, ArH); 7.88 (d (J = 2.9 Hz), 3 H, ArH); 7.53 (d (J = 8.4 Hz), 2 H, ArH); 7.45 (d (J = 8.7 Hz) d (J = 2.9 Hz), 3 H, ArH); 7.25 (d (J = 8.8 Hz), 3 H, ArH); 6.97 (d (J = 8.9 Hz) d (J = 3.1 Hz), 12 H, ArH); 4.28 (s, 2 H, - $\text{C}_6\text{H}_4\text{COOCH}_2$ -); 4.13 (t (J = 6.8 Hz), 6 H, - $\text{CH}_2\text{COO}(\text{CH}_2)_9\text{CH}_2\text{OCO}$ -); 4.03 (m, 18 H, - $\text{C}_6\text{H}_4\text{OCH}_2$ , - $\text{CH}_2\text{COOCH}_2$ -); 3.64 (t (J = 6.4 Hz), 6 H, - $\text{C}(\text{CH}_2\text{OCH}_2)_3$ ); 3.46 (s, 6 H, - $\text{C}(\text{CH}_2\text{O})_3$ ); 3.22 (s, 1 H, - $\text{C}\equiv\text{CH}$ ); 2.50 (t (J = 6.5 Hz), 6 H, - $\text{CH}_2\text{COO}$ -); 1.81 (m, 12 H, - $\text{C}_6\text{H}_4\text{OCH}_2\text{CH}_2$ -); 1.50 (m, 24 H, - $\text{C}_6\text{H}_4\text{OCH}_2\text{CH}_2\text{CH}_2$ -, - $\text{CH}_2\text{COOCH}_2\text{CH}_2(\text{CH}_2)_6\text{CH}_2\text{CH}_2\text{OCO}$ -); 1.20 (m, 36 H, - $\text{CH}_2\text{COOCH}_2\text{CH}_2(\text{CH}_2)_6$ -); 1.04 (t (J = 7.4 Hz) d (J = 2.6 Hz), 18 H, - $\text{CH}_3$ )

$^{13}\text{C}$  NMR (100.4 MHz,  $\text{CDCl}_3$ )  $\delta_{\text{C}}$  (ppm): 171.7, 165.6, 165.0, 164.7, 164.2, 163.8, 163.7, 148.4, 148.2, 132.5, 132.5, 132.2, 130.5, 129.5, 127.2, 126.8, 125.1, 121.5, 121.1, 114.5, 114.4, 82.88, 80.17, 69.83, 68.12, 68.08, 67.02, 65.72, 64.72, 44.74, 35.09, 31.21, 31.03, 29.55, 29.48, 29.34, 29.28, 28.69, 28.48, 25.98, 25.91, 19.28, 13.92

MALDI-TOF MS:  $m/z = 2436.9$  (M + Na) $^+$

IR ( $\text{cm}^{-1}$ ): 3256, 3078, 2932, 2862, 1728, 1605, 1512, 1466, 1420, 1250, 1157, 1119, 1057, 1003, 972, 849, 764, 694, 640

Elemental analysis: calcd (%) for  $\text{C}_{140}\text{H}_{172}\text{O}_{35}$ : C 69.63, H 7.18; found: C 69.65, H 7.30

# **Chapter 6**

## **1:3 Type Janus LCs**

## 6.1 Summary

The dendritic building blocks described in Chapter 5 serve to assemble the diphenylacetylene moiety that will form the core in the “Janus” molecular architecture (Fig 6.1). In this chapter materials with a segregated molecular structure were described, which based on pentaerythritol on one side and a single chain on the other side of the diphenylacetylene scaffold. Different mesogenic groups or segregating substituents (A, B in Fig 6.1) are attached to the core in a ratio of 1:3 respectively.

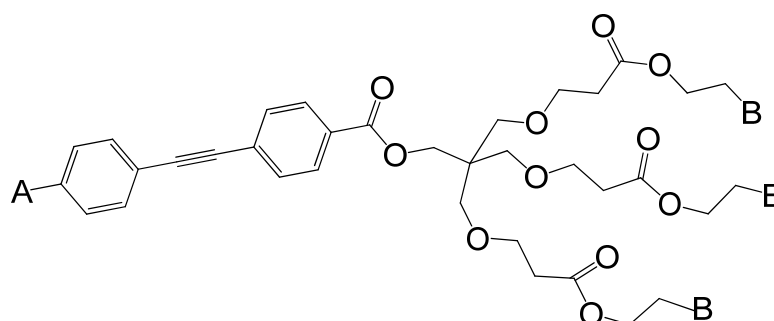


**Figure 6.1** 1:3 type Janus LC

This type of molecule still presents a distorted tetrahedral configuration, based on the multipede structure induced by PE. The three identical mesogenic units on pentaerythritol largely determine the mesomorphic behaviour of the entire molecule, whereas the chain on the opposite side serves to fine-tune this behaviour or to induce microphase segregation.

These series of 1:3 (that is, 1A:3B in the general structure) can be also viewed as PE multipedes with three identical mesogenic arms linked to PE by flexible spacers, which induce the mesomorphic behaviour. The fourth arm is actually to prepare the diphenylacetylene moiety which is directly anchored on PE without a spacer.

Three families of materials are described in this chapter, separated according to the nature of the terminal chain, A, on the diphenylacetylene arm with different segregation abilities (pentyl, perfluorodecyl and methyltriethylene glycol). For each

one, the mesogenic units, B, are either cyanobiphenyl-based (end-on) or PDAB-based (end-on), as described in previous chapters, or a perfluorinated chain.

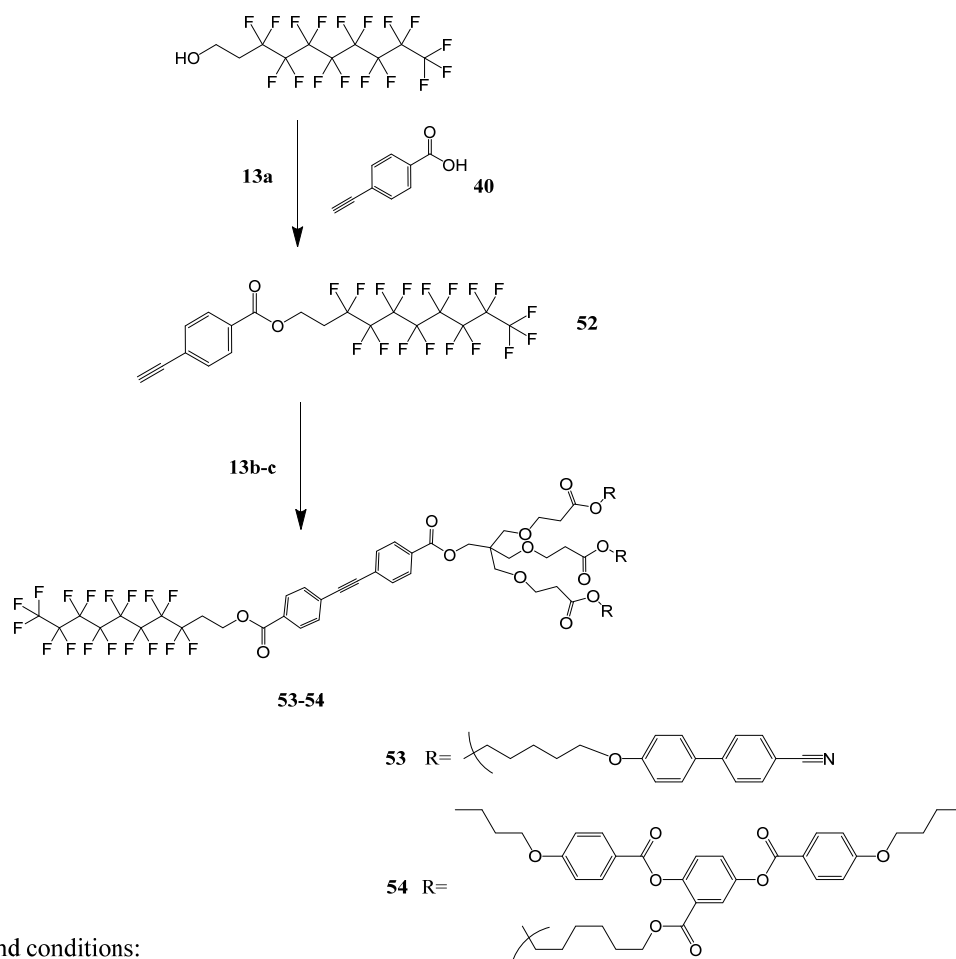
## 6.2 Synthesis

In all the cases the materials were synthesised following the same convergent strategy, that is, the Sonogashira coupling of the corresponding aromatic iodide and the alkynyl fragments described in Chapter 5.

1-Ethynyl-4-pentyl benzene was used to introduce an aliphatic chain to the asymmetric structure. It was combined to the dendron **47** to produce the diphenylacetylene arm, followed by the deprotection of the t-butyl ester to generate the tri-acid. Three different mesogens with hydroxyl groups at the end of the flexible spacer were attached to the dendritic branches via Steglich esterification to yield materials **49**, **50** and **51** (Scheme 12). For this family, the Sonogashira coupling was carried out before introducing the mesogenic units in order to prevent the loss of the valuable dendritic mesogen.



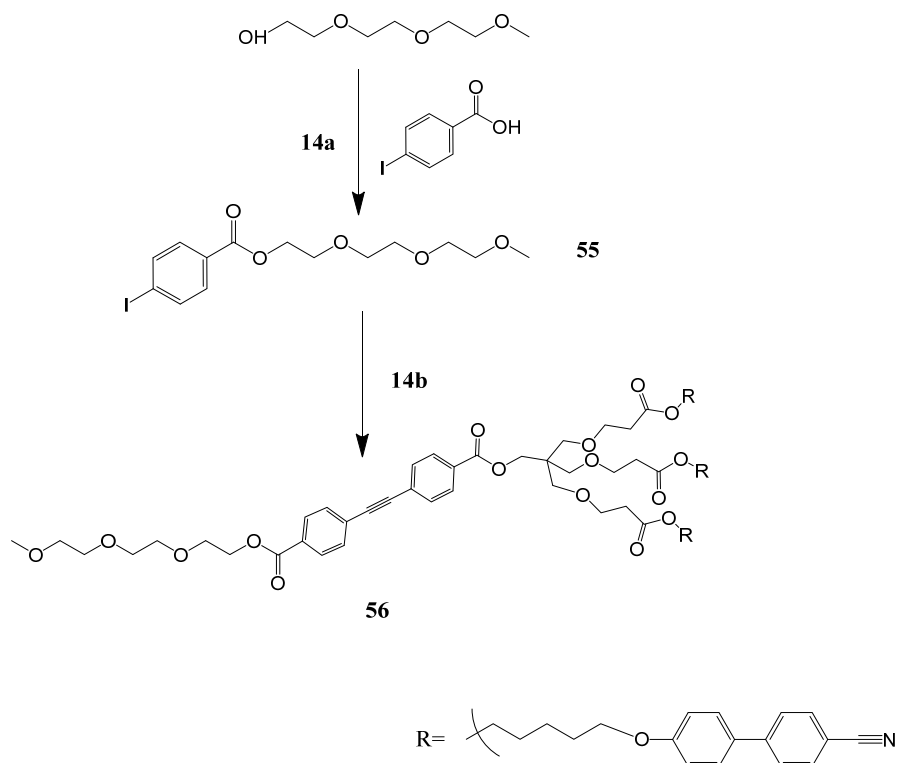
Alternatively, the fluorinated chain was attached to the 4-ethynylbenzoic acid (**52**), and the alkyne coupled to the dendritic mesogens **37** and **38** to produce **53** and **54** via Sonogashira coupling (Scheme 13).



Reagents and conditions:  
 13a - EDAC, DMAP, CH<sub>2</sub>Cl<sub>2</sub>  
 13b - **37**, Pd(PPh<sub>3</sub>)<sub>2</sub>Cl<sub>2</sub>, CuI, Et<sub>3</sub>N, Toluene  
 13c - **38**, Pd(PPh<sub>3</sub>)<sub>2</sub>Cl<sub>2</sub>, CuI, Et<sub>3</sub>N, Toluene

**Scheme 13**

A similar procedure was adopted to make the polyphilic molecule **56**, where the terminal chain on the diphenylacetylene arm is the hydrophilic methyltriethylenglycol (Scheme 14).



Reagents and conditions:  
 14a - EDAC, DMAP, CH<sub>2</sub>Cl<sub>2</sub>  
 14b - **44**, Pd(PPh<sub>3</sub>)<sub>2</sub>Cl<sub>2</sub>, CuI, Et<sub>3</sub>N

**Scheme 14**

The 1:3 Janus dendrimers combine the asymmetric dendritic structures and the rigid diphenyl acetylene cores, so their NMR spectra are combinations of the spectra of the two fragments that form the supermolecule as described in Chapter 5. The key information was gleaned from <sup>13</sup>C which showed the presence of the two distinct alkyne carbon environments and from the integration of protons on the different branches, which showed the formation of the desired products. MALDI-TOF MS was also used to ascertain the macromolecular structure and its monodispersity, without any sign of incomplete substitution of the PE branches.

### 6.3 Mesomorphic behaviour

Differential scanning calorimetry and polarized light optical microscopy were used to identify the liquid crystal behavior of the 1:3 Janus materials (Table 4).

No	g	Cr	Col	SmA	N	Iso
<b>49</b>	-	• 42.5 [14.3]	-	• 50.0 [6.1]	-	•
<b>50</b>	• -0.2	-	-	-	• 56.2 [1.4]	•
<b>51</b>	• 5.6	-	-	-	• 65.6 [2.2]	•
<b>53</b>	• 4.8	-	•*	•*	59.9 [6.2]	-
<b>54</b>	• 11.3	-	-	-	• 52.4 [1.1]	•
<b>56</b>	• -7.0	-	-	-	• 7.9 [0.4]	•

Note (\*): Overlapping transition peak, see discussion below

**Table 4** Transition temperatures (T/°C) and associated enthalpies ( $[\Delta H/\text{KJmol}^{-1}]$ ) of the 1:3 Janus materials

It is noticeable that all the materials with mesogenic units in the PE side, **50-56**, are liquid-crystalline at room temperature, and none of them crystallise at all, only show the glass transition below room temperature. The phase sequence g-Col-SmA-Iso was observed in compound **53** by POM; however the range of the SmA phase is very short, and the endotherms of the Col-SmA and SmA-Iso liq transitions on the DSC thermogram are overlapped, which made it difficult to obtain an accurate value for the transition temperature. However, by running the sample in DSC with lower heating and cooling rate, the overlapping of peaks can be observed more clearly (Fig 6.2), though a perfect analysis is still impossible. A rough estimate can be obtained from the DSC curve of heating at 1 °C/min, at around 59.5 °C and 60.7 °C for the Col-SmA and SmA-Iso transitions respectively.

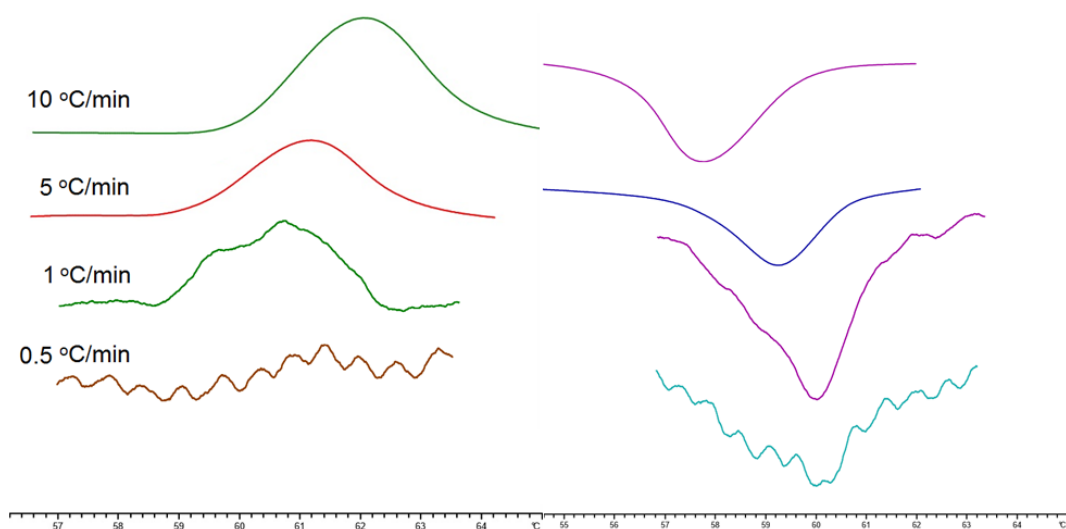


**Figure 6.2** Heating and cooling of compound **53** around the Col-SmA-Iso transition with different rate

In general the samples needed long annealing times to form clearly identifiable textures. The focal-conic fan texture of compound **49** with three perfluorinated chains is similar to that of the mesogenic dendrons **36** and **43**. Upon cooling, the focal-conic domains are formed gradually and the hyperbola and ellipse pairs can be observed clearly (Plate 9).



**Plate 9** The focal-conic fan texture of compound **49**, 49.5 °C (x200)

The schlieren texture of nematic phase forms on cooling **50** from the isotropic liquid. Both two and four brush defects were in the texture, indicated the presence of the nematic phase (Plate 10).

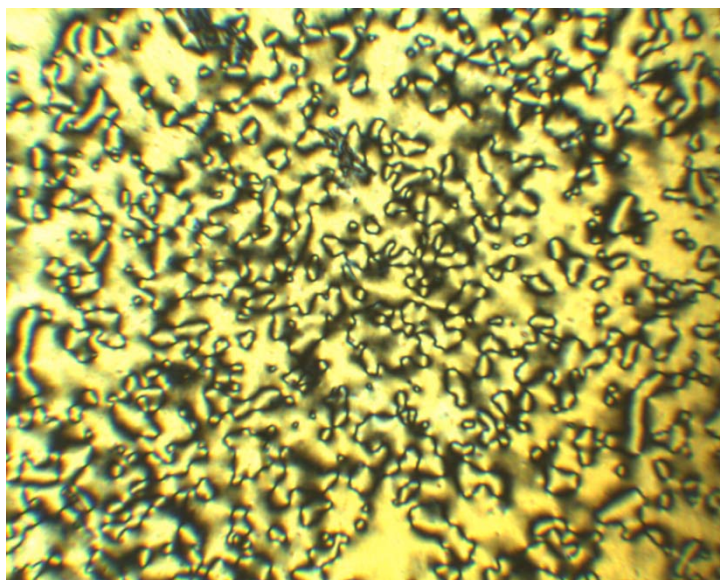
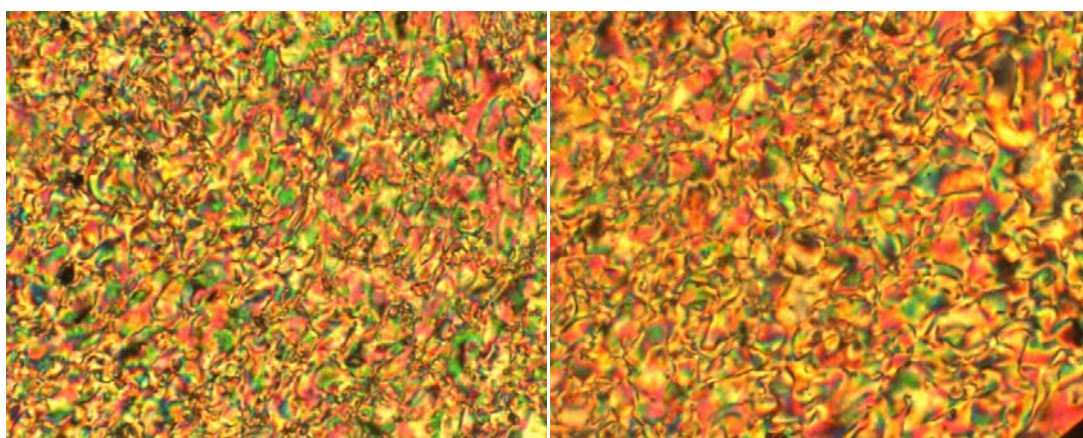


**Plate 10** The schlieren texture of compound **50**, 54 °C (x200)

Compound **51** and **54** with three side-on PDAB mesogenic units also display the schlieren texture of the nematic phase, similar to all their relatives (Plate 11).

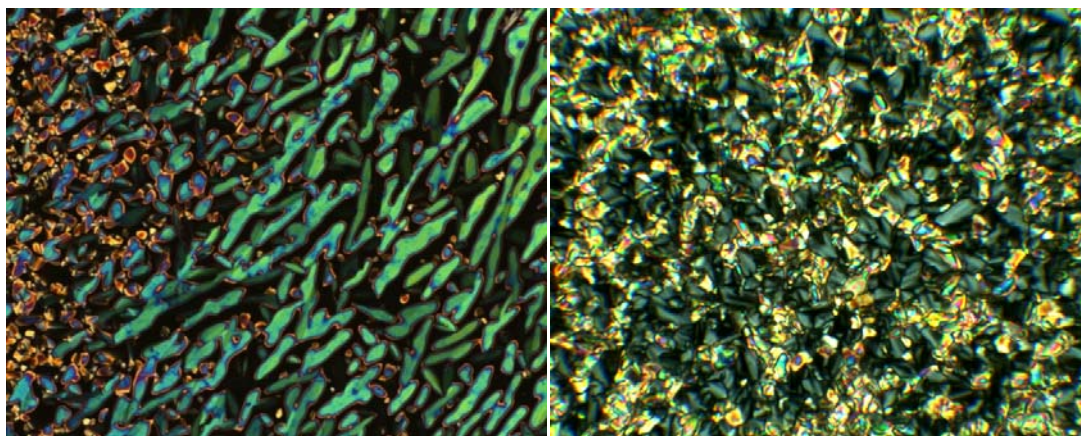


(a)

(b)

**Plate 11** The schlieren textures of compound (a) **51**, 61 °C; (b) **54**, 52 °C (x200)

Cooling just below the clearing point, compound **53** exhibits a mixed texture in which both the SmA focal-conic domains and the Col<sub>hex</sub> spine-like defects can be observed (Plate 12 a). The texture of the columnar phase is visible in the majority in the sample (Plate 12 a, right), however the hyperbola and ellipse pairs are also present (Plate 12 a, left). Further cooling to 58 °C results in a pure columnar phase, showing areas where the phase naturally coalesces from the liquid state (Plate 12 b, dark regions) and others that transformed from the SmA focal-conic fans (Plate 12 b, bright regions). This unique texture points to the existence of the SmA phase which has a quite short range and only forms partially in the sample.



(a)

(b)

**Plate 12** Textures of **53**: (a) Mixed focal-conic fan texture and spine-like texture, 61 °C, and (b) pseudo focal-conic fan texture, 58 °C (x200)

#### 6.4 Discussion

In general, the Janus 1:3 Janus dendrimers (**49**, **40**, **51**) show higher glass transitions and isotropisation temperatures than the related dendritic precursors (**44**, **45**, **46**), which may be due to the enhanced rigidity and anisotropy imparted by diphenylacetylene in comparison to phenylacetylene. Additionally, the introduction of diphenylacetylene and its terminal chain has little effect on the mesophase type exhibited, except in compound **50**.

Compound **50** and its related dendritic precursors **37** and **44** all contain three cyanobiphenyl mesogenic units. However, **50** exhibits only the nematic phase, unlike **37** and **44** which show SmA and nematic phases. In the absence of strong microsegregation, the reason of the disappearance of the lamellar phase might be the elongated fourth arm. If this arm is short, the molecules might be able to pack in the lamellar structure (as in **37** and **44** where the short arm is phenylacetylene, see Fig 5.6 top), whereas if the arm is long (as in **50**, where the arm is pentyldiphenylacetylene), the increased disorder may disturb the association in the smectic A phase and only the nematic phase is observed (Fig 6.3 top).

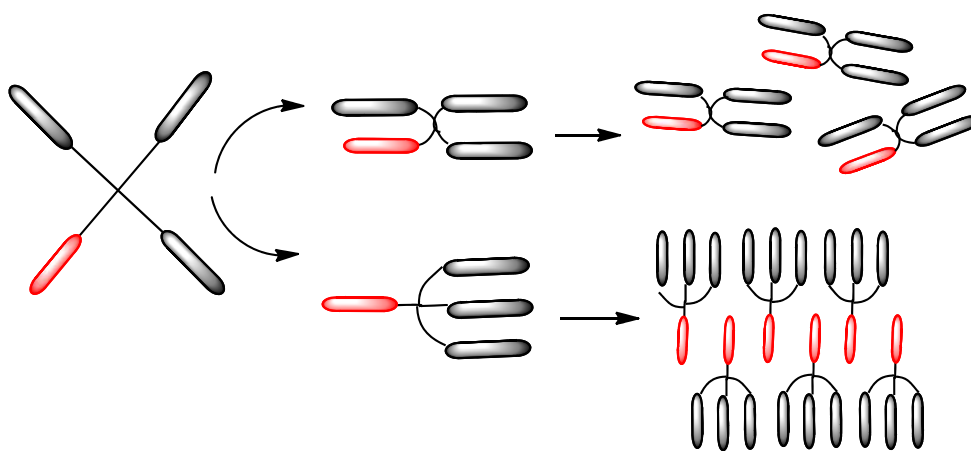


**Figure 6.3** Possible conformations of the 1:3 Janus dendrimers with substituted diphenylacetylene arm (red) and cyanobiphenyl (black) and their mesophase structures (top: nematic; bottom: smectic)

In comparison, **50** and **51** where mesomorphism is generated by the presence of mesogenic units in the PE arms, whereas compound **49** without mesogenic units but with three perfluorinated chains instead, is nevertheless liquid crystalline and shows the SmA phase (Plate 9). The much stronger microsegregation between the stiff perfluorinated chains and the pentyl diphenylacetylene unit successfully leads to the formation of the SmA phase. The melting point of **49** is higher than those of **36** and **43** whereas the SmA-Iso liq transition temperature is almost the same, yielding a mesophase with shorter range. The competition between the microphase segregation and the steric effect might result in a fluctuating bilayer and a reduction of the

stability of the SmA phase. However, the exact mesophase structure can only be ascertained by X-ray diffraction measurements.

Compound **51** with three laterally attached PDAB mesogenic units exhibits only the nematic phase. In comparison with the related dendrons **38** and **45**, the overall molecular shape of **51** is elongated, which ensures a more stable nematic. The side-on PDAB mesogenic unit which does not favour the lamellar packing completely inhibited the presence of smectic phases.

Comparison of **53** and **50** shows that by attaching a stiff perfluorinated chain onto the multipede with three cyanobipenyl mesogenic units (**53**) instead of the alkyl chain (**50**), the strong segregation effect between the perfluorinated chain and cyanobiphenyl groups forces the molecule take a pronounced cone shape (Fig 6.4). In this conformation the nematic phase is totally suppressed, and the strong microphase segregation induces the formation of the SmA phase (probably with a bilayer structure) albeit over a very short temperature range. On further cooling, increased interfacial curvature of the molecular assemblies promotes a more stable disoctic arrangement of the molecules which drives the transition to the columnar phase. However, it must be emphasised that this is only a tentative explanation, and requires X-Ray diffraction analysis to be verified.

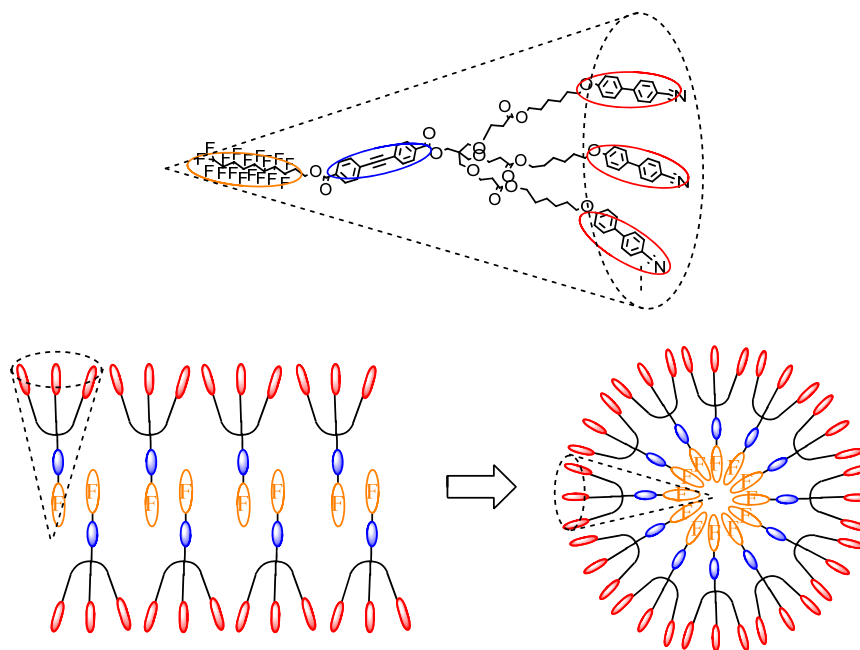
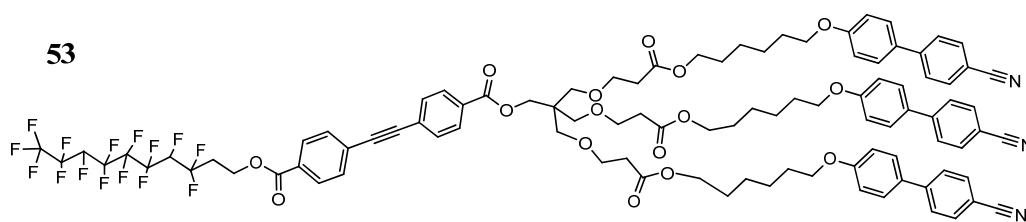
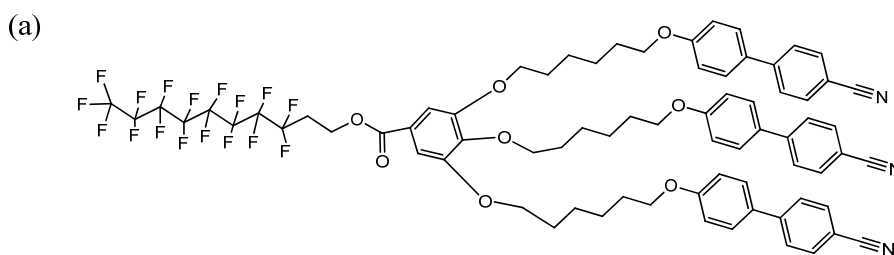


**Figure 6.4** The cone shape of compound **53** and the proposed packing of the mesogens showing the transition from the lamellar to the discotic arrangement

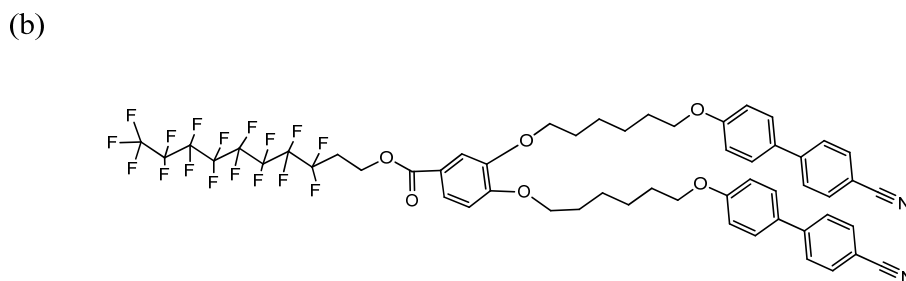
The mesomorphic behaviour of **53**, induced by strong microphase segregation, is related to that observed in similar 1:3 Janus-type derivatives reported by Yoshizawa (Fig 6.5 (a)) [32]. The asymmetric oligomer (a) also has three end-on cyanobiphenyl mesogenic units and the perfluorinated chain, and exhibits smectic A phase and a cubic phase. Microphase segregation induces the formation of a stable SmA phase with bilayer structure; however the steric effect is still important in the bilayer, resulting in a fluctuating lamellar structure. This fluctuating arrangement can easily deform and on cooling a transition to a bicontinuous cubic phase takes place. Additionally, when only two cyanobiphenyl groups are present (Fig 6.5 b) the hexagonal columnar phase is formed as well as the SmA phase, but not the cubic phase. Both (a) and (b) have much higher mesophase stability than **53** which may be caused by the more compact molecular packing allowed by the planar conformation of the phenyl ring as anchoring point as opposed to the tetrahedral pentaerythritol.



g 4.8 Col SmA 59.9 I



Cr 83.2 Cub 141.1 SmA 154.9 I



Cr 62.2 Col 134.2 SmA 170.6 I

**Figure 6.5** Janus LC molecules with cyanobiphenyls and a perfluorinated chain

Despite the strong smectic phase inducing effect of the perfluorinated chain, Janus compound **54** still exhibited only the nematic phase since the three side-on PDAB mesogenic units have much stronger nematic phase inducing ability, which inhibits the tendency to form the smectic A phase. The microsegregation effect induced by one fluorinated chain is not enough to counteract the steric hindrance caused by the three side-on mesogenic units, precluding the formation of the smectic A phase. Compared to **51**, the increased polarity of **54** caused a higher glass transition temperature; However the N-I transition temperature was notably reduced, which might be due to the potential of the smectic phase forming effect versus the nematic phase, thereby bringing down the nematic phase stability.

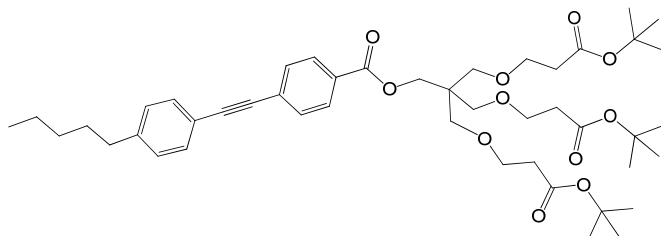
Amphiphilic Janus dendrimer **56**, with one methyltriethylene glycol chain on the diphenylacetylene arm, is isotropic at room temperature and exhibits the nematic phase when cooling down to about 6 °C. Compared to the perfluorinated chain, the flexible triethylene glycol chain doesn't lead to microphase segregation, resulting in the formation of only a nematic phase for **56**. Moreover, the liquid crystal phase stability is the lowest among the family of 1:3 Janus dendrimers. This might be caused by the longer and much more flexible chain attached to the diphenylacetylene arm, which can interfere with the interactions between the cyanobiphenyl cores.

## 6.5 Concluding remarks

Two synthetic routes were implemented to prepare three families of 1:3 Janus-type LCs. Though their structures are similar to LC mutipedes, the increased incompatibility between the differently decorated branches allowed the Janus LCs to exhibit a more varied mesophase behaviour. The microphase segregation effect can be observed between incompatible moieties; the cyanobiphenyl groups and the perfluorinated chain successfully segregate into SmA layers, whereas lower incompatibility usually results in the nematic phase being formed. The diphenylacetylene group also influences the mesophase behaviour with its own rigidity and anisotropy contributing to the system, though it can also induce more disorder disturbing the smectic layer formation in cyanobiphenyl derivatives, leading to the formation of the nematic phase.

## 6.6 Experimental

### 2,2,2-Tris(3-tert-butoxy-3-oxopropyl)ethyl 4-(4-pentylphenylethynyl)benzoate (**47**)

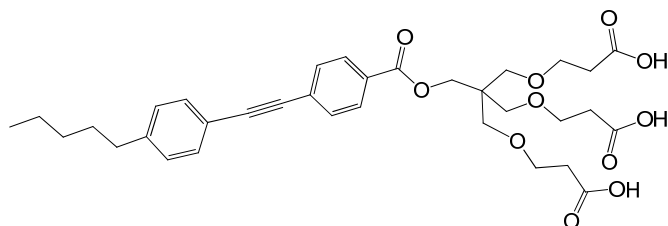


A Schlenk flask containing 2,2,2-tris(3-tert-butoxy-3-oxopropyl)ethyl 4-iodobenzoate (**34**) (0.5 g; 0.67 mmol), Pd(PPh<sub>3</sub>)<sub>2</sub>Cl<sub>2</sub> (22 mg; 0.03 mmol) and CuI (6 mg; 0.03 mmol) was degassed and flushed with argon. Triethylamine (20 mL) flushed with argon for 20 min was transferred via a cannula followed by the addition of 1-ethynyl-4-pentyl benzene (0.14 mL; 0.73 mmol) by syringe. The reaction mixture was stirred at room temperature for 20 h. The solvent was then removed by evaporation, and the product was isolated from the residue by column chromatography, eluting with hexane then dichloromethane to give **47** as a colorless oil.

Yield: 0.47 g (89%)

<sup>1</sup>H NMR (400 MHz, CDCl<sub>3</sub>) δH (ppm): 7.99 (d (J = 8.5 Hz), 2 H, ArH); 7.57 (d (J = 8.5 Hz), 2 H, ArH); 7.46 (d (J = 8.2 Hz), 2 H, ArH); 7.18 (d (J = 8.2 Hz), 2 H, ArH); 4.32 (s, 2 H, -COOCH<sub>2</sub>-); 3.62 (t (J = 6.4 Hz), 6 H, -C(CH<sub>2</sub>OCH<sub>2</sub>-)<sub>3</sub>); 3.49 (s, 6 H, -C(CH<sub>2</sub>O-)<sub>3</sub>); 2.62 (t (J = 7.7 Hz), 2 H, -C<sub>6</sub>H<sub>4</sub>CH<sub>2</sub>-); 2.43 (t (J = 6.4 Hz), 6 H, -CH<sub>2</sub>COO-); 1.62 (m, 2 H, -C<sub>6</sub>H<sub>4</sub>CH<sub>2</sub>CH<sub>2</sub>-); 1.43 (s, 27 H, -C(CH<sub>3</sub>)<sub>3</sub>); 1.32 (m, 4 H, -C<sub>6</sub>H<sub>4</sub>CH<sub>2</sub>CH<sub>2</sub>(CH<sub>2</sub>)<sub>2</sub>-); 0.89 (t (J = 6.9 Hz), 3 H, -CH<sub>2</sub>CH<sub>3</sub>)

**2,2,2-Tris(3-hydroxyl-3-oxopropyl)ethyl 4-(4-pentylphenylethynyl)benzoate (48)**

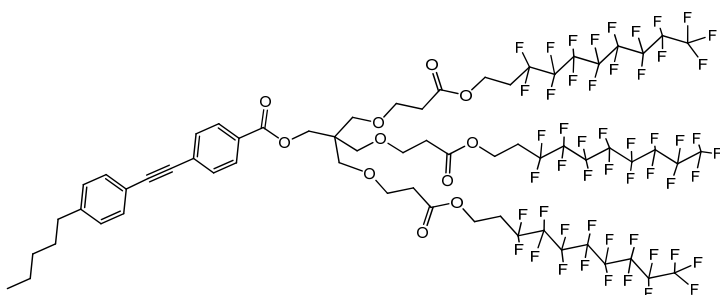


The tri-ester **47** (0.46 g; 0.58 mmol) was dissolved in dichloromethane (10 mL) and trifluoroacetic acid (1.3 mL; 17.3 mmol). The mixture was stirred for 20 h at room temperature. The solvent was removed by evaporation under reduced pressure, and the residue was left in desiccator over P<sub>2</sub>O<sub>5</sub> for 35 h to give the tri-acid **48** as a yellow solid.

Yield: 0.36 g (99%)

<sup>1</sup>H NMR (400 MHz, CDCl<sub>3</sub>) δH (ppm): 7.80 (d (J = 8.6 Hz), 2 H, ArH); 7.58 (d (J = 8.6 Hz), 2 H, ArH); 7.47 (d (J = 8.2 Hz), 2 H, ArH); 7.19 (d (J = 8.2 Hz), 2 H, ArH); 4.31 (s, 2 H, -COOCH<sub>2</sub>-); 3.61 (t (J = 6.3 Hz), 6 H, -C(CH<sub>2</sub>OCH<sub>2</sub>-)<sub>3</sub>); 3.49 (s, 6 H, -C(CH<sub>2</sub>O-)<sub>3</sub>); 2.64 (t (J = 7.7 Hz), 2 H, -C<sub>6</sub>H<sub>4</sub>CH<sub>2</sub>-); 2.56 (t (J = 6.4 Hz), 6 H, -CH<sub>2</sub>COO-); 1.61 (m, 2 H, -C<sub>6</sub>H<sub>4</sub>CH<sub>2</sub>CH<sub>2</sub>-); 1.33 (m, 4 H, -C<sub>6</sub>H<sub>4</sub>CH<sub>2</sub>CH<sub>2</sub>(CH<sub>2</sub>)<sub>2</sub>-); 0.88 (t (J = 6.9 Hz), 3 H, -CH<sub>2</sub>CH<sub>3</sub>)

**2,2,2-Tris(3-(3,3,4,4,5,5,6,6,7,7,8,8,9,9,10,10,10-heptafluorodecyloxy)-3-oxopropyl)ethyl 4-(4-pentylphenylethynyl)benzoate (49)**



The tri-acid **48** (0.04 g; 0.06 mmol) and 1H,1H,2H,2H-perfluorodecanol (0.09 g; 0.2 mmol) were dissolved in tetrahydrofuran (10 mL) with N,N'-dicyclohexylcarbodiimide (0.05 g; 0.23 mmol) and 4-(dimethylamino)pyridine (0.024

g; 0.2 mmol). The mixture was stirred under argon for 72 h at room temperature. The solvent was removed by evaporation, and the product was isolated from the crude by column chromatography, eluting with 1:10 ethyl acetate/dichloromethane to yield **49** as white crystals.

Yield: 0.07 g (57%)

$^1\text{H}$  NMR (400 MHz,  $\text{CDCl}_3$ )  $\delta\text{H}$  (ppm): 7.97 (d ( $J = 8.5$  Hz), 2 H,  $\text{ArH}$ ); 7.57 (d ( $J = 8.5$  Hz), 2 H,  $\text{ArH}$ ); 7.45 (d ( $J = 8.2$  Hz), 2 H,  $\text{ArH}$ ); 7.17 (d ( $J = 8.2$  Hz), 2 H,  $\text{ArH}$ ); 4.37 (t ( $J = 6.5$  Hz), 6 H,  $-\text{CH}_2\text{COOCH}_2-$ ); 4.28 (s, 2 H,  $-\text{C}_6\text{H}_4\text{COOCH}_2-$ ); 3.66 (t ( $J = 6.2$  Hz), 6 H,  $-\text{C}(\text{CH}_2\text{OCH}_2-)_3$ ); 3.47 (s, 6 H,  $-\text{C}(\text{CH}_2\text{O}-)_3$ ); 2.62 (t ( $J = 7.7$  Hz), 2 H,  $-\text{C}_6\text{H}_4\text{CH}_2-$ ); 2.54 (t ( $J = 6.3$  Hz), 6 H,  $-\text{CH}_2\text{COO}-$ ); 2.46 (m, 6 H,  $-\text{CH}_2\text{COOCH}_2\text{CH}_2-$ ); 1.31 (m, 8 H,  $-\text{C}_6\text{H}_4\text{CH}_2(\text{CH}_2)_4-$ ); 0.89 (t ( $J = 6.9$  Hz), 3 H,  $-\text{CH}_3$ )

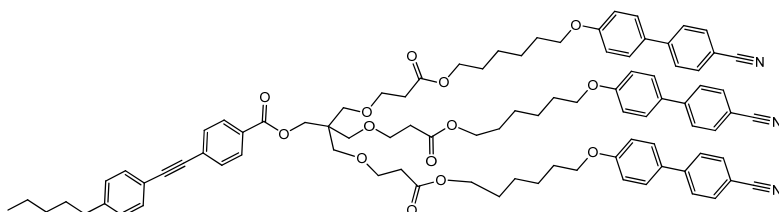
$^{13}\text{C}$  NMR (100.4 MHz,  $\text{CDCl}_3$ )  $\delta\text{C}$  (ppm): 171.2, 165.8, 144.2, 131.7, 131.5, 129.5, 129.5, 128.6, 128.4, 119.9, 92.78, 88.04, 69.75, 66.70, 64.34, 56.40, 44.75, 35.99, 34.87, 31.51, 31.00, 30.71, 30.49, 30.28, 29.79, 22.59, 14.08

MALDI-TOF MS:  $m/z = 2003.2$  ( $\text{M} + \text{K}$ ) $^+$

IR ( $\text{cm}^{-1}$ ): 2924, 2870, 2214, 1736, 1605, 1458, 1366, 1204, 1142, 1111, 1011, 964, 856, 772, 702, 656, 556, 525

Elemental analysis: calcd (%) for  $\text{C}_{64}\text{H}_{51}\text{F}_{51}\text{O}_{11}$ : C 39.12, H 2.62; found: C 39.41, H 2.85

**2,2,2-Tris(3-(6-(4'-cyanobiphenyl-4-yloxy)hexyloxy)-3-oxopropylloxymethyl)-ethyl 4-(4-pentylphenylethynyl)benzoate (50)**



The tri-acid **48** (0.1 g; 0.16 mmol) and 4,4'-(6-hydroxyhexyloxy)cyanobiphenyl (0.17 g; 0.56 mmol) were dissolved in tetrahydrofuran (10 mL) with  $\text{N,N}'$ -dicyclohexylcarbodiimide (0.12 g; 0.57 mmol) and 4-(dimethylamino)pyridine (0.06

g; 0.48 mmol). The reaction was stirred under argon for 72 h at room temperature. The solvent was removed by evaporation, and the product was isolated by column chromatography, eluting with 1:10 ethyl acetate/dichloromethane, to yield **50** as a white sticky solid.

Yield: 0.11 g (47%)

$^1\text{H}$  NMR (400 MHz,  $\text{CDCl}_3$ )  $\delta\text{H}$  (ppm): 7.97 (d (J = 8.5 Hz), 2 H, ArH); 7.67 (d (J = 8.6 Hz), 6 H, ArH); 7.62 (d (J = 8.6 Hz), 6 H, ArH); 7.55 (d (J = 8.5 Hz), 2 H, ArH); 7.50 (d (J = 8.8 Hz), 6 H, ArH); 7.43 (d (J = 8.2 Hz), 2 H, ArH); 7.16 (d (J = 8.2 Hz), 2 H, ArH); 6.96 (d (J = 8.8 Hz), 6 H, ArH); 4.30 (s, 2 H,  $-\text{C}_6\text{H}_4\text{COOCH}_2-$ ); 4.07 (t (J = 6.7 Hz), 6 H,  $-\text{CH}_2\text{COOCH}_2-$ ); 3.97 (t (J = 6.4 Hz), 6 H,  $-\text{CH}_2\text{O}(\text{C}_6\text{H}_4)_2\text{CN}$ ); 3.67 (t (J = 6.4 Hz), 6 H,  $-\text{C}(\text{CH}_2\text{OCH}_2)_3$ ); 3.49 (s, 6 H,  $-\text{C}(\text{CH}_2\text{O}-)_3$ ); 2.61 (t (J = 7.7 Hz), 2 H,  $-\text{C}_6\text{H}_4\text{CH}_2-$ ); 2.52 (t (J = 6.4 Hz), 6 H,  $-\text{CH}_2\text{COO}-$ ); 1.79 (m, 6 H,  $-\text{CH}_2\text{COOCH}_2\text{CH}_2-$ ); 1.65 (m, 8 H,  $-\text{CH}_2\text{CH}_2\text{O}(\text{C}_6\text{H}_4)_2\text{CN}$ ,  $-\text{C}_6\text{H}_4\text{CH}_2\text{CH}_2-$ ); 1.46 (m, 12 H,  $-\text{CH}_2\text{COOCH}_2\text{CH}_2(\text{CH}_2)_2-$ ); 1.29 (m, 4 H,  $-\text{C}_6\text{H}_4\text{CH}_2\text{CH}_2(\text{CH}_2)_2-$ ); 0.89 (t (J = 6.9 Hz), 3 H,  $-\text{CH}_3$ )

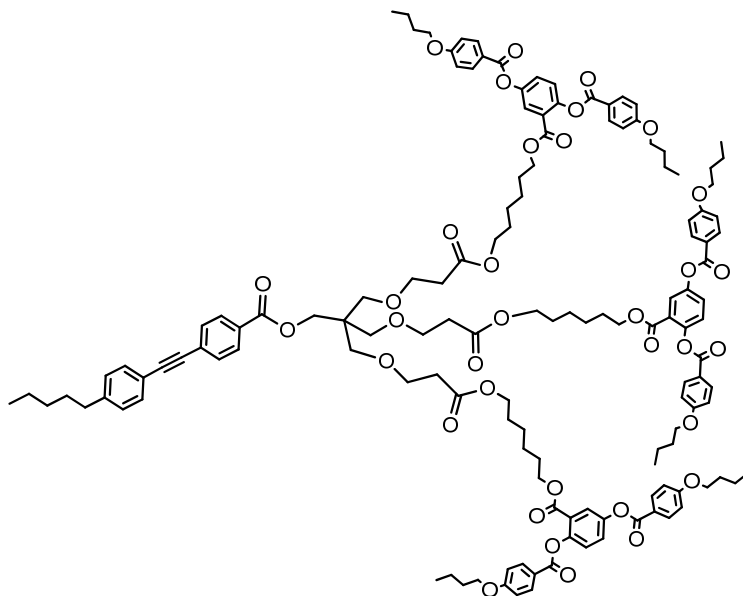
$^{13}\text{C}$  NMR (100.4 MHz,  $\text{CDCl}_3$ )  $\delta\text{C}$  (ppm): 171.7, 169.6, 159.8, 145.3, 132.7, 131.7, 131.5, 131.4, 128.7, 128.4, 127.1, 119.2, 118.3, 115.1, 110.1, 94.0, 69.89, 68.01, 67.01, 64.55, 61.14, 55.82, 41.88, 35.15, 31.53, 30.99, 29.21, 28.64, 25.83, 22.60, 16.91, 16.89, 14.12

MS:  $m/z = 1496.7$  (M + K) $^+$

IR ( $\text{cm}^{-1}$ ): 2932, 2862, 2222, 1721, 1605, 1497, 1466, 1396, 1250, 1180, 1103, 1072, 1011, 856, 818, 772, 733, 694, 656, 594, 509

Elemental analysis: calcd (%) for  $\text{C}_{91}\text{H}_{99}\text{N}_3\text{O}_{14}$ : C 74.92, H 6.84, N 2.88; found: C 74.61, H 6.78, N 2.76

**2,2,2-Tris(3-(6-(2,5-di(4-butoxybenzoyloxy)benzoyloxy)hexyloxy)-3-oxopropoxymethyl)ethyl 4-(4-pentylphenylethynyl)benzoate (51)**



The tri-acid **48** (0.1 g; 0.16 mmol) and 6-hydroxyhexyl 2,5-di(4-butoxybenzoyloxy)benzoate (**16**) (0.34 g; 0.56 mmol) were dissolved in tetrahydrofuran (10 mL) with *N,N'*-dicyclohexylcarbodiimide (0.12 g; 0.57 mmol) and 4-(dimethylamino)pyridine (0.06 g; 0.48 mmol). The reaction was stirred under argon for 72 h at room temperature. The solvent was removed by evaporation, and the product was isolated from the crude material by column chromatography, eluting with 1:5 ethyl acetate/dichloromethane, to yield **51** as a white sticky solid.

Yield: 0.13 g (34%)

$^1\text{H}$  NMR (400 MHz,  $\text{CDCl}_3$ )  $\delta$ H (ppm): 8.14 (m, 12 H, ArH); 7.95 (d (J = 8.5 Hz), 2 H, ArH); 7.87 (d (J = 2.7 Hz), 3 H, ArH); 7.54 (d (J = 8.5 Hz), 2 H, ArH); 7.44 (m, 5 H, ArH); 7.25 (d (J = 8.8 Hz), 3 H, ArH); 7.16 (d (J = 8.2 Hz), 2 H, ArH); 6.97 (d (J = 8.9 Hz) d (J = 1.9 Hz), 12 H, ArH); 4.27 (s, 2 H,  $-\text{C}_6\text{H}_4\text{COOCH}_2-$ ); 4.13 (t (J = 6.7 Hz), 6 H,  $-\text{CH}_2\text{COO}(\text{CH}_2)_5\text{CH}_2\text{OCO}-$ ); 4.04 (m, 12 H,  $-\text{C}_6\text{H}_4\text{OCH}_2-$ ); 3.97 (t (J = 6.8 Hz), 6 H,  $-\text{CH}_2\text{COOCH}_2-$ ); 3.63 (t (J = 6.5 Hz), 6 H,  $-\text{C}(\text{CH}_2\text{OCH}_2)_3$ ); 3.46 (s, 6 H,  $-\text{C}(\text{CH}_2\text{O})_3$ ); 2.60 (t (J = 7.7 Hz), 2 H,  $-\text{C}_6\text{H}_4\text{CH}_2-$ ); 2.49 (t (J = 6.4 Hz), 6 H,  $-\text{CH}_2\text{COO}-$ ); 1.80 (m, 12 H,  $-\text{C}_6\text{H}_4\text{OCH}_2\text{CH}_2-$ ); 1.50 (m, 26 H,  $-\text{C}_6\text{H}_4\text{OCH}_2\text{CH}_2\text{CH}_2-$ ,  $-\text{CH}_2\text{COOCH}_2\text{CH}_2\text{CH}_2\text{CH}_2\text{CH}_2\text{CH}_2\text{OCO}-$ ,  $-\text{C}_6\text{H}_4\text{CH}_2\text{CH}_2-$ ); 1.26 (m, 16 H,  $-\text{CH}_2\text{COOCH}_2\text{CH}_2(\text{CH}_2)_2-$ ,  $-\text{C}_6\text{H}_4\text{CH}_2\text{CH}_2(\text{CH}_2)_2-$ ); 0.99 (t (J = 7.4 Hz) d (J = 3.8 Hz), 18 H,  $-\text{O}(\text{CH}_2)_3\text{CH}_3$ ); 0.89 (t (J = 6.9 Hz), 3 H,  $-\text{C}_6\text{H}_4(\text{CH}_2)_4\text{CH}_3$ )

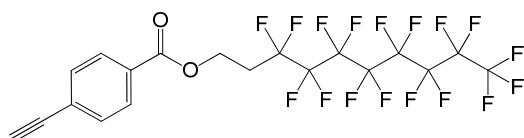
$^{13}\text{C}$  NMR (100.4 MHz,  $\text{CDCl}_3$ )  $\delta\text{C}$  (ppm): 168.5, 165.9, 165.0, 164.3, 155.1, 150.4, 149.2, 148.2, 140.3, 134.9, 132.5, 132.5, 127.2, 125.0, 122.4, 121.5, 114.5, 114.4, 113.6, 92.10, 68.12, 18.09, 67.89, 67.68, 67.00, 66.18, 65.47, 64.48, 53.89, 35.03, 31.20, 28.49, 28.39, 25.59, 25.35 19.28, 13.92

MALDI-TOF MS:  $m/z = 2392.1$  ( $\text{M} + \text{H}$ ) $^+$

IR ( $\text{cm}^{-1}$ ): 3071, 2932, 2870, 2214, 1913, 1728, 1605, 1512, 1466, 1420, 1304, 1242, 1157, 1119, 1057, 1003, 972, 910, 880, 849, 764, 694, 640, 593, 494

Elemental analysis: calcd (%) for  $\text{C}_{139}\text{H}_{162}\text{O}_{35}$ : C 69.77, H 6.82; found: C 69.55, H 6.84

### 3,3,4,4,5,5,6,6,7,7,8,8,9,9,10,10,10-heptafluorodecyl 4-ethynylbenzoate (**52**)

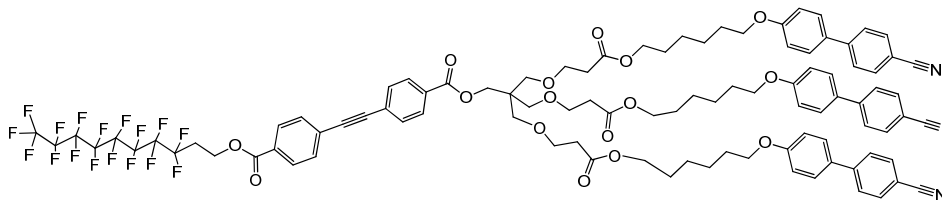


4-Ethynylbenzoic acid (0.3 g; 2 mmol) and 1H,1H,2H,2H-perfluorodecanol (0.95 g; 2 mmol) were dissolved in dichloromethane (20 mL) with 1-ethyl-3-(3-dimethylaminopropyl)carbodiimide (0.47 g; 2.5 mmol) and 4-(dimethylamino)pyridine (0.25 g; 2 mmol). The reaction was stirred under argon for 18 h at room temperature. The solvent was removed by evaporation, and the product was isolated from the crude by column chromatography, eluting with dichloromethane, to yield **52** as white crystals.

Yield: 1.03 g (88%)

$^1\text{H}$  NMR (400 MHz,  $\text{CDCl}_3$ )  $\delta\text{H}$  (ppm): 7.99 (d ( $J = 8.3$  Hz), 2 H,  $\text{ArH}$ ); 7.56 (d ( $J = 8.4$  Hz), 2 H,  $\text{ArH}$ ); 4.63 (t ( $J = 6.4$  Hz), 2 H,  $-\text{COOCH}_2-$ ); 3.25 (s, 1 H,  $-\text{C}\equiv\text{CH}$ ); 2.61 (m, 2 H,  $-\text{COOCH}_2\text{CH}_2-$ )

**2,2,2-Tris(3-(6-(4'-cyanobiphenyl-4-yloxy)hexyloxy)-3-oxopropylloxymethyl)-ethyl 3,3,4,4,5,5,6,6,7,7,8,8,9,9,10,10,10-heptafluorodecyl 4,4'-(1,2-ethynediyl)bibenzoate (53)**



The dendritic 4-iodobenzene ester **37** (0.1 g; 0.07 mmol) was dissolved in toluene (5 mL) and added to a solution of 4-ethynyl heptafluorodecylbenzoate (**52**) (46 mg; 0.08 mmol) in triethylamine (5 mL). The solution was purged with argon for 15 min. A catalytic mixture of Pd(PPh<sub>3</sub>)<sub>2</sub>Cl<sub>2</sub> (10 mg; 0.014 mmol) and CuI (3 mg; 0.014 mmol) was added into the solution and the reaction was stirred for 20 h at room temperature. The solvent was removed by evaporation, and the product was removed from the crude by column chromatography, eluting with 1:10 ethyl acetate/dichloromethane, to yield **53** as a yellow sticky solid.

Yield: 0.14 g (91%)

<sup>1</sup>H NMR (400 MHz, CDCl<sub>3</sub>) δH (ppm): 8.01 (d (J = 8.5 Hz) d (J = 4.2 Hz), 4 H, ArH); 7.67 (d (J = 8.5 Hz), 6 H, ArH); 7.60 (m, 10 H, ArH); 7.51 (d (J = 8.8 Hz), 6 H, ArH); 6.96 (d (J = 8.8 Hz), 6 H, ArH); 4.64 (t (J = 6.4 Hz), 2 H, -CF<sub>2</sub>CH<sub>2</sub>CH<sub>2</sub>-); 4.31 (s, 2 H, -CH<sub>2</sub>C(CH<sub>2</sub>O-)<sub>3</sub>); 4.07 (t (J = 6.7 Hz), 6 H, -C<sub>6</sub>H<sub>4</sub>OCH<sub>2</sub>-); 3.97 (t (J = 6.4 Hz), 6 H, -CH<sub>2</sub>COOCH<sub>2</sub>-); 3.66 (t (J = 6.4 Hz), 6 H, -C(CH<sub>2</sub>OCH<sub>2</sub>-)<sub>3</sub>); 3.48 (s, 6 H, -C(CH<sub>2</sub>O-)<sub>3</sub>); 2.60 (m, 8 H, -CH<sub>2</sub>COO-, -CF<sub>2</sub>CH<sub>2</sub>-); 1.80 (m, 6 H, -CH<sub>2</sub>CH<sub>2</sub>O(C<sub>6</sub>H<sub>4</sub>)<sub>2</sub>CN); 1.65 (m, 6 H, -CH<sub>2</sub>COOCH<sub>2</sub>CH<sub>2</sub>-); 1.45 (m, 12 H, -CH<sub>2</sub>COOCH<sub>2</sub>CH<sub>2</sub>(CH<sub>2</sub>)<sub>2</sub>-)

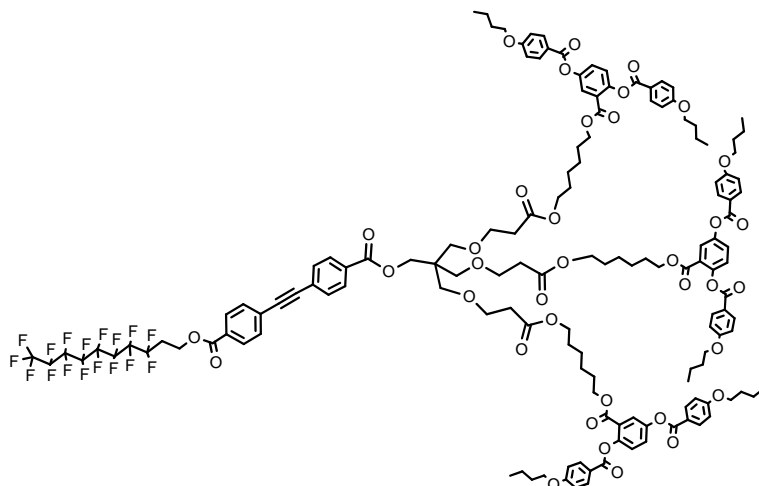
<sup>13</sup>C NMR (100.4 MHz, CDCl<sub>3</sub>) δ<sub>C</sub> (ppm): 171.7, 159.8, 145.3, 132.7, 131.8, 131.4, 129.8, 128.4, 127.1, 119.2, 115.1, 110.2, 91.82, 91.48, 68.00, 67.05, 64.56, 44.77, 35.13, 29.21, 28.63, 25.82

MALDI-TOF MS: m/z = 1900.6 (M + Na)<sup>+</sup>

IR (cm<sup>-1</sup>): 3048, 2932, 2862, 2222, 2083, 1736, 1605, 1497, 1466, 1396, 1366, 1227, 1180, 1103, 1011, 818, 756, 694, 656, 517

Elemental analysis: calcd (%) for C<sub>97</sub>H<sub>92</sub>N<sub>3</sub>O<sub>16</sub>F<sub>17</sub>: C 62.01, H 4.94, N 2.24; found: C 61.99, H 5.05, N 2.11

**2,2,2-Tris(3-(6-(2,5-di(4-butoxybenzoyloxy)benzoyloxy)hexyloxy)-3-oxopropylloxymethyl)ethyl 3,3,4,4,5,5,6,6,7,7,8,8,9,9,10,10,10-heptafluorodecyl 4,4'-(1,2-ethynediyl)bibenzoate (54)**



The dendritic 4-iodobenzene ester **38** (0.08 g; 0.034 mmol) was dissolved in toluene (5 mL) and added in to a solution of 4-ethynyl heptafluorodecylbenzoate (**52**) (23 mg; 0.04 mmol) in triethylamine (5 mL). The solution was purged with argon for 15 min. A catalytic mixture of Pd(PPh<sub>3</sub>)<sub>2</sub>Cl<sub>2</sub> (5 mg; 0.007 mmol) and CuI (1.5 mg; 0.007 mmol) was added into the solution and the mixture was stirred for 20 h at room temperature. The solvent was taken off by evaporation under reduced pressure, and the product was obtained from the crude by column chromatography, eluting with 1:8 ethyl acetate/dichloromethane, to yield **54** as a yellow sticky solid.

Yield: 78 mg (82%)

<sup>1</sup>H NMR (400 MHz, CDCl<sub>3</sub>) δH (ppm): 8.14 (d (J = 8.9 Hz) d (J = 4.9 Hz), 12 H, ArH); 8.00 (d (J = 14.8 Hz) d (J = 8.4 Hz), 4 H, ArH); 7.87 (d (J = 2.9 Hz), 3 H, ArH); 7.59 (t (J = 8.1 Hz), 4 H, ArH); 7.44 (d (J = 8.7 Hz) d (J = 2.9 Hz), 3 H, ArH); 7.24 (d (J = 8.8 Hz), 3 H, ArH); 6.97 (d (J = 8.9 Hz) d (J = 1.8 Hz), 12 H, ArH); 4.64 (t (J = 6.4 Hz), 2 H, -CF<sub>2</sub>CH<sub>2</sub>CH<sub>2</sub>-); 4.28 (s, 2 H, -C<sub>6</sub>H<sub>4</sub>COOCH<sub>2</sub>-); 4.13 (t (J = 6.7 Hz), 6 H, -CH<sub>2</sub>COO(CH<sub>2</sub>)<sub>5</sub>CH<sub>2</sub>OCO-); 4.04 (d (J = 4.1 Hz) t (J = 6.5 Hz), 12 H, -C<sub>6</sub>H<sub>4</sub>OCH<sub>2</sub>-); 3.98 (t (J = 6.7 Hz), 6 H, -CH<sub>2</sub>COOCH<sub>2</sub>-); 3.63 (t (J = 6.5 Hz), 6 H, -

$C(CH_2OCH_2^-)_3$ ; 3.46 (s, 6 H,  $-C(CH_2O^-)_3$ ); 2.62 (m, 2 H,  $-CF_2CH_2^-$ ); 2.50 (t (J = 6.5 Hz), 6 H,  $-CH_2COO^-$ ); 1.80 (m, 12 H,  $-C_6H_4OCH_2CH_2^-$ ); 1.50 (m, 24 H,  $-C_6H_4OCH_2CH_2CH_2^-$ ,  $-CH_2COOCH_2CH_2CH_2CH_2CH_2CH_2OCO^-$ ); 1.22 (m, 12 H,  $-CH_2COOCH_2CH_2(CH_2)_2^-$ ); 0.99 (t (J = 7.4 Hz) d (J = 3.6 Hz), 18 H,  $-CH_3$ )

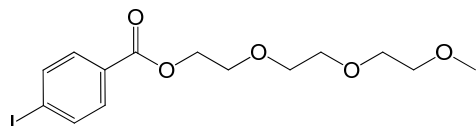
$^{13}C$  NMR (100.4 MHz,  $CDCl_3$ )  $\delta_C$  (ppm): 171.6, 165.6, 165.6, 165.0, 164.7, 164.2, 163.8, 163.7, 148.4, 148.2, 132.5, 132.5, 131.8, 131.8, 129.8, 129.6, 129.3, 127.9, 127.2, 125.1, 125.1, 125.0, 121.5, 121.1, 114.5, 114.4, 91.81, 91.28, 69.82, 68.24, 68.12, 68.09, 67.00, 65.46, 64.48, 44.75, 38.80, 35.04, 31.20, 30.44, 29.01, 28.50, 28.39, 25.59, 23.82, 23.08, 19.28, 14.15, 13.92, 11.05

MALDI-TOF MS:  $m/z = 2833.9$  ( $M + Na$ ) $^+$

IR ( $cm^{-1}$ ): 3071, 2940, 2870, 1736, 1605, 1512, 1466, 1419, 1227, 1211, 1157, 1057, 1003, 972, 849, 756, 694, 640, 509

Elemental analysis: calcd (%) for  $C_{145}H_{155}O_{37}F_{17}$ : C 61.92, H 5.55; found: C 61.80, H 5.73

### Methyloxyethyloxyethyloxyethyl 4-iodobenzoate (**55**)

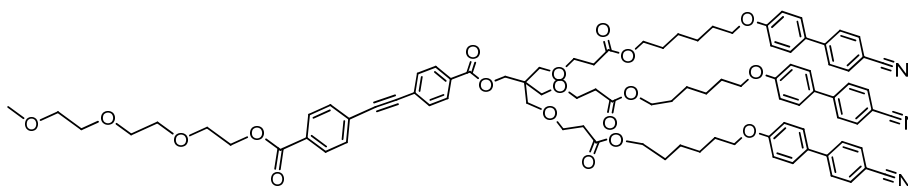


4-Iodobenzoic acid (0.5 g; 2 mmol) and methyl triethyleneglycol (0.33 g; 2 mmol) were dissolved in dichloromethane (20 mL) with 1-ethyl-3-(3-dimethylaminopropyl)carbodiimide (0.46 g; 2.4 mmol) and 4-(dimethylamino)pyridine (0.25 g; 2 mmol). The reaction was stirred under argon for 20 h at room temperature. The mixture was washed with water, dried over  $MgSO_4$ , and the solvent was removed by evaporation. The product was isolated from the crude by column chromatography, eluting with 1:1 ethyl acetate/petroleum ether, to yield the **55** as a colorless oil.

Yield: 0.64 g (81%)

$^1\text{H}$  NMR (400 MHz,  $\text{CDCl}_3$ )  $\delta\text{H}$  (ppm): 7.80 (d ( $J = 8.7$  Hz), 2 H,  $\text{ArH}$ ); 7.76 (d ( $J = 8.7$  Hz), 2 H,  $\text{ArH}$ ); 4.46 (t ( $J = 4.8$  Hz), 2 H,  $-\text{COOCH}_2-$ ); 3.82 (t ( $J = 4.8$  Hz), 2 H,  $-\text{COOCH}_2\text{CH}_2-$ ); 3.71 (m, 2 H,  $-\text{COO}(\text{CH}_2)_2\text{OCH}_2-$ ); 3.65 (m, 4 H,  $-\text{COO}(\text{CH}_2)_2\text{OCH}_2\text{CH}_2\text{OCH}_2-$ ); 3.53 (m, 2 H,  $-\text{CH}_2\text{OCH}_3-$ ); 3.37 (s, 3 H,  $-\text{OCH}_3$ )

**Methyloxylethyloxylethyloxylethyl 2,2,2-Tris(3-(6-(4'-cyanobiphenyl-4-yloxy)-hexyloxy)-3-oxopropylloxymethyl)ethyl (56)**



The dendritic 4-ethynylbenzene ester **44** (80 mg; 0.061 mmol) was dissolved in toluene (5 mL), then **55** (27 mg; 0.067 mmol) and triethylamine (5 mL) was added to the solution. The solution was purged with argon for 15 min. A catalytic mixture of  $\text{Pd}(\text{PPh}_3)_2\text{Cl}_2$  (10 mg; 0.014 mmol) and  $\text{CuI}$  (3 mg; 0.014 mmol) was added into the solution and the mixture was stirred for 20 h at room temperature. The solvent was taken off under reduced pressure, and the product was obtained from the crude by column chromatography, eluting with 3:2 ethyl acetate/hexane, to yield the **56** as a yellow oil.

Yield: 56 mg (58%)

$^1\text{H}$  NMR (400 MHz,  $\text{CDCl}_3$ )  $\delta\text{H}$  (ppm): 8.02 (d ( $J = 14.7$  Hz) d ( $J = 8.5$  Hz), 4 H,  $\text{ArH}$ ); 7.68 (d ( $J = 8.5$  Hz), 6 H,  $\text{ArH}$ ); 7.60 (m, 10 H,  $\text{ArH}$ ); 7.51 (d ( $J = 8.8$  Hz), 6 H,  $\text{ArH}$ ); 6.96 (d ( $J = 8.8$  Hz), 6 H,  $\text{ArH}$ ); 4.49 (m, 2 H,  $-\text{COOCH}_2\text{CH}_2\text{O}-$ ); 4.31 (s, 2 H,  $-\text{CH}_2\text{C}(\text{CH}_2\text{O}-)_3$ ); 4.07 (t ( $J = 6.7$  Hz), 6 H,  $-\text{CH}_2\text{O}(\text{C}_6\text{H}_4)_2\text{CN}$ ); 3.97 (t ( $J = 6.4$  Hz), 6 H,  $-\text{CH}_2\text{COOCH}_2-$ ); 3.84 (m, 2 H,  $-\text{COOCH}_2\text{CH}_2\text{O}-$ ); 3.72 (m, 2 H,  $-\text{COO}(\text{CH}_2)_2\text{OCH}_2-$ ); 3.66 (m, 10 H,  $-\text{COO}(\text{CH}_2)_2\text{OCH}_2\text{CH}_2\text{OCH}_2-$ ,  $-\text{C}(\text{CH}_2\text{OCH}_2)_3$ ); 3.54 (m, 2 H,  $-\text{CH}_2\text{OCH}_3-$ ), 3.49 (s, 6 H,  $-\text{C}(\text{CH}_2\text{O}-)_3$ ); 3.37 (s, 3 H,  $-\text{OCH}_3$ ); 2.53 (t ( $J = 6.4$  Hz), 6 H,  $-\text{CH}_2\text{COO}-$ ); 1.80 (m, 6 H,  $-\text{CH}_2\text{CH}_2\text{O}(\text{C}_6\text{H}_4)_2\text{CN}$ ); 1.65 (m, 6 H,  $-\text{CH}_2\text{COOCH}_2\text{CH}_2-$ ); 1.45 (m, 12 H,  $-\text{CH}_2\text{COOCH}_2\text{CH}_2(\text{CH}_2)_2-$ )

$^{13}\text{C}$  NMR (100.4 MHz,  $\text{CDCl}_3$ )  $\delta\text{C}$  (ppm): 171.7, 166.0, 165.7, 159.8, 145.3, 132.7, 131.8, 131.7, 131.4, 130.3, 130.1, 129.8, 129.6, 128.7, 128.4, 127.4, 127.1, 119.2,

115.1, 110.1, 91.54, 91.44, 72.01, 70.78, 70.74, 70.70, 69.89, 69.26, 68.00, 67.06, 64.69, 64.55, 64.47, 59.15, 44.78, 35.14, 29.21, 28.64, 25.83

MALDI-TOF MS:  $m/z = 1600.7 (M + Na)^+$

IR ( $\text{cm}^{-1}$ ): 3048, 2932, 2862, 2222, 1736, 1605, 1489, 1466, 1396, 1242, 1180, 1103, 1018, 856, 818, 764, 694, 633, 532

Elemental analysis: calcd (%) for  $\text{C}_{94}\text{H}_{103}\text{N}_3\text{O}_{19}$ : C 71.51, H 6.58, N 2.66; found: C 71.26, H 6.70, N 2.49

# **Chapter 7**

## **3:3 Type Janus LCs**

## 7.1 Summary

The dendritic building blocks described in Chapter 5 can also serve to assemble Janus LC materials containing two branched halves, each carrying three mesogens/segregating moieties, which can be manipulated independently. The two independent halves were assembled to form the diphenylacetylene core. In this chapter two families of Janus liquid-crystalline materials were described. The two mesogenic/functional sub-units, A and B, were covalently attached to two different branching units, based on either PE or gallic acid respectively, as depicted in Fig 7.1; the type of functional group and the way of attachment to the central scaffold, as well as the varieties of the connecting group were explored as tools for creating supermolecular systems with amphiphilic halves.

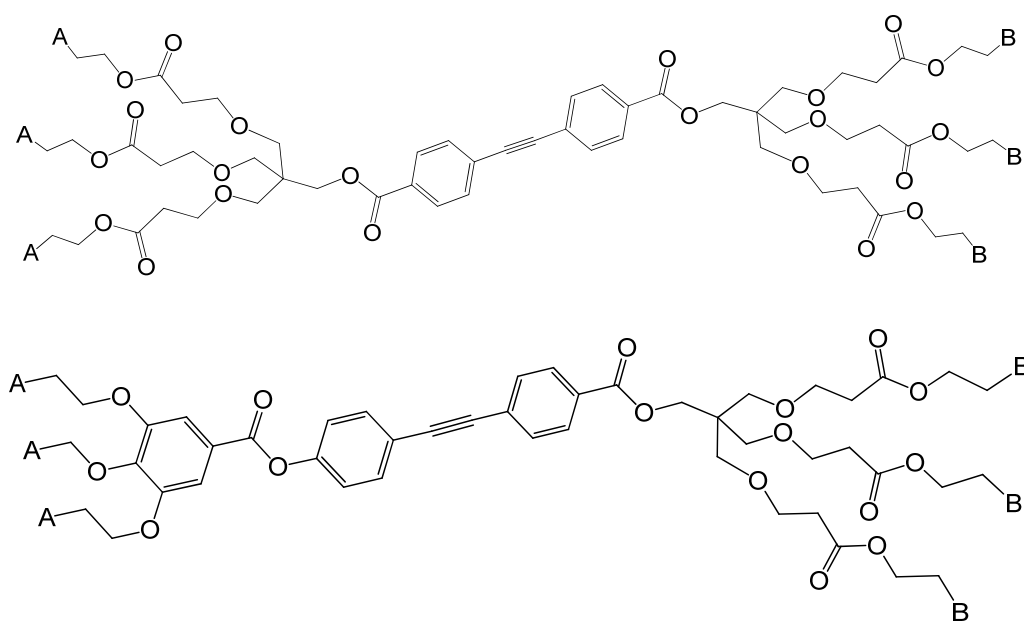


**Figure 7.1** Two types of 3:3 Janus LCs

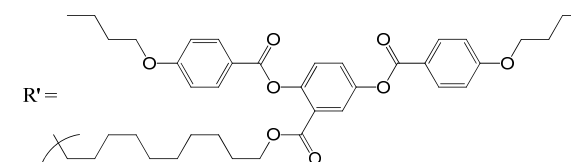
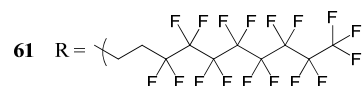
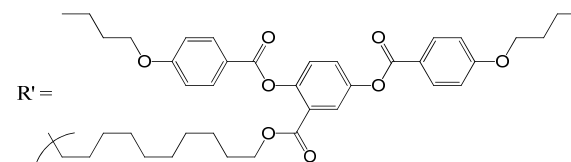
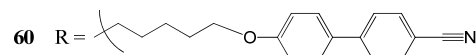
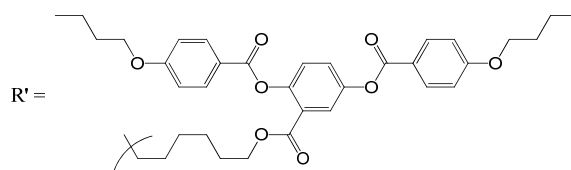
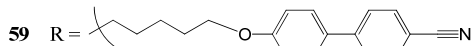
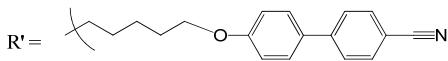
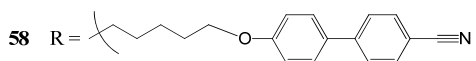
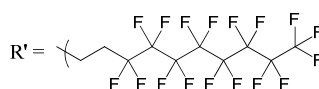
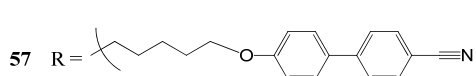
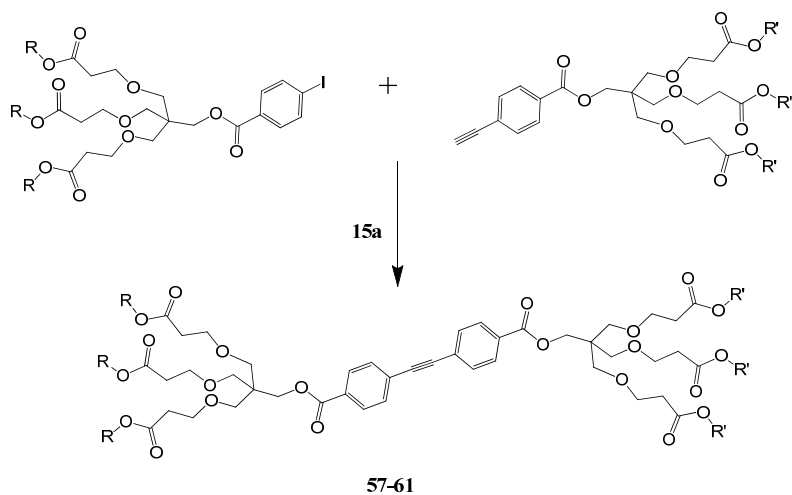
The 3:3 type molecules take the rigid diphenylacetylene as the central core, and each half with a dendritic scaffold, which generates an overall dumbbell-shaped architecture. 3:3 Refers to 3A:3B (three units of type A and three units of type B) in the general structure. Aliphatic chain spacers between the mesogenic moieties and the central scaffold introduce flexibility to the system, which decouples the motions

of the mesogenic units from the central scaffold, allowing their own ordering for the creation of a mesophase.

A family of 3:3 type LC molecules was synthesized on the basis of the dendritic mesogens made previously. These macromolecules contain two types of the central scaffold, one with two PE multipedes and another with a tri-substituted benzyl ester on one side (Fig 7.1). A series of mesogenic/functional sub-units were attached to the central scaffold to build the supermolecular LC system.

## 7.2 Synthesis

The first family of materials consists of mesogenic dendrons based on pentaerythritol for both halves of the molecule. The coupling of the appropriated mesogenic PE dendrons, described in Chapter 5, with iodo- and ethynyl- groups respectively via the Sonogashira reaction produces the Janus dendrimer LC materials **57~61** (Scheme 15). These materials have two different lobes on either side of the diphenylacetylene core. Toluene was chosen as the solvent, since the supermolecular starting materials have relatively poor solubility in triethylamine.

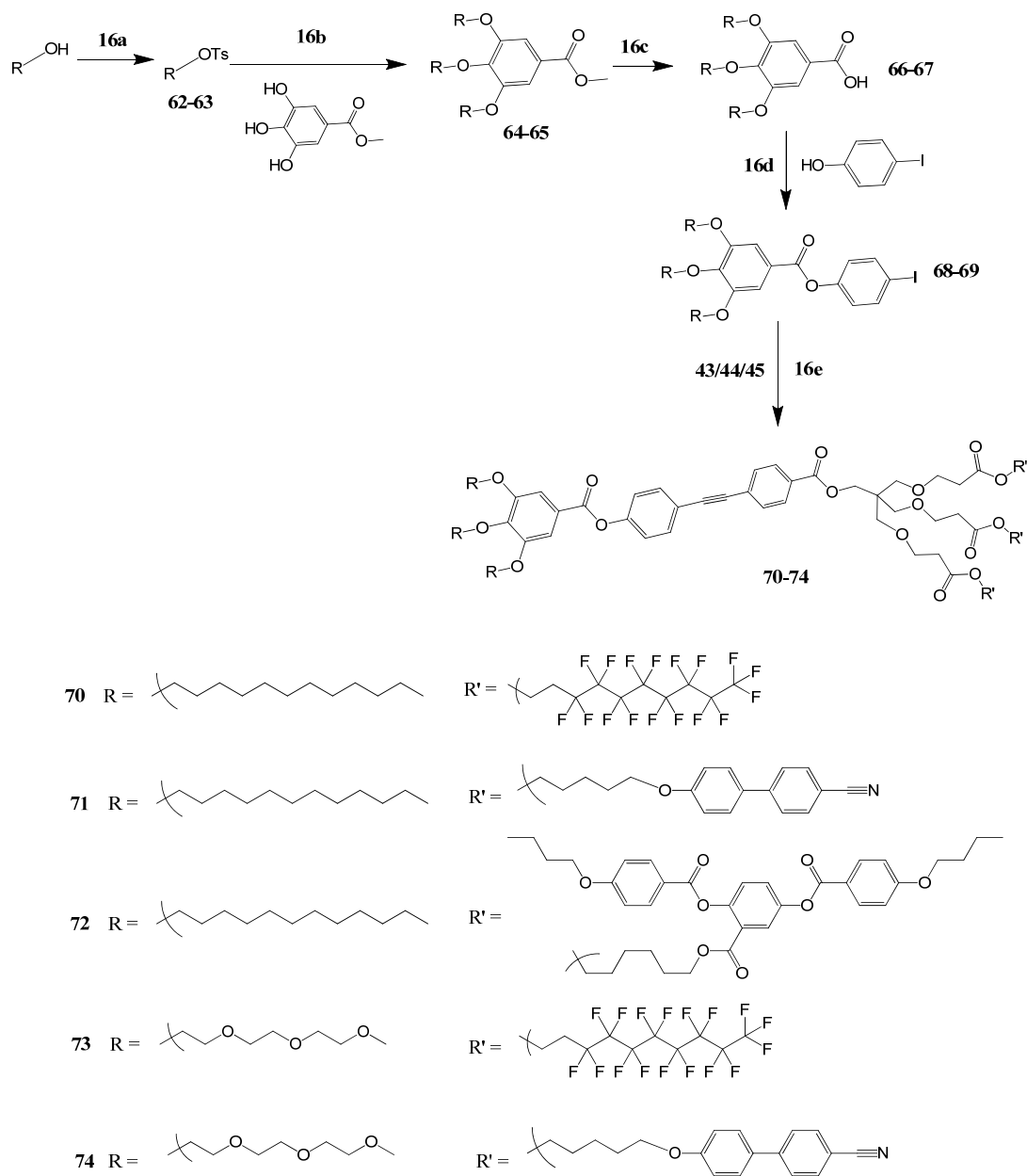


Reagents and conditions:  
15a - Pd(PPh<sub>3</sub>)<sub>2</sub>Cl<sub>2</sub>, CuI, Et<sub>3</sub>N, Toluene

### Scheme 15

The other family of materials consists of two types of mesogenic dendrons on the diphenylacetylene core. One is based on PE as before, and the other one is a dendron block based on gallic acid (a benzoate scaffold made from 3,4,5-hydroxybenzoate ester), on which the aliphatic or fluorinated chains were attached before deprotection

and esterification (**62-67**) (Scheme 16). Supramolecular Janus LCs **70-74** were synthesized via Sonogashira coupling of the gallate iodobenzoates with the appropriate alkynyl PE derivatives.



Reagents and conditions:

16a - TsCl, DMAP, Et<sub>3</sub>N, CH<sub>2</sub>Cl<sub>2</sub>

16b - K<sub>2</sub>CO<sub>3</sub>, DMF, 80 °C

16c - (i) KOH/H<sub>2</sub>O, EtOH, THF, 100 °C; (ii) HCl

16d - EDAC, DMAP, CH<sub>2</sub>Cl<sub>2</sub>

16e - Pd(PPh<sub>3</sub>)<sub>2</sub>Cl<sub>2</sub>, CuI, Et<sub>3</sub>N, Toluene

**Scheme 16**

The Sonogashira coupling between the dendritic mesogens usually results in yields of around 50%, lower than the similar reaction from the simpler building blocks in chapters 5 and 6. The original idea of introducing aliphatic chains or hydrophilic PEG group using PE as the scaffold did not work successfully as the same as other mesogenic units which use the PE derivative as the dendron scaffold. The esterification reactions of tri-acids **35** or **42** and the long chain alcohols didn't work well, so the 3,4,5-substituted benzoate ester was adopted instead of the PE derivatives.

In the Janus molecules the ratio between two types of mesogenic units and the diphenyl acetylene core is 3:3:1, which can be determined by  $^1\text{H}$  NMR. The chemical shift of protons in the dendritic mesogenic starting material is almost the same in the Janus co-dendrimer, except for the diphenyl acetylene core part (Fig 7.2).

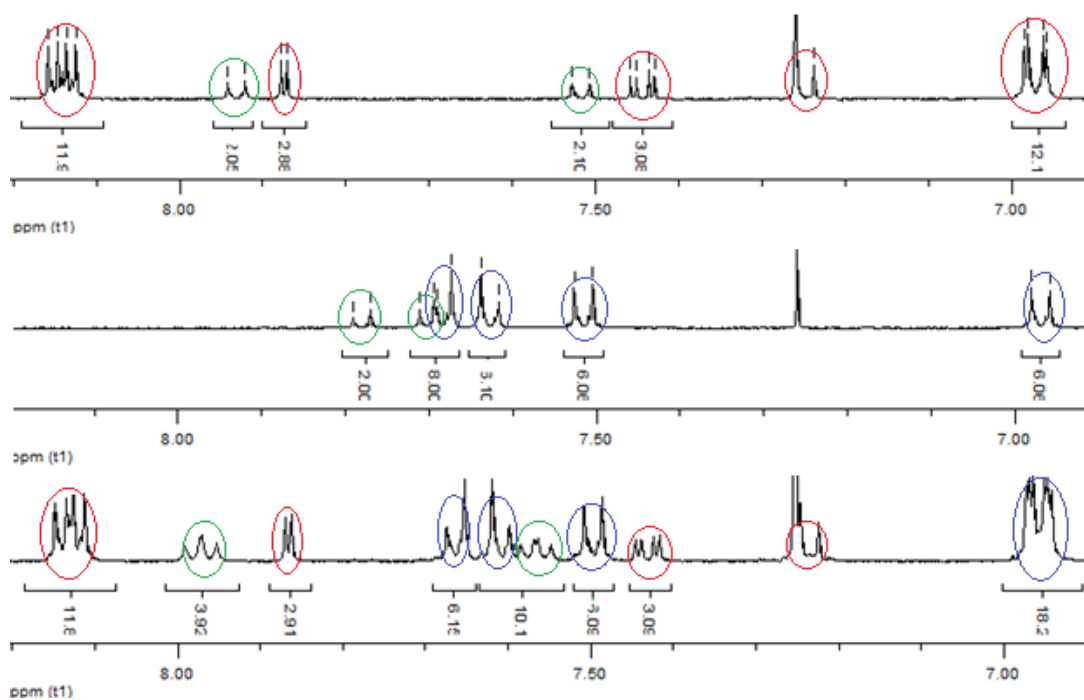


**Figure 7.2**  $^1\text{H}$  NMR of **45** (top), **37** (middle) and **59** (bottom); chemical shift changes of the protons on the diphenylacetylene core (green circle) while the protons on PDAB (red circle) and CB (blue circle) units unchanged

The protons on the identical chains attached to methyl 3,4,5-hydroxybenzoate generated two group of peaks with 1:2 integration (Fig 7.3), since the three branches are not in same chemical environment (one *para*- and two *meta*-), which is different from the dendrons of PE derivatives in which the three branches are chemically identical.

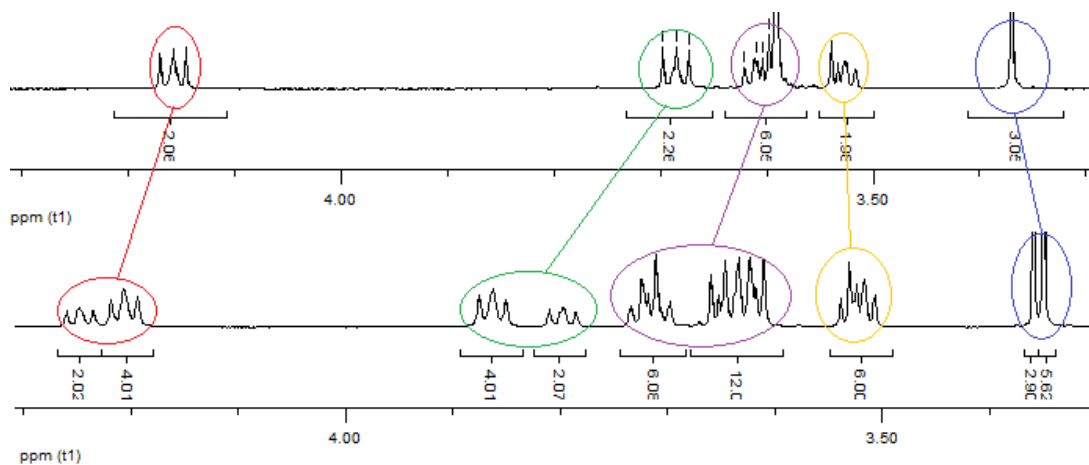


**Figure 7.3** <sup>1</sup>H NMR of the TEG region in **63** (top) and **65** (bottom) and the 1:2 split peaks

The large molecular structure was also identified by  $^{13}\text{C}$  NMR, MALDI-TOF MS and elemental analysis. The MALDI-TOF MS spectrum of **59** and **72** shown in Fig 7.4 showing that the coupling of the two building blocks had taken part to yield the Janus molecular structure.

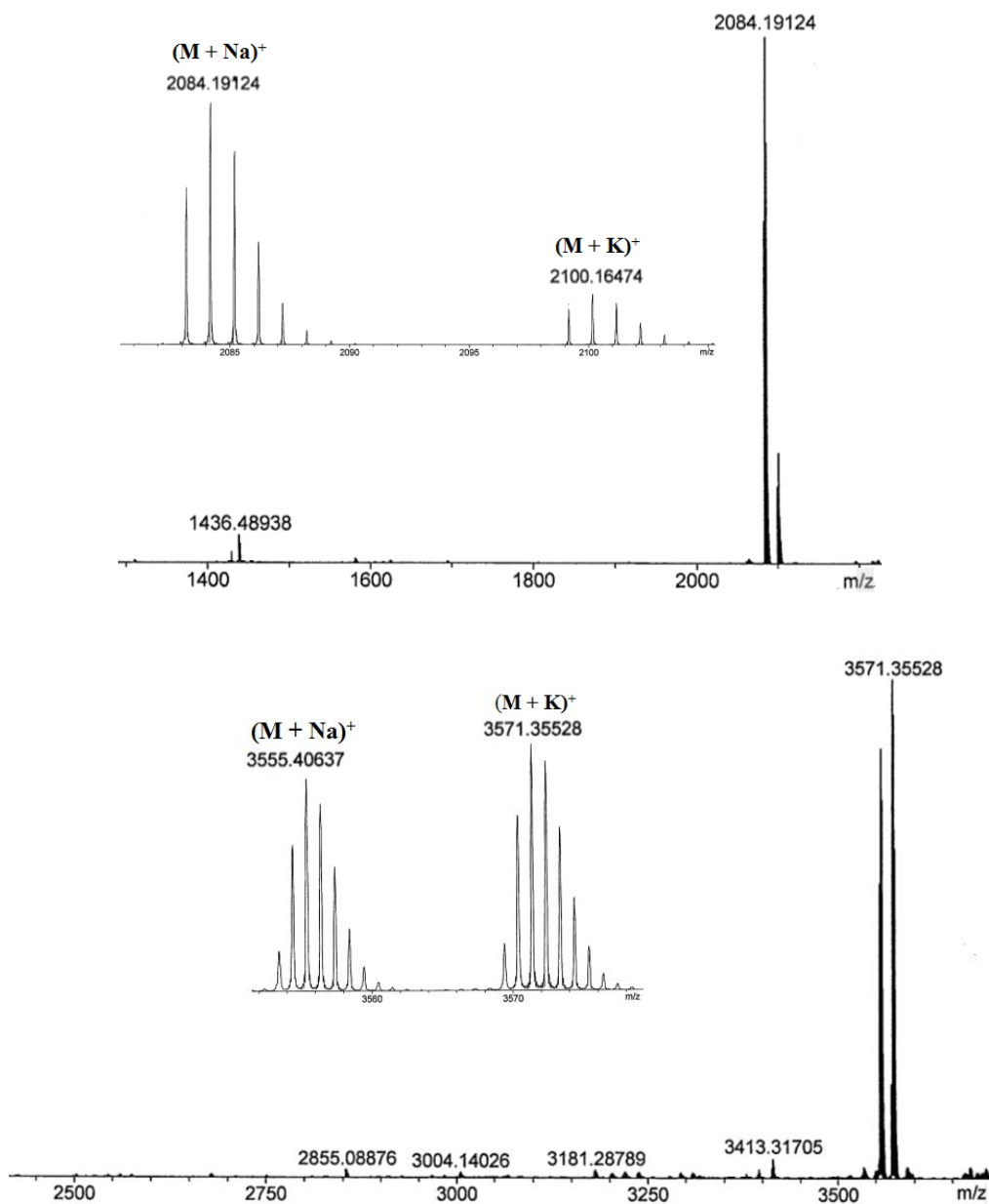


**Figure 7.4** MALDI-TOF MS of **72** (top) and **59** (bottom)

### 7.3 Mesomorphic behaviour

All of the 3:3 Janus materials were examined by DSC and POM. The phase transition temperatures and associated enthalpies for the two families of materials are collected in Table 5. Just as a reminder, the family of materials **57-61** are based on PE for both sides, whereas the **70-74** family contains PE on one side and gallate on the other.

No	g	Cr	X	X'	Cub	SmA	N	Iso		
57		• 49.0 [27.8]	• 56.8 [23.2]	•*	65	•*	68	• 171 [1.2]	-	•
58	• 10.3	-	-	-	-	-	-	• 50.0 [1.5]	-	•
59	• 11.4	-	-	-	-	-	-	• 59.8 [2.5]	-	•
60	• -1.1	-	-	-	-	-	-	• 46.9 [3.4]	-	•
61	• 5.3	-	-	-	-	•	-	115 [0.9]	-	•
70	-	• 82.4 [125]	-	-	-	•	-	109 [1.6]	-	•
71	-	• 30.1 [28.4]	• 36.9 [2.7]	-	-	•	-	49.7 [5.1]	-	•
72	• -1.7	-	-	-	-	-	-	• 34.1 [0.7]	-	•
73	-	• 24.3 [14.6]	-	-	-	•	-	69.0 [1.1]	-	•
74	• 22.4	-	-	-	-	-	-	-	-	•

Note (\*): Mesophases observed by POM only

**Table 5** Transition temperatures ( $T/^{\circ}\text{C}$ ) and associated enthalpies ( $[\Delta H/\text{KJmol}^{-1}]$ ) of the 3:3 Janus dendrimers

All the phase transition behaviours were identified by differential scanning calorimetry and the texture of the liquid crystal phases were observed by polarized light optical microscopy. In all cases the natural textures resulting from cooling from

the isotropic liquid were studied; in some cases long periods of annealing were needed to obtain clearly identifiable textures as is common for these types of macromolecular material.

Compound **57** (3CB:3R<sub>F</sub>) has a tendency to adopt homeotropic ordering at high temperature. During the cooling process, the birefringence of the focal-conic fans gradually becomes visible. Hyperbola and ellipse pairs can be found in the texture, which is a signature of the SmA phase (Plate 13). An optically extinct texture was also observed on cooling the SmA phase, assigned tentatively to a cubic phase.

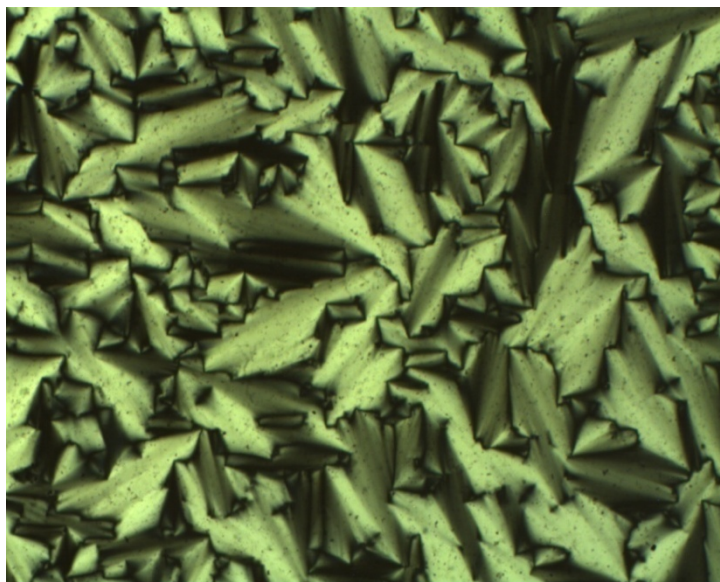


**Plate 13** Focal-conic fan texture of **57**, 100 °C (x200)

The typical schlieren texture of nematic phase formed from isotropic liquid of compound **58** (3CB:3CB). The  $m = \pm 1/2$  and  $m = \pm 1$  disclinations (2- and 4-brush singularities) can be clearly seen from the picture (Plate 14).

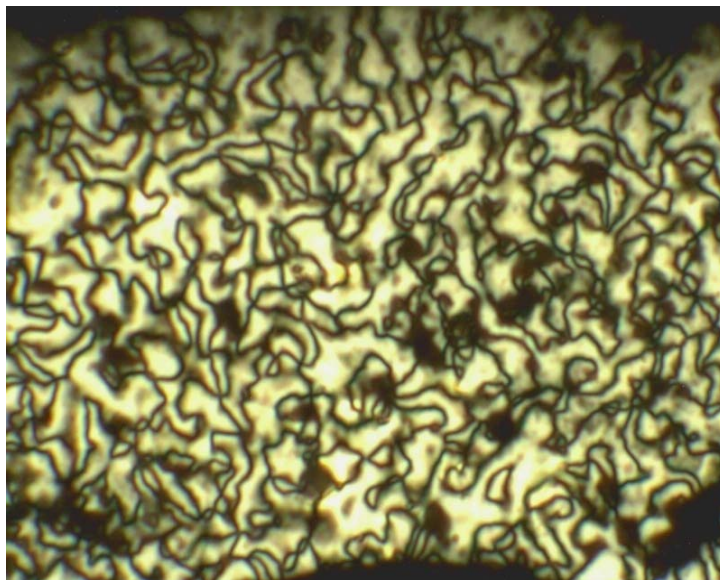


**Plate 14** The schlieren texture of **58**, 50 °C (x200)

In analogy to the texture of all the other compounds with the side-on PDAB mesogenic units, the texture of **59** (3CB:3PDAB) also shows a highly birefringent schlieren texture, which is typical of the nematic phase (Plate 15).



**Plate 15** The schlieren texture of **59**, 58 °C (x200)

The related material **60** (3CB:3PDAB) exhibits a typical schlieren texture for the nematic phase. The 2- and 4-brush singularities can be found in the picture, present the character of a nematic phase (Plate 16).

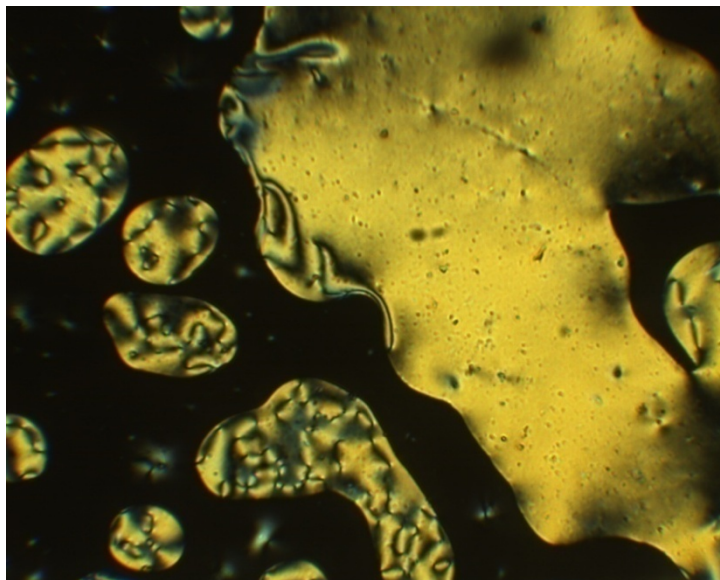


**Plate 16** The schlieren texture of **60**, 57 °C (x200)

Upon cooling **61** (3PDAB:3R<sub>F</sub>) from the isotropic liquid, the focal-conic fans formed and coalesced showing the hyperbola/ellipse pairs, which together with the presence of homeotropic black areas, indicated the existence of a smectic A phase (Plate 17).

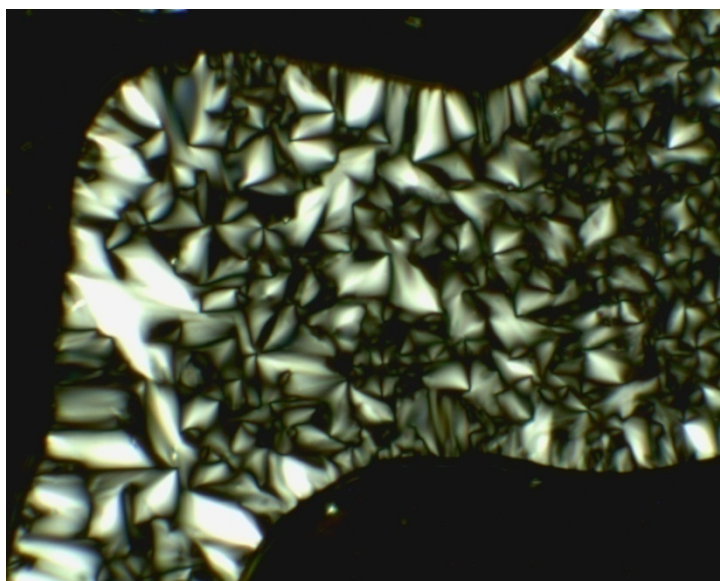


**Plate 17** Focal-conic fan texture of **61**, 108 °C (x200)

Many discontinuous oily streaks in a mainly homeotropic background were found in the texture of compound **70** (3R<sub>H</sub>:3R<sub>F</sub>). This type of birefringence is caused by the dislocations in the homeotropic alignment at the boundary of the sample, identifying it as the SmA phase. This type of materials with fluorinated chains tends to show strong homeotropic tendency (Plate 18).

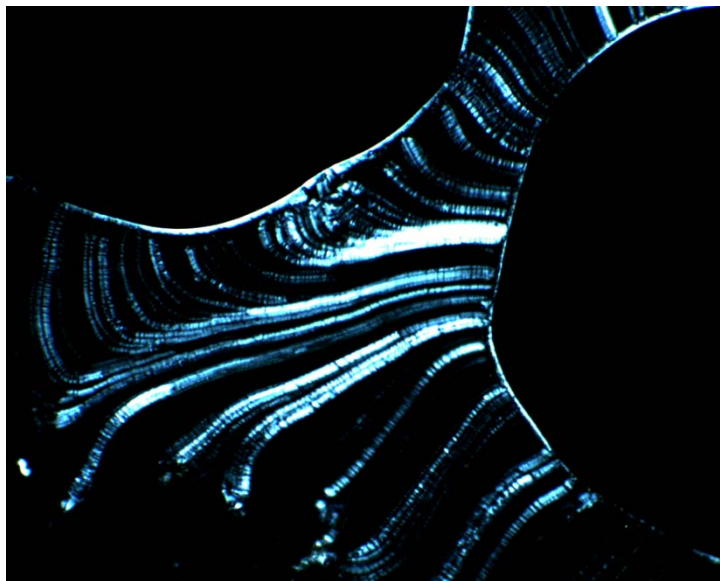


**Plate 18** Oily streaks texture of **70**, 105 °C (x200)

The textures of **71** (3CB:3R<sub>H</sub>) and **72** (3PDAB:3R<sub>H</sub>) are those typical of the SmA and nematic phases respectively, and resemble the textures found for the related compounds of the first family (Plates 19 and 20). Similarly, material **73** (3TEG:3R<sub>F</sub>), without any mesogenic units, exhibits the SmA phase.

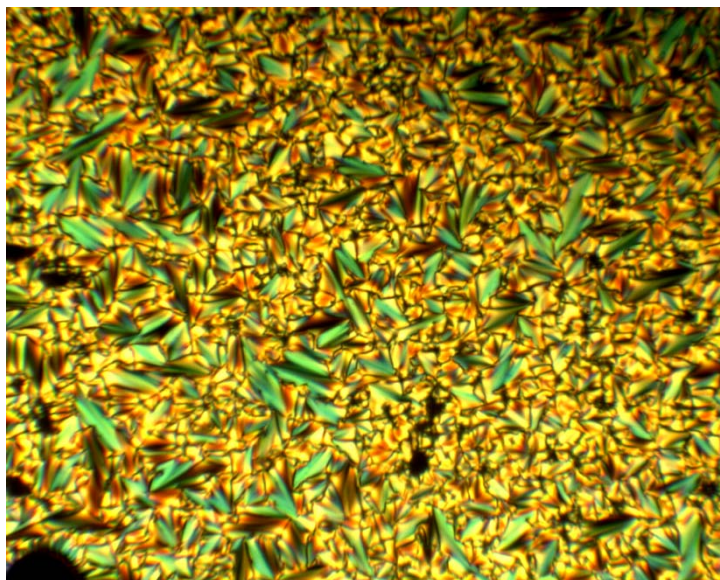


**Plate 19** Focal-conic fan texture of **71**, 49 °C (x200)



**Plate 20** The schlieren texture of **72**, 32 °C (x200)

## 7.4 Discussion

The 3:3 Janus dendrimers have a dumbbell shape caused by the conical shape of the dendrons attached to the diphenylacetylene core. In such a topology, the self-assembly of the molecules is affected by the competing effects of phase segregation and steric requirements. Ultimately, the phase structure formed will depend on the relative cross-sectional area of the two sides of the molecule and the segregation that they impose on each other. Additionally, the requirement to minimise the free volume between the molecules to achieve a stable mesophase must also be met. To minimize the overall volume and to pack more effectively, the free space around the core section of the molecule is intended to be occupied by the other molecules; but the mesogenic units require side to side interactions to achieve the parallel alignment of the molecules, which seems hard to satisfy for this type of geometry (Fig 7.5). If the lateral interactions between the molecules cannot overcome the space filling effect, a layered structure will not be formed and only nematic phase will result. The competition between steric/microphase segregation effect in smectic layers will be further discussed in later sections.

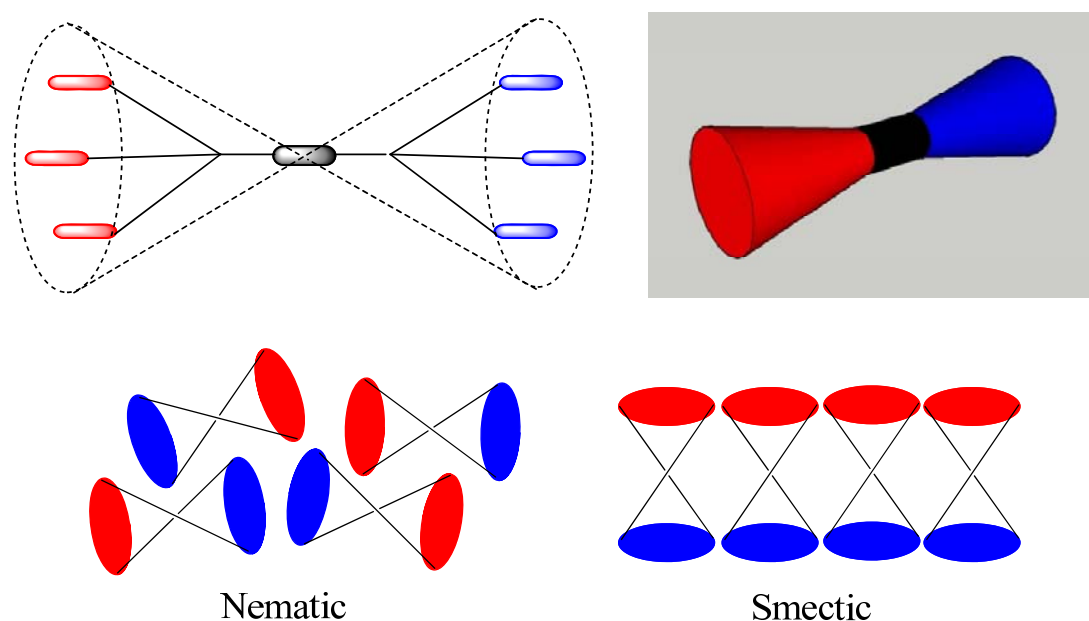


**Figure 7.5** The dumbbell topology of the 3:3 Janus dendrimers and the different mesophases controlled by steric/microphase segregation effect

The symmetric dendrimer **58** (3CB:3CB), which is not actually “Janus”-like, has three cyanobiphenyl mesogenic units on each side of the dendritic scaffold and exhibits a nematic phase at room temperature. Looking back to all its precursors with only cyanobiphenyl units (**37**, **44** and **50**), it can be found that they all exhibit the nematic phase. The peripheral cyanobiphenyls cannot have a strong lateral affinity to induce a stable lamellar smectic phase, which might be easily disturbed by other factors. In the 3:3 type, the presence of smectic A phase is inhibited by the inefficient space filling, producing only a roughly orientational ordering of the molecules which leads to the nematic phase (see Fig 7.5). The nematic phase stability of compound **50** is was similar to its relatives, since the molecule is merely a combination of two identical parts which do not change too much the properties.

Almost all of the Janus materials with side-on mesogens exhibit the nematic phase at room temperature, with a range of approximately 40 °C, and the crystallisation process is suppressed, showing only the glass transition. This behaviour is typical of supermolecular LCs. Janus compound **59** (3CB:3PDAB) and **60** (3CB:3PDAB) are decorated with three cyanobiphenyl mesogenic units for one side and three side-on mesogenic units for the other side, with different spacer lengths. As in previous occasions, the laterally attached mesogenic units are not likely to be segregated in a lamellar arrangement but still have a strong tendency to keep the orientational order to induce a liquid crystal phase. Since the cyanobiphenyls mesogenic units are not able to induce a stable smectic phase, the Janus compounds **59** and **60** exhibit only the nematic phase. It can be also found for both that the glass transition temperature and nematic phase stability are related to the of the length of the spacer which links the core and the side on mesogenic units, increasing of which enhanced the flexibility and also affects the overall shape of the supermolecule making it wider. Comparison of **59** and **58** shows that the introduction of the side-on mesogens has little impact on the clearing point, resulting in a slightly higher isotropisation temperature for **59** than **58**.

The molecule design of compound **59** and **60** are based on the first Janus type supermolecule LC synthesized by Saez et. al [30] (Fig 7.6). The combination of different mesogenic units on each side of the system allowed the molecular recognition from one side to the other, modifying their self-assembling behaviour. The Janus material **60** (3CB:3PDAB) has a similar mesophase behaviour to the Janus

compound (a), whereas compound (b) also exhibits a chiral smectic C phase at room temperature. The formation of the lamellar phase is really unusual considering the tendency of the laterally attached mesogenic unit to suppress the lamellar structure. It is remarkable that **60** has similar glass transition and isotropisation temperatures to those of (a) and (b).

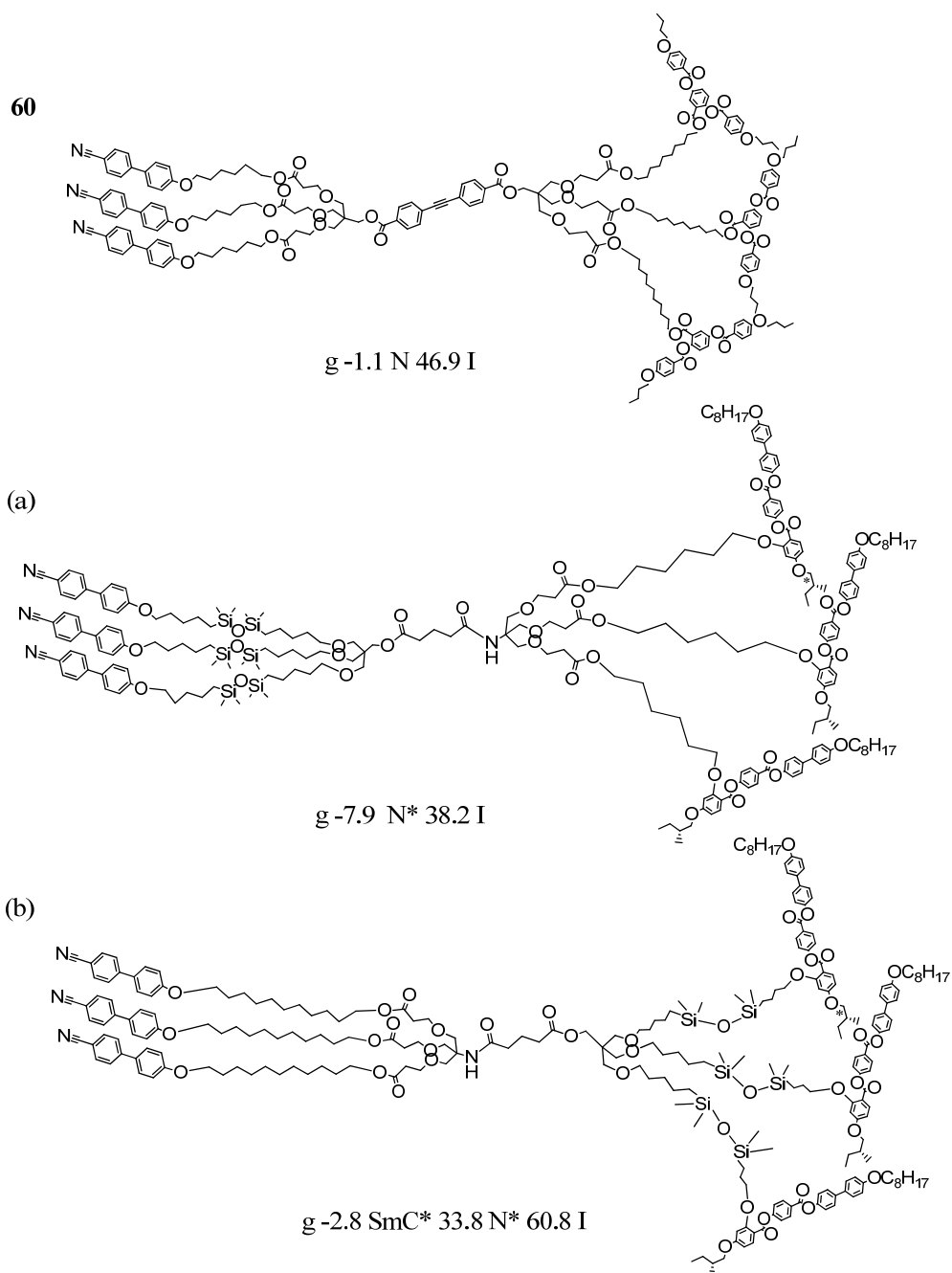


**Figure 7.6** Janus LCs containing end-on and side-on mesogenic units

Unlike the cyanobiphenyl end-on mesogenic groups, introducing a perfluorinated chain usually leads to a much more stable lamellar arrangement, due to the increasing of polarity, stiffness and microphase segregation. Compound **61** (3R<sub>F</sub>:3PDAB) with three laterally attached mesogenic units and three perfluorinated chain exhibits only smectic A phase with a quite wide temperature range (~110 °C), indicating the successful microphase segregation even with the side-on mesogenic units on the other side of the molecule, which usually causes difficulty in the lateral packing. It is remarkable that the microphase segregation of the fluorinated chains is able to counteract the reluctance of the side-on mesogens to adopt a lamellar structure. Though the nematic phase was suppressed, the side-on mesogenic units also have a noticeable effect on the phase transition behaviour of **61**, which prevented the crystallisation upon rapid cooling which is always observed in the compounds with perfluorinated chains; however, the Janus compound is still able to crystallize on cooling at a very slow rate at room temperature. These effects are explained by the strong competition between the opposing tendencies to microphase segregation of the fluorinated chains and nematic tendency of the laterally attached mesogens. As expected, the clearing point of the SmA phase in **61** is lower than that of **57** because the side-on mesogens introduce more disorder in the system.

Compared to compound **61**, the terminally attached mesogenic units favour a compact lamellar packing, which can also be proved by the crystallization of **57** at room temperature. Unlike most of the other Janus LCs, compound **57** also exhibits two other unidentified mesophases and also a rare cubic phase between the SmA phase and the crystalline state. Among all of the 3:3 type Janus LCs, compound **57** can be regarded as the only one with two types of end-on rigid mesogenic units which favours a strong lateral interaction between the mesogens. An interesting phenomenon was found in the SmA phase of compound **57**, that is the birefringence of the texture is somehow affected by the temperature: the lower the temperature, the brighter the texture. The degree of order of the molecules in layers varies with temperature, and determines the birefringence of the phase. This may also explain the formation of the cubic phase since the higher ordering of the molecules in this type of Janus system may generate a modulated smectic layer (see in later section), the cubic phase thus appears at a lower temperature. The relationship between the bicontinuous cubic phase (Cub<sub>v</sub>) and a SmA layer has been studied in the

amphiphilic LC oligomers with a semiperfluorinated chain discussed before in section 1.4.4 [32].

By replacing one of the pentaerythritol hemispheres of the Janus design by a flat aromatic ring, this hemisphere of the 3:3 Janus molecule no longer takes a cone shape but a more flat configuration (Fig 7.6). This means that the cone angle required by the gallate unit is smaller than that required by PE. Thus, the free space around the core was reduced and more compact packing can be achieved, which may stabilize the lamellar mesophases of the supermolecular mesogens. As an example, a smectic A phase with a high smectic phase stability was exhibited by compound **70** with three perfluorinated chains and three hydrocarbon chains. The biphenyl acetylene core was also effectively elongated which increase the rigidity and polarisability, resulting in a more stable smectic phase, as well as a much higher melting point than the similar compound **49**. Apart from microphase segregation, the long aliphatic chains pack through Van der Waals interactions but also introduce enough flexibility to the system to lower the melting point, thereby maintain the presence of the smectic A phase.

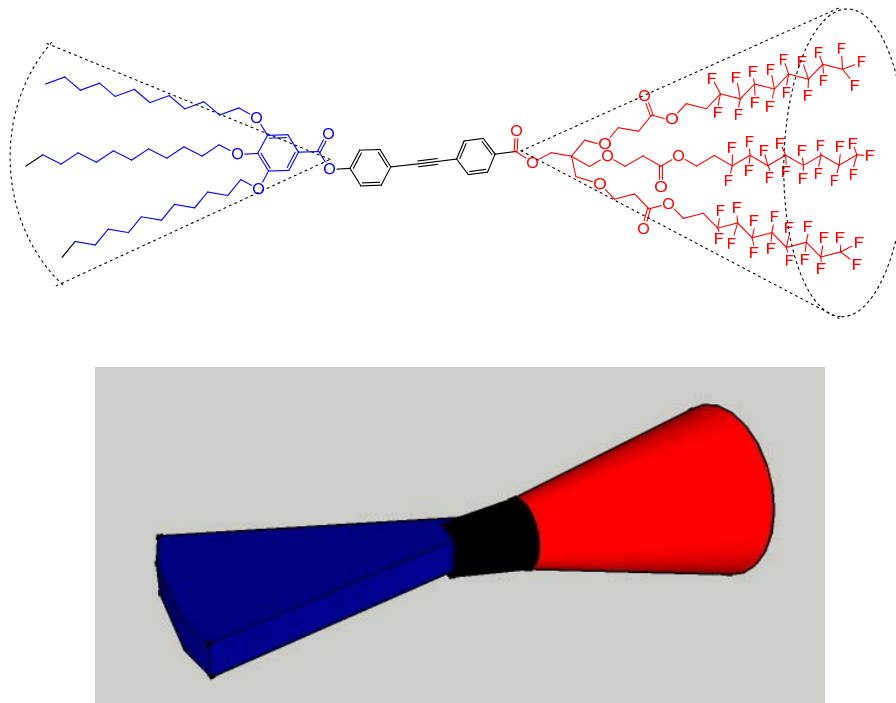


**Figure 7.7** Molecular topology of the asymmetric dendritic scaffold with PE and gallate units

The notable smectic phase inducing ability of the 3,4,5-decyloxy benzoate moiety was further observed in compound **71** (3R<sub>H</sub>:3CB), in which three cyanobiphenyl mesogenic units are combined with the trialkoxygallate. The Janus 3:3 type dendrimer exhibits only smectic phases, which is quite uncommon since the others dendrimers/mutipedes mainly decorated with cyanobiphenyl units usually possess a nematic phase (**37** and **44**) or even only nematic phase (**50** and **58**). Compared to the other 3:3 Janus smectogens, the entropy of SmA-I transition of **71** is relatively higher, which may cause a more ordered structure. The ordered and compact packing of molecules can be also proved by the crystallization of compound **71** at room temperature, which is rarely observed in similar dendritic compounds possessing cyanobiphenyl units. However, compound **72** (3R<sub>H</sub>:3PDAB) with three side-on mesogenic units still only exhibits a nematic phase. Compared to compound **61** which presents smectic phase with high mesophase stability, it can be seen that the smectic phase inducing ability of the long alkyl chains is still much weaker than the perfluorinated chains. Without the lamellar structure, the long alkyl chains can only introduce isotropy and flexibility to the system, which results in a lower N-I transition temperature of **71** compared to other nematogens with three side-on mesogenic units.

The introduction triethyl glycol (TEG) methyl ether chain has a noticeable effect on the overall phase behavior of the 3:3 Janus LCs. Compound **73** (3TEG:3R<sub>F</sub>) is a Janus dendrimer with three perfluorinated chains and three hydrophilic TEG chains, and compound **74** (3TEG:3CB) has three cyanobiphenyl instead of the perfluorinated chains. As observed in the 1:3 type Janus dendrimer **56**, the TEG group tends to reduce both the glass transition and isotropic transition temperature, due to the greater flexibility induced. Compared to **49**, the melting point of compound **73** was lowered by almost 20 °C; on the other hand, the mesophase is almost 20 °C more stable than **49**, due to the elongated rigid core. Thus a smectic A phase with much wider range was produced by the simultaneous enhancement due to the core and the TEG groups. Unlike **73**, the Janus dendrimer **74** is not mesomorphic at all. Some trends can be derived from comparison of **50**, **56** and **74** (Table 6). From **50** to **56**, it can be seen the introduction of the long TEG group greatly reduces the nematic phase stability rather than the glass transition temperature. From **56** to **74** the vitrification point is further lowered, however the isotropic transition temperature

might be lowered much more, which might bring it below the glass transition, resulting in the disappearing of any liquid crystal phase. Even the elongated rigid core could not compete with the the flexible TEG groups in maintaining the mesophase. This trend indicated the strong mesophase disturbing effect of the polyethylene glycol chain, at least as a periphery group adopted in this Janus type of mesogens.

No	Unit 1	Units 2	Core	g	N	Iso
<b>50</b>	CB x 3	R <sub>H</sub>	2 rings	● -0.2	● 56	●
<b>56</b>	CB x 3	TEG	2 rings	● -7	● 7.8	●
<b>74</b>	CB x 3	TEG x 3	3 rings	● -22.4	-	●

**Table 6** Comparison of the stuctures and the LC behaviors of **50**, **56** and **74**

### 7.5 Microphase segregation and steric effect in 3:3 Janus LCs

The discussion above of the LC behaviour is mainly based on the topology and interaction of the supermolecular mesogens. Since the Janus-like molecules are closely related to the concept of an amphiphile regarding microphase segergation, the “incompatibility leads to positional order” principle can be also applied on the 3:3 Janus LCs to a certain degree.

The unusual effect of PEG chain on the LC behavior deduced before can be also checked with microsegregation theory. According to the calculation of the cohesive energy density (CED,  $c$ ) [27], the PEG chain should have higher incompatibility with the perfluorinated chain rather than the aliphatic chain ( $\delta_{\text{PEG}} \approx 20 \text{ MPa}^{1/2}$ ,  $\delta_{\text{RH}} \approx 17.5 \text{ MPa}^{1/2}$  and  $\delta_{\text{RF}} \approx 12 \text{ MPa}^{1/2}$ ). However the SmA phase stability of compound **73** is much lower than **70**, which coincide with the mesophase supression effect observed in Table 7.

Apart from the PEG chain groups, all the 3:3 Janus LC molecules with other types of peripheral moieties agree with the microsegregation theory, which can be seen from

the relationship between the degree of incompatibility and the SmA phase stability (Fig 7.8).

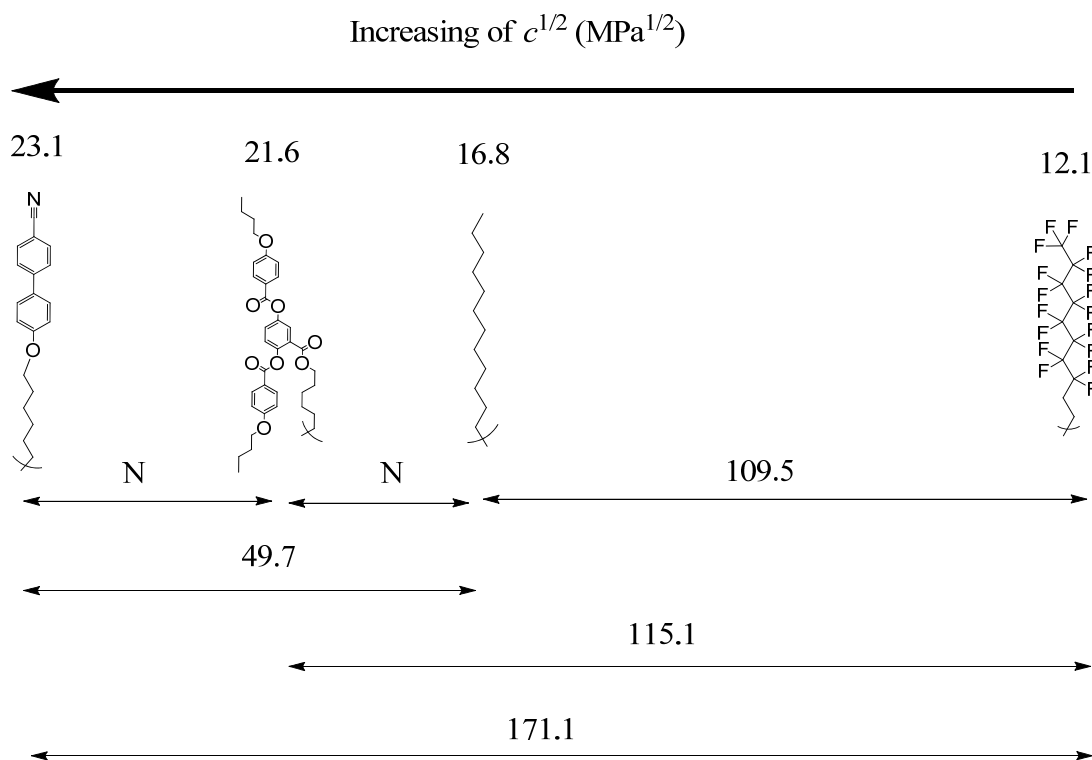


**Figure 7.8** SmA-I transition temperature ( $^{\circ}\text{C}$ ) of 3:3 Janus LCs with all combinations of peripheral moieties, roughly coincide with the incompatibility based on CED ( $\delta^2$ ), ignoring the influence of volume fraction ( $f$ ) and central scaffold for simplification

From Fig 7.8, it can be found that the incompatibility between the side-on PDAB mesogenic unit and cyanobiphenyl/aliphatic chain is too low for good microphase segregation, which leaves only the nematic phase; however there are enough difference in the CED value between cyanobiphenyl and aliphatic chain, so a SmA phase with phase stability at  $49.7^{\circ}\text{C}$  is exhibited by the Janus molecule with three cyanobiphenyl groups and three aliphatic chains. The perfluorinated chain has the lowest CED value far from the others; the Janus molecules with perfluorinated chains always show stable smectic phases. The SmA phase stability of perfluorinated chain-containing compound is directly related to the CED value of the other periphery groups,  $109.5^{\circ}\text{C}$  for the long alkyl chain,  $115.1^{\circ}\text{C}$  for the PDAB side-on

mesogenic unit and 171 °C for the cyanobiphenyl group which is a very stable SmA phase induced by the highest incompatibility. Though the amphiphilic model is quite simplified since it ignored the effect of the volume fraction ( $f$ ) and central/dendritic scaffold structure, the consistency in the stability-incompatibility is still remarkable, which proves that such a Janus LC system is an ideal model for good microphase segregation manipulation.

Since the 3:3 type Janus compounds have unique dumbbell structure, the free space generated affects the molecular packing in the smectic layers as shown in Fig 7.5. The reduced molar entropy per mesogen may give an idea about the order in the mesophase for a series of compounds with a common perfluorinated chain (Table 8).

No	Low CED Group	High CED Group	T <sub>SmA-I</sub> (°C)	ΔH (KJmol <sup>-1</sup> )	ΔS/R
57	R <sub>F</sub>	CB	171.1	1.2	0.3
61	R <sub>F</sub>	PDAB (side-on)	115.1	0.9	0.3
73	R <sub>F</sub>	TEG	69.0	1.1	0.4
70	R <sub>F</sub>	R <sub>H</sub>	109.4	1.6	0.5
71	R <sub>H</sub>	CB	49.7	5.1	1.9

**Table 8** Reduced molar entropy (ΔS/R) of SmA-I transition in 3:3 Janus LCs

Compared to the LC multipedes or the 1:3 type Janus LCs, it can be found the 3:3 type Janus compounds usually have higher smectic phase stability, due to the stronger microphase segregation caused by the higher number of segregating chains. Additionally, the SmA-Iso transition enthalpy was remarkably reduced, along with the transition entropy. This indicated a much more disordered alignment within the SmA phase which is barely seen for low molar mass mesogens.

Influenced by the dumbbell topology, the alignment of molecules simply by packing them side by side generates a lot of free space which is not conducive to a stable mesophase (Fig 7.9 (a)). A reduction in free volume could be achieved by tilting the

molecules with respect to each other, but this introduces a certain disorder in the alignment of the mesogens. Additionally, the tilting may be dependent on the strength of the microphase segregation effect. Strong segregation of the incompatible segments results in a worse alignment of the mesogens (Fig 7.9 (b)), whereas if there isn't strong segregation vertical slippage of the molecules results in a better alignment of the mesogens (Fig. 7.9 (c)). This may explain why a higher isotropisation temperature of the 3:3 Janus LC usually associated with a lower reduced molar entropy per mesogen, as described in Table 8.

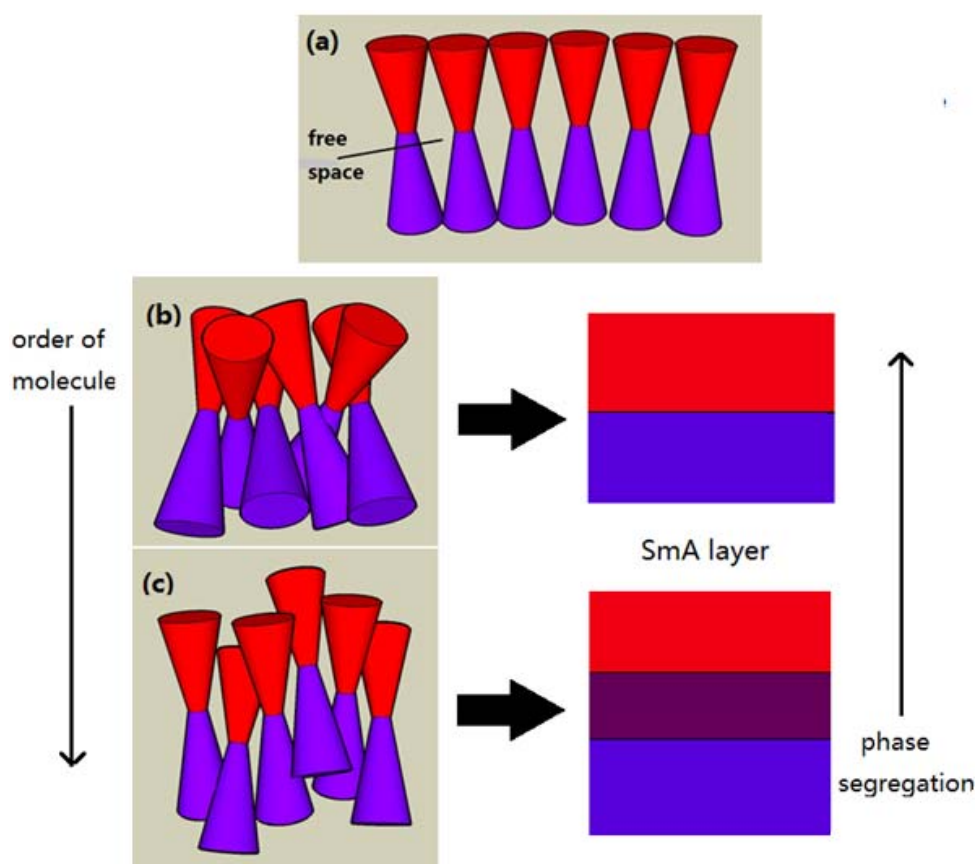


**Figure 7.9** Different arrangement of Janus molecules in the layer: (a) packing side by side; (b) orientational disordered packing; (c) packing with vertical slippage. The free space was reduced by the twist arrangement (b, c) than the more regulated way of packing (a)

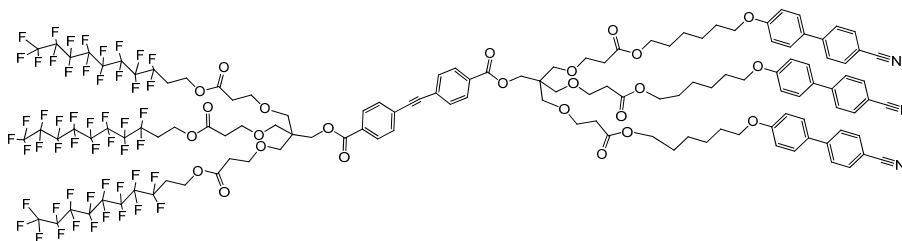
Again as a matter of fact, the dumbbell shape of the 3:3 Janus LCs is just a simplified model, since the flexible aliphatic spacers allow a relatively free motion of the mesogenic units and the central scaffold units. The actual situation is much more complicated; the disorder may not only exist in the molecule alignment, but also in the intermolecule and intramolecule positions, which is mainly related to the size, structure and attachment of the periphery groups. However its still a good model which provided a concise explanation of the abnormal mesophase behaviour, which can be taken into consideration in the further design of supermolecular amphiphilic systems.

## 7.6 Concluding remarks

A series of 3:3 type Janus supermolecular LCs were developed. Two types of mesogenic units (cyanobiphenyl, phenylene dibenzoate) and three types of terminal chains on the buiding segment (hydrocarbon chain, perfluorinated chain and triethylene glycol) were adopted as amphiphilic (chemically incompatible) pairs. In these types of Janus LCs which are highly functionalized, the effect of central core and dendritic scaffold on the mesomorphic behaviour is not quite as simple as in lower LC oligomers where the LC behaviour is mainly controlled by the peripheral groups. According to the peripheral moieties, the Janus compounds exhibit either nematic or smectic phases; and the mesomorphic behaviour can be explained either by the competition effect between mesogenic units, or by the microphase segregation effect. Considering the dumbbell molecular shape, the steric effect is crucial in the molecular alignment in the smectic layers, which depends on the relative cross-sectional area of each half of the molecule, and the competition between microphase segregation and steric effects results in either highly disordered alignment of mesogens in SmA phase, or the total supression of any mesophases with positional order. A unique cubic phase is also observed in compound **57**, probably induced by strong microsegregation. All these distinct mesomorphic behaviors prove that these types of Janus LC compounds have great potential in the research of the self-recognition of nanostructures and are therefore of value of further studies.

## 7.7 Experimental

### **2,2,2-Tris(3-(6-(4'-cyanobiphenyl-4-yloxy)hexyloxy)-3-oxopropylloxymethyl)-ethyl 2,2,2-tris(3-(3,3,4,4,5,5,6,6,7,7,8,8,9,9,10,10,10-heptafluorodecyloxy)-3-oxopropylloxymethyl)ethyl 4,4'-(1,2-ethynediyl)bibenzoate (57)**



The dendritic 4-iodobenzene ester **37** (50 mg; 0.035 mmol) was dissolved in toluene (5 mL) and added in to a solution of dendritic 4-ethynylbenzene ester **43** (64 mg; 0.035 mmol) in triethylamine (5 mL). Argon was then flushed through the solution for 15 min. A catalytic mixture of Pd(PPh<sub>3</sub>)<sub>2</sub>Cl<sub>2</sub> (10 mg; 0.014 mmol) and CuI (3 mg; 0.014 mmol) was added into the solution and the mixture was stirred for 20 h at room temperature. The solvent was taken off, and the product was isolated from the crude by column chromatography, eluting with 1:5 ethyl acetate/dichloromethane, to yield **57** as a yellow solid.

Yield: 56 mg (52%)

<sup>1</sup>H NMR (400 MHz, CDCl<sub>3</sub>) δ<sub>H</sub> (ppm): 7.99 (d (J = 8.4 Hz) d (J = 3.5 Hz), 4 H, ArH); 7.68 (d (J = 8.6 Hz), 6 H, ArH); 7.60 (m, 10 H, ArH); 7.51 (d (J = 8.8 Hz), 6 H, ArH); 6.96 (d (J = 8.8 Hz), 6 H, ArH); 4.37 (t (J = 6.5 Hz), 6 H, -CF<sub>2</sub>CH<sub>2</sub>CH<sub>2</sub>-); 4.30 (d (J = 8.1 Hz), 4 H, -CH<sub>2</sub>C(CH<sub>2</sub>O-)<sub>3</sub>); 4.07 (t (J = 6.7 Hz), 6 H, -C<sub>6</sub>H<sub>4</sub>OCH<sub>2</sub>-); 3.98 (t (J = 6.4 Hz), 6 H, -CH<sub>2</sub>COOCH<sub>2</sub>CH<sub>2</sub>CH<sub>2</sub>-); 3.66 (t (J = 6.3 Hz) d (J = 2.5 Hz), 12 H, -C(CH<sub>2</sub>OCH<sub>2</sub>-)<sub>3</sub>); 3.48 (d (J = 7.9 Hz), 12 H, -C(CH<sub>2</sub>O-)<sub>3</sub>); 2.48 (m, 18 H, -CH<sub>2</sub>COO-, -CF<sub>2</sub>CH<sub>2</sub>-); 1.80 (m, 6 H, -CH<sub>2</sub>CH<sub>2</sub>O(C<sub>6</sub>H<sub>4</sub>)<sub>2</sub>CN); 1.65 (m, 6 H, -CH<sub>2</sub>COOCH<sub>2</sub>CH<sub>2</sub>CH<sub>2</sub>-); 1.45 (m, 12 H, -CH<sub>2</sub>COOCH<sub>2</sub>CH<sub>2</sub>(CH<sub>2</sub>)<sub>2</sub>-)

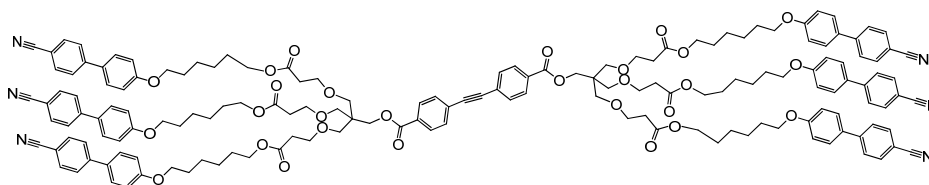
<sup>13</sup>C NMR (100.4 MHz, CDCl<sub>3</sub>) δ<sub>C</sub> (ppm): 171.7, 171.2, 165.7, 165.6, 159.8, 145.3, 132.6, 131.7, 131.4, 130.3, 129.6, 128.4, 127.4, 127.1, 119.2, 115.1, 110.2, 91.44, 91.39, 69.85, 69.73, 67.99, 67.05, 66.71, 64.54, 56.41, 44.76, 35.10, 34.88, 30.72, 30.51, 30.29, 29.20, 28.63, 25.81

MALDI-TOF MS: m/z = 3126.7 (M + Na)<sup>+</sup>

IR (cm<sup>-1</sup>): 3032, 2940, 2870, 2222, 1736, 1605, 1489, 1466, 1396, 1227, 1211, 1142, 1103, 1018, 918, 818, 748, 702, 656, 525

Elemental analysis: calcd (%) for C<sub>131</sub>H<sub>120</sub>N<sub>3</sub>O<sub>25</sub>F<sub>51</sub>: C 50.67, H 3.90, N 1.35; found C 50.91, H 3.99, N 1.28

**Bis(2,2,2-tris(3-(6-(4'-cyanobiphenyl-4-yloxy)hexyloxy)hexyloxy)-3-oxopropylloxymethyl)-ethyl) 4,4'-(1,2-ethynediyl)bibenzoate (58)**



The dendritic 4-iodobenzene ester **37** (55 mg; 0.04 mmol) and the dendritic 4-ethynylbenzene ester **44** (51 mg; 0.04 mmol) were dissolved in toluene (5 mL). Argon was then flushed through the solution for 15 min. A catalytic mixture of Pd(PPh<sub>3</sub>)<sub>2</sub>Cl<sub>2</sub> (10 mg; 0.014 mmol) and CuI (2.5 mg; 0.014 mmol) was added into the solution and the mixture was stirred for 20 h at room temperature. The solvent was taken off by evaporation under vacuum, and the product was separated from the crude by column chromatography, eluting with 1:5 ethyl acetate/dichloromethane, to yield **58** as a yellow sticky solid.

Yield: 47 mg (45%)

<sup>1</sup>H NMR (400 MHz, CDCl<sub>3</sub>) δ<sub>H</sub> (ppm): 7.98 (m, 4 H, ArH); 7.67 (d (J = 8.5 Hz), 12 H, ArH); 7.62 (d (J = 8.5 Hz), 12 H, ArH); 7.56 (m, 4 H, ArH); 7.50 (d (J = 8.8 Hz), 12 H, ArH); 6.96 (d (J = 8.8 Hz), 4.31 (s, 4 H, -C<sub>6</sub>H<sub>4</sub>COOCH<sub>2</sub>-); 4.07 (t (J = 6.7 Hz), 12 H, -C<sub>6</sub>H<sub>4</sub>OCH<sub>2</sub>-); 3.98 (t (J = 6.4 Hz), 12 H, -CH<sub>2</sub>COOCH<sub>2</sub>-); 3.66 (t (J = 6.4 Hz), 12 H, -C(CH<sub>2</sub>OCH<sub>2</sub>-)<sub>3</sub>); 3.48 (s, 12 H, -C(CH<sub>2</sub>O-)<sub>3</sub>); 2.53 (t (J = 6.4 Hz), 12 H, -CH<sub>2</sub>COO-); 1.80 (m, 12 H, -CH<sub>2</sub>CH<sub>2</sub>O(C<sub>6</sub>H<sub>4</sub>)<sub>2</sub>CN); 1.65 (m, 12 H, -CH<sub>2</sub>COOCH<sub>2</sub>CH<sub>2</sub>-); 1.45 (m, 24 H, -CH<sub>2</sub>COOCH<sub>2</sub>CH<sub>2</sub>(CH<sub>2</sub>)<sub>2</sub>-)

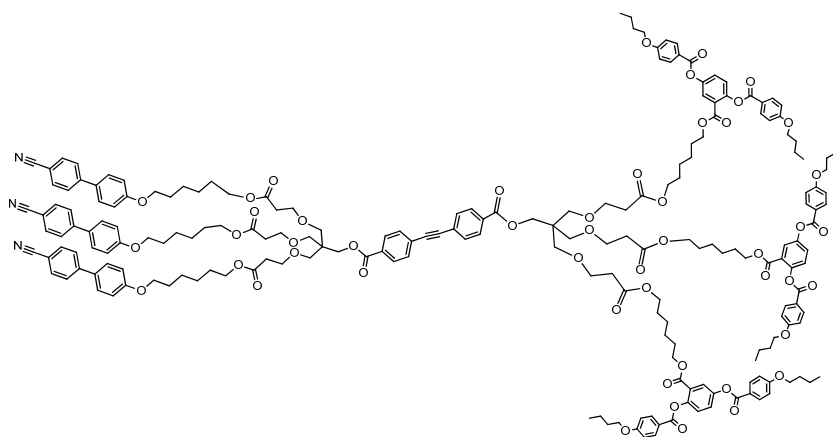
<sup>13</sup>C NMR (100.4 MHz, CDCl<sub>3</sub>) δ<sub>C</sub> (ppm): 171.7, 165.6, 159.8, 145.3, 132.7, 131.8, 131.4, 130.4, 129.6, 128.4, 127.1, 119.2, 115.1, 110.1, 91.48, 69.86, 68.00, 67.05, 64.55, 44.78, 35.12, 29.20, 28.64, 25.81

MALDI-TOF MS:  $m/z = 2620.1$  ( $M + Na$ )<sup>+</sup>

IR ( $\text{cm}^{-1}$ ): 3040, 2932, 2862, 2222, 1728, 1605, 1489, 1466, 1396, 1366, 1242, 1173, 1103, 1072, 1011, 910, 818, 764, 733, 656, 532

Elemental analysis: calcd (%) for  $\text{C}_{158}\text{H}_{168}\text{N}_6\text{O}_{28}$ : C 73.02, H 6.51, N 3.23; found: C 73.22, H 6.31, N 3.00

**2,2,2-Tris(3-(6-(2,5-di(4-butoxybenzoyloxy)benzoyloxy)hexyloxy)-3-oxopropyl-oxymethyl)ethyl 2,2,2-tris(3-(6-(4'-cyanobiphenyl-4-yloxy)hexyloxy)-3-oxopropyl-oxymethyl)ethyl 4,4'-(1,2-ethynediyl)bibenzoate (59)**



The dendritic 4-iodobenzene ester **37** (50 mg; 0.035 mmol) and the dendritic 4-ethynylbenzene ester **45** (80 mg; 0.035 mmol) were dissolved separately in toluene (10 mL), and triethylamine (5 mL) was added to the solution. Argon was then flushed through the solution for 15 min. A catalytic mixture of  $\text{Pd}(\text{PPh}_3)_2\text{Cl}_2$  (10 mg; 0.014 mmol) and  $\text{CuI}$  (3 mg; 0.014 mmol) was added into the solution and reacted for 20 h at room temperature. The solvent was taken off, and the product was isolated from the crude by column chromatography, eluting with 1:1 ethyl acetate/hexane, to yield **59** as a slight yellow sticky solid.

Yield: 71 mg (57%)

$^1\text{H}$  NMR (400 MHz,  $\text{CDCl}_3$ )  $\delta_{\text{H}}$  (ppm): 8.14 (d ( $J = 8.8$  Hz) d ( $J = 5.4$  Hz), 12 H,  $\text{ArH}$ ); 7.98 (m, 4 H,  $\text{ArH}$ ); 7.87 (d ( $J = 2.8$  Hz), 3 H,  $\text{ArH}$ ); 7.67 (d ( $J = 8.3$  Hz), 6 H,  $\text{ArH}$ ); 7.62 (d ( $J = 8.4$  Hz), 6 H,  $\text{ArH}$ ); 7.57 (d ( $J = 8.2$  Hz) d ( $J = 6.4$  Hz), 4 H,  $\text{ArH}$ ); 7.50 (d ( $J = 8.7$  Hz), 6 H,  $\text{ArH}$ ); 7.44 (d ( $J = 8.7$  Hz) d ( $J = 2.9$  Hz), 3 H,  $\text{ArH}$ ); 7.24

(d (J = 8.8 Hz), 3 H, ArH); 6.96 (m, 18 H, ArH); 4.29 (d (J = 11.2 Hz), 4 H, -C<sub>6</sub>H<sub>4</sub>COOCH<sub>2</sub>-); 4.13 (t (J = 6.7 Hz), 6 H, -C<sub>6</sub>H<sub>3</sub>COOCH<sub>2</sub>-); 4.05 (m, 18 H, -C<sub>6</sub>H<sub>4</sub>OCH<sub>2</sub>-); 3.98 (t (J = 6.4 Hz), 12 H, -CH<sub>2</sub>COOCH<sub>2</sub>-); 3.65 (m, 12 H, -C(CH<sub>2</sub>OCH<sub>2</sub>-)<sub>3</sub>); 3.47 (d (J = 10.8 Hz), 12 H, -C(CH<sub>2</sub>O-)<sub>3</sub>); 2.51 (d (J = 11.1 Hz) t (J = 6.4 Hz), 12 H, -CH<sub>2</sub>COO-); 1.80 (m, 18 H, -C<sub>6</sub>H<sub>4</sub>OCH<sub>2</sub>CH<sub>2</sub>-); 1.65 (m, 6 H, -CH<sub>2</sub>(CH<sub>2</sub>)<sub>4</sub>O(C<sub>6</sub>H<sub>4</sub>)<sub>2</sub>CN); 1.46 (m, 36 H, -C<sub>6</sub>H<sub>4</sub>OCH<sub>2</sub>CH<sub>2</sub>CH<sub>2</sub>-, -CH<sub>2</sub>COOCH<sub>2</sub>CH<sub>2</sub>CH<sub>2</sub>CH<sub>2</sub>CH<sub>2</sub>OCO-, -CH<sub>2</sub>CH<sub>2</sub>(CH<sub>2</sub>)<sub>2</sub>O(C<sub>6</sub>H<sub>4</sub>)<sub>2</sub>CN); 1.22 (m, 12 H, -CH<sub>2</sub>COOCH<sub>2</sub>CH<sub>2</sub>(CH<sub>2</sub>)<sub>2</sub>CH<sub>2</sub>CH<sub>2</sub>OCO-); 0.99 (t (J = 7.4 Hz) d (J = 3.6 Hz), 18 H, -CH<sub>3</sub>)

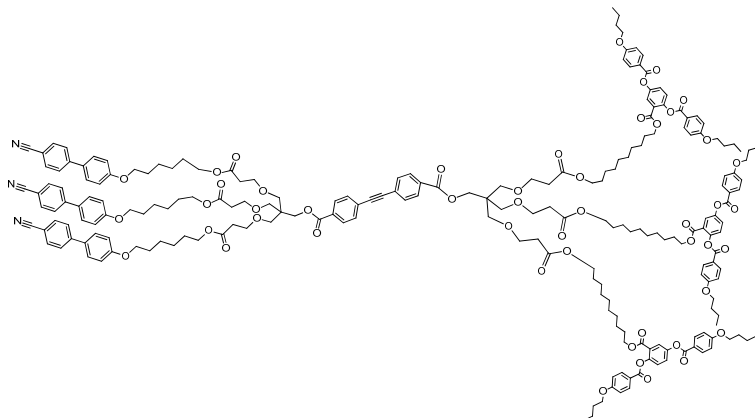
<sup>13</sup>C NMR (100.4 MHz, CDCl<sub>3</sub>) δ<sub>C</sub> (ppm): 171.7, 171.6, 165.6, 165.0, 164.7, 164.2, 163.8, 163.7, 159.8, 148.4, 148.2, 145.3, 132.7, 132.5, 132.5, 131.8, 131.7, 131.4, 130.3, 129.6, 128.4, 127.4, 127.2, 127.1, 125.1, 125.1, 125.0, 121.5, 121.1, 119.2, 115.1, 114.5, 114.4, 110.1, 91.57, 91.38, 69.84, 69.80, 68.12, 68.09, 67.99, 67.05, 67.01, 65.46, 64.55, 64.48, 44.76, 35.13, 35.04, 31.20, 29.21, 28.64, 28.50, 28.39, 25.83, 25.59, 19.28, 13.93

MALDI-TOF MS: m/z = 3553.4 (M + Na)<sup>+</sup>

IR (cm<sup>-1</sup>): 3071, 2940, 2870, 2222, 1736, 1605, 1512, 1489, 1466, 1420, 1366, 1242, 1165, 1111, 1065, 1003, 972, 910, 849, 818, 756, 741, 694, 640, 516

Elemental analysis: calcd (%) for C<sub>206</sub>H<sub>231</sub>N<sub>3</sub>O<sub>49</sub>: C 70.03, H 6.59, N 1.19; found: C 69.78, H 6.69, N 1.17

**2,2,2-Tris(3-(6-(2,5-di(4-butoxybenzoyloxy)benzoyloxy)decyloxy)-3-oxopropyl-oxymethyl)ethyl 2,2,2-tris(3-(6-(4'-cyanobiphenyl-4-yloxy)hexyloxy)-3-oxopropyl)ethyl 4,4'-(1,2-ethynediyl)bibenzoate (60)**



The dendritic 4-iodobenzene ester **37** (28 mg; 0.02 mmol) and the dendritic 4-ethynylbenzene ester **46** (50 mg; 0.02 mmol) were dissolved separately in toluene (10 mL), and triethylamine (5 mL) was added to the solution. Argon was then flushed through the solution for 15 min. A catalytic mixture of Pd(PPh<sub>3</sub>)<sub>2</sub>Cl<sub>2</sub> (10 mg; 0.014 mmol) and CuI (3 mg; 0.014 mmol) were added into the solution and the mixture was stirred 24 h at room temperature. The solvent was taken off, and the product was obtained from the crude by column chromatography, eluting with 1:1.2 ethyl acetate/hexane, to yield **60** as a slight yellow sticky solid.

Yield: 37 mg (50%)

<sup>1</sup>H NMR (400 MHz, CDCl<sub>3</sub>) δ<sub>H</sub> (ppm): 8.14 (d (J = 8.9 Hz) d (J = 5.3 Hz), 12 H, ArH); 7.99 (d (J = 8.2 Hz) d (J = 1.3 Hz), 4 H, ArH); 7.88 (d (J = 2.9 Hz), 3 H, ArH); 7.59 (d (J = 8.4 Hz) d (J = 1.8 Hz), 4 H, ArH); 7.44 (d (J = 8.7 Hz) d (J = 2.9 Hz), 3 H, ArH); 7.25 (d (J = 8.8 Hz), 3 H, ArH); 6.97 (d (J = 8.9 Hz) d (J = 3.3 Hz), 12 H, ArH); 4.37 (t (J = 6.6 Hz), 6 H, -CF<sub>2</sub>CH<sub>2</sub>CH<sub>2</sub>OCO-); 4.29 (d (J = 4.1 Hz), 4 H, -C<sub>6</sub>H<sub>4</sub>COOCH<sub>2</sub>-); 4.13 (t (J = 6.8 Hz), 6 H, -C<sub>6</sub>H<sub>3</sub>COOCH<sub>2</sub>-); 4.04 (m, 18 H, -C<sub>6</sub>H<sub>4</sub>OCH<sub>2</sub>-, -COOCH<sub>2</sub>(CH<sub>2</sub>)<sub>9</sub>-); 3.65 (m, 12 H, -C(CH<sub>2</sub>OCH<sub>2</sub>-)<sub>3</sub>); 3.47 (s, 12 H, -C(CH<sub>2</sub>O-)<sub>3</sub>); 2.48 (m, 18 H, -CH<sub>2</sub>COO-, -CF<sub>2</sub>CH<sub>2</sub>-); 1.81 (m, 12 H, -C<sub>6</sub>H<sub>4</sub>OCH<sub>2</sub>CH<sub>2</sub>-); 1.51 (m, 24 H, -C<sub>6</sub>H<sub>4</sub>OCH<sub>2</sub>CH<sub>2</sub>CH<sub>2</sub>-, -CH<sub>2</sub>COOCH<sub>2</sub>CH<sub>2</sub>(CH<sub>2</sub>)<sub>6</sub>CH<sub>2</sub>CH<sub>2</sub>OCO-); 1.20 (m, 36 H, -CH<sub>2</sub>COOCH<sub>2</sub>CH<sub>2</sub>(CH<sub>2</sub>)<sub>6</sub>CH<sub>2</sub>CH<sub>2</sub>OCO-); 1.03 (t (J = 7.4 Hz) d (J = 2.1 Hz), 18 H, -CH<sub>3</sub>)

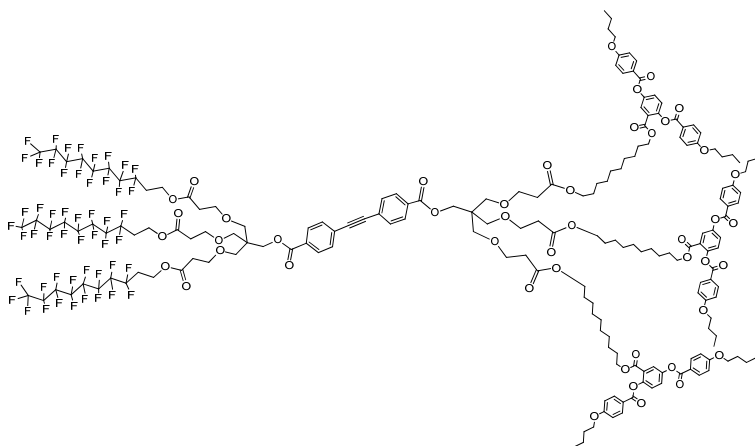
$^{13}\text{C}$  NMR (100.4 MHz,  $\text{CDCl}_3$ )  $\delta_{\text{C}}$  (ppm): 171.7, 165.0, 164.7, 164.2, 163.8, 163.7, 159.8, 148.4, 148.2, 145.3, 132.7, 132.5, 132.5, 131.8, 131.4, 129.6, 128.4, 127.1, 125.1, 121.5, 121.1, 119.2, 115.1, 114.5, 114.4, 110.2, 93.92, 90.84, 69.85, 69.81, 68.13, 68.07, 68.00, 67.04, 65.72, 64.73, 64.54, 44.78, 35.12, 31.21, 29.79, 29.56, 29.47, 29.34, 29.28, 29.21, 28.70, 28.64, 28.47, 25.99, 25.01, 25.81, 19.28, 13.92

MALDI-TOF MS:  $m/z = 3722.5$  ( $\text{M} + \text{Na}$ ) $^+$

IR ( $\text{cm}^{-1}$ ): 3071, 2924, 2862, 2222, 1736, 1605, 1512, 1489, 1466, 1420, 1366, 1242, 1227, 1211, 1157, 1111, 1057, 972, 826, 756, 694, 640, 532

Elemental analysis: calcd (%) for  $\text{C}_{218}\text{H}_{255}\text{N}_3\text{O}_{49}$ : C 70.74, H 6.94, N 1.15; found C 70.45, H 7.19, N 1.15

**2,2,2-Tris(3-(6-(2,5-di(4-butoxybenzoyloxy)benzoyloxy)decyloxy)-3-oxopropyl-oxymethyl)ethyl 2,2,2-tris(3-(3,3,4,4,5,5,6,6,7,7,8,8,9,9,10,10,10-heptafluoro-decyloxy)-3-oxopropyl)oxymethyl)ethyl 4,4'-(1,2-ethynediyl)bibenzoate (61)**



The dendritic 4-iodobenzene ester **36** (35 mg; 0.018 mmol) and the dendritic 4-ethynylbenzene ester **46** (40 mg; 0.018 mmol) were dissolved separately in toluene (10 mL) and triethylamine (5 mL) was added to the solution. Argon was then flushed through the solution for 15 min. A catalytic mixture of  $\text{Pd}(\text{PPh}_3)_2\text{Cl}_2$  (10 mg; 0.014 mmol) and  $\text{CuI}$  (3 mg; 0.014 mmol) was added into the solution and the mixture was stirred for 24 h at room temperature. The solvent was taken off, and the product was obtained from the crude by column chromatography, eluting with 1:1.5 ethyl acetate/hexane, to yield **61** as a white solid.

Yield: 24 mg (31%)

$^1\text{H}$  NMR (400 MHz,  $\text{CDCl}_3$ )  $\delta_{\text{H}}$  (ppm): 8.14 (d (J = 8.9 Hz) d (J = 5.3 Hz), 12 H, ArH); 7.99 (d (J = 8.2 Hz) d (J = 1.3 Hz), 4 H, ArH); 7.88 (d (J = 2.9 Hz), 3 H, ArH); 7.59 (d (J = 8.4 Hz) d (J = 1.8 Hz), 4 H, ArH); 7.44 (d (J = 8.7 Hz) d (J = 2.9 Hz), 3 H, ArH); 7.25 (d (J = 8.8 Hz), 3 H, ArH); 6.97 (d (J = 8.9 Hz) d (J = 3.3 Hz), 12 H, ArH); 4.37 (t (J = 6.6 Hz), 6 H,  $-\text{CF}_2\text{CH}_2\text{CH}_2\text{OCO}-$ ); 4.29 (d (J = 4.1 Hz), 4 H,  $-\text{C}_6\text{H}_4\text{COOCH}_2-$ ); 4.13 (t (J = 6.8 Hz), 6 H,  $-\text{C}_6\text{H}_3\text{COOCH}_2-$ ); 4.04 (m, 18 H,  $-\text{C}_6\text{H}_4\text{OCH}_2-$ ,  $-\text{COOCH}_2(\text{CH}_2)_9-$ ); 3.65 (m, 12 H,  $-\text{C}(\text{CH}_2\text{OCH}_2-)_3$ ); 3.47 (s, 12 H,  $-\text{C}(\text{CH}_2\text{O}-)_3$ ); 2.48 (m, 18 H,  $-\text{CH}_2\text{COO}-$ ,  $-\text{CF}_2\text{CH}_2-$ ); 1.81 (m, 12 H,  $-\text{C}_6\text{H}_4\text{OCH}_2\text{CH}_2-$ ); 1.51 (m, 24 H,  $-\text{C}_6\text{H}_4\text{OCH}_2\text{CH}_2\text{CH}_2-$ ,  $-\text{CH}_2\text{COOCH}_2\text{CH}_2(\text{CH}_2)_6\text{CH}_2\text{CH}_2\text{OCO}-$ ); 1.20 (m, 36 H,  $-\text{CH}_2\text{COOCH}_2\text{CH}_2(\text{CH}_2)_6\text{CH}_2\text{CH}_2\text{OCO}-$ ); 1.03 (t (J = 7.4 Hz) d (J = 2.1 Hz), 18 H,  $-\text{CH}_3$ )

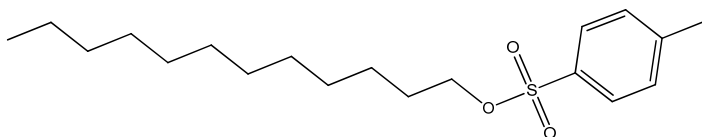
$^{13}\text{C}$  NMR (100.4 MHz,  $\text{CDCl}_3$ )  $\delta_{\text{C}}$  (ppm): 171.7, 171.2, 165.0, 164.7, 164.2, 163.8, 163.7, 148.4, 148.2, 132.5, 132.5, 131.7, 129.6, 127.2, 125.1, 121.5, 121.1, 114.5, 114.4, 69.79, 69.71, 68.12, 68.07, 67.03, 66.70, 65.72, 64.73, 44.76, 35.09, 34.87, 31.21, 29.56, 29.47, 29.34, 29.28, 28.70, 28.47, 25.99, 19.28, 13.91

MALDI-TOF MS:  $m/z = 4229.1$  ( $\text{M} + \text{Na}$ ) $^+$

IR ( $\text{cm}^{-1}$ ): 2924, 2862, 1736, 1605, 1512, 1466, 1420, 1242, 1157, 1111, 1065, 1011, 972, 849, 756, 741, 694, 648, 556

Elemental analysis: calcd (%) for  $\text{C}_{191}\text{H}_{207}\text{O}_{46}\text{F}_{51}$ : C 54.52, H 4.96; found: C 55.02, H 4.98

### Dodecyl tosylate (62)



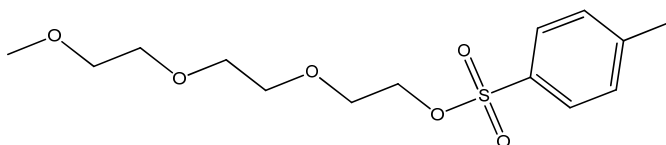
To a stirred solution of dodecan-1-ol (4.66 g; 25 mmol) in anhydrous dichloromethane was added triethylamine (6.3 g; 62.5 mmol), tosyl chloride (9.5 g; 50 mmol) and 4-(dimethylamino)pyridine (0.15 g; 1.25 mmol) at room temperature. The mixture continued to be stirred for 18 h, and diluted with ethyl acetate. After

removing the precipitate, the filtrate was subjected to evaporation, and the product was purified by column chromatography eluting with 1:1 dichloromethane/petroleum to yield **62** as a colourless oil.

Yield: 7.74 g (91%)

$^1\text{H}$  NMR (400 MHz,  $\text{CDCl}_3$ )  $\delta_{\text{H}}$  (ppm): 7.79 (d (J = 8.3 Hz), 2 H, ArH); 7.34 (d (J = 8.1 Hz), 2 H, ArH); 4.01 (t (J = 6.5 Hz), 2 H,  $-\text{OCH}_2-$ ); 2.45 (s, 3 H,  $-\text{C}_6\text{H}_4\text{CH}_3$ ); 1.62 (m, 2 H,  $-\text{OCH}_2\text{CH}_2-$ ); 1.26 (m, 18 H,  $-\text{OCH}_2\text{CH}_2(\text{CH}_2)_9-$ ); 0.88 (t (J = 6.9 Hz), 3 H,  $-\text{CH}_3$ )

### Methoxyethoxyethoxyethyl tosylate (**63**)

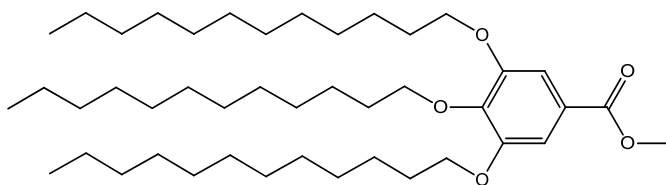


To a stirred solution of methylene glycol (0.82 g; 5 mmol) in anhydrous dichloromethane was added triethylamine (1.26 g; 12.5 mmol), tosyl chloride (1.9 g; 10 mmol) and 4-(dimethylamino)pyridine (0.03 g; 0.25 mmol) at room temperature. The mixture continued to be stirred for 18 h, and then diluted with ethyl acetate. After removing the precipitate, the filtrate was subjected to evaporation, and the product was purified by column chromatography eluting with 1:20 ethanol/dichloromethane to yield **63** as a colorless oil.

Yield: 1.51 g (95%)

$^1\text{H}$  NMR (400 MHz,  $\text{CDCl}_3$ )  $\delta_{\text{H}}$  (ppm): 7.80 (d (J = 8.4 Hz), 2 H, ArH); 7.34 (d (J = 8.0 Hz), 2 H, ArH); 4.16 (m, 2 H,  $-\text{O}_2\text{SOCH}_2-$ ); 3.69 (m, 2 H,  $-\text{O}_2\text{SOCH}_2\text{CH}_2-$ ); 3.61 (m, 6 H,  $-\text{CH}_2\text{CH}_2\text{OCH}_2\text{CH}_2\text{OCH}_3$ ); 3.53 (m, 2 H,  $-\text{CH}_2\text{OCH}_3$ ); 3.37 (s, 3 H,  $-\text{OCH}_3$ ); 2.45 (s, 3 H,  $-\text{C}_6\text{H}_4\text{CH}_3$ )

### Methyl 3,4,5-dodecyloxybenzoate (**64**)

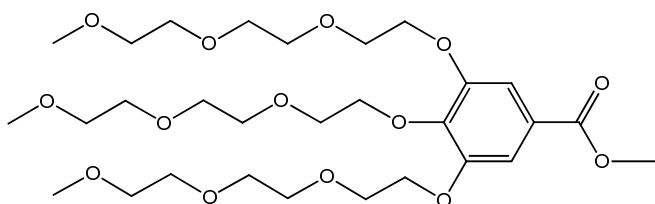


A mixture of methyl 3,4,5-trihydroxybenzoate (0.46 g; 2.5 mmol), **62** (2.8 g; 8.25 mmol), potassium carbonate (3.45 g; 25 mmol) and dimethylformamide (100 mL) was heated to 80 °C for 24 h. After the solvent was removed by evaporation, aq HCl was added and the crude product was extracted with dichloromethane. The combined organic layers were washed with aq HCl and brine, and dried over Na<sub>2</sub>SO<sub>4</sub>. After filtration, the solvent was removed and the product was isolated by column chromatography, using 1:1 dichloromethane/petroleum ether, to yield **64** as a white solid.

Yield: 1.61 g (93%)

<sup>1</sup>H NMR (400 MHz, CDCl<sub>3</sub>) δ<sub>H</sub> (ppm): 7.25 (s, 2 H, ArH); 4.01 (m, 6 H, -C<sub>6</sub>H<sub>2</sub>OCH<sub>2</sub>-); 3.89 (s, 3 H, -COOCH<sub>3</sub>); 1.77 (m, 6 H, -OCH<sub>2</sub>CH<sub>2</sub>-); 1.46 (m, 6 H, -OCH<sub>2</sub>CH<sub>2</sub>CH<sub>2</sub>-); 1.26 (m, 48 H, -OCH<sub>2</sub>CH<sub>2</sub>CH<sub>2</sub>(CH<sub>2</sub>)<sub>8</sub>-); 0.88 (t (J = 6.8 Hz), 9 H, -CH<sub>3</sub>)

### Methyl 3,4,5-methoxyethoxyethoxyethoxybenzoate (**65**)



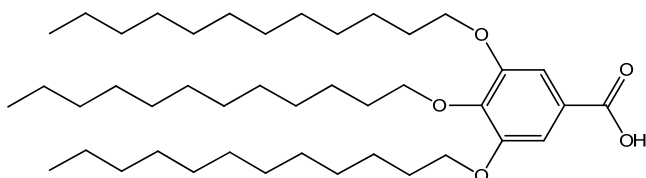
A mixture of methyl 3,4,5-trihydroxybenzoate (0.25 g; 1.36 mmol), **63** (1.51 g; 4.7 mmol), potassium carbonate (1.88 g; 13.6 mmol) and dimethylformamide (20 mL) was heated to 80 °C for 24 h. After the solvent was removed, aq HCl was added and the crude product was extracted with dichloromethane. The combined organic layers were washed with aq HCl and brine, and dried over Na<sub>2</sub>SO<sub>4</sub>. After filtration, the

solvent was removed and the product was purified by column chromatography, using 3% EtOH in dichloromethane, to yield **65** as a colorless oil.

Yield: 0.78 g (92%)

$^1\text{H}$  NMR (400 MHz,  $\text{CDCl}_3$ )  $\delta_{\text{H}}$  (ppm): 7.28 (s, 2 H, ArH); 4.20 (m, 6 H, - $\text{C}_6\text{H}_2\text{OCH}_2$ -); 3.86 (m, 7 H, - $\text{COOCH}_3$ , - $\text{C}_6\text{H}_2\text{OCH}_2$ -); 3.79 (m, 2 H, - $\text{C}_6\text{H}_2\text{OCH}_2\text{CH}_2$ -); 3.72 (m, 6 H, - $\text{C}_6\text{H}_2\text{OCH}_2\text{CH}_2\text{OCH}_2$ -); 3.62 (m, 12 H, - $\text{CH}_2\text{OCH}_2\text{CH}_2\text{OCH}_3$ ); 3.53 (m, 6 H, - $\text{CH}_2\text{OCH}_3$ ); 3.37 (s, 9 H, - $\text{OCH}_3$ )

### 3,4,5-Dodecyloxybenzoic acid (**66**)

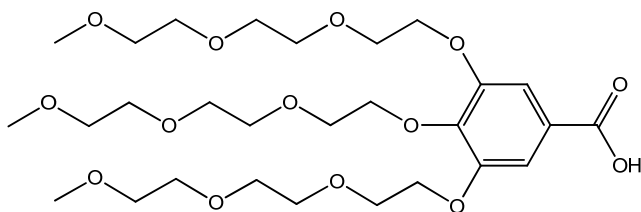


Compound **64** (1.61 g; 2.34 mmol) was dissolved in tetrahydrofuran (30 mL). NaOH (0.94 g; 23.4 mmol) dissolved in water (30 mL) was then added to the solution along with a few drops of methanol. The reacting mixture was heated under reflux at 100 °C for 16 h, then allowed to cool down to room temperature and acidified with 2M HCl. The organic layer was then removed by evaporation leaving a white precipitate in the aqueous layer, extracted three times with dichloromethane, and washed with HCl. The solvent was taken off *in vacuo* to yield **66** as a white solid.

Yield: 1.15 g (73%)

$^1\text{H}$  NMR (400 MHz,  $\text{CDCl}_3$ )  $\delta_{\text{H}}$  (ppm): 7.30 (s, 2 H, ArH); 4.03 (m, 6 H, - $\text{C}_6\text{H}_2\text{OCH}_2$ -); 1.78 (m, 6 H, - $\text{OCH}_2\text{CH}_2$ -); 1.47 (m, 6 H, - $\text{OCH}_2\text{CH}_2\text{CH}_2$ -); 1.26 (m, 48 H, - $\text{OCH}_2\text{CH}_2\text{CH}_2(\text{CH}_2)_8$ -); 0.88 (t (J = 6.9 Hz), 9 H, - $\text{CH}_3$ )

### 3,4,5-Methoxyethoxyethoxyethoxybenzoic acid (**67**)

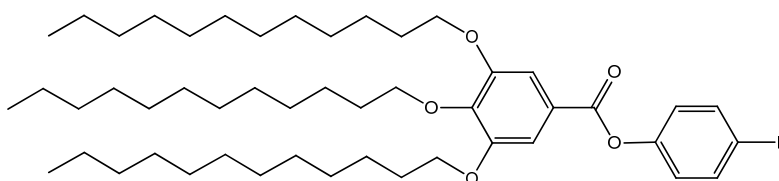


Compound **65** (0.7 g; 1.12 mmol) was dissolved in a mixture of THF (8 mL), MeOH (8 mL), and 1M aqueous KOH (8 mL). Then solid KOH (0.76 g, 13.5 mmol) was added. The mixture was heated under reflux at 100 °C for 12 h. The solvent was removed under reduced pressure and the solid residue was dissolved in water (40 mL). Addition of concentrated HCl (5 mL) to the solution caused precipitation of a yellowish solid. The solid was filtered and then dissolved in acetone. The solution was dried over MgSO<sub>4</sub> and the solvent removed under reduced pressure affording **67** as a slight yellow oil.

Yield: 0.66 g (97%)

<sup>1</sup>H NMR (400 MHz, CDCl<sub>3</sub>)  $\delta_H$  (ppm): 7.35 (s, 2 H, ArH); 4.24 (m, 2 H, -C<sub>6</sub>H<sub>2</sub>OCH<sub>2</sub>-); 4.20 (m, 4 H, -C<sub>6</sub>H<sub>2</sub>OCH<sub>2</sub>-); 3.87 (m, 4 H, -C<sub>6</sub>H<sub>2</sub>OCH<sub>2</sub>CH<sub>2</sub>-); 3.80 (m, 2 H, -C<sub>6</sub>H<sub>2</sub>OCH<sub>2</sub>CH<sub>2</sub>-); 3.73 (m, 6 H, -C<sub>6</sub>H<sub>2</sub>OCH<sub>2</sub>CH<sub>2</sub>OCH<sub>2</sub>-); 3.65 (m, 12 H, -CH<sub>2</sub>OCH<sub>2</sub>CH<sub>2</sub>OCH<sub>3</sub>); 3.54 (m, 6 H, -CH<sub>2</sub>OCH<sub>3</sub>); 3.38 (s, 9 H, -OCH<sub>3</sub>)

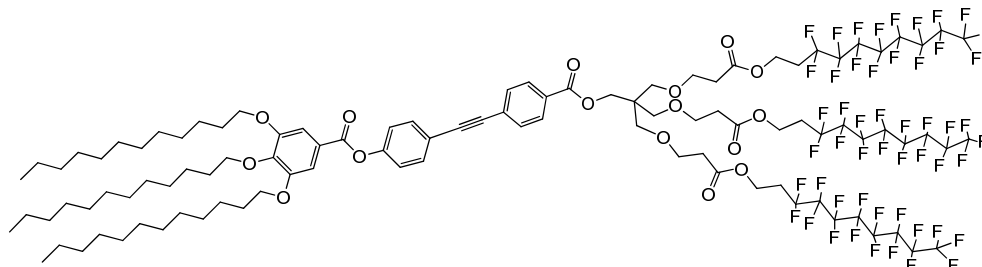
### 4-Iodophenyl 3,4,5-dodecyloxybenzoate (**68**)



Compound **66** (1.15 g; 1.7 mmol) and 4-iodophenol (0.41 g; 1.87 mmol) were dissolved in dichloromethane (25 mL) with 1-ethyl-3-(3-dimethylaminopropyl)carbodiimide (0.39 g; 2 mmol) and 4-(dimethylamino)pyridine (20 mg; 0.17 mmol). The reaction was stirred under argon for 18 h at room temperature. The solvent was removed by evaporation, and the product was obtained



**4-(4-(2,2,2-Tris(3-(3,3,4,4,5,5,6,6,7,7,8,8,9,9,10,10,10-heptafluorodecyloxy)-3-oxopropyl)oxy)methyl)ethyloxycarbonyl)phenylethynyl)phenyl 3,4,5-dodecyl-oxybenzoate (70)**



The dendritic 4-ethynylbenzene ester **43** (70 mg; 0.039 mmol), **68** (34 mg; 0.039 mmol) and triethylamine (5 mL) were added to a degassed shlenk tube. Argon was then flushed through the solution for 15 min. A catalytic mixture of Pd(PPh<sub>3</sub>)<sub>2</sub>Cl<sub>2</sub> (4 mg; 0.006 mmol) and CuI (1 mg; 0.006 mmol) was added into the solution and the mixture was stirred for 18 h at room temperature. The solvent was taken off, and the product was obtained from the crude by column chromatography, eluting with 1:5 ethyl acetate/petroleum ether, to yield **70** as a yellow crystal.

Yield: 46 mg (45%)

<sup>1</sup>H NMR (400 MHz, CDCl<sub>3</sub>) δ<sub>H</sub> (ppm): 7.98 (d (J = 8.4 Hz), 2 H, ArH); 7.59 (d (J = 8.4 Hz) d (J = 5.4 Hz), 4 H, ArH); 7.39 (s, 2 H, ArH); 7.21 (d (J = 8.6 Hz), 2 H, ArH); 4.37 (t (J = 6.5 Hz), 6 H, -CH<sub>2</sub>COOCH<sub>2</sub>-); 4.28 (s, 2 H, -COOCH<sub>2</sub>C(CH<sub>2</sub>O-)<sub>3</sub>); 4.04 (m, 6 H, -C<sub>6</sub>H<sub>2</sub>OCH<sub>2</sub>-); 3.66 (t (J = 6.2 Hz), 6 H, -C(CH<sub>2</sub>OCH<sub>2</sub>-)<sub>3</sub>); 3.47 (s, 6 H, -C(CH<sub>2</sub>O-)<sub>3</sub>); 2.48 (m, 12 H, -CH<sub>2</sub>CF<sub>2</sub>-, -CH<sub>2</sub>COO-); 1.79 (m, 6 H, -C<sub>6</sub>H<sub>2</sub>OCH<sub>2</sub>CH<sub>2</sub>-); 1.48 (m, 6 H, -OCH<sub>2</sub>CH<sub>2</sub>CH<sub>2</sub>-); 1.25 (m, 48 H, -OCH<sub>2</sub>CH<sub>2</sub>CH<sub>2</sub>(CH<sub>2</sub>)<sub>8</sub>-); 0.87 (m, 9 H, -CH<sub>3</sub>)

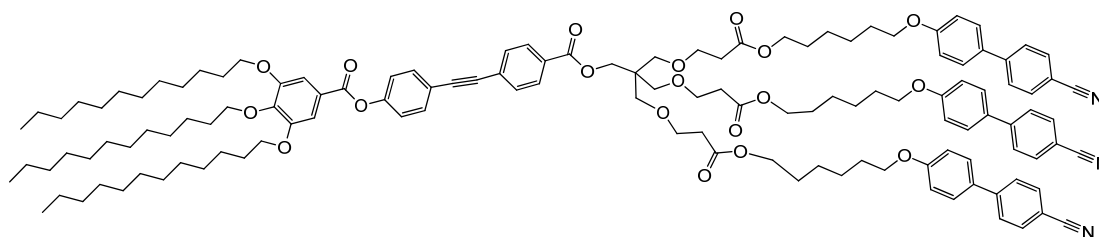
<sup>13</sup>C NMR (100.4 MHz, CDCl<sub>3</sub>) δ<sub>C</sub> (ppm): 171.2, 165.7, 164.8, 153.1, 151.4, 143.3, 133.0, 131.6, 129.8, 129.5, 128.0, 123.6, 122.2, 120.4, 118.6, 112.8, 110.8, 110.6, 108.7, 91.68, 88.75, 73.70, 69.75, 69.36, 66.71, 64.39, 56.41, 44.76, 39.16, 34.88, 32.01, 30.73, 30.51, 30.44, 30.29, 29.79, 29.73, 29.66, 29.58, 29.49, 29.38, 26.17, 22.78, 14.20

MALDI-TOF MS: m/z = 2589.7 (M + Na)<sup>+</sup>

IR (cm<sup>-1</sup>): 2916, 2855, 1759, 1744, 1589, 1504, 1466, 1427, 1366, 1342, 1196, 1142, 1111, 972, 856, 702, 656, 556, 532

Elemental analysis: calcd (%) for C<sub>102</sub>H<sub>117</sub>O<sub>16</sub>F<sub>51</sub>: C 47.71, H 4.59; found C 48.01, H 4.65

**4-(4-(2,2,2-Tris(3-(6-(4'-cyanobiphenyl-4-yloxy)hexyloxy)-3-oxopropoxy-methyl)ethyloxycarbonyl)phenylethynyl)phenyl 3,4,5-dodecyloxybenzoate (71)**



The dendritic 4-ethynylbenzene ester **44** (60 mg; 0.046 mmol) was dissolved in toluene (5 mL) and added to a degassed shlenk tube with **68** (44 mg; 0.05 mmol) and triethylamine (5 mL). Argon was then flushed through the solution for 15 min. A catalytic mixture of Pd(PPh<sub>3</sub>)<sub>2</sub>Cl<sub>2</sub> (5 mg; 0.007 mmol) and CuI (1 mg; 0.006 mmol) was added into the solution and the mixture was stirred for 24 h at room temperature. The solvent was taken off, and the product was obtained from the crude by column chromatography, eluting with 1:10 ethyl acetate/dichloromethane, and then recrystallization from dichloromethane/ethanol to yield **71** as white crystals.

Yield: 23 mg (22%)

<sup>1</sup>H NMR (400 MHz, CDCl<sub>3</sub>) δ<sub>H</sub> (ppm): 7.99 (d (J = 8.5 Hz), 2 H, ArH); 7.67 (d (J = 8.6 Hz), 6 H, ArH); 7.62 (d (J = 8.6 Hz), 6 H, ArH); 7.58 (d (J = 8.6 Hz) d (J = 3.6 Hz), 4 H, ArH); 7.51 (d (J = 8.8 Hz), 6 H, ArH); 7.40 (s, 2 H, ArH); 7.20 (d (J = 8.7 Hz), 2 H, ArH); 6.96 (d (J = 8.8 Hz), 6 H, ArH); 4.31 (s, 2 H, -C<sub>6</sub>H<sub>4</sub>COOCH<sub>2</sub>-); 4.06 (m, 12 H, -CH<sub>2</sub>O(C<sub>6</sub>H<sub>4</sub>)<sub>2</sub>CN, -OCH<sub>2</sub>(CH<sub>2</sub>)<sub>10</sub>CH<sub>3</sub>); 3.98 (t (J = 6.4 Hz), 6 H, -CH<sub>2</sub>COOCH<sub>2</sub>-); 3.67 (t (J = 6.4 Hz), 6 H, -C(CH<sub>2</sub>OCH<sub>2</sub>-)<sub>3</sub>, -CH<sub>2</sub>OCH<sub>2</sub>CH<sub>2</sub>OCH<sub>3</sub>); 3.49 (s, 6 H, -C(CH<sub>2</sub>O-)<sub>3</sub>); 2.53 (t (J = 6.4 Hz), 6 H, -CH<sub>2</sub>COO-); 1.80 (m, 12 H, -CH<sub>2</sub>CH<sub>2</sub>O(C<sub>6</sub>H<sub>4</sub>)<sub>2</sub>CN, -OCH<sub>2</sub>CH<sub>2</sub>(CH<sub>2</sub>)<sub>9</sub>CH<sub>3</sub>); 1.65 (m, 6 H, -CH<sub>2</sub>COOCH<sub>2</sub>CH<sub>2</sub>-);

1.36 (m, 66 H,  $-\text{CH}_2\text{COOCH}_2\text{CH}_2(\text{CH}_2)_2-$ ,  $-\text{OCH}_2\text{CH}_2(\text{CH}_2)_9\text{CH}_3$ ); 0.88 (m, 9 H,  $-\text{CH}_3$ )

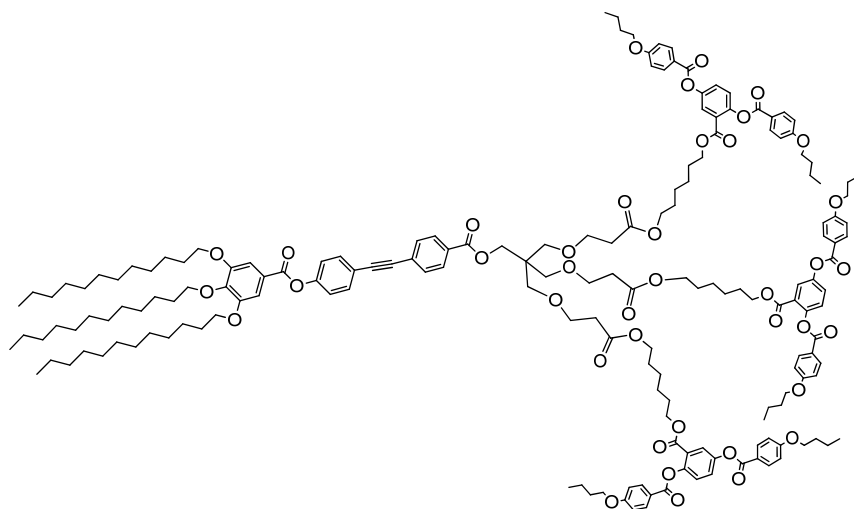
$^{13}\text{C}$  NMR (100.4 MHz,  $\text{CDCl}_3$ )  $\delta_{\text{C}}$  (ppm): 171.7, 165.8, 164.8, 159.8, 153.1, 151.4, 145.3, 143.3, 133.0, 132.7, 131.6, 131.4, 129.9, 129.6, 128.4, 127.9, 127.1, 123.6, 122.2, 120.3, 119.2, 115.1, 110.1, 108.7, 91.77, 88.83, 73.71, 69.89, 69.38, 68.00, 67.06, 64.64, 64.55, 44.78, 35.15, 32.03, 30.45, 29.84, 29.80, 29.74, 29.68, 29.50, 29.47, 29.39, 29.22, 28.65, 26.19, 25.84, 22.80, 14.23

MALDI-TOF MS:  $m/z = 2084.2$  ( $\text{M} + \text{Na}$ ) $^+$

IR ( $\text{cm}^{-1}$ ): 3071, 2916, 2855, 2222, 1736, 1605, 1497, 1466, 1427, 1366, 1242, 1180, 1111, 1011, 856, 818, 764, 725, 656, 532

Elemental analysis: calcd (%) for  $\text{C}_{129}\text{H}_{165}\text{N}_3\text{O}_{19}$ : C 75.15, H 8.07, N 2.04; found: C 74.96, H 8.06, N 1.97

**4-(4-(2,2,2-Tris(6-(2,5-di(4-butoxybenzoyloxy)benzoyloxy)hexyloxy)-3-oxo-propyloxymethyl)ethyloxycarbonyl)phenylethynyl)phenyl 3,4,5-dodecyloxybenzoate (72)**



The dendritic 4-ethynylbenzene ester **45** (80 mg; 0.036 mmol) was dissolved in toluene (5 mL) and added to a degassed shlenk tube with **68** (31 mg; 0.036 mmol) and triethylamine (5 mL). Argon was then flushed through the solution for 15 min. A catalytic mixture of  $\text{Pd}(\text{PPh}_3)_2\text{Cl}_2$  (4 mg; 0.006 mmol) and  $\text{CuI}$  (1 mg; 0.006 mmol)

was added into the solution and the mixture was stirred for 18 h at room temperature. The solvent was taken off, and the product was isolated from the crude by column chromatography, eluting with 1:2.5 ethyl acetate/petroleum ether, to yield **72** as a white sticky solid.

Yield: 30 mg (28%)

$^1\text{H}$  NMR (400 MHz,  $\text{CDCl}_3$ )  $\delta_{\text{H}}$  (ppm): 8.14 (d (J = 8.9 Hz) d (J = 6.1 Hz), 12 H, ArH); 7.97 (d (J = 8.5 Hz), 2 H, ArH); 7.88 (d (J = 2.9 Hz), 3 H, ArH); 7.58 (m, 4 H, ArH); 7.44 (d (J = 8.7 Hz) d (J = 2.9 Hz), 3 H, ArH); 7.39 (s, 2 H, ArH); 7.25 (d (J = 8.7 Hz), 3 H, ArH); 7.20 (d (J = 8.7 Hz), 2 H, ArH); 6.97 (d (J = 8.7 Hz), 12 H, ArH); 4.28 (s, 2 H,  $-\text{C}_6\text{H}_4\text{COOCH}_2-$ ); 4.14 (t (J = 6.7 Hz), 6 H,  $-\text{CH}_2\text{COO}(\text{CH}_2)_5\text{CH}_2\text{OCO}-$ ); 4.04 (m, 18 H,  $-\text{C}_6\text{H}_4\text{OCH}_2-$ ,  $-\text{OCH}_2(\text{CH}_2)_{10}\text{CH}_3$ ); 3.98 (t (J = 6.8 Hz), 6 H,  $-\text{CH}_2\text{COOCH}_2-$ ); 3.64 (t (J = 6.5 Hz), 6 H,  $-\text{C}(\text{CH}_2\text{OCH}_2)_3$ ); 3.46 (s, 6 H,  $-\text{C}(\text{CH}_2\text{O})_3$ ); 2.50 (t (J = 6.5 Hz), 6 H,  $-\text{CH}_2\text{COO}-$ ); 1.80 (m, 18 H,  $-\text{C}_6\text{H}_4\text{OCH}_2\text{CH}_2-$ ,  $-\text{OCH}_2\text{CH}_2(\text{CH}_2)_9\text{CH}_3$ ); 1.50 (m, 30 H,  $-\text{C}_6\text{H}_4\text{OCH}_2\text{CH}_2\text{CH}_2-$ ,  $-\text{CH}_2\text{COOCH}_2\text{CH}_2\text{CH}_2\text{CH}_2\text{CH}_2\text{CH}_2\text{OCO}-$ ,  $-\text{OCH}_2\text{CH}_2\text{CH}_2(\text{CH}_2)_8\text{CH}_3$ ); 1.26 (m, 60 H,  $-\text{CH}_2\text{COOCH}_2\text{CH}_2(\text{CH}_2)_2-$ ,  $-\text{OCH}_2\text{CH}_2\text{CH}_2(\text{CH}_2)_8\text{CH}_3$ ); 0.99 (t (J = 7.4 Hz) d (J = 3.0 Hz), 18 H,  $-\text{O}(\text{CH}_2)_3\text{CH}_3$ ); 0.88 (m, 6 H,  $-\text{O}(\text{CH}_2)_{11}\text{CH}_3$ )

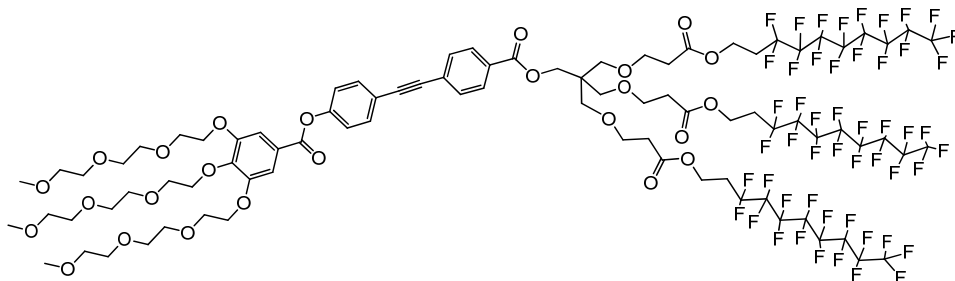
$^{13}\text{C}$  NMR (100.4 MHz,  $\text{CDCl}_3$ )  $\delta_{\text{C}}$  (ppm): 171.6, 165.7, 165.0, 164.8, 164.7, 164.2, 163.8, 163.7, 153.1, 151.3, 148.4, 148.2, 143.2, 133.1, 132.5, 132.5, 131.6, 129.5, 127.8, 127.2, 125.1, 125.1, 125.0, 123.6, 122.2, 121.5, 121.1, 120.4, 114.5, 114.4, 108.6, 88.87, 73.69, 69.82, 69.35, 68.12, 67.00, 65.47, 64.49, 44.75, 35.05, 32.02, 31.21, 30.45, 30.19, 29.84, 29.80, 29.74, 29.68, 29.50, 29.39, 28.50, 28.39, 26.19, 25.59, 22.79, 19.28, 14.22, 13.93

MALDI-TOF MS:  $m/z = 3018.6$  (M + Na) $^+$

IR ( $\text{cm}^{-1}$ ): 3071, 2924, 2855, 1751, 1605, 1512, 1466, 1427, 1366, 1312, 1242, 1211, 1157, 1111, 157, 1003, 972, 849, 756, 694, 640, 548

Elemental analysis: calcd (%) for  $\text{C}_{177}\text{H}_{228}\text{O}_{40}$ : C 70.97, H 7.67; found: C 80.00, H 7.86

**4-(4-(2,2,2-Tris(3-(3,3,4,4,5,5,6,6,7,7,8,8,9,9,10,10,10-heptafluorodecyloxy)-3-oxopropyl)oxy)methyl)ethyloxycarbonyl)phenylethynyl)phenyl 3,4,5-methoxyethyloxyethyloxyethyloxybenzoate (73)**



The dendritic 4-ethynylbenzene ester **43** (72 mg; 0.04 mmol) was dissolved in toluene (5 mL), then **69** (33 mg; 0.06 mmol) and triethylamine (5 mL) were added to the solution. Argon was then flushed through the solution for 15 min. A catalytic mixture of Pd(PPh<sub>3</sub>)<sub>2</sub>Cl<sub>2</sub> (8 mg; 0.011 mmol) and CuI (2 mg; 0.011 mmol) was added into the solution and the mixture was stirred for 18 h at room temperature. The solvent was taken off, and the product was obtained from the crude by column chromatography, eluting with 1:20 methanol/ethyl acetate, to yield **73** as a yellow crystal.

Yield: 30 mg (28%)

<sup>1</sup>H NMR (400 MHz, CDCl<sub>3</sub>) δ<sub>H</sub> (ppm): 7.98 (d (J = 8.4 Hz), 2 H, ArH); 7.60 (d (J = 8.4 Hz) d (J = 6.0 Hz), 4 H, ArH); 7.45 (s, 2 H, ArH); 7.21 (d (J = 8.7 Hz), 2 H, ArH); 4.37 (t (J = 6.6 Hz); -CH<sub>2</sub>COOCH<sub>2</sub>-); 4.25 (m, 8 H, -CH<sub>2</sub>C(CH<sub>2</sub>O-)<sub>3</sub>, -C<sub>6</sub>H<sub>2</sub>OCH<sub>2</sub>-); 3.89 (m, 4 H, -C<sub>6</sub>H<sub>2</sub>OCH<sub>2</sub>CH<sub>2</sub>-); 3.85 (m, 2 H, -C<sub>6</sub>H<sub>2</sub>OCH<sub>2</sub>CH<sub>2</sub>-); 3.74 (m, 6 H, -C<sub>6</sub>H<sub>2</sub>O(CH<sub>2</sub>)<sub>2</sub>OCH<sub>2</sub>-); 3.66 (m, 18 H, -C(CH<sub>2</sub>OCH<sub>2</sub>-)<sub>3</sub>, -CH<sub>2</sub>OCH<sub>2</sub>CH<sub>2</sub>OCH<sub>3</sub>); 3.54 (m, 6 H, -CH<sub>2</sub>OCH<sub>3</sub>); 3.47 (s, 6 H, -C(CH<sub>2</sub>O-)<sub>3</sub>); 3.38 (s, 3 H, -OCH<sub>3</sub>); 3.37 (s, 6 H, -OCH<sub>3</sub>); 2.55 (t (J = 6.2 Hz), 6 H, -CH<sub>2</sub>COO-); 2.47 (m, 6 H, -CH<sub>2</sub>CF<sub>2</sub>-)

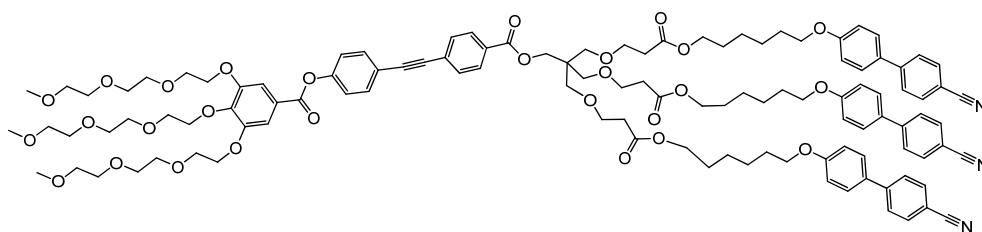
<sup>13</sup>C NMR (100.4 MHz, CDCl<sub>3</sub>) δ<sub>C</sub> (ppm): 171.2, 152.6, 151.3, 133.1, 131.6, 129.8, 129.5, 128.7, 123.9, 122.1, 109.8, 91.64, 88.78, 72.60, 72.01, 70.93, 70.79, 70.67, 69.71, 69.07, 66.71, 64.38, 59.12, 56.45, 56.42, 56.37, 44.76, 34.88, 32.02, 30.73, 30.51, 30.29, 29.79, 29.46, 29.31, 22.78, 14.21

MALDI-TOF MS: m/z = 2523.6 (M + Na)<sup>+</sup>

IR (cm<sup>-1</sup>): 3078, 2924, 2855, 1728, 1597, 1458, 1435, 1366, 1335, 1227, 1196, 1142, 1111, 964, 856, 702, 656, 610, 556, 517

Elemental analysis: calcd (%) for C<sub>87</sub>H<sub>87</sub>O<sub>25</sub>F<sub>51</sub>: C 41.77, H 3.51; found: C 41.96, H 3.39

**4-(4-(2,2,2-tris(3-(6-(4'-cyanobiphenyl-4-yloxy)hexyloxy)-3-oxopropoxy-methyl)ethyloxycarbonyl)phenylethynyl)phenyl 3,4,5-methoxyethyloxyethyloxybenzoate (74)**



The dendritic 4-ethynylbenzene ester **44** (78 mg; 0.06 mmol) was dissolved in toluene (5 mL), then **69** (65 mg; 0.08 mmol) and triethylamine (5 mL) was added to the solution. Argon was then flushed through the solution for 15 min. A catalytic mixture of Pd(PPh<sub>3</sub>)<sub>2</sub>Cl<sub>2</sub> (8 mg; 0.011 mmol) and CuI (2 mg; 0.011 mmol) was added to the solution and the mixture was stirred for 18 h at room temperature. The solvent was taken off, and the product was obtained from the crude by column chromatography eluting with 1:20 methanol/ethyl acetate to yield **74** as a yellow oil.

Yield: 24 mg (20%)

<sup>1</sup>H NMR (400 MHz, CDCl<sub>3</sub>) δ<sub>H</sub> (ppm): 7.99 (d (J = 8.4 Hz), 2 H, ArH); 7.66 (d (J = 8.5 Hz), 6 H, ArH); 7.61 (d (J = 8.5 Hz), 6 H, ArH); 7.57 (d (J = 8.6 Hz) d (J = 2.4 Hz), 4 H, ArH); 7.50 (d (J = 8.8 Hz), 6 H, ArH); 7.44 (s, 2 H, ArH); 7.19 (d (J = 8.6 Hz), 2 H, ArH); 6.96 (d (J = 8.8 Hz), 6 H, ArH); 4.31 (s, 2 H, -C<sub>6</sub>H<sub>4</sub>COOCH<sub>2</sub>-); 4.27 (m, 2 H, -C<sub>6</sub>H<sub>2</sub>OCH<sub>2</sub>-); 4.22 (m, 4 H, -C<sub>6</sub>H<sub>2</sub>OCH<sub>2</sub>-); 4.07 (t (J = 6.7 Hz), 6 H, -CH<sub>2</sub>O(C<sub>6</sub>H<sub>4</sub>)<sub>2</sub>CN); 3.97 (t (J = 6.4 Hz), 6 H, -CH<sub>2</sub>COOCH<sub>2</sub>-); 3.88 (m, 4 H, -C<sub>6</sub>H<sub>2</sub>OCH<sub>2</sub>CH<sub>2</sub>-); 3.82 (m, 2 H, -C<sub>6</sub>H<sub>2</sub>OCH<sub>2</sub>CH<sub>2</sub>-); 3.74 (m, 6 H, -C<sub>6</sub>H<sub>2</sub>OCH<sub>2</sub>CH<sub>2</sub>OCH<sub>2</sub>-); 3.65 (m, 18 H, -C(CH<sub>2</sub>OCH<sub>2</sub>)<sub>3</sub>, -CH<sub>2</sub>OCH<sub>2</sub>CH<sub>2</sub>OCH<sub>3</sub>); 3.54 (m, 6 H, -CH<sub>2</sub>OCH<sub>3</sub>); 3.49 (s, 6 H, -C(CH<sub>2</sub>O)<sub>3</sub>); 3.37 (s, 3 H, -OCH<sub>3</sub>); 3.36 (s, 6 H, -

OCH<sub>3</sub>); 2.52 (t (J = 6.4 Hz), 6 H, -CH<sub>2</sub>COO-); 1.79 (m, 6 H, -CH<sub>2</sub>CH<sub>2</sub>O(C<sub>6</sub>H<sub>4</sub>)<sub>2</sub>CN); 1.65 (m, 6 H, -CH<sub>2</sub>COOCH<sub>2</sub>CH<sub>2</sub>-); 1.45 (m, 12 H, -CH<sub>2</sub>COOCH<sub>2</sub>CH<sub>2</sub>(CH<sub>2</sub>)<sub>2</sub>-)

<sup>13</sup>C NMR (100.4 MHz, CDCl<sub>3</sub>) δ<sub>C</sub> (ppm): 171.7, 165.7, 164.5, 159.8, 152.6, 151.3, 145.3, 143.5, 133.1, 132.6, 131.6, 131.4, 129.9, 129.6, 128.4, 128.3, 127.9, 127.1, 123.8, 122.2, 120.4, 119.2, 115.1, 110.1, 109.8, 91.74, 88.85, 72.61, 72.00, 70.92, 70.78, 70.69, 70.65, 69.89, 69.70, 69.07, 68.00, 67.06, 64.55, 59.13, 44.77, 35.15, 29.21, 28.64, 25.83

MALDI-TOF MS: m/z = 2018.0 (M + Na)<sup>+</sup>

IR (cm<sup>-1</sup>): 3071, 2932, 2870, 2222, 1728, 1605, 1497, 1466, 1427, 1335, 1250, 1180, 1103, 1034, 964, 856, 818, 764, 633, 532

Elemental analysis: calcd (%) for C<sub>114</sub>H<sub>135</sub>N<sub>3</sub>O<sub>28</sub>: C 68.62, H 6.82, N 2.11; found: C 68.53, H 6.89, N 1.94

# **Chapter 8**

# **Hexaphenylbenzenes**

## 8.1 Introduction

An alternative synthetic approach to dendritic macromolecules consists of the transformation of a dendritic core to produce a larger assembly. This strategy has been elegantly demonstrated by Fréchet on the convergent synthesis of new benzene-cored dendrimers via the cobalt-catalysed cyclotrimerisation of an alkyne dendritic precursor [44].

The [2+2+2] cycloaddition of alkynes catalysed by noble metals generates a benzene ring [45]. When the alkyne is a disubstituted diphenylacetylene, the cyclotrimerisation affords the hexasubstituted hexaphenylbenzene (HPB) derivative. New self-assembling materials have been designed based on hexaphenylbenzene, one of the smallest rigid star-shaped polyphenylenes, as the dendritic core.

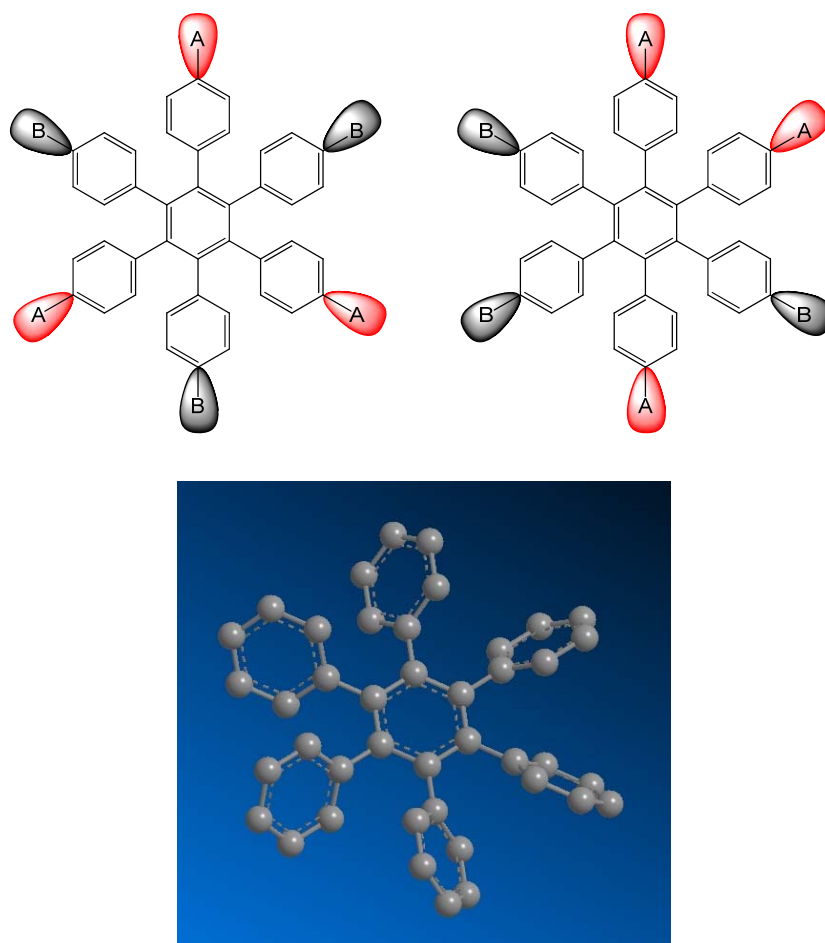


**Figure 8.1** Structure and topology of hexaphenylbenzene molecule

In the most stable conformation of the HPB molecule, the six phenyl rings on the periphery are twisted out of the plane of the central benzene ring, caused by the steric congestion (Fig 8.1 bottom). Although the disc-like shape of the entire molecule is appealing, it doesn't have the ideal planar conformation and it doesn't have aromatic conjugation, but it can still be used as the rigid core of a dendritic material.

In this chapter, several symmetric and asymmetric dendritic supermolecular LCs based on hexaphenylbenzene are presented together with their physical properties and mesophase behaviour. They are synthesised by the cobalt-catalysed cyclotrimerisation of the diphenylacetylene LC oligomers materials presented in previous chapters.

## 8.2 Synthesis

The [2+2+2] cycloaddition of alkynes catalysed by cobalt complexes yields the corresponding benzene derivatives. Hexaphenylbenzene derivatives can be obtained from a variety of diphenylacetylene derivatives since this reaction exhibits a high degree of chemoselectivity towards carbon-carbon triple bonds, rendering the reaction tolerant to many functional groups [45].

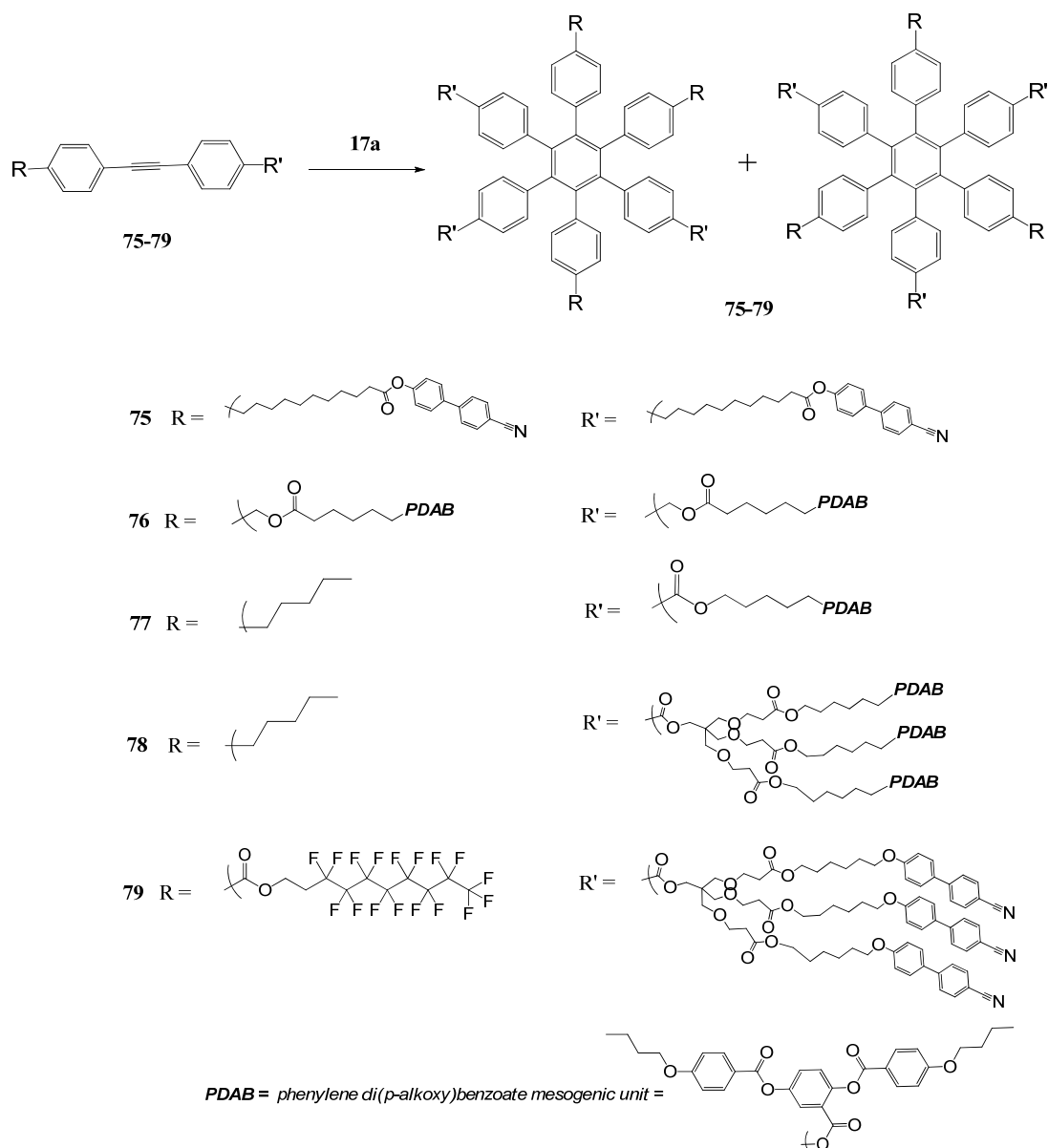
When the diphenylacetylene is substituted with dendrons, the reaction affords the corresponding hexaphenylbenzene surrounded by six dendrons on the peripheral phenyl rings in a convergent fashion. This strategy is not only expeditious but, more importantly, overcomes the very serious problem of incomplete functionalization of a multifunctional core, mainly when bulky dendrons are meant to be attached to the core by a divergent methodology. Thus, six dendrons can be placed in *one reaction* on the periphery of the core without any possibility of having either penta-, tetra- ... etc substitution. This remarkable transformation shows how powerful appropriate design can be in order to circumvent the issue of partial substitution in dendrimers.

Additionally, if the starting acetylene is unsymmetrical, two possible isomers are produced in the reaction: the 1,3,5-trisubstituted benzene and the 1,2,4-trisubstituted benzene (Fig. 8.1 top). If an unsymmetrical diphenylacetylene derivative is used, the symmetrical and unsymmetrical hexaphenylbenzenes are produced. More

importantly, when the dissimilar arms of the diphenylacetylene have different self-assembling behaviours, this transformation gives access to two isomers of disc-like hexaphenylbenzene derivatives that have different geometries and therefore different self-assembling directionalities, ultimately affording “*Janus*” discs (Fig. 8.1).

The structure of HPB can be obtained easily from the diphenylacetylenes previously synthesized. The alkynes were cyclotrimerized using  $\text{Co}_2(\text{CO})_8$  as the catalyst with exhaustive exclusion of air at high temperature to yield the hexaphenylbenzene derivatives (Scheme 17). A number of diphenylacetylene derivatives were used, either those containing only one mesogen at either side of the diphenylacetylene or those carrying the dendrons with three mesogens.

The symmetric mesogenic dimmers **32** and **24** were trimerized to give the symmetric HPB molecules **75** and **76**, while the asymmetric diphenylacetylenes **19**, **51** and **53** give the combination of the two isomers which are difficult to separate further.



Reagents and conditions:

17a -  $\text{Co}_2(\text{CO})_8$ , 1,4-dioxane, 125 °C

### Scheme 17

This reaction is very sensitive to oxygen impurities and traces of moisture so the reactions were carried out under argon, air was rigorously excluded from the reaction mixture and rigorously dry dioxane was used. From the mesogenic LC oligomers and the 1:3 type Janus dendrimers, the mesogenic hexaphenyl benzenes (HPBs) can be made by one step trimerization. However, depending on the nature of the starting diphenylacetylene the reaction worked differently. For the LC oligomers the reaction worked much better, while for the dendrimers with more bulky groups there were

always low conversion and a series of by-products were found, and the yield was usually quite low (< 20%). Another problem was the separation of the isomers resulting from the cyclotrimerisation of unsymmetrical starting acetylenes, which have very similar polarities. Considerable time and effort was dedicated to solve the problems of separation, however even after repeated column chromatography the isomers could not be totally resolved, resulting in very substantial loss of material. Given the small scale of the reactions and considering the quite small amount of the isomers mixture handled, it might be wise to give up separating them and instead use the mixture as a whole. Fortunately, the mixture of the isomers also has very interesting physical properties and mesophase behaviour, which is still worthy of study. The detail will be stated in later sections. The  $^1\text{H}$  NMR spectra of the HPB supermolecules are similar to their starting material, since there isn't too much change about the chemical environment of most of the protons. The major difference comes from the protons on the diphenylacetylene core, which involves most of the process of alkyne trimerization (Fig 8.2). Due to the shielding effect, the protons on the HPB core usually need long relaxation times ( $T_1$ ) and the integration is less than expected, especially for the more bulky substituted HPBs with dendritic structures. Due to the complexity of the  $^1\text{H}$  NMR spectra of the mixture of the 1,3,5- and the 1,2,4- isomers, it is impossible to deduce their relative ratio. This ratio is typically ~30:70% in much simpler systems. Since the isomers have the same molecular weight, they are also indistinguishable in the MALDI-TOF spectra.

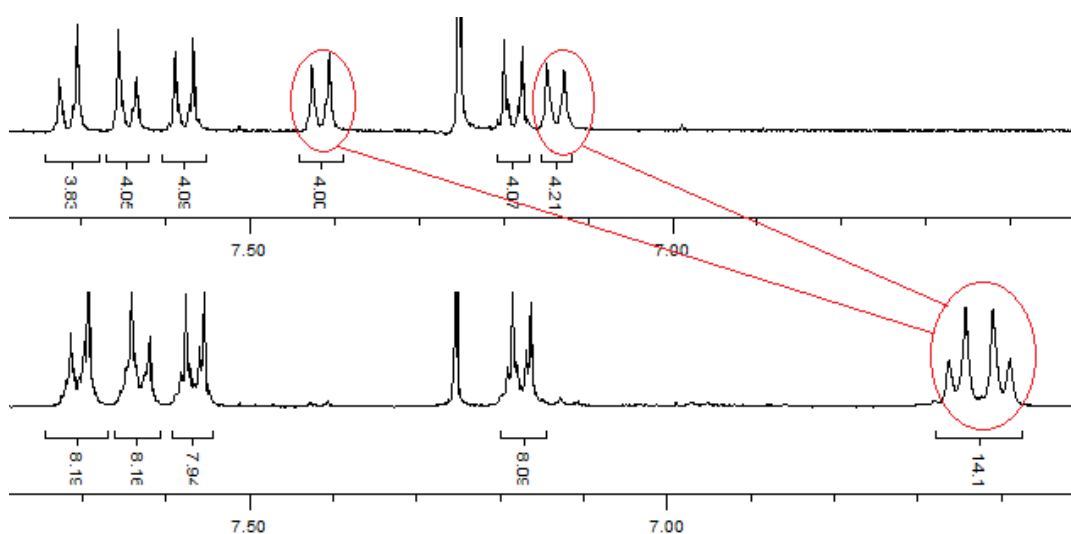


**Figure 8.2** Change of the chemical shift of the protons in the core section (red circle) from dimer **32** (top) to hexamer **75** (bottom)

The materials were also characterized by  $^{13}\text{C}$  NMR, which showed in the simpler cases the formation of the central benzene ring by the disappearance of the resonances of the alkyne carbons at  $\sim 90$  ppm and the appearance of the new benzene carbon resonance in the aromatic region. However, with unsymmetrical alkynes and dendritic alkynes, it is virtually impossible to follow this transformation. The presence of the mixture of two isomers generated by the unsymmetrical alkynes is not only proven by the  $^1\text{H}$  and  $^{13}\text{C}$  NMR, but also by the two close spots on the TLC, although further separation is impractical.

MALDI-TOF MS was the most useful technique for the characterization of these materials; it showed the presence of the hexamers without any residual acetylene, and was useful to ascertain that all the mesogenic arms were intact after the reaction, with no sign of cleavage of the mesogenic arms from the core during the cyclotrimerisation. The MALDI-TOF MS spectrum for material **75** and **79** is shown in Fig 8.3, demonstrating the formation of the intact supermolecular LCs.

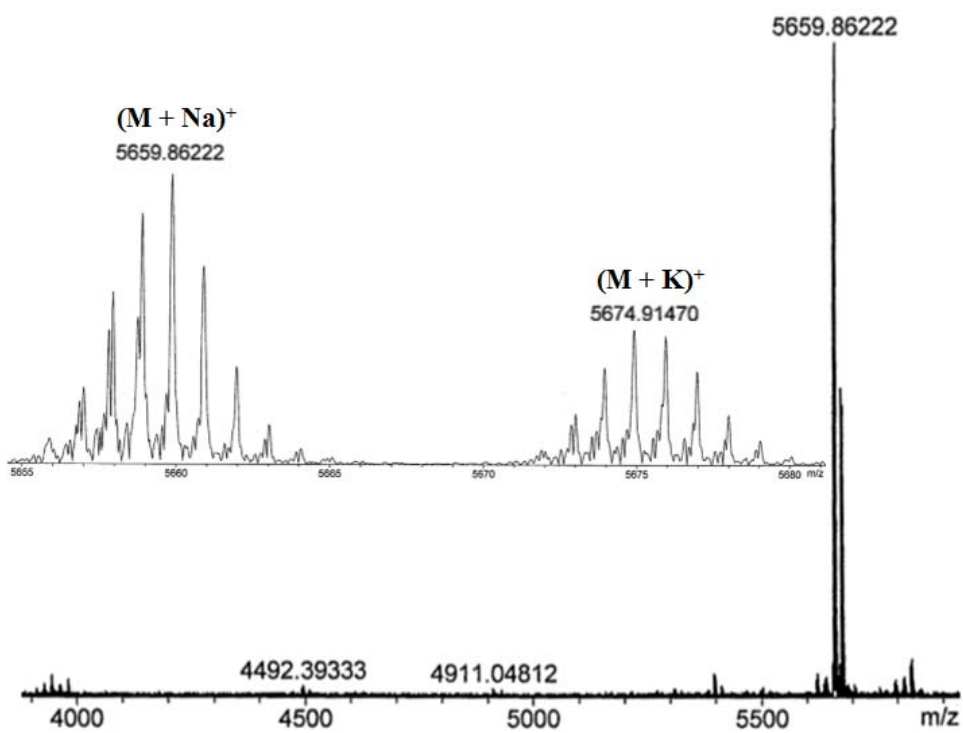
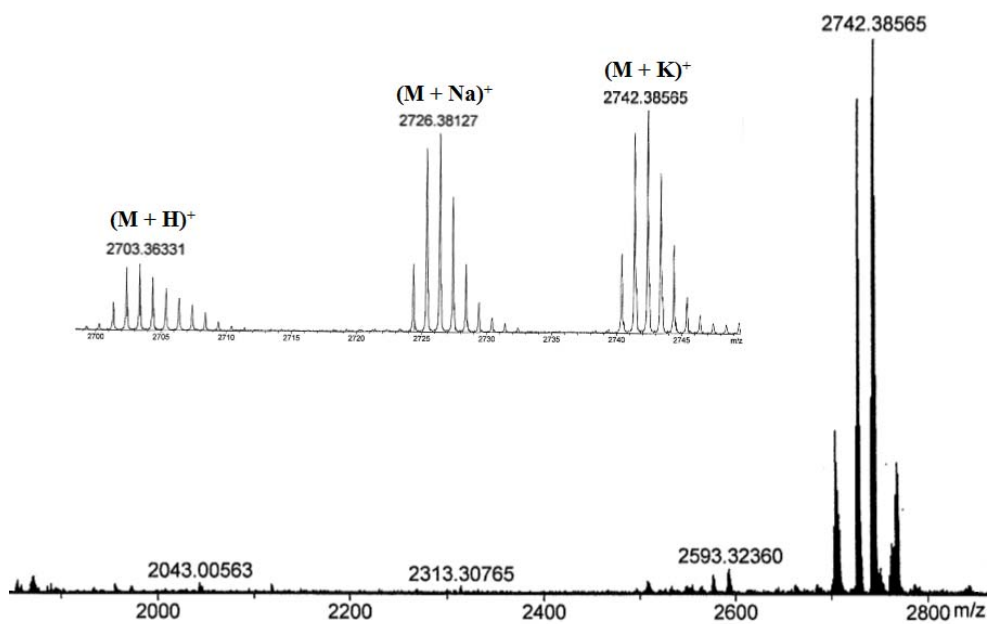


**Figure 8.3** MALDI-TOF MS of compound **75** (top) and **79** (bottom)

### 8.3 Mesomorphic properties

The substituted hexaphenyl benzenes were examined by DSC and POM. The transition temperatures and associated enthalpies are collected in Table 8.

No	g	Cr	Col	SmA	N	Iso
75	-	• 142.1 [89.6]	-	• 159.3 [4.3]	-	•
76	• 27.0	-	-	-	• 68.7 [5.2]	•
77	• 28.5	-	-	-	-	•
78	• 20.0	-	-	-	• 49.8 [3.7]	•
79	• 11.9	-	• 43.7 [19.9]	•	-	•

**Table 8** Transition temperatures ( $T/^{\circ}\text{C}$ ) and associated enthalpies ( $[\Delta H/\text{KJmol}^{-1}]$ ) of the hexaphenylbenzene derivatives (HPBs)

Polarized light optical microscopy was used to observe the LC phase behaviour of the substituted HPBs. As before, the materials needed long periods of annealing in order to obtain well developed textures. All the photomicrographs presented are with x100 or x200 magnification.

The typical focal-conic fan texture of smectic A phase was exhibited by compound **73**. The relatively large and well formed fans indicate the strong tendency of a lamellar phase assembling. The hyperbola/ellipse pairs and the parallel black lines on the fans all proved the formation of Dupin cyclides as well as the SmA phase.

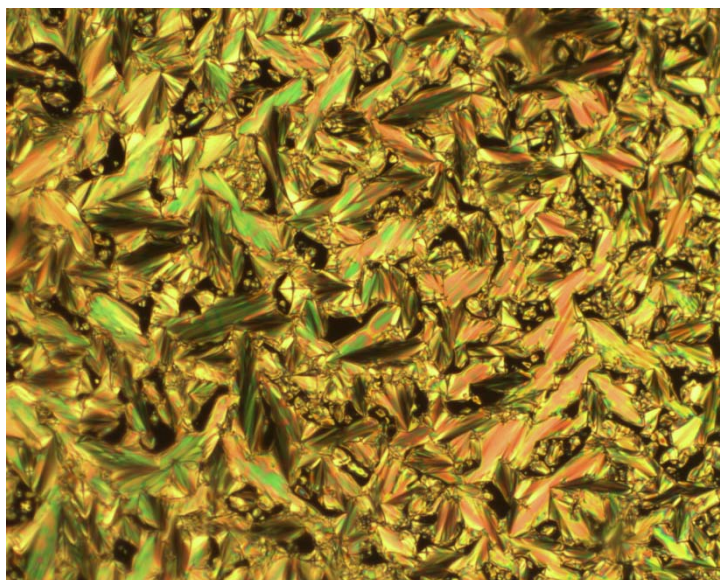
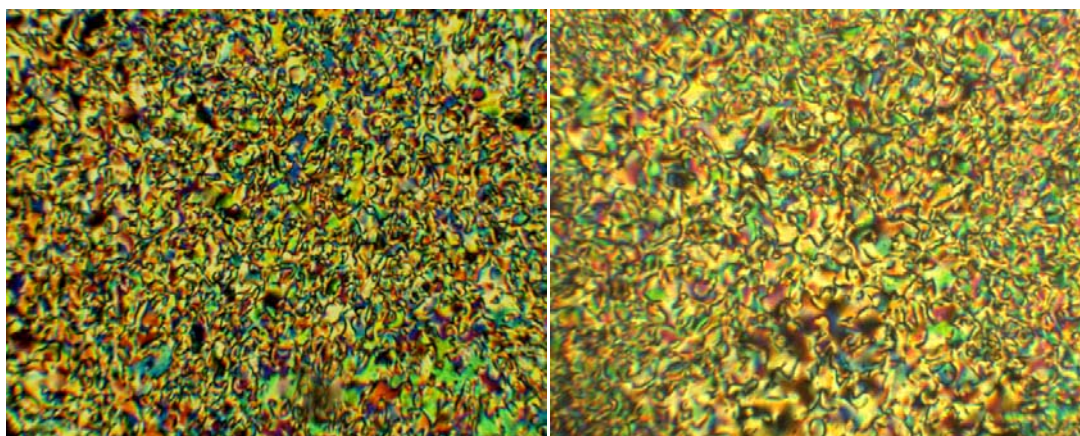


**Plate 21** Focal-conic fan texture of **73**, 135 °C (x100)

Random black curves and the countless 4- and 2- brushes disclinations are all present in the textures of the nematic phase for compounds **74** and **77**. There are also small black areas which imply the homeotropic alignment of the molecules (Plate 22).



(a)

(b)

**Plate 22** Schlieren texture of (a) **74**, 72 °C; (b) **77**, 48 °C (x200)

The spine-like texture of **79** formed very slowly. This might be caused by the slow intermixing process of the two isomers. The bright and dark sections on the batonnets as well as the black homeotropic regions allow identification of it as a Col<sub>hex</sub> phase (Plate 23).

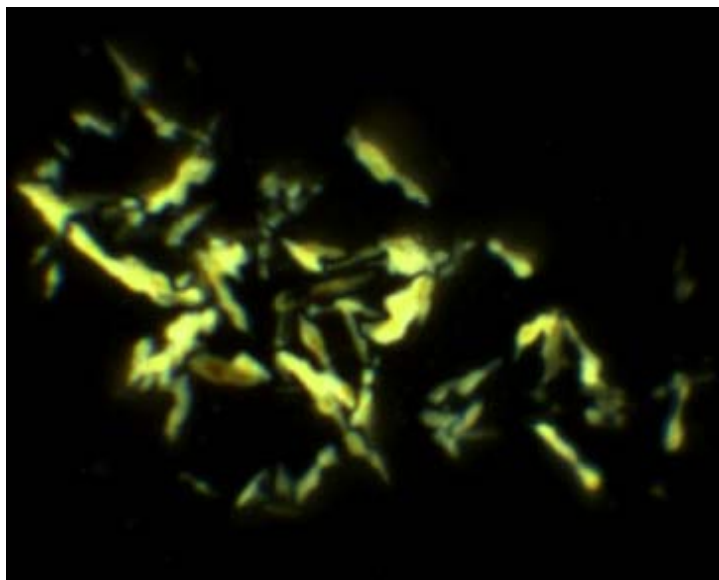


**Plate 23** Spine-like texture of **79**, 54 °C (x200)

#### 8.4 Discussion

It is clear that the HPBs that have a single mesogen in each arm do not present a columnar phase. This might be caused by the twist of the peripheral phenyl rings of the core which produced a propeller-like topology of the core rather than a flat disc, thus precluding the stacking of the disc-like cores needed to form a columnar arrangement. These materials might be also viewed as a mixed rod-disc system, similar to those reported in the literature; however, six rods might be able to overcome the discotic tendency resulting in a calamitic-type phase rather than a columnar arrangement [16] (see section 1.3.4). Secondly, at least for some of the HPBs with dendritic branches, such as **78**, the HPB core is relatively small compared with the peripheral part of the molecule.

Compound **75** has a symmetric structure of six cyanobiphenyl groups linked to the HPB core by long hydrocarbon chain spacers. A smectic A phase with high

isotropisation temperature was observed, indicating the stability of the lamellar assembling. It is tentatively proposed that the HPB group is placed in the middle and the cyanobiphenyl groups are separated into opposite sides of the core, forming a bilayer of the mesogenic units, in effect segregating the rod-like mesogens from the disc-like core (Fig 8.4). In comparison with the dumbbell-shaped hexamer **58**, which also has six cyanobiphenyl end-on mesogenic units and only exhibits a nematic phase, compound **75** has a structure more conducive to lamellar arrangement. This might due to the combination of a number of factors. The high incompatibility between the cyanobiphenyl mesogenic groups and the HPB core may play a part. The fact that hexa-substituted HPB molecule **75** also has a flatter topology compared to the dumbbell conformation of compound **58**, which produces less free space and better packing, and the presence of a long alkyl spacer.

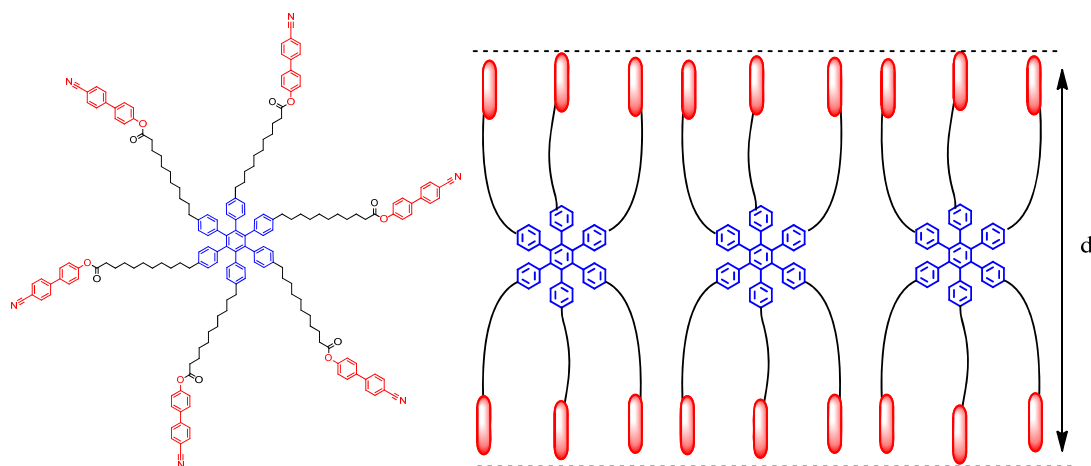


**Figure 8.4** The tentatively proposed molecular arrangement in the smectic layered packing of compound **75**

Similar to most of the compounds with the PDAB side-on mesogenic units, compound **76** also exhibits a nematic phase with wide temperature range. Due to the lateral attachment of the mesogenic units, the microphase segregation such as for compound **75** is unlikely to happen. In the nematic phase of **76**, the side-on mesogenic groups are aligned roughly perpendicular to the plane of the HPB core (since the spacer is relatively short), allowing the parallel orientation of all the mesogenic groups without short range correlation of the HPB cores (Fig 8.5).

However, it must be emphasised again that this is only a tentative explanation which requires further investigation. The relatively high enthalpy of the N-I transition indicated an ordered alignment in the nematic phase induced by the six periphery mesogenic units. Unlike compound **76**, the substituted HPB **77** with only three laterally attached mesogenic units is not mesomorphic at all. Obviously, for such a broadened system which is neither actually rod-like nor disc-like, three mesogenic units are not enough for inducing an ordered liquid crystal phase.

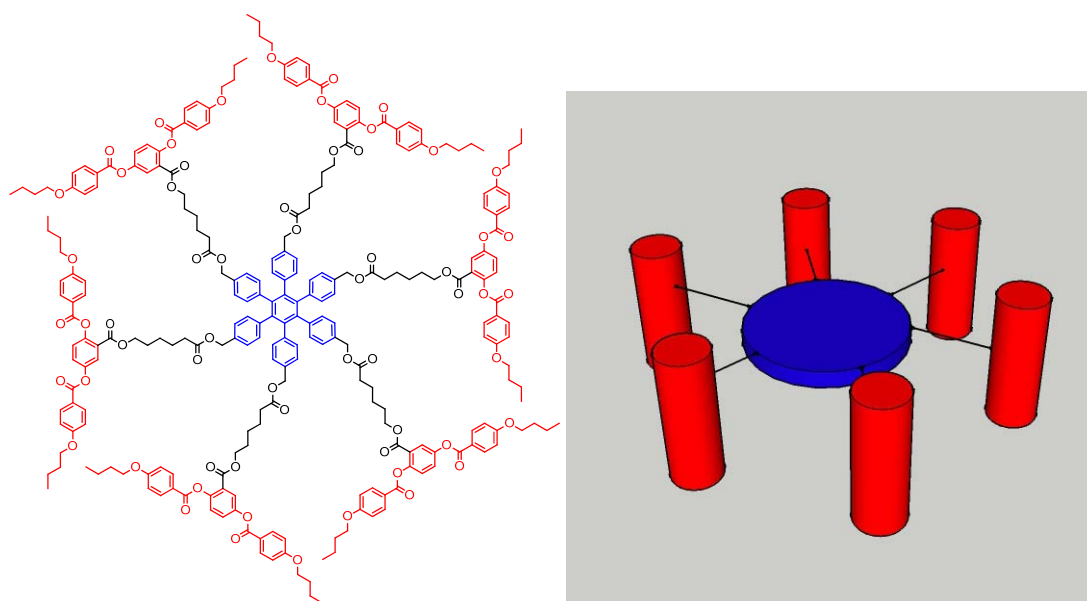


**Figure 8.5** The postulated molecular topology of **76**, showing the perpendicular position of the core and the mesogenic units in **76**

By trimerization of the 1:3 type Janus dendrimer **54**, the substituted HPB **78** was obtained in the form of a mixture of two 1,3,5- and 1,2,4- isomers (Fig 8.6 top). An enantiotropic nematic phase at room temperature was still observed, indicated the miscibility of the two steric isomers. Similar to **76**, the HPB **78** with dendritic branches has nine laterally attached PDAB mesogenic units on the periphery of the macromolecule; however, due to the tetrahedral topology of the PE dendritic scaffold, the side-on mesogenic units are unlikely to be aligned perpendicular to the plain of the HPB core (Fig 8.6 bottom). Compared to the dendrimers with three laterally attached mesogenic units, the nematic phase stability of **78** is a little bit

lower, however the enthalpy of N-I transition is higher, indicating a more ordered mesophase due to the more regular alignment of the macromolecules within the liquid crystal phase.

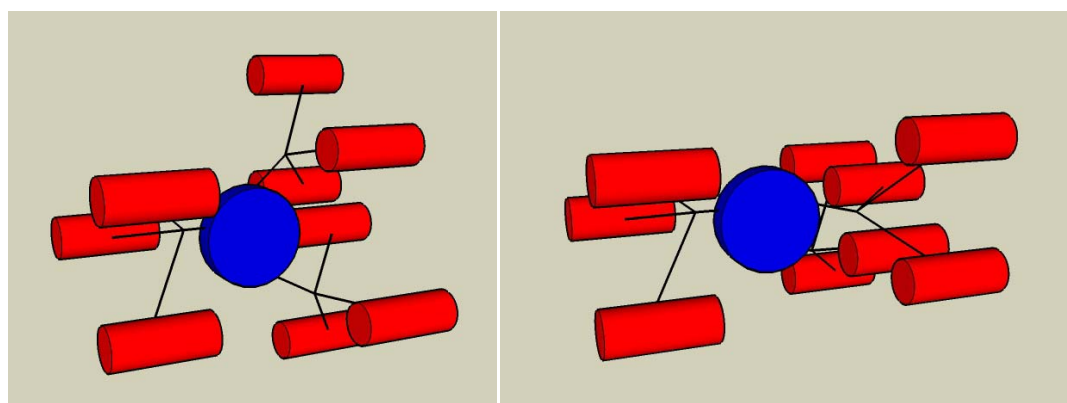
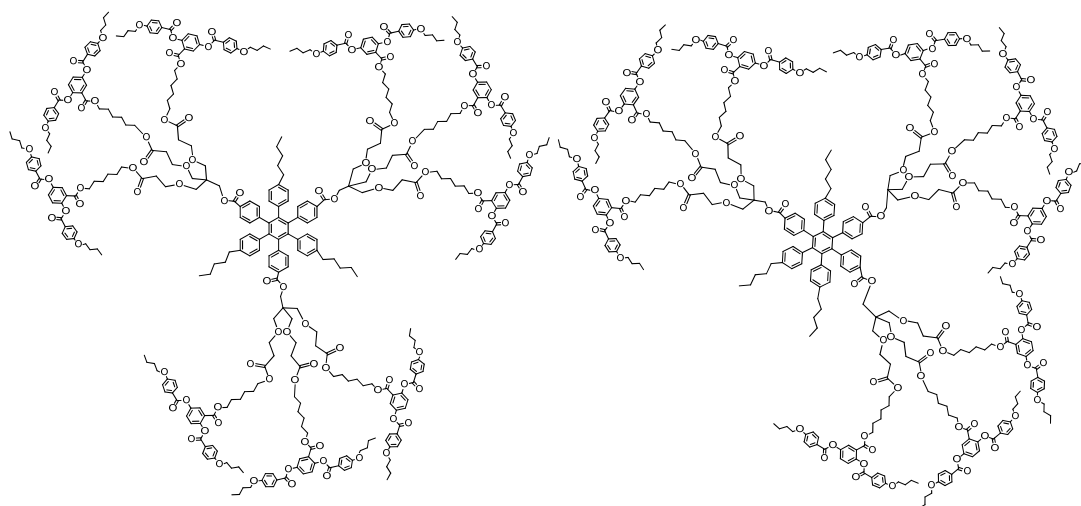


**Figure 8.6** The molecular structure of the isomers of **78** (top) and the cartoons showing the parallel position of the core and the mesogenic units (bottom) of the two isomers of **78** (left, 1,3,5-substituted; right, 1,2,4-substituted)

Another mixture of HPB isomers **79** was made from the trimerization of the 1:3 type Janus compound **53** (1R<sub>F</sub>:3CB) which has three cyanobiphenyl groups and one perfluorinated chain. A hexagonal columnar phase was observed at room temperature. Compared to the symmetric HPB **75** with six cyanobiphenyl groups that

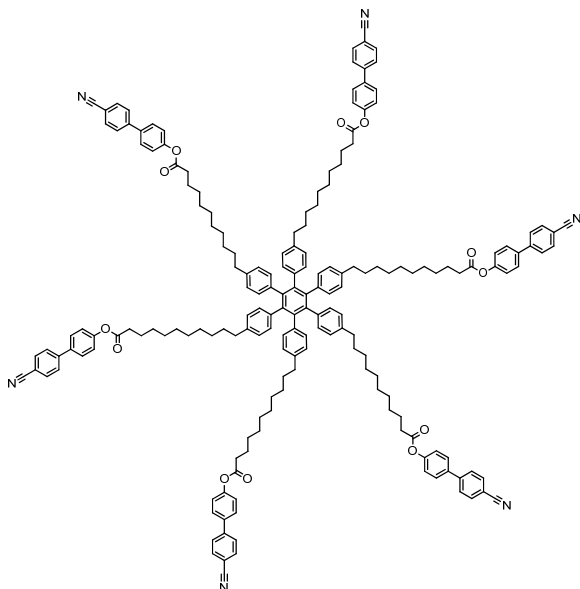
exhibits a stable SmA phase, there are more mesogenic units at the periphery for the supermolecule **79**, increasing the molecular interfacial curvature. The increased density of mesogens makes for better space filling around the core. Regarding the fluorinated chains, they are bulky and stiff, aiding also the effective space filling around the HPB core; additionally they impose considerable microphase segregation from the cyanobiphenyl mesogens and from the HPB core. All these factors put together point to the formation of disc-like units that can pack in a columnar arrangement. However, the exact way in which the cyanobiphenyl mesogenic units may segregate from the fluorinated chains to form the mesophase and the mesophase structure can only be determined by X-Ray diffraction, therefore any model proposed here would be purely speculative.

### 8.5 Concluding remarks

The alkyne trimerization of the diphenylacetylene-based LC oligomers and dendrimers afforded five new supermolecular hexaphenyl benzene (HPB) derivatives. However the trimerization of the unsymmetrical mesogens yielded a mixture of isomers which is hard to separate. The mixtures were treated as unit in the study of liquid crystal properties. Though the HPB mesogens have a disc-like core, they exhibit the SmA and N phases. Due to the high incompatibility between the cyanobiphenyl mesogenic units and the HPB core, it is tentatively proposed that microsegregation occurs in the cyanobiphenyl-containing HPB supermolecular mesogen, resulting in stable mesophases with positional order (SmA and Col). In the HPB mesogens with side-on PDAB groups, the flexible spacer allowed the PDAB mesogenic units to align with each other to form the nematic phase; however compound **77** with 3 PDAB groups is not mesomorphic, which indicated that a certain number of mesogenic units is required to introduce the orientational order to the supermolecular systems. The HPB supermolecular mesogens offers an elegant route to macromolecular systems to explore the relationship between intramolecular conformation and mesophase behaviour as well as microsegregation in complicated LC systems.

## 8.6 Experimental and chemicals

### 1,2,3,4,5,6-Hexa(4-(10(4,4'-cyanobiphenyloxy)carbonyl)decyl)phenyl)benzene (75)



Bis(4-(10-(4,4'-cyanobiphenyloxy)carbonyl)decyl)phenyl)acetylene (**32**) (0.1 g; 0.11 mmol) was dissolved in 1,4-dioxane (5 mL). Argon was purged into the solution for 15 mins and dicobalt octacarbonyl (5 mg; 0.015 mmol) was added. The mixture was stirred for 20 h at 125 °C under Argon. After cooling and removal of the solvent, the product was obtained from the residue by column chromatography using 1:10 ethyl acetate/dichloromethane, and then recrystallised from ethanol to give **73** as a white solid.

Yield: 82 mg (82%)

$^1\text{H}$  NMR (400 MHz,  $\text{CDCl}_3$ )  $\delta_{\text{H}}$  (ppm): 7.71 (d ( $J = 8.5$  Hz), 12 H, ArH); 7.64 (d ( $J = 8.6$  Hz), 12 H, ArH); 7.57 (d ( $J = 8.7$  Hz), 12 H, ArH); 7.18 (d ( $J = 8.6$  Hz), 12 H, ArH); 6.63 (d ( $J = 21.3$  Hz) d ( $J = 8.1$  Hz), 24 H, ArH); 2.57 (t ( $J = 7.5$  Hz), 12 H,  $-\text{C}_6\text{H}_4\text{CH}_2$ ); 2.33 (t ( $J = 7.4$  Hz), 12 H,  $-\text{CH}_2\text{COO}-$ ); 1.75 (m, 12 H,  $-\text{CH}_2\text{CH}_2\text{COO}-$ ); 1.33 (m, 72 H,  $-\text{C}_6\text{H}_4\text{CH}_2(\text{CH}_2)_3-$ ,  $-(\text{CH}_2)_3\text{CH}_2\text{COO}-$ ); 1.11 (m, 12 H,  $-\text{C}_6\text{H}_4\text{CH}_2(\text{CH}_2)_3\text{CH}_2-$ )

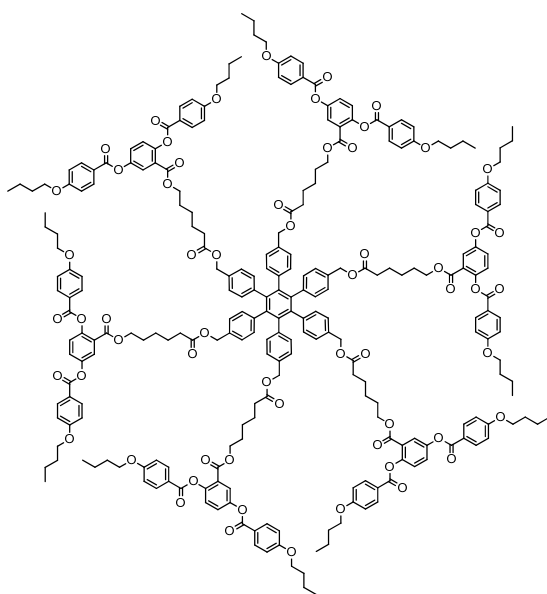
$^{13}\text{C}$  NMR (100.4 MHz,  $\text{CDCl}_3$ )  $\delta_{\text{C}}$  (ppm): 172.3, 151.3, 144.8, 140.4, 139.1, 138.4, 136.8, 132.7, 131.5, 128.4, 127.7, 126.5, 122.4, 118.9, 111.1, 35.43, 34.48, 31.32, 29.73, 29.66, 29.0, 29.42, 29.25, 28.98, 25.02

MALDI-TOF MS:  $m/z = 2724.4 (M + Na)^+$

IR ( $\text{cm}^{-1}$ ): 3048, 2916, 2847, 2222, 1736, 1697, 1605, 1489, 1466, 1412, 1389, 1242, 1204, 1165, 1134, 1003, 918, 826, 725, 563, 532

Elemental analysis: calcd (%) for  $\text{C}_{186}\text{H}_{192}\text{N}_6\text{O}_{12}$ : C 82.63, H 7.16, N 3.11; found: C 82.44, H 7.35, N 2.84

**1,2,3,4,5,6-Hexa(4-(6-(2,5-di(4-butoxybenzoyloxy)benzoyloxy)hexylcarbonyloxy)methyl)phenyl)benzene (76)**



4,4'-(1,2-Ethynediyl)benzyl bis(6-(2,5-Di(4-butoxybenzoyloxy)benzoyloxy)hexan)ate (**24**) (0.1 g; 0.07 mmol) was dissolved in 1,4-dioxane (10 mL), and argon was purged into the solution for 15 mins and dicobalt octacarbonyl (3 mg; 0.01 mmol) was added. The mixture was stirred for 20 h at 125 °C under Argon. After cooling and removal of the solvent, the product was isolated from the residue by column chromatography, eluting with 1:5 ethyl acetate/dichloromethane, and then recrystallised from ethanol to yield **74** as a white crystal.

Yield: 70 mg (70%)

$^1\text{H}$  NMR (400 MHz,  $\text{CDCl}_3$ )  $\delta_{\text{H}}$  (ppm): 8.12 (d ( $J = 8.9$  Hz), 24 H, *ArH*); 7.86 (d ( $J = 2.9$  Hz), 6 H, *ArHc*); 7.43 (d ( $J = 8.8$  Hz) d ( $J = 2.9$  Hz), 6 H, *ArHb*); 7.24 (d ( $J = 8.7$  Hz), 6 H, *ArHa*); 6.94 (d ( $J = 11.6$  Hz) d ( $J = 8.9$  Hz), 24 H, *ArH*); 6.75 (s, 24 H,

ArH); 4.80 (s, 12 H,  $-\text{COOCH}_2\text{C}_6\text{H}_4-$ ); 4.11 (t (J = 6.8 Hz), 12 H,  $-\text{COOCH}_2\text{CH}_2-$ ); 4.02 (m, 24 H,  $-\text{C}_6\text{H}_4\text{OCH}_2-$ ); 2.16 (t (J = 7.5 Hz), 12 H,  $-\text{CH}_2\text{COO}-$ ); 1.78 (m, 24 H,  $-\text{C}_6\text{H}_4\text{OCH}_2\text{CH}_2-$ ); 1.47 (m, 48 H,  $-\text{C}_6\text{H}_4\text{OCH}_2\text{CH}_2\text{CH}_2-$ ,  $-\text{COOCH}_2\text{CH}_2\text{CH}_2\text{CH}_2\text{CH}_2\text{COO}-$ ); 1.23 (m, 12 H,  $-\text{CH}_2\text{CH}_2\text{CH}_2\text{CH}_2\text{CH}_2-$ ); 0.98 (m, 36 H,  $-\text{CH}_3$ )

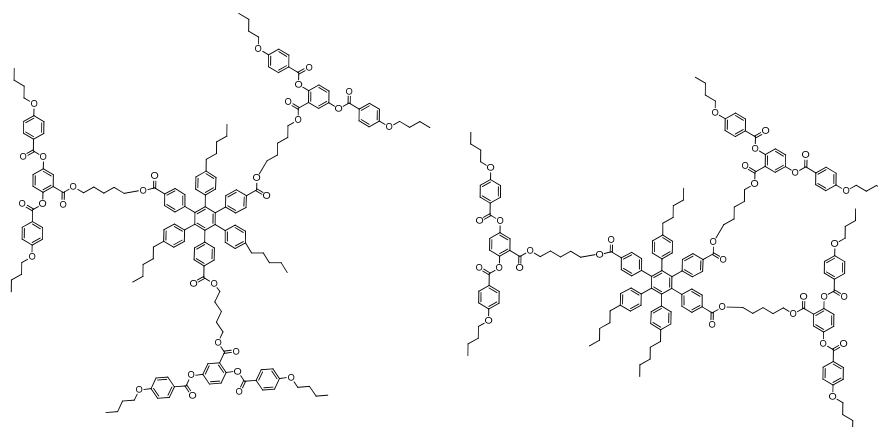
$^{13}\text{C}$  NMR (100.4 MHz,  $\text{CDCl}_3$ )  $\delta_{\text{C}}$  (ppm): 173.1, 165.0, 164.7, 164.1, 163.8, 163.7, 148.4, 148.2, 140.1, 140.1, 133.1, 132.5, 132.5, 131.4, 127.2, 126.1, 125.1, 125.1, 124.9, 121.4, 121.1, 114.5, 68.12, 68.06, 65.63, 65.32, 33.95, 31.20, 28.18, 25.42, 24.47, 19.28, 13.94

MALDI-TOF MS:  $m/z = 4350.7$  ( $\text{M} + \text{Na}$ ) $^+$

IR ( $\text{cm}^{-1}$ ): 3078, 2955, 2870, 1728, 1605, 1512, 1466, 1420, 1381, 1242, 1157, 1057, 964, 910, 841, 764, 733, 694, 640, 548

Elemental analysis: calcd (%) for  $\text{C}_{258}\text{H}_{270}\text{O}_{60}$ : C 71.55, H 6.28; found: C 71.25, H 6.41

**1,3,5-Tris(4-pentylphenyl)-2,4,6-tris(4-(6-(2,5-di(4-butoxybenzoyloxy)benzoyloxy)hexylcarbonyloxymethyl)phenyl)benzene and 1,2,4-Tris(4-pentylphenyl)-3,5,6-tris(4-(6-(2,5-di(4-butoxybenzoyloxy)benzoyloxy)hexylcarbonyloxymethyl)phenyl)benzene (77)**



Asymmetric monomer **19** (0.1 g; 0.12 mmol) was dissolved in 1,4-dioxane (5 mL), and argon was purged into the solution for 15 mins and dicobalt octacarbonyl (4 mg; 0.012 mmol) was added. The mixture was stirred for 24 h at 125 °C under Argon.

After cooling and removal of the solvent, the product was isolated from the residue by column chromatography, eluting with 1:3 ethyl acetate/petroleum ether, and then recrystallised from ethanol to yield **75** as a yellow crystal.

Yield: 53 mg (53%)

$^1\text{H}$  NMR (400 MHz,  $\text{CDCl}_3$ )  $\delta_{\text{H}}$  (ppm): 8.13 (m, 12 H, ArH); 7.88 (t (J = 2.6 Hz), 3 H, ArH); 7.51 (m, 6 H, ArH); 7.46 (d (J = 8.7 Hz) t (J = 3.0 Hz), 3 H, ArH); 7.25 (d (J = 8.7 Hz) d (J = 1.4 Hz), 3 H, ArH); 6.98 (d (J = 9.0 Hz) d (J = 2.3 Hz), 6 H, ArH); 6.91 (m, 12 H, ArH); 6.63 (m, 12 H, ArH); 4.15 (m, 6 H,  $-\text{C}_6\text{H}_3\text{COOCH}_2-$ ); 4.04 (m, 18 H,  $-\text{C}_6\text{H}_4\text{COOCH}_2-$ ,  $-\text{C}_6\text{H}_4\text{OCH}_2-$ ); 2.30 (m, 6 H,  $-\text{C}_6\text{H}_4\text{CH}_2-$ ); 1.79 (m, 12 H,  $-\text{C}_6\text{H}_4\text{OCH}_2\text{CH}_2-$ ); 1.51 (m, 24 H,  $-\text{COOCH}_2\text{CH}_2-$ ,  $-\text{C}_6\text{H}_4\text{OCH}_2\text{CH}_2\text{CH}_2-$ ); 1.34 (m, 12 H,  $-\text{C}_6\text{H}_4\text{CH}_2(\text{CH}_2)_2-$ ); 1.18 (m, 6 H,  $-\text{COOCH}_2\text{CH}_2\text{CH}_2-$ ); 1.02 (m, 24 H,  $-\text{O}(\text{CH}_2)_3\text{CH}_3$ ,  $-\text{C}_6\text{H}_4(\text{CH}_2)_3\text{CH}_2-$ ); 0.78 (m, 9 H,  $-\text{C}_6\text{H}_4(\text{CH}_2)_4\text{CH}_3$ )

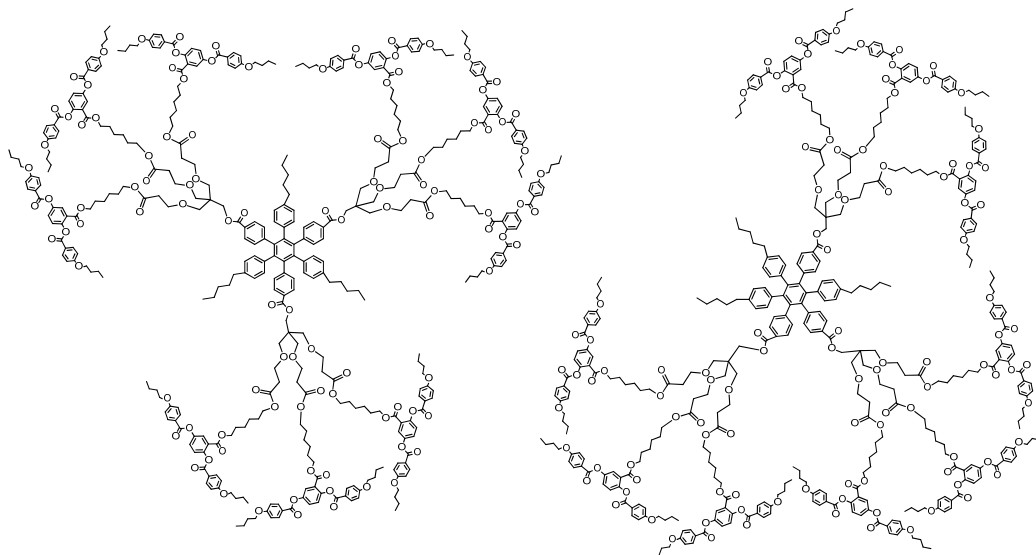
$^{13}\text{C}$  NMR (100.4 MHz,  $\text{CDCl}_3$ )  $\delta_{\text{C}}$  (ppm): 166.7, 166.5, 165.0, 164.7, 164.2, 163.8, 163.7, 148.4, 148.1, 145.9, 145.8, 145.7, 141.1, 140.6, 140.2, 140.0, 139.9, 139.8, 139.6, 139.2, 137.1, 137.0, 136.9, 132.5, 131.5, 131.4, 131.1, 131.0, 128.2, 128.0, 127.3, 127.2, 127.0, 127.0, 125.1, 125.0, 121.4, 121.1, 114.5, 114.4, 68.13, 68.01, 65.35, 64.59, 64.53, 35.26, 35.15, 31.21, 30.99, 30.86, 30.70, 30.47, 29.80, 28.34, 28.21, 22.55, 22.47, 22.40, 19.29, 14.11, 14.08, 13.93

MALDI-TOF MS:  $m/z = 2622.2$  (M + Na) $^+$

IR ( $\text{cm}^{-1}$ ): 3024, 2940, 2870, 1751, 1605, 1512, 1427, 1358, 1227, 1157, 1057, 1011, 972, 849, 756, 694, 571, 525

Elemental analysis: calcd (%) for  $\text{C}_{162}\text{H}_{174}\text{O}_{30}$ : C 74.75, H 6.70; found: C 74.61, H 6.88

**1,3,5-Tris(4-pentylphenyl)-2,4,6-tris(4-(2,2,2-tris(3-(6-(2,5-di(4-butoxybenzoyloxy)benzoyloxy)hexyloxy)-3-oxopropyl)oxymethyl)ethoxy)carbonyl)phenyl)benzene and 1,2,4-Tris(4-pentylphenyl)-3,5,6-tris(4-(2,2,2-tris(3-(6-(2,5-di(4-butoxybenzoyloxy)benzoyloxy)hexyloxy)-3-oxopropyl)oxymethyl)ethoxy)carbonyl)phenyl)benzene (78)**



Asymmetric 1:3 Janus LC monomer **51** (0.1 g; 0.04 mmol) was dissolved in 1,4-dioxane (5 mL), and argon was purged into the solution for 15 min and dicobalt octacarbonyl (2 mg; 0.006 mmol) was added in. The mixture was stirred for 30 h at 125 °C under Argon. After cooling and removal of the solvent, the product was purified by column chromatography, eluting with 1:1.2 ethyl acetate/hexane and then recrystallised from dichloromethane/ethanol to yield **77** as a white sticky solid.

Yield: 24 mg (24%)

$^1\text{H}$  NMR (400 MHz,  $\text{CDCl}_3$ )  $\delta_{\text{H}}$  (ppm): 8.13 (m, 36 H, ArH); 7.87 (m, 9 H, ArH); 7.45 (m, 15 H, ArH); 7.24 (m, 9 H, ArH); 6.96 (m, 36 H, ArH); 6.89 (m, 6 H, ArH); 6.63 (m, 12 H, ArH); 4.21 (m, 24 H,  $-\text{C}_6\text{H}_4\text{COOCH}_2-$ ,  $-\text{CH}_2\text{COO}(\text{CH}_2)_5\text{CH}_2\text{OCO}-$ ); 4.03 (m, 36 H,  $-\text{C}_6\text{H}_4\text{OCH}_2-$ ); 3.97 (m, 18 H,  $-\text{CH}_2\text{COOCH}_2-$ ); 3.61 (m, 18 H,  $-\text{C}(\text{CH}_2\text{OCH}_2)_3$ ); 3.40 (m, 18 H,  $-\text{C}(\text{CH}_2\text{O})_3$ ); 2.48 (m, 18 H,  $-\text{C}_6\text{H}_4\text{CH}_2-$ ); 2.32 (m, 6 H,  $-\text{C}_6\text{H}_4\text{CH}_2-$ ); 1.79 (m, 36 H,  $-\text{C}_6\text{H}_4\text{OCH}_2\text{CH}_2-$ ); 1.50 (m, 72 H,  $-\text{C}_6\text{H}_4\text{OCH}_2\text{CH}_2\text{CH}_2-$ ,  $-\text{CH}_2\text{COOCH}_2\text{CH}_2\text{CH}_2\text{CH}_2\text{CH}_2\text{CH}_2\text{OCO}-$ ); 1.25 (m, 54 H,  $-\text{CH}_2\text{COOCH}_2\text{CH}_2(\text{CH}_2)_2-$ ,  $-\text{C}_6\text{H}_4\text{CH}_2\text{CH}_2(\text{CH}_2)_3-$ ); 1.01 (m, 54 H,  $-\text{O}(\text{CH}_2)_3\text{CH}_3$ ); 0.87 (m, 9 H,  $-\text{C}_6\text{H}_4(\text{CH}_2)_4\text{CH}_3$ )

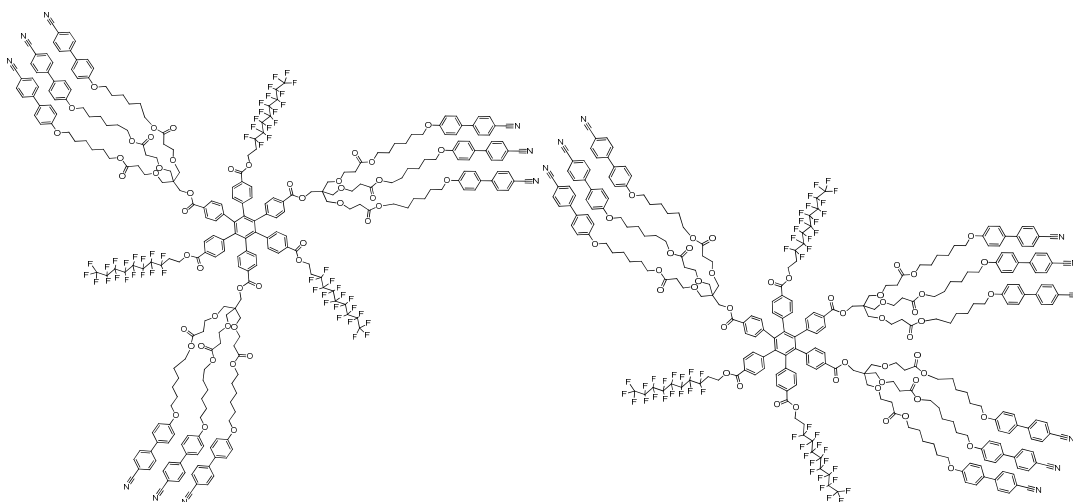
$^{13}\text{C}$  NMR (100.4 MHz,  $\text{CDCl}_3$ )  $\delta_{\text{C}}$  (ppm): 171.5, 165.0, 164.7, 164.1, 163.8, 163.7, 148.4, 148.2, 132.5, 132.5, 127.2, 125.1, 125.0, 125.0, 121.5, 121.1, 114.5, 114.4, 68.11, 68.08, 66.90, 65.47, 64.45, 34.96, 31.20, 28.50, 28.39, 25.59, 19.27, 13.92

MALDI-TOF MS:  $m/z = 7197.3$  ( $\text{M} + \text{Na}$ ) $^+$

IR ( $\text{cm}^{-1}$ ): 3071, 2932, 2870, 1728, 1605, 1512, 1466, 1420, 1366, 1242, 1211, 1157, 1119, 1057, 1003, 972, 910, 880, 849, 756, 694, 640, 548

Elemental analysis: calcd (%) for  $\text{C}_{417}\text{H}_{486}\text{O}_{105}$ : C 69.77, H, 6.82; found C 69.52, H 6.79

**1,3,5-Tris(4-(3,3,4,4,5,5,6,6,7,7,8,8,9,9,10,10,10-heptafluorodecyloxy-carbonyl)phenyl)-2,4,6-tris(4-(2,2,2-tris(3-(6-(4'-cyanobiphenyl-4-yloxy)-hexyloxy)-3-oxopropyl)oxy)methyl)ethyloxycarbonyl)phenyl)benzene and 1,2,4-Tris(4-(3,3,4,4,5,5,6,6,7,7,8,8,9,9,10,10,10-heptafluorodecyloxy-carbonyl)-phenyl)-3,5,6-tris(4-(2,2,2-tris(3-(6-(4'-cyanobiphenyl-4-yloxy)hexyloxy)-3-oxopropyl)oxy)methyl)ethyloxycarbonyl)phenyl)benzene (79)**



Asymmetric 1:3 Janus LC monomer **19** (80 mg; 0.04 mmol) was dissolved in 1,4-dioxane (5 mL), and argon was purged into the solution for 15 mins and dicobalt octacarbonyl (2 mg; 0.006 mmol) was added in. The mixture was stirred for 30 h at 125 °C under Argon. After cooling and removal of the solvent, the product was purified by column chromatography, eluting with 1:1.1 ethyl acetate/petroleum ether,

and then recrystallised from dichloromethane/ethanol to yield **78** as a yellow sticky solid.

Yield: 15 mg (19%)

$^1\text{H}$  NMR (400 MHz,  $\text{CDCl}_3$ )  $\delta_{\text{H}}$  (ppm): 7.67 (m, 18 H, ArH); 7.61 (m, 18 H, ArH); 7.56 (m, 12 H, ArH); 7.50 (m, 12 H, ArH); 6.96 (m, 18 H, ArH); 6.90 (m, 12 H, ArH); 4.55 (m, 6 H,  $-\text{CF}_2\text{CH}_2\text{CH}_2-$ ); 4.25 (m, 6 H,  $-\text{CH}_2\text{C}(\text{CH}_2\text{O}-)_3$ ); 4.06 (m, 18 H,  $-\text{C}_6\text{H}_4\text{OCH}_2-$ ); 3.97 (m, 18 H,  $-\text{CH}_2\text{COOCH}_2-$ ); 3.63 (m, 18 H,  $-\text{C}(\text{CH}_2\text{OCH}_2-)_3$ ); 3.43 (m, 18 H,  $-\text{C}(\text{CH}_2\text{O}-)_3$ ); 2.52 (m, 24 H,  $-\text{CH}_2\text{COO}-$ ,  $-\text{CF}_2\text{CH}_2-$ ); 1.77 (m, 18 H,  $-\text{CH}_2\text{CH}_2\text{O}(\text{C}_6\text{H}_4)_2\text{CN}$ ); 1.62 (m, 18 H,  $-\text{CH}_2\text{COOCH}_2\text{CH}_2-$ ); 1.44 (m, 36 H,  $-\text{CH}_2\text{COOCH}_2\text{CH}_2(\text{CH}_2)_2-$ )

$^{13}\text{C}$  NMR (100.4 MHz,  $\text{CDCl}_3$ )  $\delta_{\text{C}}$  (ppm): 171.6, 159.8, 145.3, 145.2, 132.7, 131.4, 128.4, 128.3, 127.1, 119.2, 115.1, 110.2, 69.79, 69.69, 67.98, 66.96, 66.88, 64.96, 64.51, 44.68, 44.55, 35.01, 29.20, 28.63, 25.83

MALDI-TOF MS:  $m/z = 5655.9$  ( $\text{M} + \text{Na}$ ) $^+$

IR ( $\text{cm}^{-1}$ ): 3032, 2940, 2870, 2222, 1736, 1605, 1497, 1466, 1373, 1219, 1180, 1103, 1018, 856, 818, 733, 702, 656, 532

Elemental analysis: calcd (%) for  $\text{C}_{291}\text{H}_{276}\text{N}_9\text{O}_{48}\text{F}_{51}$ : C 62.01, H 4.94, N 2.24; found: C 61.74, H 4.97, N 2.12

# **Chapter 9**

## **Overall**

### **Conclusion**

This project mainly focused on the synthesis and LC properties of the Janus LCs and their relatives. According to the process of building up of the supermolecular LC system, the LC monomers based on PDAB (side-on decorated), LC oligomers (dimers and trimers with a linear connection), dendritic LC multipedes based on PE scaffold, 1:3 and 3:3 type Janus LCs, and a few of advanced HPB LC supermolecules, were separately described.

Eight PDAB monomers with different terminal groups on the side-on aliphatic chain were synthesized from various routes. Designed originally as a good nematogen, most of the PDAB monomeric mesogens exhibit stable nematic phases though there is disorder induced by the side-on chains. The mesomorphic behaviour is influenced by the terminal group and also length of the spacer. A terminal group with high polarity or polarisability can assist the anisotropic conjugated aromatic core thus strengthen the stability of the nematic phase, whereas a longer spacer will induce more disorder to the system and causes a reduction in the phase stability, with a small odd-even effect.

Three LC oligomers were developed via both convergent and divergent synthetic routes. With the side-on PDAB mesogenic units, the T-shaped and H-shaped oligomers present similar mesomorphic behaviour to the monomeric mesogens, which indicated the parallel alignment of the rigid mesogenic cores in the favored conformation. The linear shaped trimer with two end-on CB moieties exhibit a very stable nematic phase due to the accumulated anisotropy of the three mesogenic units. None of the oligomers shows a smectic phase, caused by both the steric effect and the weak microphase segregation in the symmetric trimers.

As building blocks of the Janus LCs, seven dendritic LC multipedes with a PE scaffold were synthesized. The mesomorphic behaviour of a multipede was determined by the three identical peripheral groups attached on PE: the perfluorinated chains can always lead to microphase segregation and form SmA phase; side-on PDAB mesogenic units prefer the nematic phase with no positional order, and the end-on CB groups usually induce a SmA phase with a short range nematic phase, which may be caused by an extended conformation. The different moieties on the fourth arm (iodophenyl/ethylphenyl) do not cause too much difference in the mesophase behaviour. The mesophase inducing abilities of the

mesogenic units (and also the perfluorinated chain) can be observed in the homogeneous LC multipedes as accordance for their interaction in Janus LCs.

Six of 1:3 Type Janus LCs were developed. Compared to the LC multipedes, the fourth arm in 1:3 Type Janus LC is elongated; the newly formed diphenylacetylene core further enhanced the overall LC phase stability, and the chain group attached on to the core can lead to microsegregation with the mesogenic units on the other side of the molecule. The strong microphase segregation in the molecule with one perfluorinated chain and three CB groups presents a hexagonal columnar phase instead of SmA phase; however it still cannot compete with the steric effect caused by the side-on PDAB mesogenic units which prefer nematic phase. On the other hand, one hydrocarbon chain or one TEG chain didn't lead to a better microphase segregation but increased the disorder, resulting in only a nematic phase being formed when combined with end-on or side-on mesogenic units.

All of the three types of chain groups (hydrocarbon, perfluorinated and TEG) and also side-on and end-on mesogenic units were used as peripheral groups of the 3:3 type Janus LCs. A total of ten Janus LCs were synthesized via Sonogashira couplings; for the hydrocarbon and TEG chain, gallic acid was used as the dendritic scaffold instead of PE. The interaction of the phase inducing ability can be observed in the Janus LCs: nematic phase favored side-on PDAB groups totally suppressed the SmA phase lead by CB mesogenic units, but surpassed by the segregation effect of three perfluorinated chains, results in the only Janus LC exhibiting a smectic phase with side-on mesogenic units. Strong segregation effect between three CB groups and three perfluorinated chains generates a series mesophases with positional order, including a cubic phase, unique among all the materials presented. Due to the microsegregation inducing ability, perfluorinated chains can always lead to stable SmA phases. With lower microphase segregation effects, the hydrocarbon and TEG chain cannot lead to stable smectic phases; however the segregation between three hydrocarbon chains and three CB groups still generated a SmA phase, whereas three TEG chains always brought down the mesophase stability, sometimes result in no LC phase at all. It was also found that the SmA phase stability is related to the reduced molar enthalpy per mesogen in these Janus LCs, due to the competition between microphase segregation and steric effect.

Five supermolecular LC hexaphenylbenzenes were prepared, with three, six or nine mesogenic units on the periphery via alkyne trimerization of the diphenylacetylene core. The mesomorphic behaviours in this family are largely dependent on the interactions between the HPB core and the mesogenic units; not only the type, but also the density of mesogenic units, determines the type of mesophase formed. With three side-on PDAB mesogenic units, the HPB is not mesomorphic; however with six and nine PDABs, the nematic phase is found. The HPB with six end-on CB groups exhibit a SmA phase via microsegregation between the discotic core and the calamitic mesogenic units; microphase segregation also occurs in the HPB with nine CBs, however an increased density of peripheral groups results in the formation of a columnar phase instead of smectic phases.

From all of the research above, it can be concluded that the liquid crystal properties of a supermolecular system is mainly controlled by the type and quantity of mesogenic unit, the structure of the central dendritic scaffold, the steric effect and also the microphase segregation effect among incompatible moieties, which is especially important for the Janus type LCs with a remarkable self-recognition capabilities. These factors must be taken into careful consideration in the design of more advanced supermolecular LC architectures in the future.

## Appendix 1 Experimental Techniques

### 1. $^1\text{H}$ and $^{13}\text{C}$ Nuclear Magnetic Resonance (NMR)

NMR spectra were collected on a Jeol ECS400 and a Jeol ECX400 spectrometer.  $\text{CDCl}_3$  and  $\text{D}_6\text{-DMSO}$  were used as the solvent, and the sample was processed with a total scan of 16~512 for the  $^1\text{H}$  NMR and 256~8192 for the  $^{13}\text{C}$  NMR, according to the quantity of the sample. Tetramethylsilane (TMS) was used as the internal standard, and the chemical shifts are record in parts per million (ppm) downfield from the TMS signal. The NMR data was analyzed with MestReC Nova ver. 4.8.6.0 software.

### 2. Mass Spectroscopy (MS)

The ESI MS data of low molar mass product ( $\text{MW} < 1000$ ) were recorded on a Bruker micrOTOF Agilent series 1200LC MS spectrometer. The MALDI-TOF MS data of the samples with high molar mass ( $\text{MW} > 1000$ ) were recorded on a Solarix FTMS spectrometer with 9.4-Tesla superconducting magnet, in which the dihydroxybenzoic acid (DHB,  $m/z = 154.0$ ) was used as the matrix.

### 3. Elemental Analysis (CHN)

Elemental analysis was performed on an Exeter Analytical Inc. CE-440 Elemental Analyzer. S-Benzylthiuronium chloride was used as the checking standard.

### 4. Infra-red Spectroscopy (IR)

Infrared spectra were recorded on a Shimadzu IR prestige-21 FT-IR spectrometer, with samples prepared on KBr disc. The spectra were analyzed by Shimadzu IRsolution ver. 1.30 software.

## 5. Differential Scanning Calorimetry (DSC)

Heat flow curves of the LC products were determined by a Mettler DSC 822e differential scanning calorimetry, calibrated with an indium standard. The samples were heated/cooled with a rate of 10 °C/min, and the phase transition temperatures and enthalpies were determined by the second heating cycle. The DSC spectra were analyzed using STAR ver. 8.10 software.

## 6. Polarized Light Optical Microscopy (POM)

The mesomorphic properties of the materials were investigated by a combination of a Zeiss Axioskop 40 microscopy together with a Mettler FT82HT hot stage and FP90 central processor. The photographs of the LC textures were taken during cooling of the sample from isotropic liquid state with x100 or x200 magnification, by a Infinity X (color) camera along with the Infinity Capture Application ver. 3.7.5 software. Some of the LC materials were annealed for a long time in order to obtain the LC texture, usually > 10 h.

## 7. Chemicals and solvents

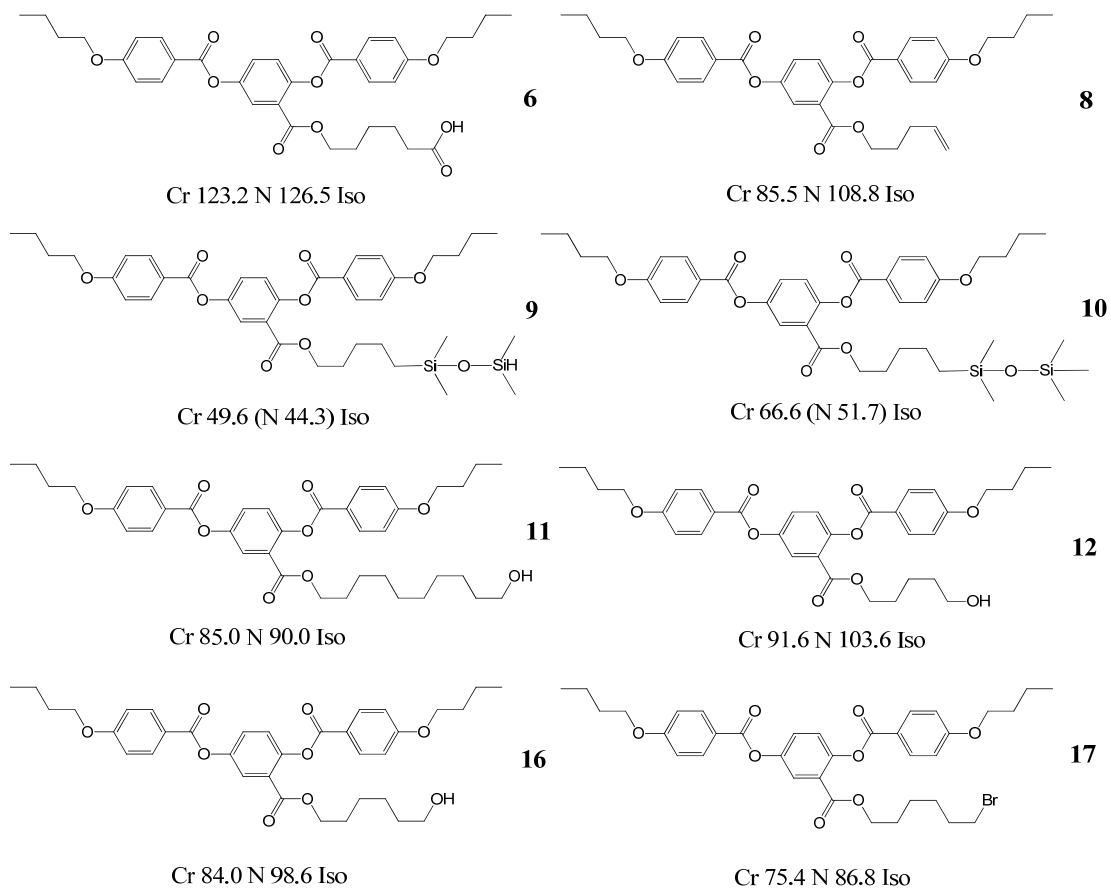
The starting materials, catalysts and inorganic chemicals were obtained from Sigma-Aldrich, Alfa Aesar, Fisher Scientific and FluoroChem, using without further purification. 4,4'-(6-Hydroxyhexyloxy)cyanobiphenyl was synthesized by I. M. Saez in a previous project. The solvents for normal reaction and column chromatography were obtained from Fisher Scientific and VWR Chemicals; anhydrous solvents for moisture sensitive reactions were purchased from Sigma-Aldrich.

## 8. Thin Layer Chromatography (TLC) and Columnar Chromatography

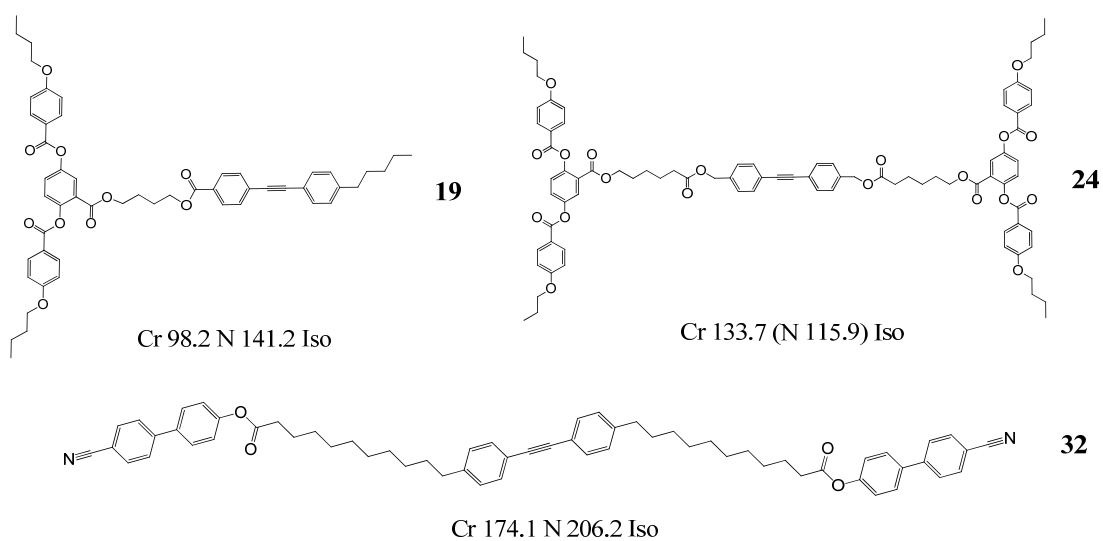
Thin Layer Chromatography was performed on TLC Silica gel 60 F<sub>254</sub> on aluminium sheets, obtained from Merck KGaA. Columnar chromatography was carried out with

high-purity flash grade silica gel with a pore size 60 Å, 220-440 mesh particle size, purchased from Fluka Analytical.

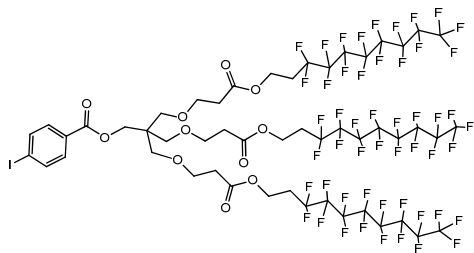
## Appendix 2 List of Compounds



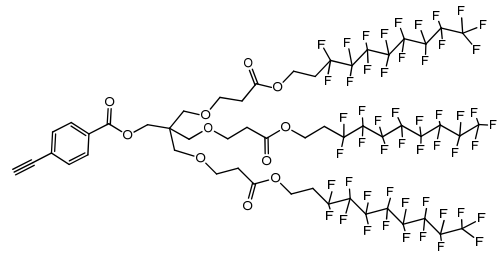
### PDB LC Monomers



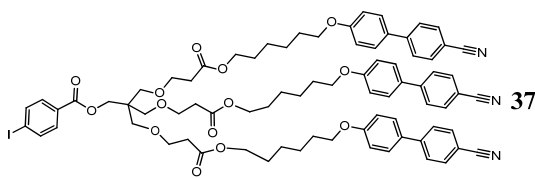
### LC Oligomers



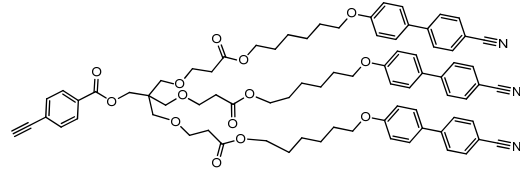
Cr 37.4 SmA 49.1 Iso



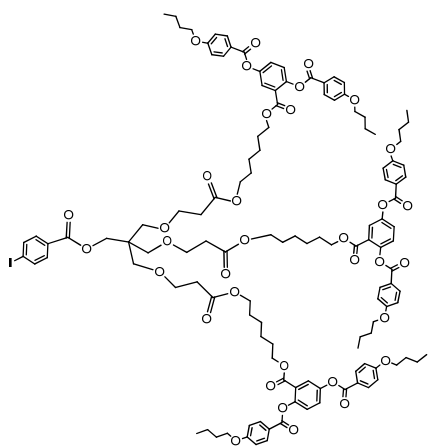
Cr 31.5 SmA 49.2 Iso



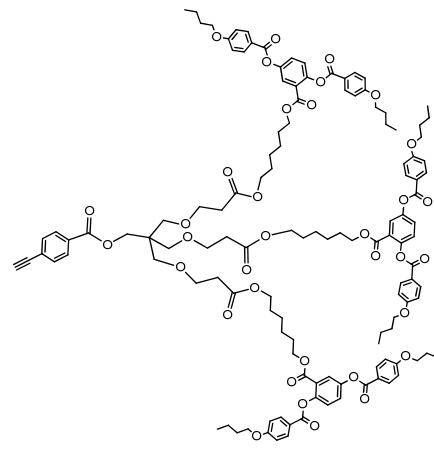
g 1.7 SmA 33.7 N 37.1 Iso



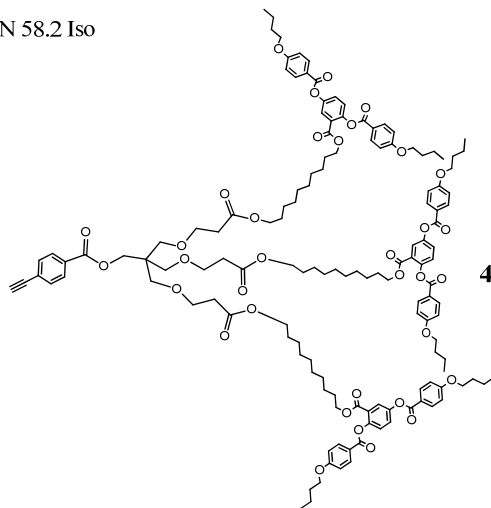
g 2.0 SmA Col N 43.9 Iso



g 0.5 N 58.2 Iso

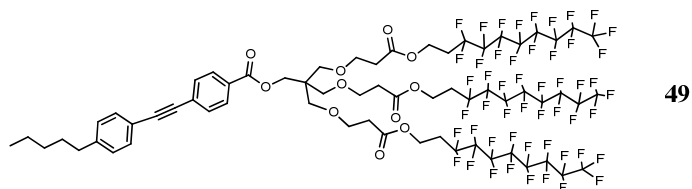


g 3.2 N 56.1 Iso

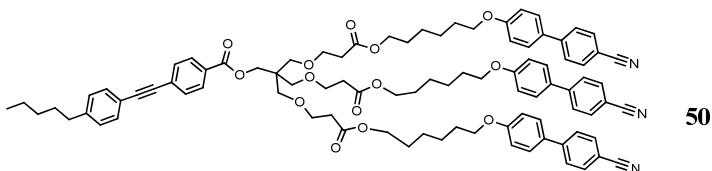


g -2.1 N 59.8 Iso

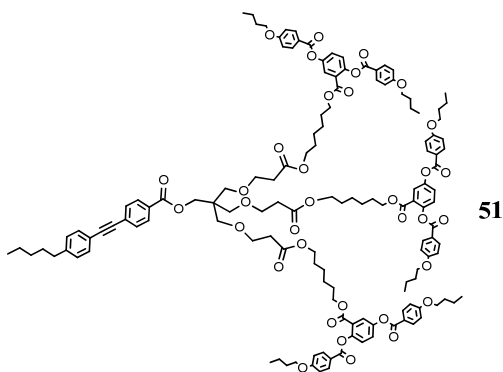
**LC Multipedes**



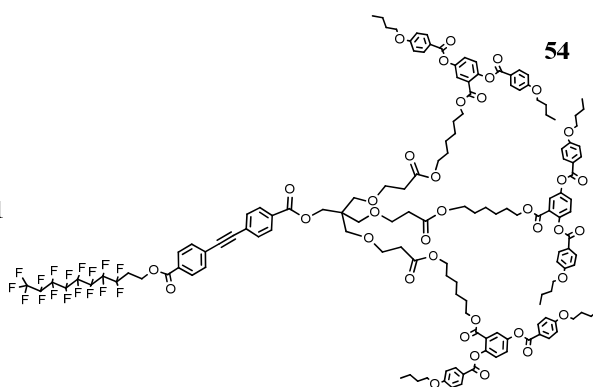
Cr 42.5 SmA 50.0 Iso



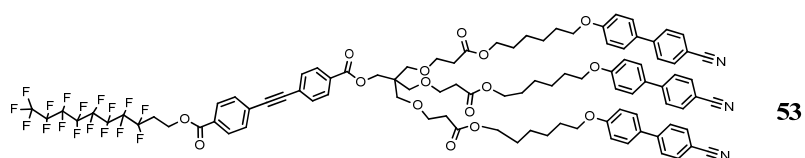
g -0.2 N 56.2 Iso



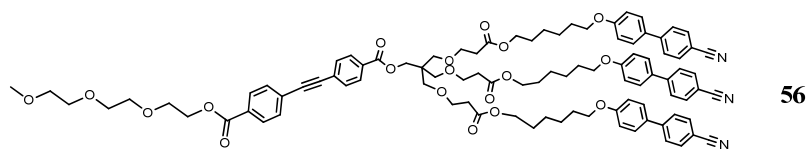
g 5.6 N 65.6 Iso



g 11.3 N 52.4 Iso

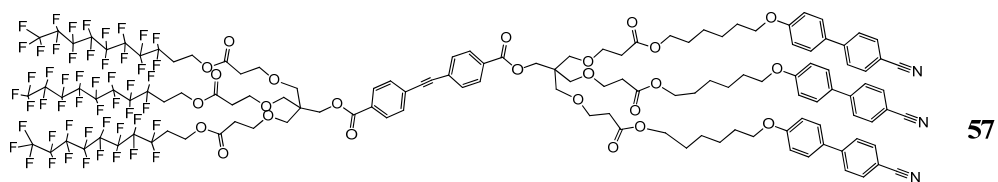


g 4.8 Col SmA 59.9 Iso

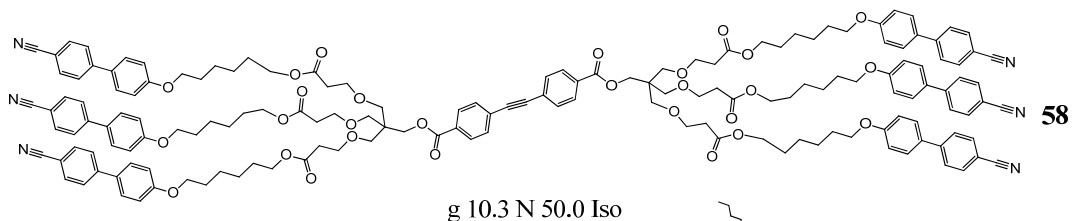


g -7.0 N 7.9 Iso

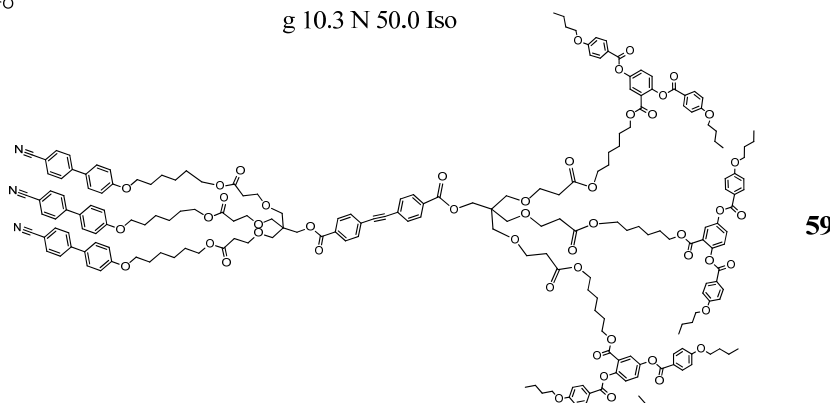
**1:3 Type Janus LCs**



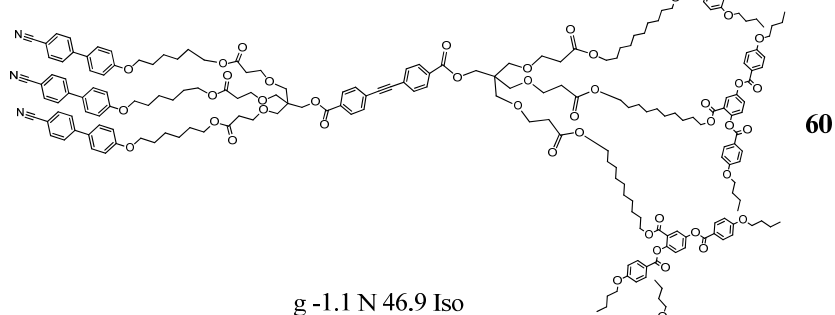
Cr 49.0 X 56.8 X' 65.0 Cub 68.0 SmA 171.1 Iso



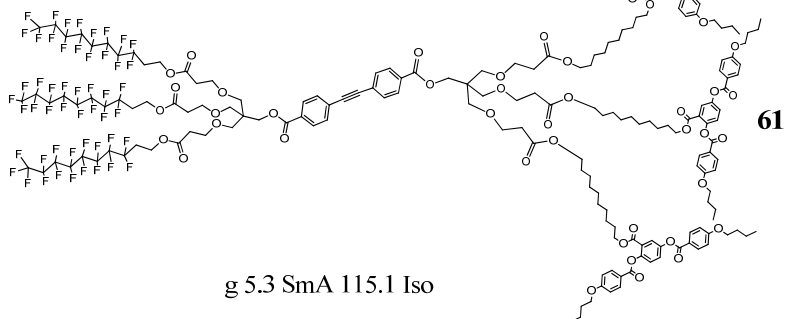
g 10.3 N 50.0 Iso



g 11.4 N 59.8 Iso

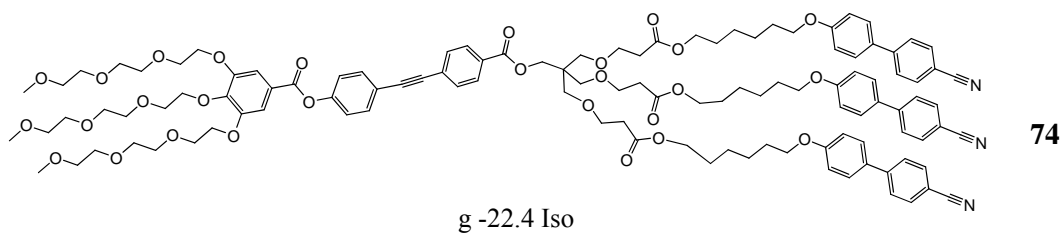
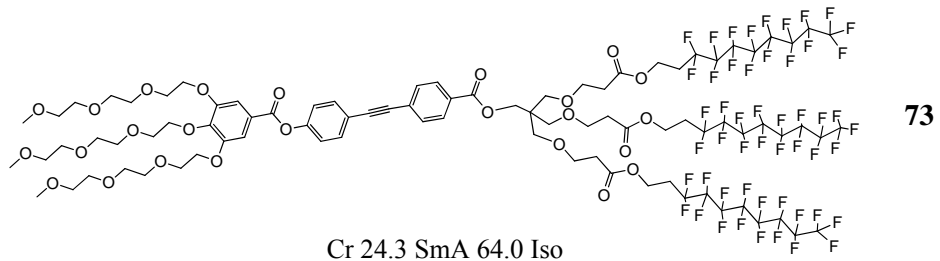
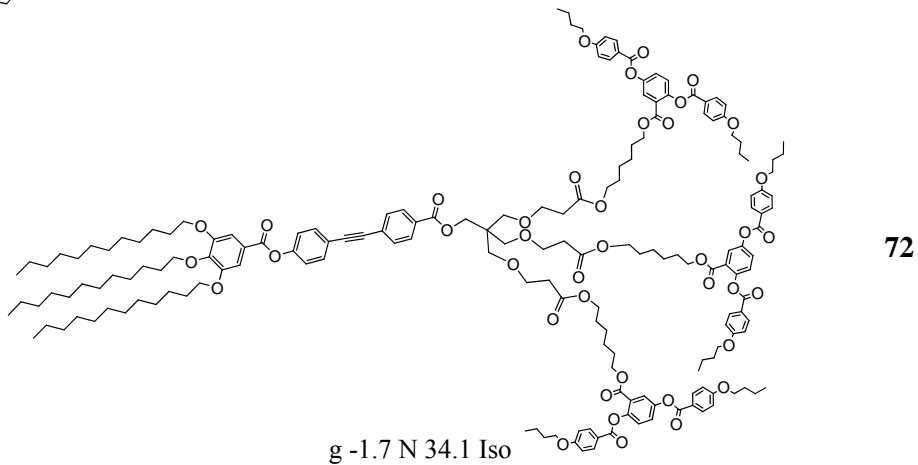
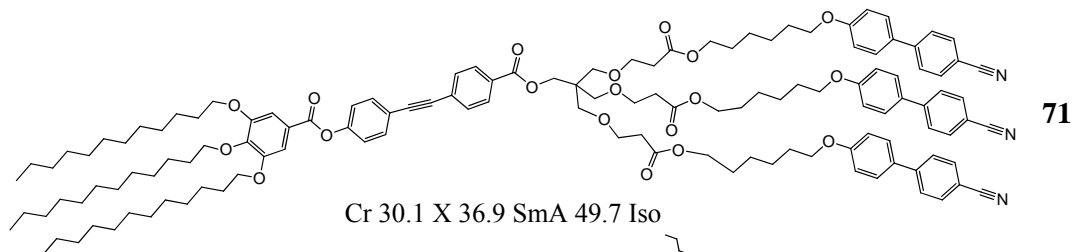
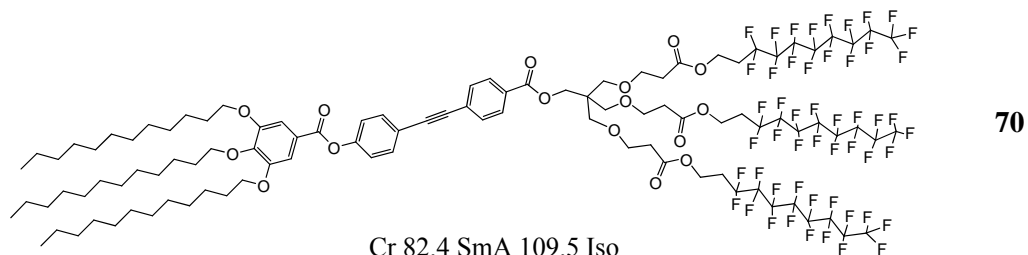


g -1.1 N 46.9 Iso

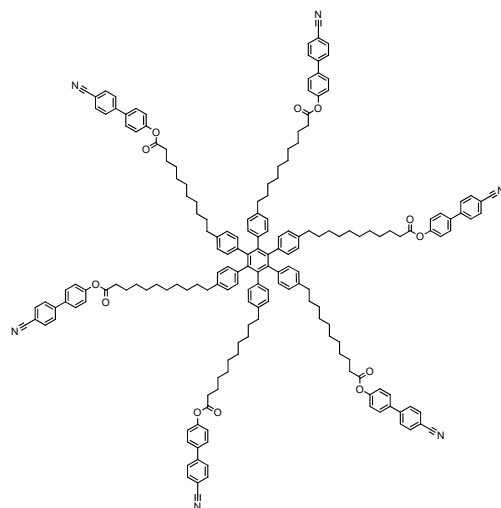


g 5.3 SmA 115.1 Iso

### 3:3 Type Janus LCs

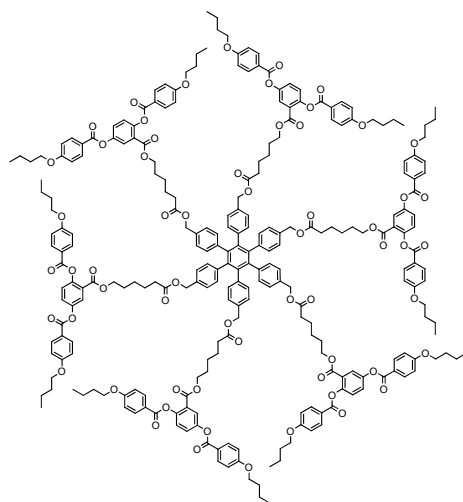


### 3:3 Type Janus LCs



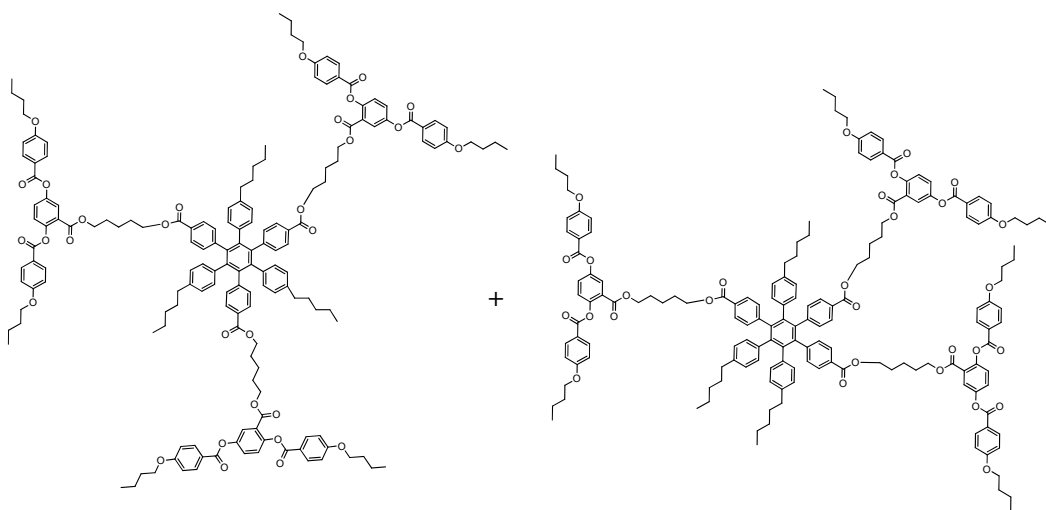
75

Cr 142.1 SmA 159.3 Iso



76

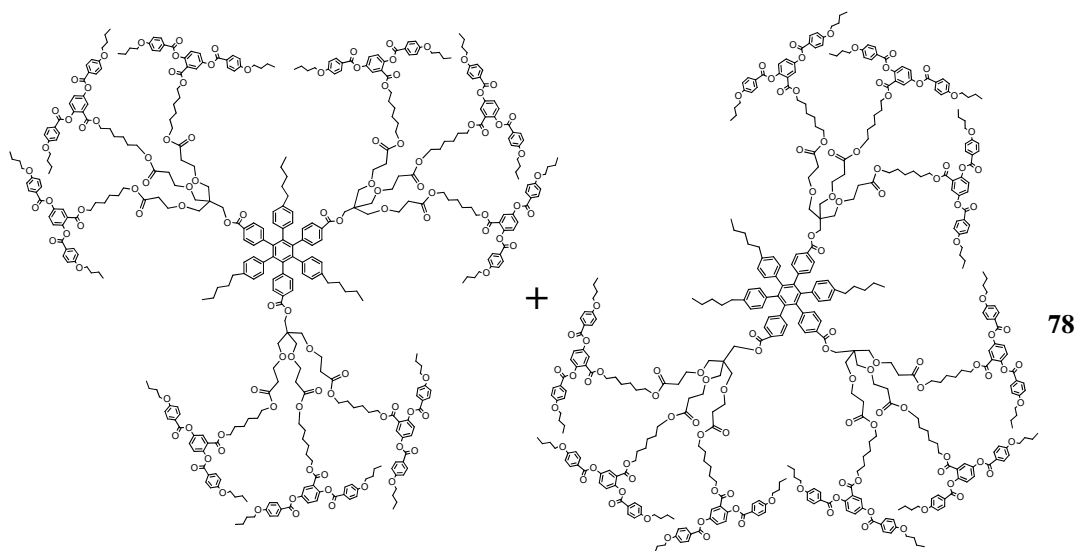
g 27.0 N 68.7 Iso



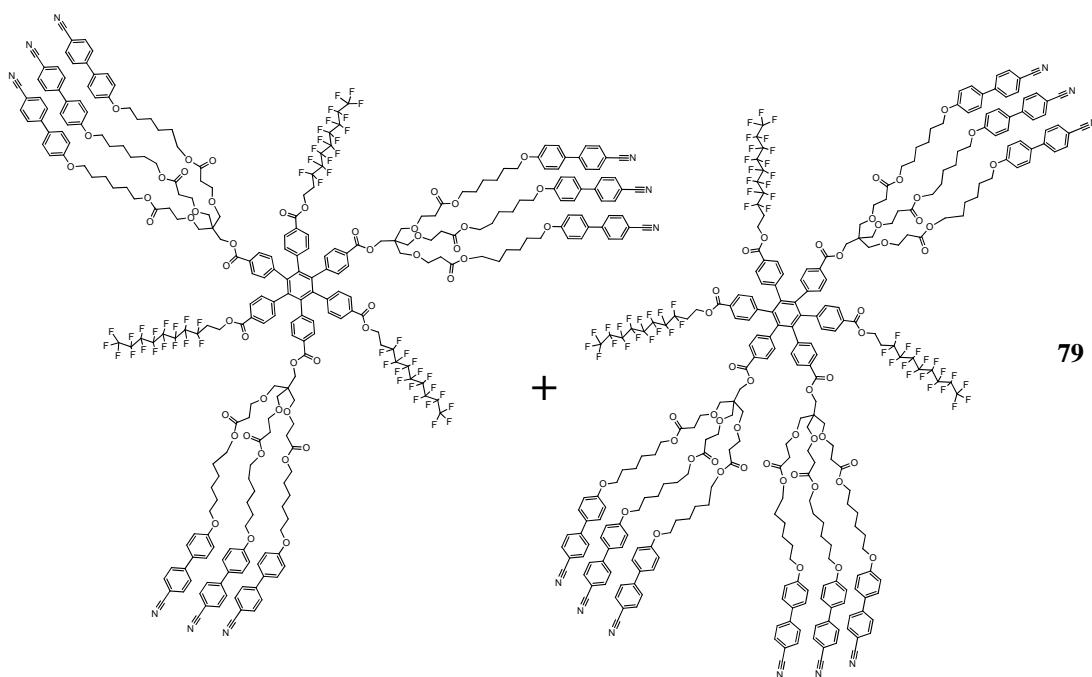
77

g 28.5 Iso

### Hexaphenylbenzenes



g 20.0 N 49.8 Iso



g 11.9 Col 43.7 Iso

**Hexapheylbenzenes**

## Abbreviations and Acronyms

9-BBN	9-borabicyclo(3.3.1)nonane
Ar	aromatic
Bn	benzyl
<sup>t</sup> Bu	tert-butyl
CB	cyanobiphenyl
CED	cohesive energy density
CHN	elemental analysis (carbon, hydrogen and nitrogen)
Col	columnar phase
Cr	crystal state
Cub	cubic phase
d (in NMR spectra)	doublet
DCC	N,N-dicyclohexylcarbodiimide
DHP	dihydropyran
DMAP	4-dimethylaminopyridine
DMF	dimethyl formamide
DSC	differential scanning calorimetry
EDAC	1-ethyl-3-(3-dimethylaminopropyl)carbodiimide
ESI	electrospray ionization
Et	ethyl
<i>f</i> (in microsegregation)	volume fraction
g	glass state
HPB	hexaphenylbenzene (derivative)
I/Iso	isotropic state
IR	infrared spectroscopy
J (in NMR spectra)	coupling constant (Hz)
LC	liquid crystal
m (in continuum theory)	strength of disclination
m (in NMR spectra)	multiplet
MALDI	matrix-assisted laser desorption/ionization
MCPBA	meta-chloroperbenzoic acid
Me	methyl
MS	mass spectrometry

N	nematic phase
N*	chiral nematic phase
N <sub>B</sub>	biaxial nematic phase
N <sub>D</sub>	discotic nematic phase
NMR	nuclear magnetic resonance spectroscopy
OCB	alkoxy-cyanobiphenyl
PDAB	phenylene dibenzoate (derivative)
PE	pentaerythritol
PEG	polyethylene glycol
Ph	phenyl
POM	polarized light optical microscopy
ppm	parts per million
PTSA	<i>p</i> -toluenesulfonic acid
R <sub>F</sub>	perfluorinated hydrocarbon chain
R <sub>H</sub>	hydrocarbon chain
s (in NMR spectra)	singlet
SmA	smectic A phase
SmC	smectic C phase
SmCP	polar smectic C phase
SmX	unidentified smectic phase
t (in NMR spectra)	triplet
TCBO	tricyanobiphenyl oligomer
TEG	triethylene glycol
TFA	trifluoroacetic acid
THF	tetrahydrofuran
THP	tetrahydropyran
TLC	thin layer chromatography
TMSA	trimethylsilyl acetylene
TOF	time-of-flight mass spectrometer
X (in liquid crystal phases)	unidentified mesophase
χ (in microsegregation)	interaction parameter

## References

1. D. Demus, J. W. Goodby, G. W. Gray, H.-W. Spiess and V. Vill, *Handbook of Liquid Crystals, Vol I-III*, Wiley-VCH, Weinheim, 1998.
2. P. J. Collings and M. Hird, *Introduction to Liquid Crystal: Chemistry and Physics*, Taylor & Francis, London, 2004.
3. a) I. M. Saez and J. W. Goodby, *Struct. Bond.*, 2008, **128**, 1; b) I. M. Saez and J. W. Goodby, *Supramolecular Soft Matter*, p. 301, Wiley, Weinheim, 2011; c) I. M. Saez, unpublished results.
4. C. Viney, T. P. Russell, L. E. Depero and R. J. Twieg, *Mol. Cryst. Liq. Cryst.*, 1989, **168**, 63.
5. X. Bao and L. R. Dix, *Mol. Cryst. Liq. Cryst.*, 1996, **281**, 291.
6. M. Hird, J. W. Goodby, R. A. Lewis and K. J. Toyne, *Mol. Cryst. Liq. Cryst.*, 2003, **401**, 115.
7. P. Oswald and P. Pieranski, *Smectic and Columnar Liquid Crystals*, CRC press, Taylor & Francis, Boca Raton, 2006.
8. a) J. W. Emsley, G. R. Luckhurst, G. N. Shilstone and I. Sage, *Mol. Cryst. Liq. Cryst.*, 1984, **102**, 223; b) G. R. Luckhurst, *Liq. Cryst.*, 2005, **32**, 1335; c) C. T. Imrie and P. A. Henderson, *Chem. Soc. Rev.*, 2007, **36**, 2096.
9. W. S. Bae, J. W. Lee and J. I. Jin, *Liq. Cryst.*, 2001, **28**, 59.
10. W. Weissflog, D. Demus, S. Diele, P. Nitschke and W. Wedler, *Liq. Cryst.*, 1989, **5**, 111.
11. C. T. Imrie and G. R. Luckhurst, *J. Mater. Chem.*, 1998, **8**, 1339.
12. C. V. Yelamaggad, S. K. Prasad, G. G. Nair, I. S. Shashikala, D. S. S. Rao, C. V. Lobo and S. Chandrasekhar, *Angew. Chem., Int. Ed.*, 2004, **43**, 3429.
13. R. Eidenschink, F.-H. Kreuzer and W.-H. Dejeu, *Liq. Cryst.*, 1990, **8**, 879.

14. I. M. Saez and J. W. Goodby, *J. Mater. Chem.*, 2003, **13**, 2727.
15. a) J. P. Straley, *Phys. Rev. A.*, 1973, **10**, 1881; b) P. G. De Gennes and J. Prost, *The Physics of Liquid Crystals, 2nd ed.*, Clarendon Press, Oxford, 1993; c) A. G. Vanakaras, S. C. Mcgrother, G. Jackson and D. J. Photinos, *Mol. Cryst. Liq. Cryst.*, 1998, **323**, 199; d) R. W. Date and D. W. Bruce, *J. Am. Chem. Soc.*, 2003, **125**, 9012; e) P. H. J. Kouwer and G. H. Mehl, *J. Am. Chem. Soc.*, 2003, **125**, 11172.
16. H. K. Bisoyi, V. A. Raghunathan and S. Kumar, *Chem. Commun.*, 2009, 7003.
17. G. R. Newkome, C. N. Moorefield and F. Vögtle, *Dendritic Molecules: Concepts, Syntheses, Perspectives*, Wiley, Weinheim, 1996.
18. A. Kishimura, T. Yamashita, K. Yamaguchi and T. Aida, *Nat. Mater.*, 2005, **4**, 546.
19. D. Lagnoux, T. Darbre, M. L. Schmitz and J.-L. Reymond, *Chem. Eur. J.*, 2005, **11**, 3941.
20. a) B. M. Rosen, C. J. Wilson, D. A. Wilson, M. Peterca, M. R. Imam and V. Percec, *Chem. Rev.*, 2009, **109**, 6275; b) V. Percec, W. D. Cho, G. Ungar and D. J. P. Yeardley, *J. Am. Chem. Soc.*, 2001, **123**, 1302.
21. a) B. Donnio, S. Buathong, I. Bury and D. Guillon, *Chem. Soc. Rev.* 2007, **36**, 1495; b) V. Percec and M. Kawasumi, *Macromolecules*, 1992, **25**, 3843; c) S. Buathong, L. Gehringer, B. Donnio and D. Guillon, *Compt. Rend. Chim.*, 2009, **12**, 138.
22. K. Lorenz, D. Holter, B. Stuhn, R. Mulhaupt and H. Frey, *Adv. Mater.*, 1996, **8**, 414.
23. a) R. Elsaber, G. H. Mehl, J. W. Goodby and D. J. J. Photinos, *Chem. Commun.*, 2000, 851; b) B. Donnio and D. Guillon, *Adv. Polym. Sci.*, 2006, **201**, 45; c) S. Campidelli, T. Brandmüller, A. Hirsch, I. M. Saez, J. W. Goodby and R. Deschenaux, *Chem. Commun.*, 2006, 4282; d) I. M. Saez, J. W. Goodby and R. M. Richardson, *Chem. Eur. J.*, 2001, **7**, 2758.
24. G. H. Mehl and J. W. Goodby, *Chem. Commun.*, 1999, 13.

25. C. Casagrande, P. Fabre, E. Raphael and M. Veyssie, *Europhys. Lett.*, 1989, **9**, 251.
26. P-G de Gennes, *Angew. Chem. Int. Ed. Engl.*, 1992, **31**, 842.
27. C. Tschierske, *Isr. J. Chem.* 2012, **52**, 935.
28. V. Percec, D. A. Wilson, P. Leowanawat, C. J. Wilson, A. D. Hughes, M. S. Kaucher, D. A. Hammer, D. H. Levine, A. J. Kim, F. S. Bates, K. P. Davis, T. P. Lodge, M. L. Klein, R. H. DeVane, E. Aqad, B. M. Rosen, A. O. Argintaru, M. J. Sienkowska, K. Rissanen, S. Nummelin and J. Ropponen, *Science*, 2010, **328**, 1009.
29. J. Pan, M. Wen, D. Yin, B. Jiang, D. He and L. Guo, *Tetrahedron*, 2012, **68**, 2943.
30. I. M. Saez and J. W. Goodby, *Chem. Eur. J.* 2003, **9**, 4869.
31. Z. T. Nagy, B. Heinrich, D. Guillon, J. Tomczyk, J. Stumpe and B. Donnio, *J. Mater. Chem.*, 2012, **22**, 18614.
32. A. Yamaguchi, Y. Maeda, H. Yokoyama and A. Yoshizawa, *Chem. Mater.*, 2006, **18**, 5704.
33. N. Gimeno, J. Vergara, M. T. Cano, J. L. Serrano, M. B. Ros, J. Ortega, C. L. Folcia, S. Rodríguez-Conde, G. Sanz-Enguita and J. Etxebarria, *Chem. Mater.*, 2013, **25**, 286.
34. H.-J. Sun, C.-L. Wang, I.-F. Hsieh, C.-H. Hsu, R. M. V. Horn, C.-C. Tsai, K.-U. Jeong, B. Lotz and S. Z. D. Cheng, *Soft Matter*, 2012, **8**, 4767.
35. P. Keller, D. L. Thomsen III and M-H. Li, *Macromolecules*, 2002, **35**, 581.
36. D. L. Thomsen III, P. Keller, J. Naciri, R. Pink, H. Jeon, D. Shenoy and B. R. Ratna, *Macromolecules*, 2001, **34**, 5868.
37. L. Pastor, J. Barbera, M. McKenna, M. Marcos, R. Martin-Rapun, J. L. Serrano, G. R. Luckhurst and A. Mainal, *Macromolecules*, 2004, **37**, 9386.
38. S. Sia, PhD Thesis, University of Hull, 2003.

39. a) G. W. Gray and A. Mosley, *Mol. Cryst. Liq. Cryst.*, 1976, **37**, 213; b) A. Bouchta, H. T. Nguyen, M. F. Achard, F. Hardouin, C. Destrade, R. J. Twieg, A. Marroufi and N. Isaert, *Liq. Cryst.*, 1992, **12**, 575.
40. L. Gehringer, C. Bourgogne, D. Guillon and B. Donnio, *J. Mater. Chem.*, 2005, **15**, 1696.
41. Z. Li, F. W. Fowler and J. W. Lauher, *J. Am. Chem. Soc.*, 2009, **131**, 634.
42. J. D. Brand, C. Kübel, S. Ito, and K. Müllen, *Chem. Mater.*, 2000, **12**, 1638.
43. A. Dupraz, P. Guy and C. Dupuy, *Tet. Lett.*, 1996, **37**, 1240.
44. S. Hecht and J. M. J. Frechet, *J. Am. Chem. Soc.*, 1999, **121**, 4084.
45. a) H. W. Frühauf, *Chem. Rev.*, 1997, **97**, 523; b) M. Lautens, W. Klute and W. Tam, *Chem. Rev.*, 1996, **96**, 49; c) D. B. Grotjahn, *Comprehensive Organometallic Chemistry II*; Eds: E. W. Abel, F. G. A. Stone and G. Wilkinson, Pergamon: Oxford, 1995; Vol. 12, pp 741-770.